VOYAGER

SPACECRAFT Phase B, Task D

FINAL REPORT

OCTOBER 1967

Prepared for

GEORGE C. MARSHALL SPACE FLIGHT CENTER

Huntsville, Alabama

Voyager Operations
Space Vehicles Division

TRW SYSTEMS GROUP

One Space Park, Redondo Beach, California

MODEL OF TRW RECOMMENDED VOYAGER SPACECRAFT

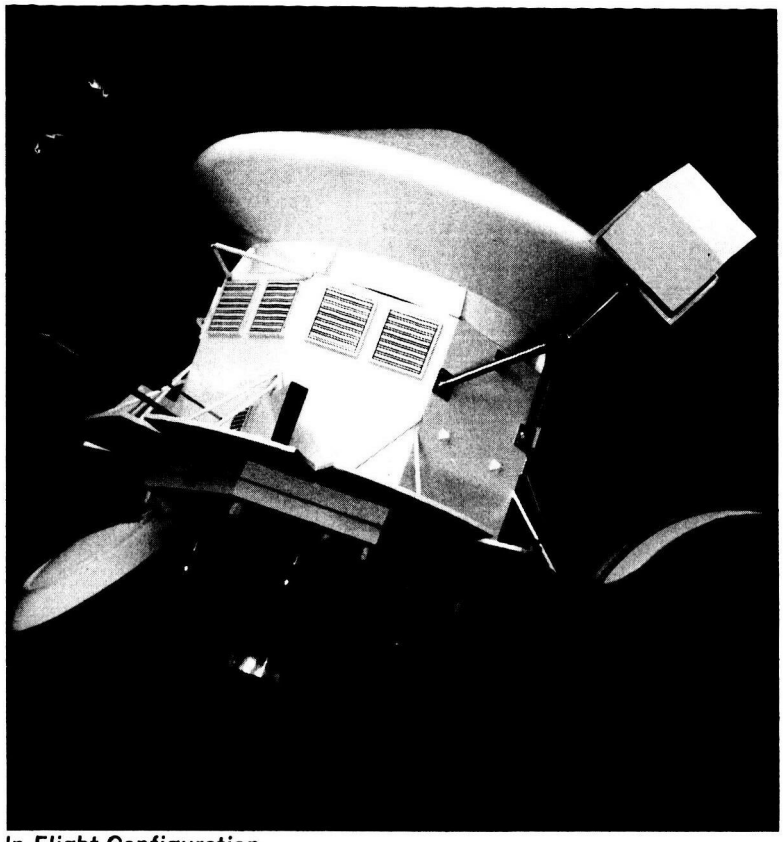

In-Flight Configuration

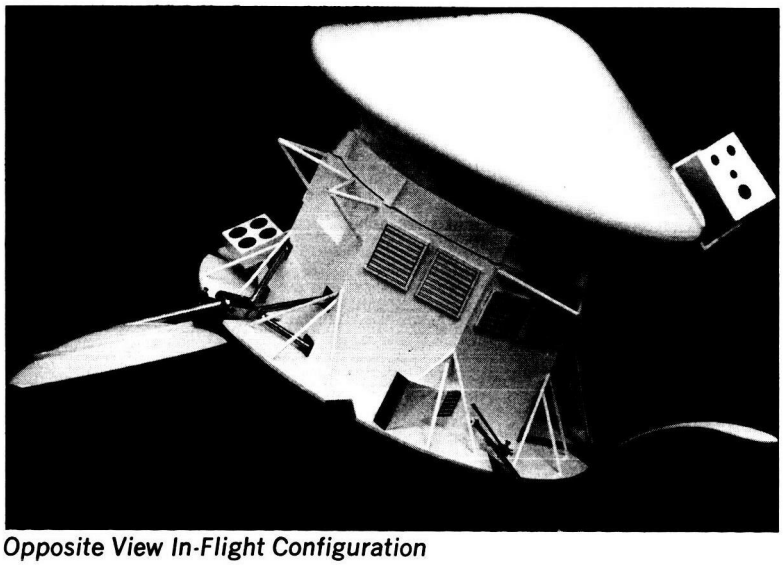

Opposite View In-Flight Configuration

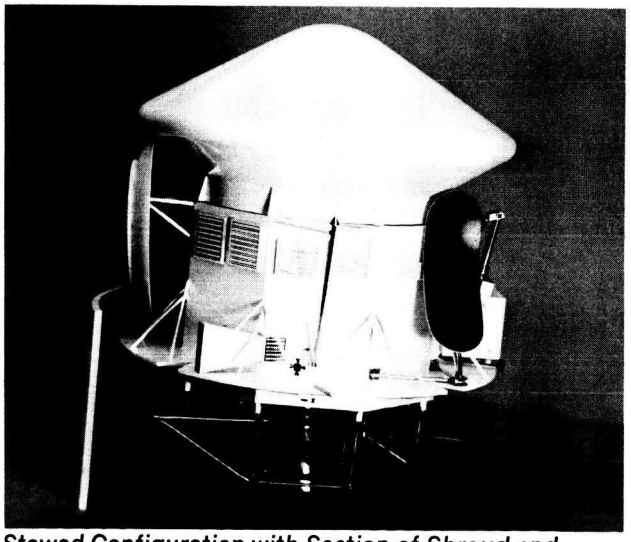

Stowed Configuration with Section of Shroud and Planetary Vehicle Adapter

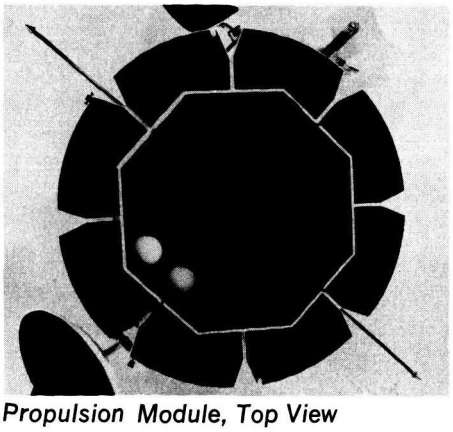

Propulsion Module, Top View

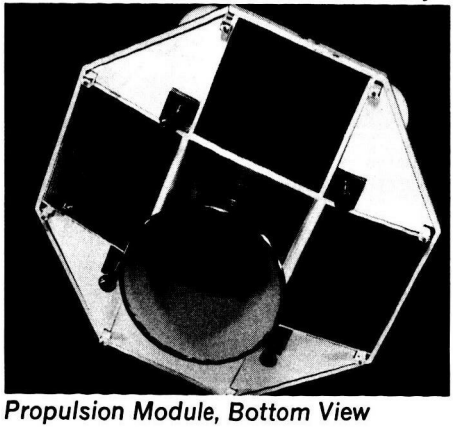

Propulsion Module, Bottom View

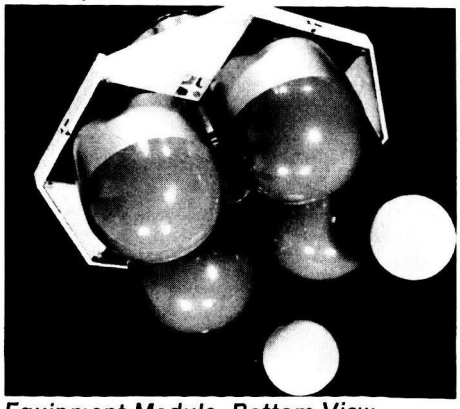

Equipment Module, Bottom View

Copy 47

VOYAGER

SPACECRAFT Phase B, Task D

FINAL REPORT

Volume 3. Spacecraft Mechanical Subsystems Definition

OCTOBER 1967

Prepared for
GEORGE C. MARSHALL SPACE FLIGHT CENTER
Huntsville, Alabama

TRW
SYSTEMS GROUP

Voyager Operations
Space Vehicles Division

One Space Park, Redondo Beach, California

CONTENTS

1. INTRODUCTION

The Voyager Spacecraft consists of a group of subsystems, mechanical and electrical. This volume describes the mechanical subsystems. These are:

- Structural subsystem, which includes the appendage release mechanisms
- Propulsion subsystem, which is designed around the LM Descent Engine
- Planetary vehicle adapter
- Temperature control subsystem

A major advantage of the TRW spacecraft is its modularity, which simplifies all the assembly, test, and checkout operations that have to be performed between manufacture and launch. The spacecraft is divided into two easily integrated yet independent units: the equipment module and the propulsion module. See Figure 1-1.

The equipment module supports and protects all electrical subsystems and the science payload. All these components can be integrated, tested, and checked out before the spacecraft is assembled, and the module can be shipped as a separate unit.

The main engine (LMDE), the backup engines (C-1), and all other components of the propulsion subsystem are in the propulsion module. The entire propulsion subsystem can therefore be assembled and tested (including engine firing tests) independently of the rest of the spacecraft. This module, too, can be shipped separately.

Only for system level tests and launch preparation need the two modules be mated. The savings in terms of time, personnel, and facilities required are significant. Schedule confidence is substantially increased.

A second major advantage of the TRW design is the key role played by the planetary vehicle adapter, which is not injected into the Martian trajectory with its planetary vehicle. This separate module includes a truss structure, which takes all planetary vehicle loads during the boost phase of the mission and distributes them to the shroud. It thereby relieves

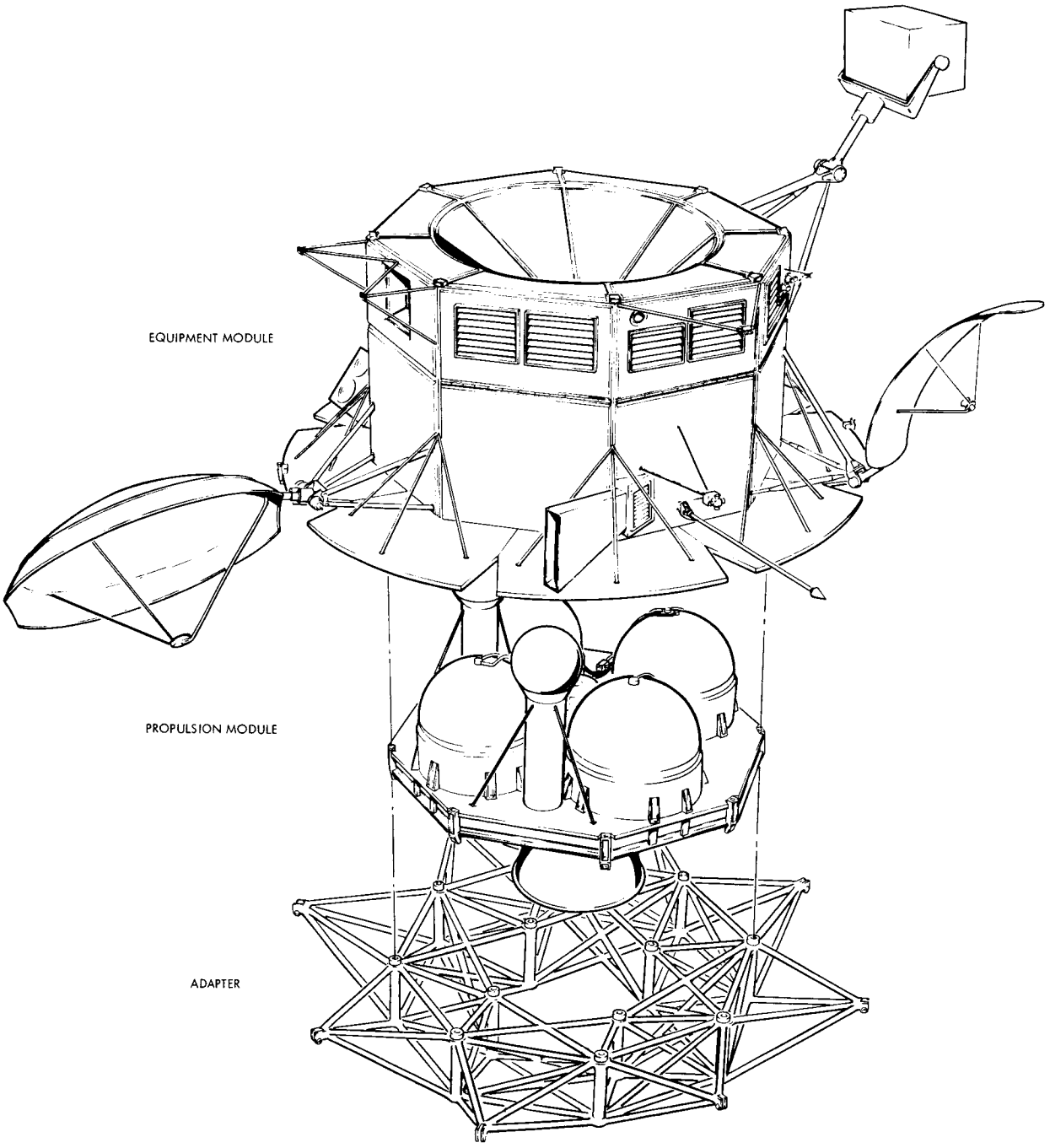

Figure 1-1

SPACECRAFT is easily separated into two discrete modules for test, checkout and shipment . . . easily integrated with simple, bolted field joint and a single electrical connector. Planetary vehicle adapter is designed to relieve spacecraft of much structural weight needed only during launch and boost.

the spacecraft of a considerable inert mass, which would otherwise have to be carried during the rest of the mission and deboosted into Mars orbit. This design therefore permits a lighter spacecraft structure and thereby increases payload capability.

The equipment module structure and the propulsion module structure each consist of a rigid framework, to which are attached panels of composite construction. These panels serve the dual purpose of protecting against meteoroid penetration and adding to structural strength and rigidity.

Integrated with the structural subsystem is a complete temperature control subsystem. This consists of insulation blankets and moldings as well as surface coatings designed to maintain required temperatures throughout the spacecraft. It also includes automatic louvers for cooling, and heaters for equipment that requires special thermal environments.

Figure 1-2 is an exploded view of the spacecraft and adapter, showing all major elements.

FOLDOUT FRAME

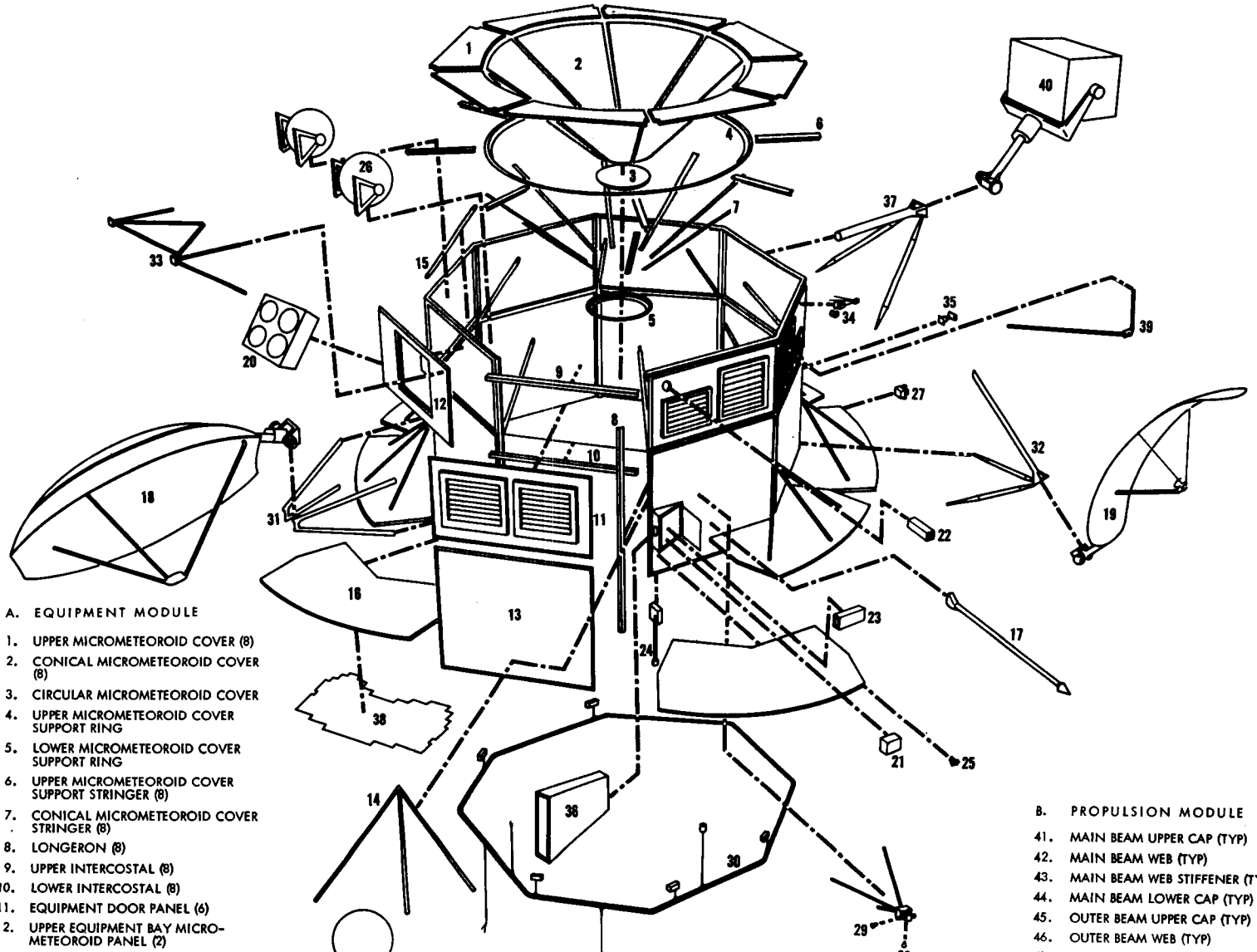

A. EQUIPMENT MODULE

1. UPPER MICROMETEOROID COVER (8)
2. CONICAL MICROMETEOROID COVER (8)
3. CIRCULAR MICROMETEOROID COVER
4. UPPER MICROMETEOROID COVER SUPPORT RING
5. LOWER MICROMETEOROID COVER SUPPORT RING
6. UPPER MICROMETEOROID COVER SUPPORT STRINGER (8)
7. CONICAL MICROMETEOROID COVER STRINGER (8)
8. LONGERON (8)
9. UPPER INTERCOSTAL (8)
10. LOWER INTERCOSTAL (8)
11. EQUIPMENT DOOR PANEL (6)
12. UPPER EQUIPMENT BAY MICRO-METEOROID PANEL (2)

B. PROPULSION MODULE

41. MAIN BEAM UPPER CAP (TYP)
42. MAIN BEAM WEB (TYP)
43. MAIN BEAM WEB STIFFENER (TYP)
44. MAIN BEAM LOWER CAP (TYP)
45. OUTER BEAM UPPER CAP (TYP)
46. OUTER BEAM WEB (TYP)

13. LOWER EQUIPMENT BAY MICRO-METEOROID PANEL (8)
14. SOLAR ARRAY SUPPORT STUT (24)
15. EQUIPMENT BAY BRACE (8)
16. SOLAR ARRAY SUBSTRATE PANEL (8)
17. LOW-GAIN ANTENNA AND DRIVE ASSEMBLY
18. HIGH-GAIN ANTENNA AND DRIVE ASSEMBLY
19. MEDIUM-GAIN ANTENNA AND DRIVE ASSEMBLY
20. UHF ANTENNA (CAPSULE RELAY LINK)
21. GYRO REFERENCE ASSEMBLY (2) ACCELEROMETER ASSEMBLY (2)
22. LIMB AND TERMINATOR CROSSING SENSOR (2)
23. CANOPUS SENSOR (2)
24. FINE SUN SENSOR (2) (2)
25. COARSE SUN SENSOR (4)
26. REACTION CONTROL PRESSURE VESSEL AND SUPPORT STRUCTURE (2)
27. PITCH THRUSTER (4)
28. YAW THRUSTER (4)
29. ROLL THRUSTER (4)
30. ELECTRIC CABLE AND WIRE HARNESS
31. HIGH-GAIN ANTENNA SUPPORT STRUCTURE
32. MEDIUM-GAIN ANTENNA SUPPORT STRUCTURE
33. HIGH-GAIN ANTENNA TIE - DOWN ASSEMBLY
34. MEDIUM-GAIN ANTENNA TIE-DOWN ASSEMBLY
35. PLANETARY SCAN PLATFORM TIE-DOWN ASSEMBLY (2)
36. CANOPUS SENSOR GLINT SHIELD (2)
37. PLANETARY SCAN PLATFORM SUPPORT STRUCTURE
38. SOLAR CELL PANEL(8) PANEL (8)
39. LOW-GAIN ANTENNA TIE-DOWN ASSEMBLY
40. PLANETARY SCAN PLATFORM AND DRIVE ASSEMBLY

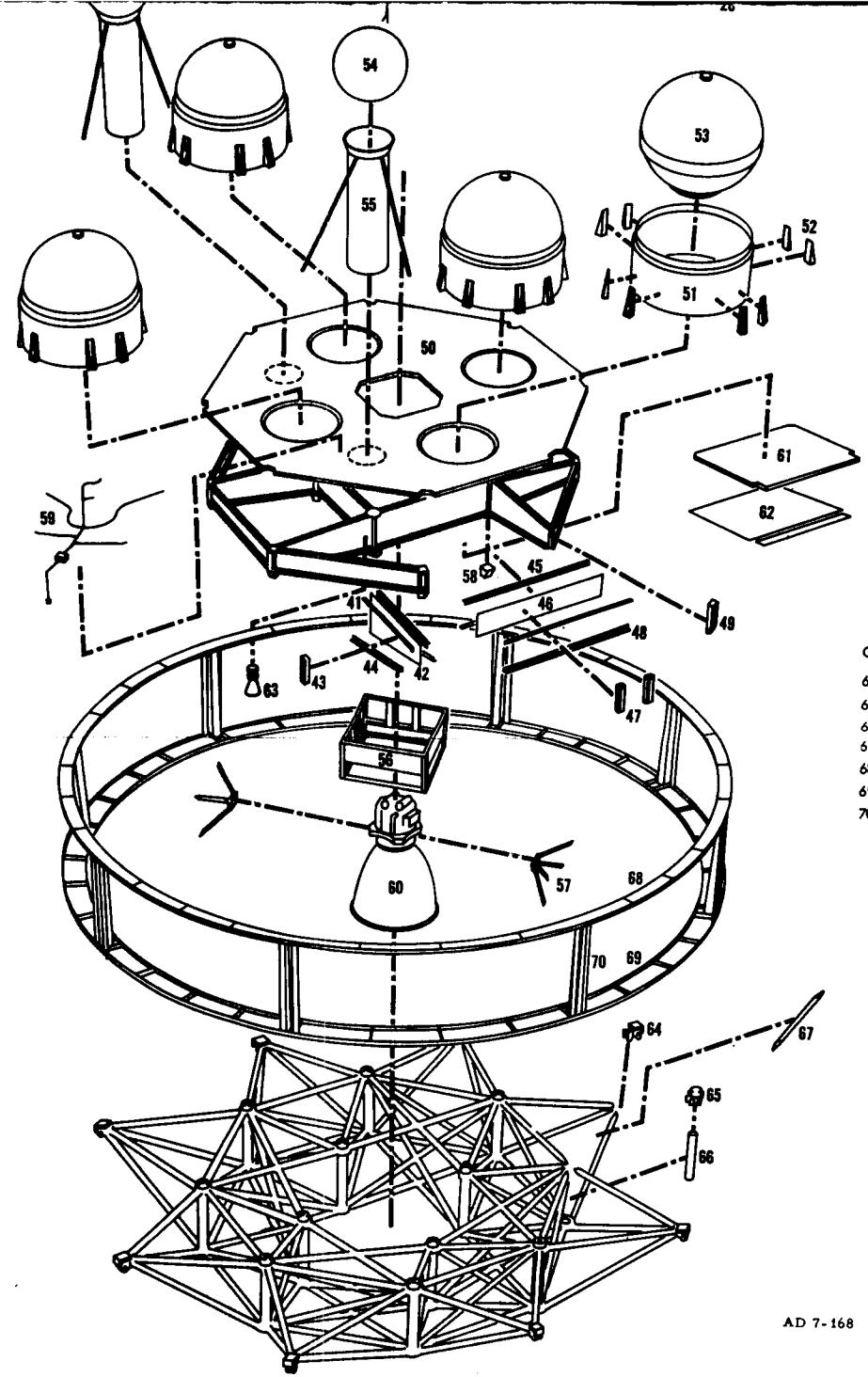

AD 7-168

47. OUTER BEAM WEB STIFFENER (TYP)
48. OUTER BEAM LOWER CAP (TYP)
49. CORNER AND ADAPTER ATTACH FITTING (8)
50. TANK SUPPORT PLATFORM
51. TANK SUPPORT SKIRT (4)
52. SKIRT SUPPORT FITTING (40)
53. PROPELLANT TANK (4)
54. PRESSURE TANK (2)
55. PRESSURANT TANK SUPPORT (2)
56. ENGINE SUPPORT BEAM ASSEMBLY
57. ENGINE TRUNION SUPPORT TRUSS ASSEMBLY (2)
58. ADAPTER ATTACH FITTING (4)
59. ELECTRICAL HARNESS
60. MODIFIED LM DESCENT ENGINE
61. SOLAR ARRAY SUBSTRATE PANEL (3)
62. SOLAR CELL PANEL (3)
63. C-1 ENGINE (4)

C. ADAPTER

64. SHROUD ATTACH FITTING (8)
65. SPACECRAFT ATTACH FITTING (2)
66. COLUMN (12)
67. TRUSS MEMBER (TYP)
68. SHROUD UPPER RING
69. SHROUD LOWER RING
70. SHROUD INTERCOSTAL (8)

Figure 1-2
EXPLODED VIEW

FOLDOUT FRAME

2. STRUCTURAL SUBSYSTEM

2.1 SUMMARY

The structural subsystem includes the basic framework of the spacecraft and various support and release mechanisms for the spacecraft and its appendages. Its primary function is to integrate with minimum weight the other subsystems comprising the spacecraft. It provides sufficient strength, rigidity, and other physical characteristics to withstand ground and mission environments and provides the required support and alignment for spacecraft components and assemblies, and the capsule. The preliminary subsystem specification is shown in Figure 2-1.

The recommended configuration of the structural subsystem features:

- Modularity of the propulsion and equipment module structures
- Minimum weight of separated spacecraft
- Direct load paths from major load items to interfaces and support points
- Removable equipment mounting panels
- Accessibility to propulsion components in mated spacecraft
- Flexibility for locating appendages and solar arrays
- Maximum utilization of primary structure as meteoroid protection
- Use of proven designs for release devices and mechanisms
- Growth capacity for increased payloads
- State-of-the-art materials and fabrication

A modular view of the complete structural subsystem and planetary vehicle adapter for the recommended configuration is shown in Figure 1-1.

The propulsion module structure provides complete support for all of the spacecraft helium and fuel tanks, the LM descent engine, the C-1 engines, and the various propulsion subsystem components. Its primary structure consists of built-up aluminum beams and a honeycomb platform

PRELIMINARY SPECIFICATION

Structural Subsystem

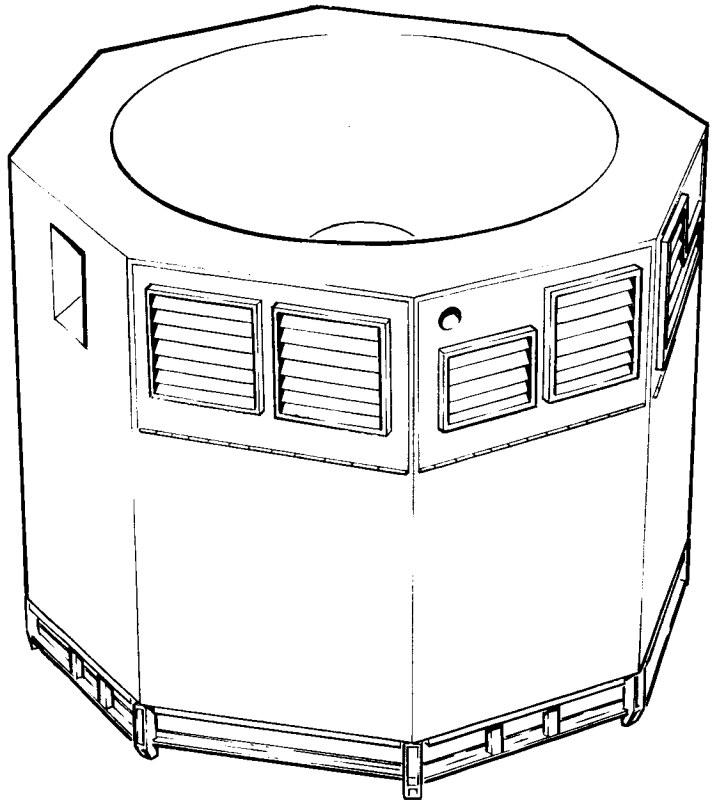

Purpose

Provides structural integration, support and environmental protection for the spacecraft subsystems and mounting provisions for the flight capsule.

SUBSYSTEM CHARACTERISTICS

The subsystem is composed of an equipment module structure and propulsion module structure plus support and release mechanisms for appendages.

Characteristics

LOAD FACTORS (LIMIT)	LONGITUDINAL		LATERAL	
Primary structures	Static	Dynamic	Static	Dynamic
1st stage burnout	+5.0		±1.0	±1.0
1st stage cutoff				
Retrofire	+2.0		±0.3	

FACTORS OF SAFETY	Yield	Ultimate
General Structure	1.00	1.25

METEOROID PROTECTION	
Spacecraft surface area	650 square feet
Mission time	284 days
Probability of zero penetration	0.87
Mission reliability	0.97

Performance Characteristics

CONFIGURATION

COMPONENT	OVERALL DIMENSIONS	WEIGHT	MATERIALS AND CONSTRUCTION
Propulsion module structure	158 in. across flats octagon taper to 57 in. square x 22 in. high	484 lb	7075 Al built up beams plus honeycomb deck
Equipment module structure	158 in. octagon x 100 in. high	1008 lb	7075 Al-semi-monocoque plus meteroid panels
Subsystem		1492 lb	

Interfaces

FLIGHT CAPSULE: 8 equally spaced bolts on a 160 in. diameter bolt circle.

PLANETARY VEHICLE ADAPTER: 12 points, 8 equally spaced on 160 in. diameter bolt circle
4 equally spaced on 80 in. diameter bolt circle

Figure 2-1

to which honeycomb tank support cylinders are attached. (See Figure 2-2.) The upper side of the deck interfaces with the equipment module while the lower caps of the beams attach to the planetary vehicle adapter.

The octagonal equipment module structure supports the equipment subsystems and the capsule. Its primary structure consists of eight vertical longerons, foam-filled honeycomb meteoroid protection panels and honeycomb equipment panels. (See Figure 2-3.) At their upper ends, the longerons provide the structural interface with the capsule and at their lower ends with the propulsion module.

The mechanical section of the subsystem provides redundant devices for retaining and releasing the four antennas and the planetary scan platform shown in Figure 1-1. In addition, it provides the mechanisms for separating the planetary vehicles from the launch vehicle.

The reliability model and assessment calculation for the structural subsystem are shown below. Including the allocated assessment of 0.97 for damaging meteoroid penetration, the probability of mission success for the entire subsystem becomes 0.964. Details of these calculations and the complete list of assumptions are found in Appendix E of Volume 2.

The weight breakdown for the structural subsystem is given in Table 2-1.

Structure Subsystem Reliability Model

$$\text{Reliability} = R_{ss} \times R_A \times R_{SM} \times (R_M)$$

$$= (0.99753)(0.99714)(0.999603)(0.97) = 0.964$$

where

R_{ss} is the spacecraft structure reliability

R_A is the adapter structure reliability

R_{SM} is the adapter separation mechanism reliability

R_M is the probability of no mission failure due to meteoroid penetration

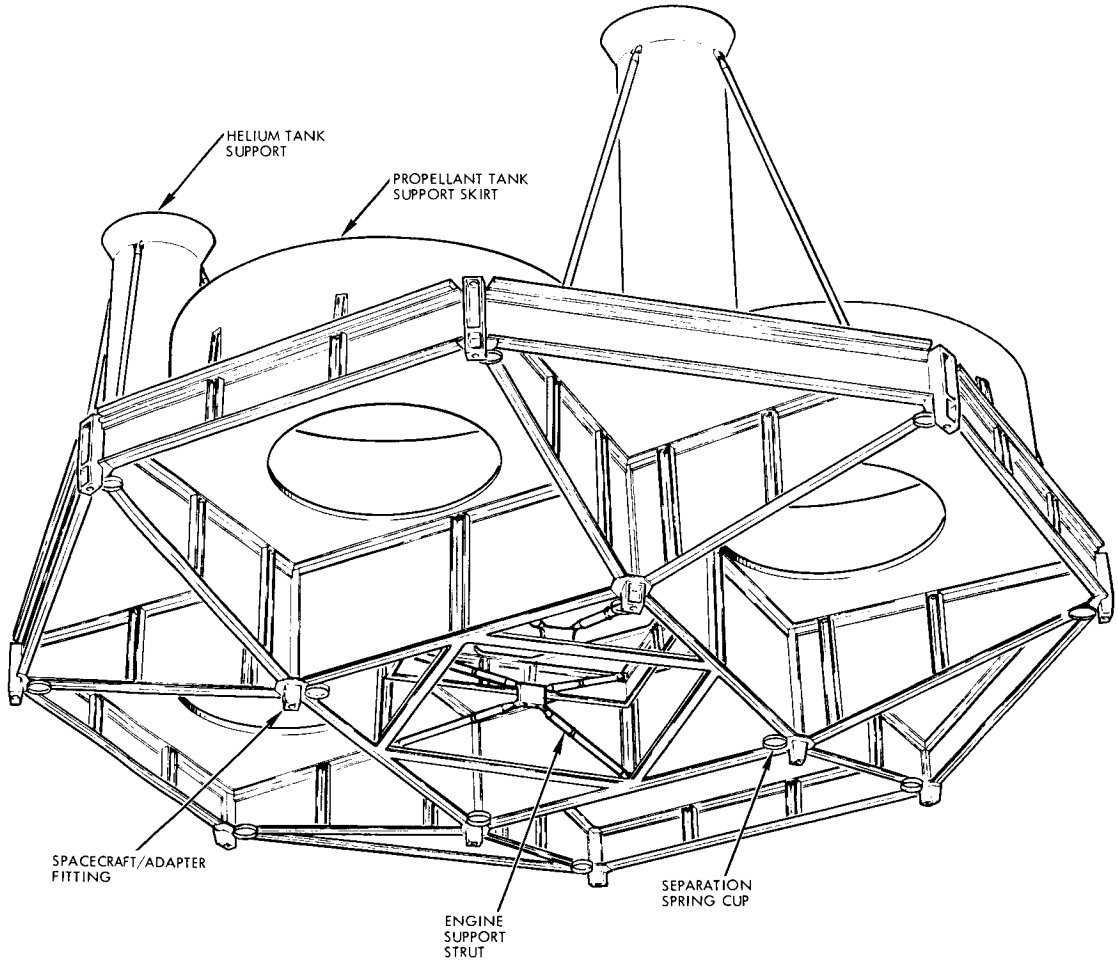

Figure 2-2

PROPULSION MODULE STRUCTURE is based on four aluminum beams, joined in a cruciform grid, which provides support for the propellant tank loads during launch and boost and transmits them to the planetary vehicle adapter by the most direct path. The structure is also designed so that all propellant lines and valves are located for maximum accessibility.

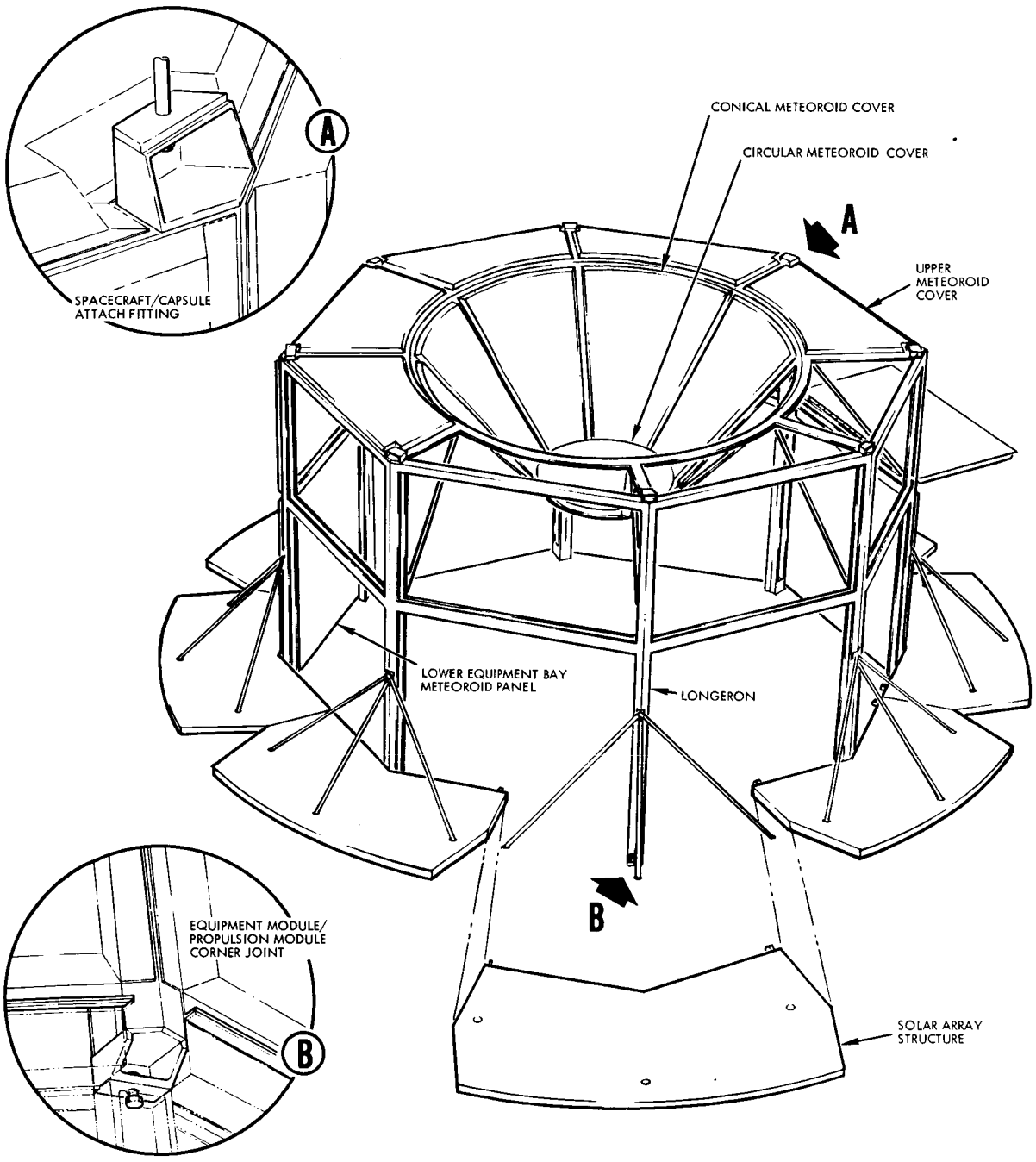

Figure 2-3

EQUIPMENT MODULE STRUCTURE provides support for capsule at upper ends of main longerons, which also provide rigid attachment points for externally mounted appendages, meteroid protection panels, and equipment mounting panels.

Table 2-1. Structure Subsystem Weight Breakdown (Recommended Configuration)

Item		Weight, (lb)
Equipment Module		1008.5
Equipment Panels	(6)	180.0
Meteoroid Protection Panels	(19)	510.0
Longerons	(8)	75.6
Rings	(5)	77.0
Radial Members	(4)	21.0
Medium Gain Antenna Supports and Release Mechanism		12.5
Low Gain Antenna Release Mechanism		2.0
High Gain Antenna Supports and Release Mechanism		22.4
PSP Supports and Release Mechanism		38.5
Solar Array Supports		35.0
Nitrogen Bottle Supports		11.0
Attachments and Miscellaneous		23.5
Propulsion Module		483.7
Main Cruciform Beams	(4)	72.0
End Beams	(8)	48.0
Center Beams	(4)	20.0
Tank Platform	(1)	136.4
Meteoroid Protection Panels	(4)	52.6
Separation System		28.6
Propellant Tank Supports		44.0
Pressurant Tank Supports		36.0
Engine Supports		31.8
Attachments and Miscellaneous		14.3
Total Structure Subsystem		1492.2

2.2 REQUIREMENTS AND CONSTRAINTS

2.2.1 Mission Constraints

The design and operation of the structural subsystem are dictated in part by several mission considerations: prelaunch operations, mission environments, and planetary quarantine.

2.2.1.1 Prelaunch Operations

Final assembly, checkout, and other prescribed activities are performed at KSC to ready the space vehicle for launch. Spacecraft prelaunch assembly and checkout are conducted at a spacecraft assembly facility. Explosive-safe facilities are used for propellant and gas loading, final spacecraft alignment and installation of the spacecraft ordnance elements. The spacecraft is also capable of on-pad propellant loading. Conformance to the range safety requirements, as delineated in AFETR 127-1 and M127-1, is essential for all pyrotechnic devices.

2.2.1.2 Launch Environment

The launch environment for the spacecraft includes:

a) Random and acoustic vibrations generated during Saturn V liftoff and flight through the transonic and maximum dynamic pressure (max. q) regions of the boost trajectory; (see Reference 1)

b) Shock loads generated during Saturn V staging; nose fairing, shroud section, and planetary vehicle separation; and appendage release events

c) Static and dynamic inertia loads during Saturn V liftoff, boost and cutoff.

2.2.1.3 Space Environment

The spacecraft structure is designed to withstand the space environments encountered during the 220-day (approximate) transit to Mars and the 2-month Martian orbit. These environments include the random vibrations generated during LM descent engine operations, response to LM descent engine startup and shutdown transients, shock loads induced during the capsule separation, and the meteoroid fluxes near earth, in interplanetary space, and near Mars.

The meteoroids that will be encountered by the Voyager spacecraft present a particularly hazardous environment from which pressurized units and sensitive electronic equipment must be protected. The particle flux, density and velocity data given in Reference 2 are used in conjunction with rational analysis to determine the amount of meteoroid protection required to meet the selected 0.97 probability of no destructive penetration (see Section 2.5). The requirement that the flight spacecraft must perform its intended mission with the capsule removed establishes the exposed area.

2.2.1.4 Planetary Quarantine

The overall probability that Mars will be contaminated prior to the calendar year 1985 by a single spacecraft shall be less than 3×10^{-5}. In addition, for a period of 13 years subsequent to launch, the integrity of all structural assemblies must be maintained and all mechanical devices used to initiate appendage separation must be contained to preclude Mars impact by any debris.

2.2.2 Design Requirements

2.2.2.1 Configuration

The following configuration requirements are satisfied by the design of the structural subsystem.

a) The spacecraft structure is sized to accommodate a capsule weight of up to 8000 pounds, on-board scientific equipment weight of up to 600 pounds and up to 16,000 pounds of propellants. This sizing is discussed in Volume 6.

b) Direct load paths are used to minimize the lengths of members and the amount of structure subject to bending.

c) Structural elements are designed for multiple functions wherever possible; for example, structural panels are used for equipment mounting, meteoroid protection and thermal environment control.

d) Structural member shapes and their materials are selected to maximize strength to weight ratios.

e) Spacecraft surface area and the number and size of mechanical joints are minimized to reduce weight, consistent with the growth potential features included in the design.

f) Where multiple panels or members are used, such as equipment mounting panels, solar array sections, meteoroid protection panels, and basic structural elements, the design of each is identical to simplify fabrication and replacement.

g) Spacecraft components and subsystem equipment are located close to the main structural elements to reduce secondary structure weight.

h) Appendages are stowed during launch to minimize loads on the appendages and their mechanisms.

i) The equipment and propulsion modules have independent structures.

j) For slosh stability, the vehicle c.g., is always forward of the geometric center of the tanks

k) For vehicle control, the spacecraft c.g.—engine gimbal arm is at least 32.5 inches.

l) The spacecraft shades the capsule during sun-stabilized flight.

m) Redundant pyrotechnic devices are employed to initiate separation of the planetary vehicle and to release all appendages. Separation and release are accomplished if either or both of the redundant devices are actuated by the electrical signal supplied.

n) Capsule separation is assumed to be the responsibility of the capsule contractor, although the initiation signal is supplied by the spacecraft.

o) Basic meteoroid protection for pressurized units and electronic equipment is provided by foam-filled sandwich structure where not constrained by other requirements.

p) State-of-the-art concepts, materials, and techniques are used in the spacecraft design. Advantage is taken of Ranger, Mariner and other NASA program experience where feasible. Standard and qualified parts and assemblies are used as applicable.

2.2.2.2 Structural Requirements

The spacecraft structure is designed to withstand simultaneously the application of design limit loads and other accompanying environmental phenomena without experiencing excessive elastic or plastic deformation where such deformation would reduce the probability of successful completion of the mission. The design limit loads are the maximum loads that may reasonably be expected to occur in service for the design conditions specified.

The spacecraft structure is designed to withstand simultaneously the application of design ultimate loads and accompanying environments without failure. Design ultimate loads are the product of the design limit loads and a factor of safety, which is 1.25 for spacecraft general structure. The ability of the design to sustain these loads will be substantiated by analysis and test.

The spacecraft structure has sufficient fatigue strength to sustain the cyclic loads imposed during ground handling, acceptance vibration tests, transportation, launch, boost, separation, orbit correction and retro-propulsion maneuvers. The planetary quarantine requirement of a 13 year subsystem life requires detailed evaluation of long-term creep and fatigue strengths and the possibility of spalling or explosion due to meteoroid impact. Of special concern are the propellant tanks. (See Section 4 of this volume.)

The design limit inertia loads imposed on the structural subsystem, derived by the logical combination of steady-state and low frequency accelerations, are presented in Table 2-2. These loads account for all launch and in-flight quasi-static and transient phenomena occuring during Sature V and LM descent engine operation. All launch inertia loads are transmitted through the spacecraft and reacted at the adapter interface. In-flight inertias are reacted by engine thrust. In addition to the above loads, secondary structure (including bracketry and component support structure) is also designed to withstand the vibration environments shown in Figures 2-4 and 2-5.

Table 2-2. Limit Structural Load Factors (g)*

	X	Y	Z	Rotation
Launch/Boost	5.0	±1.0	---	To Be Determined
	5.0	---	±1.0	
	-2.0	±1.0	---	
	-2.0	---	±1.0	
Spaceflight	1.3	±0.32	---	
Appendages and	1.3	---	±0.32	
Deployment Mechanisms	-1.0	±0.14	---	
	-1.0	---	±0.14	
Primary and Secondary	2.0	±0.30	---	
Structure	2.0	---	±0.30	
	-0.50	±0.070	---	
	-0.50	---	±0.070	

*These load factors are used to establish the strength requirements for the structural subsystem and planetary vehicle adapter.

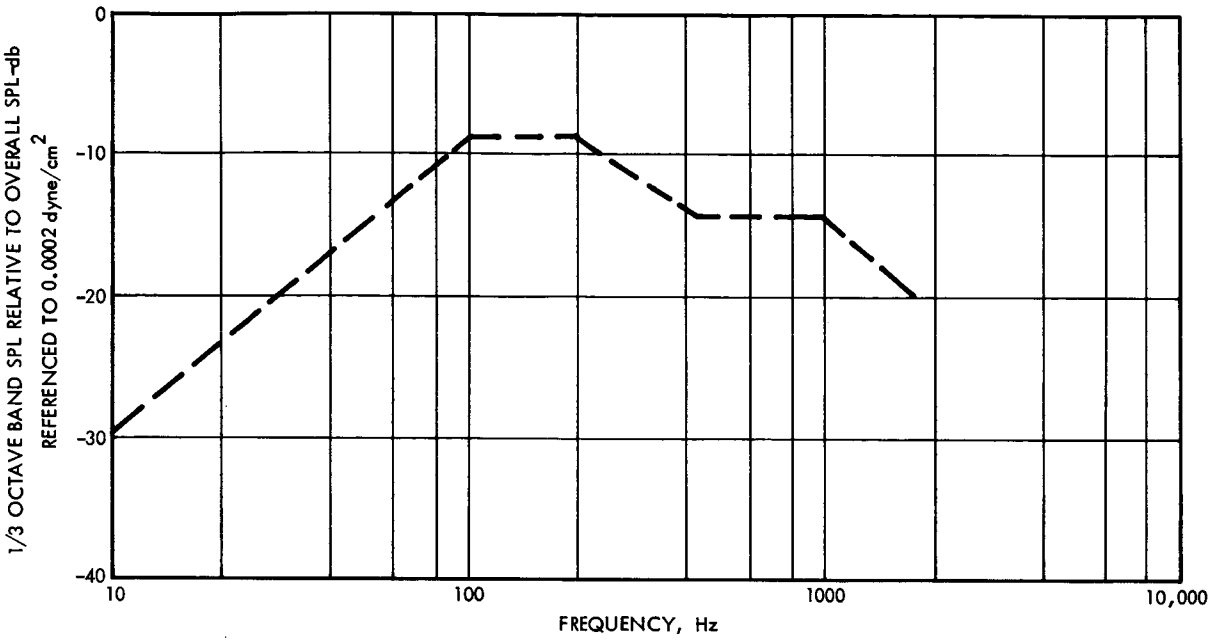

Figure 2-4

OVERALL ACOUSTIC LEVELS are critical during lift-off and boost. This curve shows criteria used to design structure to withstand acoustic environment throughout these phases of the mission.

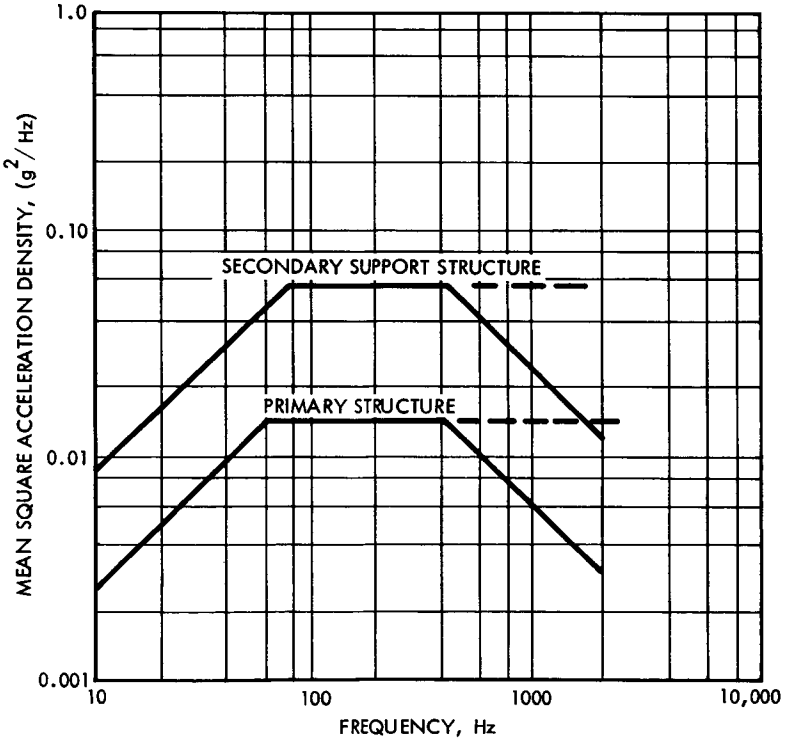

Figure 2-5

RANDOM VIBRATION ENVIRONMENT is delineated by this curve, which was used to design spacecraft structure to withstand all randomly induced vibrations.

Stiffness characteristics of major assemblies are selected to avoid deleterious coupling with launch vehicle resonant frequencies and to minimize the dynamic response of the flight capsule and appendages. In addition, the structure must not deflect so that it will violate the dynamic envelope shown in Figure 2-6.

All ground handling of the spacecraft, including transportation, hoisting and stacking shall not subject the fully loaded spacecraft structure to loads greater than plus or minus 1-1/2 g vertically and 1 g laterally. However, higher g-levels may be imposed on an unloaded spacecraft during shipping if properly designed supports are provided.

2.2.2.3 Material, Parts and Processes Requirements

All parts and materials will be selected on the basis of suitability for the intended application with emphasis on reliable performance during all phases of the mission. In addition, all parts, materials, and processes will be selected on the basis of capability to perform in accordance with requirements during the complete test and operational lifetime as established by test program evaluations and applicable specifications.

To achieve the quarantine goal, it is necessary for all structural materials and coatings to be stable in the space environment and compatible with the prelaunch decontamination procedures. For composite structures, such as plastic laminates and sandwich panels, treatment with heat or ethyline oxide (ETO) during fabrication is required so that any ejecta resulting from meteoroid impact and penetration will be sterile.

All materials will be nonmagnetic, except that a deviation will be allowed for the use of a magnetic material in a specific application when such use can be shown to enhance the probability of mission success through increased reliability or reduced technical and schedule risk.

All materials used in the spacecraft will be selected from a list of materials compiled by TRW and approved by NASA. All manufacturing processes used in spacecraft manufacture will be selected from a list of process documents compiled by TRW and approved by NASA.

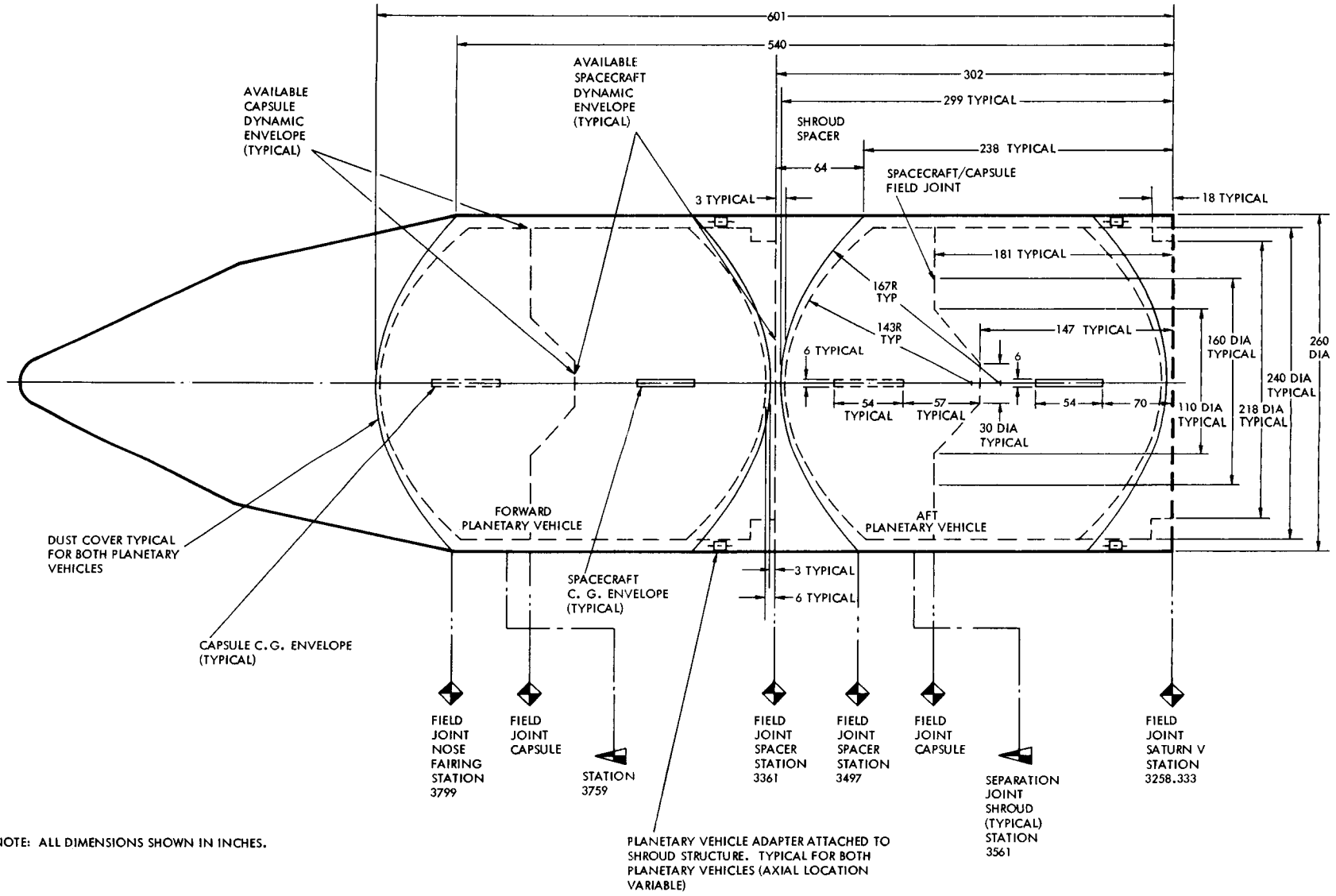

Figure 2-6

SPACECRAFT DYNAMIC ENVELOPE, as specified, determines capsule/spacecraft positions and joints. They are based on required geometry of 160-inch diameter capsule-spacecraft field joint and relative position of capsule forward of spacecraft.

2.2.2.4 Subsystem Electrical Ground References

A common electrical ground reference will be established for the subsystem. The following techniques will be used to provide the basic low-impedance reference.

a) Electrical bonding, when possible, will be accomplished by metal-to-metal contact over the entire area of surfaces which are held in mechanical contact.

b) The electrical bonding technique employed, where metal-to-metal contact is not used, will provide a bonding impedance not to exceed 2.5 milliohms DC and 80 milliohms at 20 mc across any bond.

c) The use of bonding straps will be minimized. When required, bonding straps will be of solid metal, having a length-to-width ratio not to exceed 3 to 1.

2.3 INTERFACES

This section identifies and defines the mechanical and physical interfaces and spatial relationships where applicable between the structural subsystem and the subsystems and items it must physically support. These include the

- Science subsystem
- Capsule
- Propulsion subsystem
- Planetary vehicle adapter
- Temperature control subsystem
- Electronic equipment
- Antenna assemblies
- Solar array
- Guidance and control subsystem
- Instrumentation

2.3.1 Science Subsystem

All of the science sensors of the recommended spacecraft are housed in the planetary scan platform (PSP). The PSP is mounted adjacent to spacecraft panel VI (Figure 2-7) on three tubular struts. During launch and separation, the PSP is stowed against the spacecraft to minimize support structure bending and keep it within the dynamic envelope of the launch

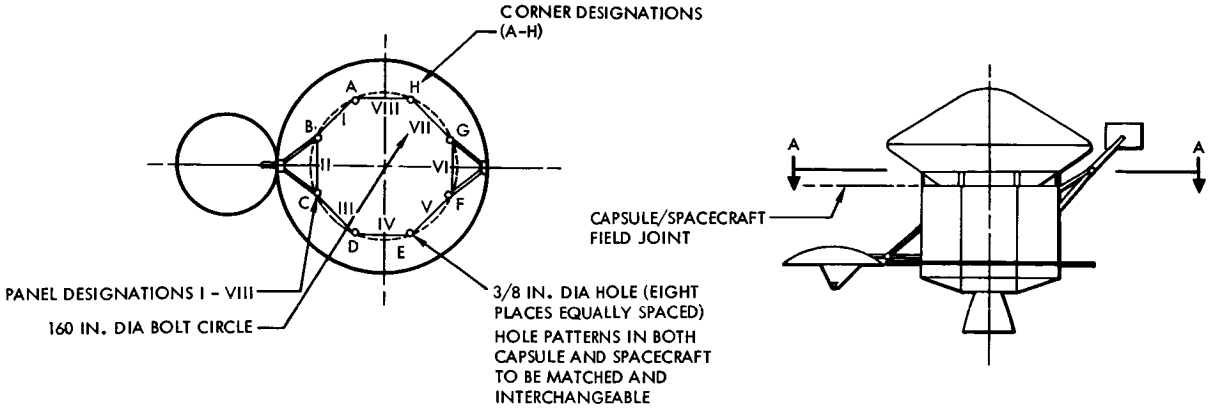

Figure 2-7

CAPSULE/SPACECRAFT MECHANICAL INTERFACE shows simple, bolted field joint which facilitates replacement of fully interchangeable capsules and spacecraft.

vehicle. The PSP is mounted so that after deployment it has an optimum view of the illuminated portion of Mars.

Areas for mounting additional science equipment are provided at equipment mounting panels III, V and VII, where they have suitable fields of view. Volume 5 contains more detailed information.

2.3.2 Capsule

Capsules weighing up to 8000 pounds can be supported by the spacecraft structure at an interchangeable field joint. The installation misalignment between a perpendicular to the plane of the capsule field joint and the spacecraft geometrical roll axis will not exceed 2 milliradians. The required diameter (per Reference 3) for the interface field joint and the capsule design envelope is illustrated in Figure 2-6.

2.3.3 Propulsion Subsystem

The propulsion subsystem consists of propellant tanks, pressurization system, engine assemblies and miscellaneous components that are supported by the propulsion module structure. (See Section 4 for propulsion subsystem details.) Propellant lines are to be secured to structure at frequent intervals to minimize their vibrational amplitudes and induced loads. Maximum accessibility to the propulsion subsystem components is required and clearance for 6 degrees of engine gimballing about the pitch and yaw axes is provided. The main engine support structure is capable of reacting the 9850 pounds descent engine thrust plus engine dynamic loads. See Figure 2-8.

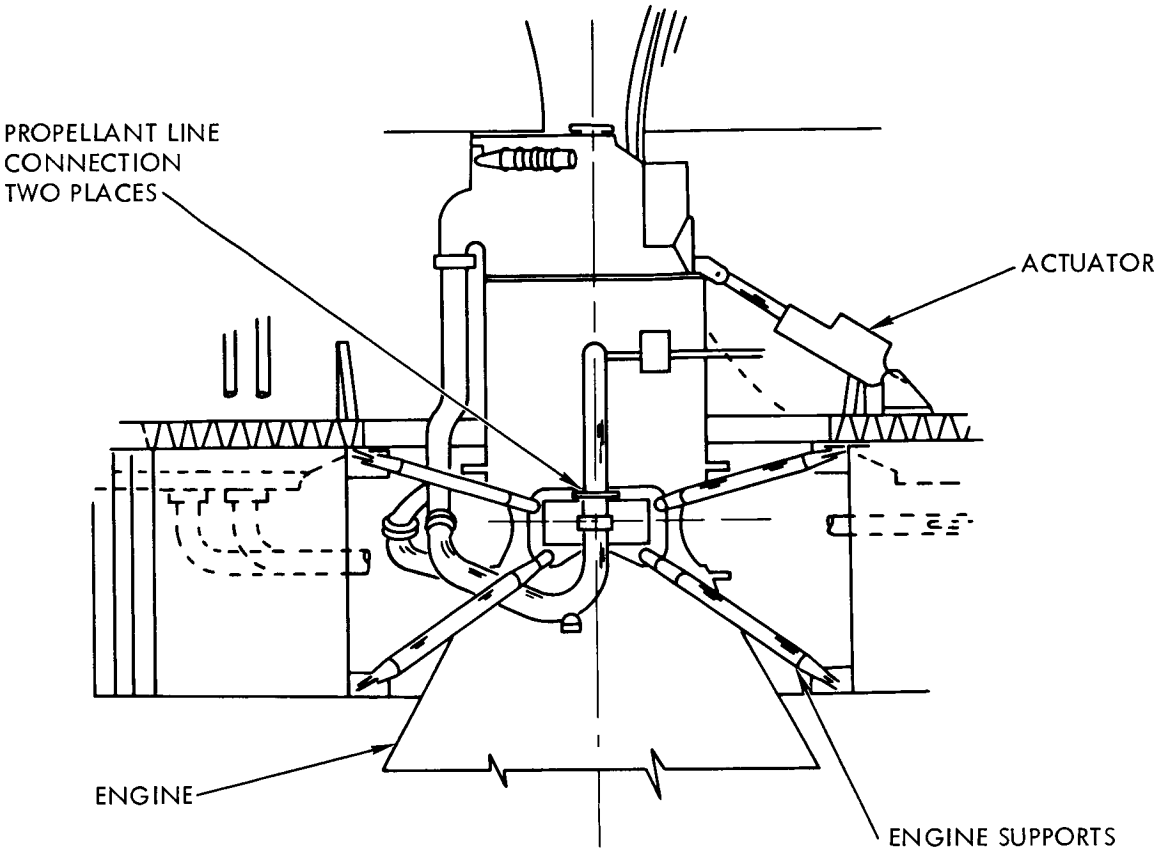

Figure 2-8

ENGINE INSTALLATION is simple. The engine is supported at its gimbal ring by a light, rigid framework which carries its loads to the main beams.

2.3.4 Planetary Vehicle Adapter

The structural subsystem transfers all planetary vehicle loads induced during the launch phase to the planetary vehicle adapter through attachments capable of in-flight separation. In addition, a field joint will be provided to facilitate removal and installation of the spacecraft. The installation misalignment between a perpendicular to the plane of the adapter field joint and the spacecraft geometrical roll axis will not exceed 2 milliradians. The adapter is described in detail in Section 3.

2.3.5 Temperature Control Subsystem

The equipment and propulsion module structures contain provisions for attaching thermal insulation on their external surfaces. In addition,

louver assemblies are installed at specified thermal radiating areas on the equipment mounting panels (see Figure 1-1). Mounting surfaces of the equipment panels will have a minimum flatness of 0.004 in/ft to enhance conductive heat transfer from the electronic equipment.

Mechanical joints between the main structure and the solar array structure, the appendages and the capsule are designed to impede heat transfer. Internal structural joints are designed to enhance conductive heat transfer. Structural surfaces will be treated to provide the thermal characteristics specified in Section 5.

2.3.6 Electronic Equipment

All electronic equipment is mounted internally on hinged removable panels located toward the forward end of the equipment module. The mounting panels rotate outboard and aft to allow access to the mounted equipment. Components of a complete subsystem will be located on a single panel to the maximum extent possible. Junction boxes on each panel, as shown in Figure 2-9, will allow the subsystem and its panel to be removed from the spacecraft for testing if required. Panel opening or removal can be accomplished even when the spacecraft is mounted in the shroud.

Harnesses will be supported at sufficient points to prevent excessive vibration or chafing. Cable loops in the system harness allow the panels to be opened without undue flexing of the harness. All components are mounted on the panels in such a manner as to insure intimate contact for efficient heat transfer.

2.3.7 Antennas

Mechanical supports capable of withstanding all induced loads and providing sufficient rigidity are provided for attaching the low, medium, and high gain S-band and UHF antennas to the spacecraft structure. All the S-band antennas are supported from the main longerons of the equipment module. (See Figure 1-1.) The UHF antenna is body-fixed to the equipment module structure at Panel I. Retention and release mechanisms are provided as required at the extremities of the antenna support booms or at stowed-position hard points on the spacecraft structure. Section 2.4.3 contains a detailed description of the antenna mounts.

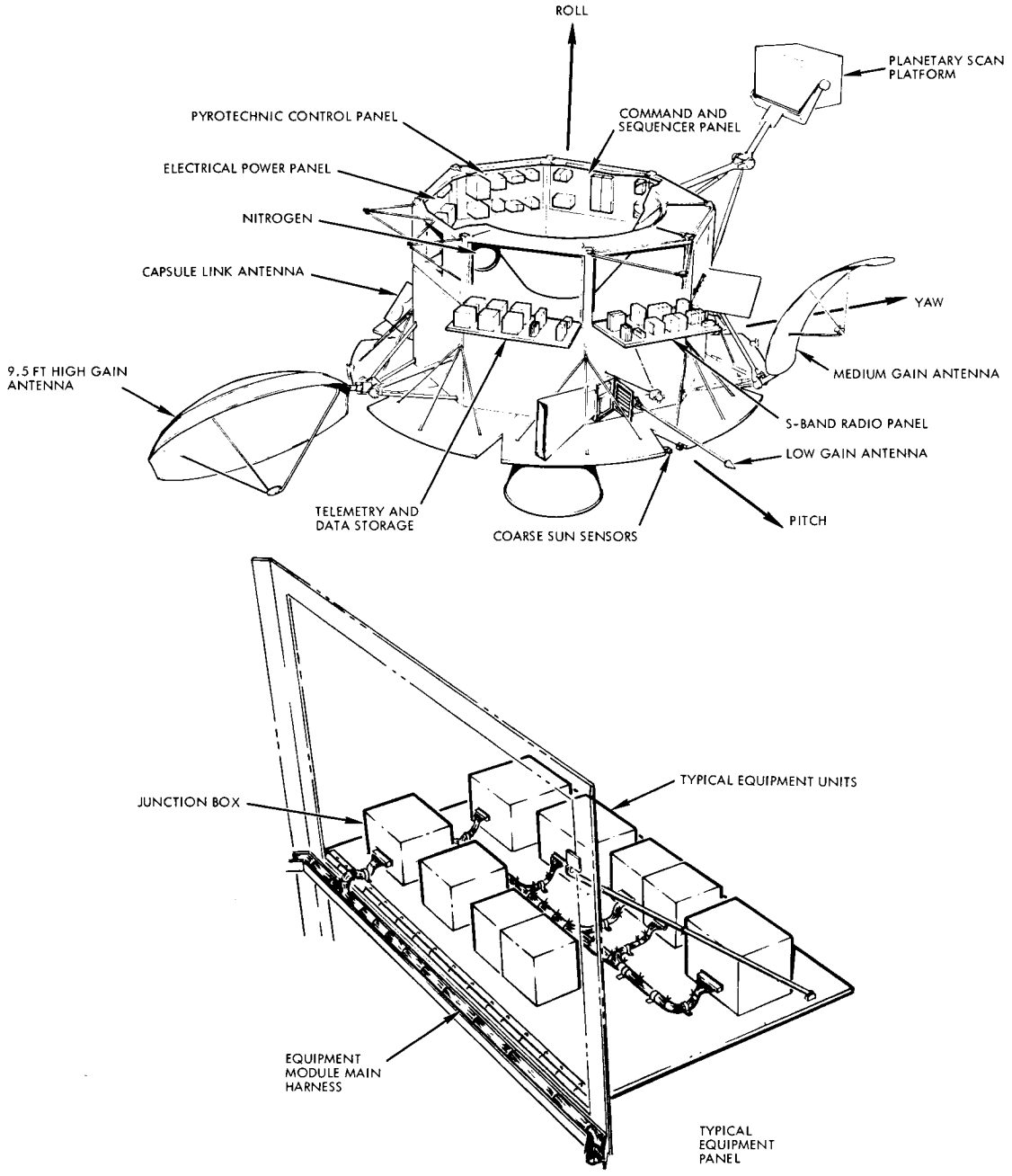

Figure 2-9

EQUIPMENT MOUNTING PANELS are designed for maximum accessibility during all spacecraft integration operations. They can be opened even after the spacecraft has been installed in its shroud compartment.

2.3.8 Solar Array

The solar array is split into two sections. The major portion of the array, consisting of eight identical, removeable panels, is fixed to the equipment module structure forming an annular area as shown in Figure 2-10. To facilitate installation and to maintain modularity for ground testing, the three solar array panels mounted on the aft facets of the propulsion module are attached to the aft end of the equipment module with removable hinged fittings. They are rotated into their installed positions after the equipment module is mated to the propulsion module (see Figure 2-11). All ties to the structure are through low-heat-transfer joints. Additional area is available on the aft surfaces of the propulsion module to accommodate growth of the solar array.

2.3.9 Guidance and Control Subsystem

Sensors are mounted to provide their required view angles and with the alignment accuracies required for optimum performance. The coarse sun sensors are mounted on the main solar array, and Canopus sensors are internally mounted on the equipment panels with glint shields. Limb and terminator crossing detectors are mounted on the equipment mounting panels along with the guidance and control electronics assembly. Twelve thrusters are supported from the equipment module and are positioned with maximum moment arms for pitch, yaw, and roll attitude control. The two nitrogen tanks which provide gas for the system are located within the equipment module. Gyro and accelerometer assemblies are rigidly attached to the equipment module on the same structure which supports the Canopus and fine sun sensors. Figure 2-12 shows the installation of the attitude control nozzles and attitude control subsystem sensors. Engine gimbal actuators are shown in Figure 2-8.

2.3.10 Instrumentation

Strain gages, accelerometers, temperature sensors, and other instrumentation provide in-flight housekeeping measurements. This instrumentation is located at critical points throughout the spacecraft. Measurements are sent through multiplexing units to the telemetry and data storage subsystem which is located on one of the hinged equipment panels.

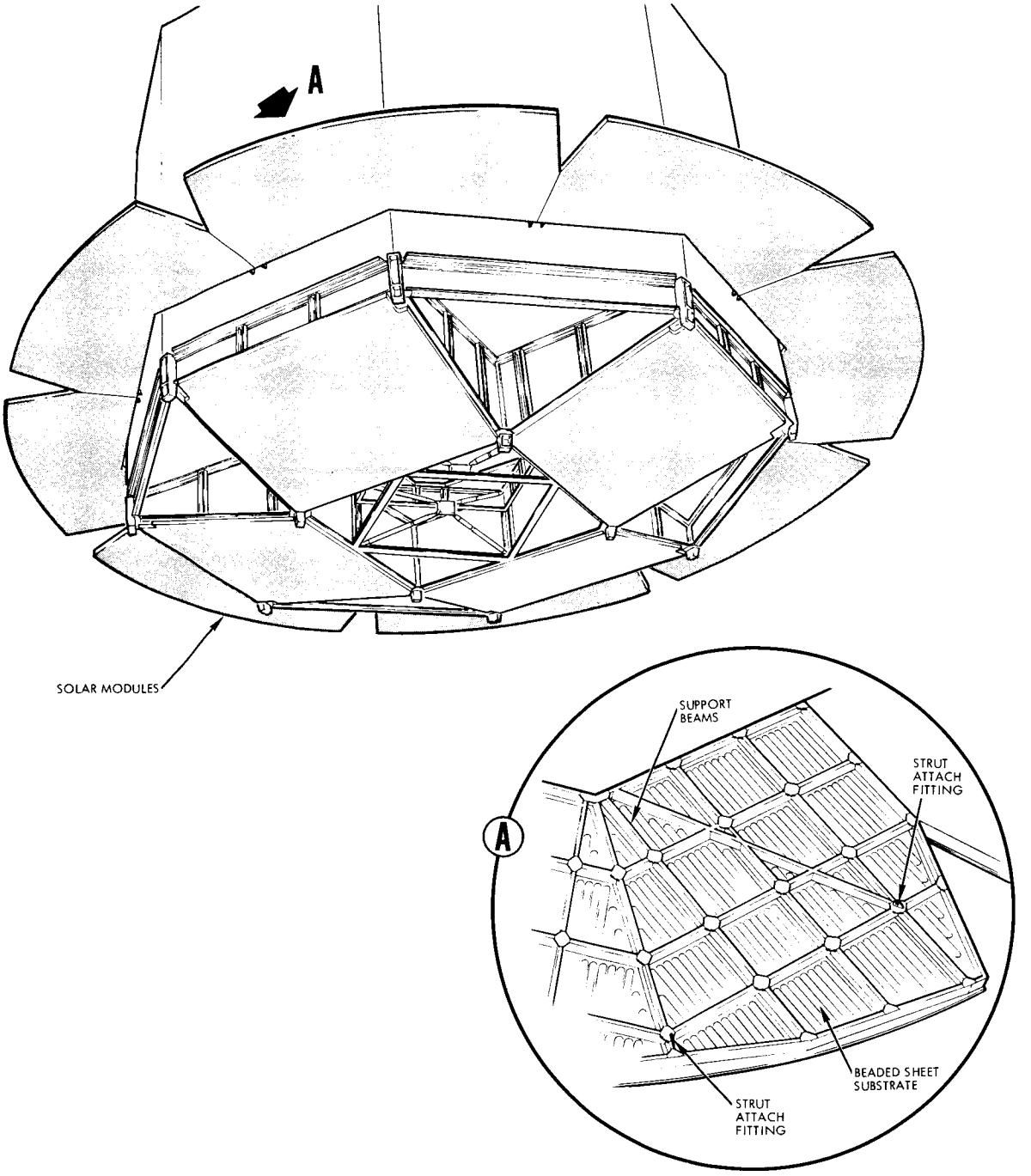

Figure 2-10
SOLAR ARRAYS consists of eight fully interchangeable panels attached to the equipment module (annular array) and three rectangular panels) attached to propulsion module (aft array).

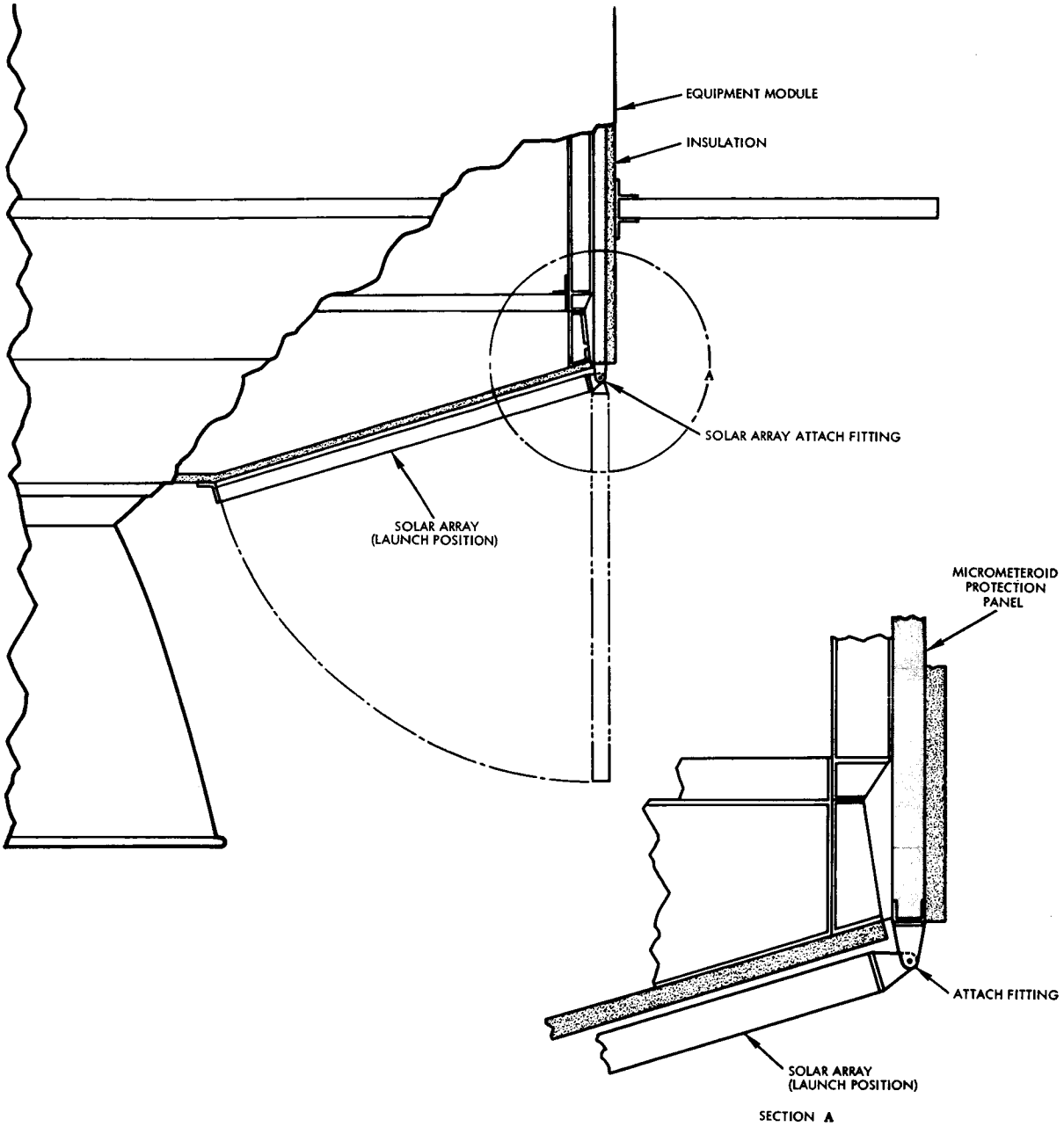

Figure 2-11

VOYAGER PRELIMINARY DESIGN-AFT SOLAR PANEL INSTALL LAYOUT.

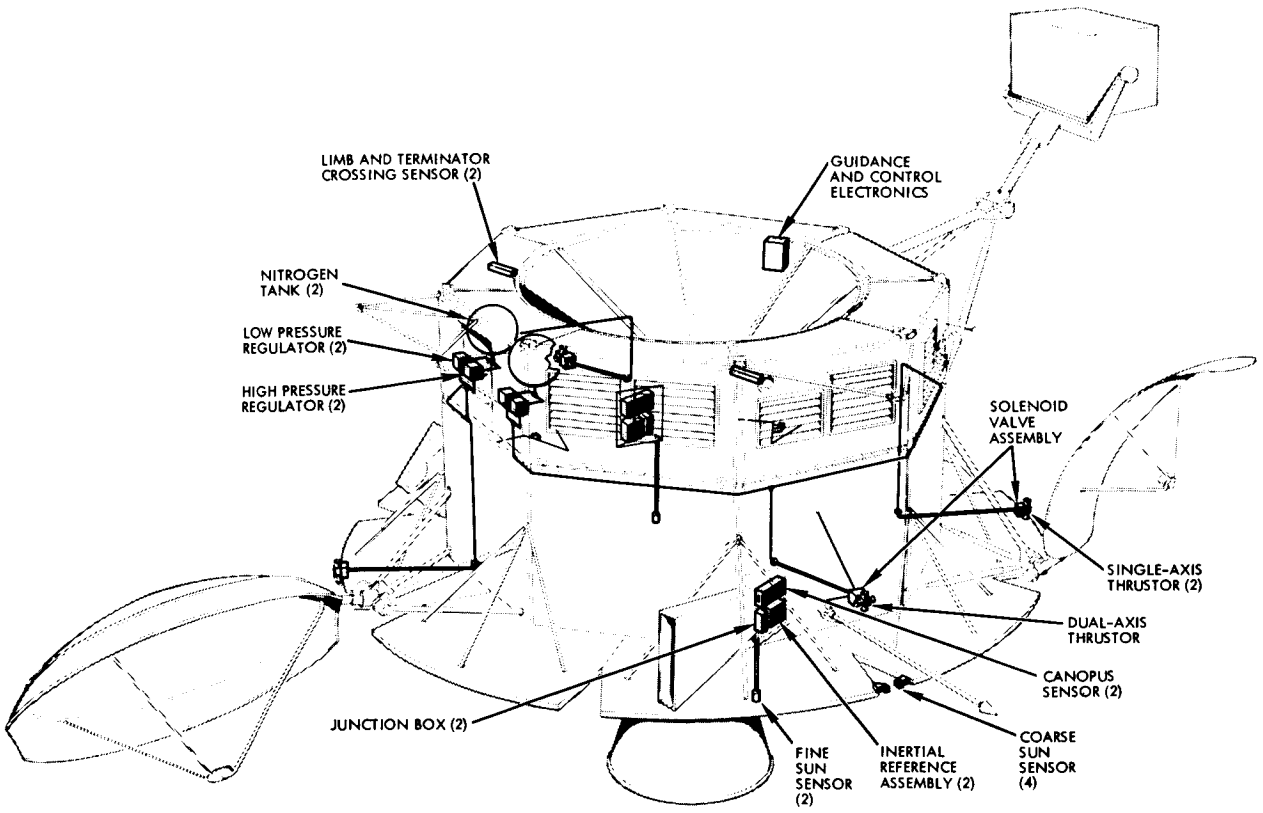

Figure 2-12

ATTITUDE CONTROL NOZZLES are mounted at maximum distance from center axis of spacecraft and supported by light, rigid, tubular tripod structure. Attitude sensors are installed at edge of annular solar array (sun sensors) and at corner of equipment module (Canopus sensor).

2.4 STRUCTURAL SUBSYSTEM DESCRIPTION

The recommended design meets the requirements and constraints of Section 2.2 and satisfies the interface requirements of Section 2.3. The structure is of aluminum alloy construction (primarily 7075-T6), lightweight, efficient and simple to manufacture and assemble.

A major advantage of the TRW design is its modularity, which has been achieved without any penalties to the structure. It simplifies all the test and checkout operations that have to be performed between manufacture and launch. The interface between the two easily integrated yet essentially independent modules is shown in Figure 2-3.

2.4.1 Equipment Module Structure

The equipment module structure supports the capsule at its forward end and accommodates all spacecraft subsystem equipment, the PSP, all spacecraft appendages, and the solar array.

The equipment module structure is octagonal in cross section, 157 inches across the flats and 100 inches high. The octagon shape has been selected, after examining many other configurations, because, it offered the most advantages. It provides nearly uniform support to the capsule at the specified 160-inch bolt circle while minimizing the number of attachments required. It also provides an efficient structural interface with the propulsion module, nearly minimum surface area, convenient hard points for mounting appendages, good structural rigidity, and flexibility for locating equipment panels without requiring major structural reinforcements.

Eight longerons carry axial loads directly from the capsule to the propulsion module interface as shown in Figure 2-3. Meteoroid protection panels shown in Figure 2-3 form the structural sides of the spacecraft and are attached to the eight longerons at the corners of the octagon to form a closed box. The major axial and bending load paths are through the longerons, with the meteoroid panels providing shear rigidity for the structure. Fittings on the longeron lower ends bolt to mating bathtub fittings on the propulsion module as shown in Figure 2-3. Similar fittings at the longeron upper ends form the attachment to the capsule (see Figure 2-3). At both the upper and lower ends of the structure, the longerons tie into octagonal frames. Intermediate frames reinforce the panel cutout areas. Additional meteoroid panels, attached to radial ribs and a central ring, close the upper end of the spacecraft below the capsule.

2.4.1.1 Equipment Mounting Panels

The forward sections of the meteoroid protection side panels contain cutouts for mounting the removable equipment panels that support the spacecraft and science electronics equipment. The panels are of honeycomb sandwich construction with 1 1/2 inch thick aluminum 1/4-0.001 core and 0.035 face sheets. In addition to providing structural support they provide meteoroid protection for the equipment and serve as radiators and louver supports for the thermal control subsystem. Each panel is hinged to a structural member at the aft end of the equipment bay and bolted to the door-land structure around its periphery. This design permits the panels to transfer spacecraft shear loads and avoids structural discon-

tinuities. The panels are designed to give a natural frequency high cnough to avoid dynamic coupling with other portions of the structure and the mounted equipment. Figure 2-9 shows several of the panels with their mounted equipment.

Additional panel area is available for growth over and above the requirements of the recommended spacecraft electronics subsystems.

2.4.1.2 Meteoroid Protection Panels

All exposed areas of the module (excluding the equipment mounting panels) are covered with meteoroid protection panels consisting of a 1-1/2 inch core of honeycomb filled with polyurethane foam sandwiched between an 0.010 inch aluminum alloy outer face sheet and an 0.030 inch aluminum alloy inner face sheet. (See Figure 2-13.) The 3/8-0.0007 honeycomb reinforces the panel and supports the lightweight foam core. Zee members around the periphery of each panel are used for attachment to the main structural members and for handling. (See Figure 2-3.) All panels are removable for maximum equipment accessibility. As stated above the removable equipment mounting panels have inherent meteoroid protection capabilities. (See Section 2.5 for details of the meteoroid penetration analysis.)

2.4.1.3 Solar Panel Substrates

The eight interchangeable solar panel substrates shown in Figure 2-9 are constructed of aluminum beaded sheet mounted on a grid-work of beams. Each of the substrate assemblies is supported along its inner edge by standoffs designed to minimize heat leakage and near its outer edge by three struts. Cutouts between the panels allow for growth in the deployable appendages.

The three rectangular solar panel substrates mounted to the aft surface of the propulsion module structure at spacecraft assembly are constructed of 3/4 inch thick aluminum honeycomb sandwich.

2.4.2 Propulsion Module Structure

The propulsion module structure supports the four main propellant tanks, the LM descent engine and other propulsion subsystem components as an independent structural assembly, consistent with the modularity concept.

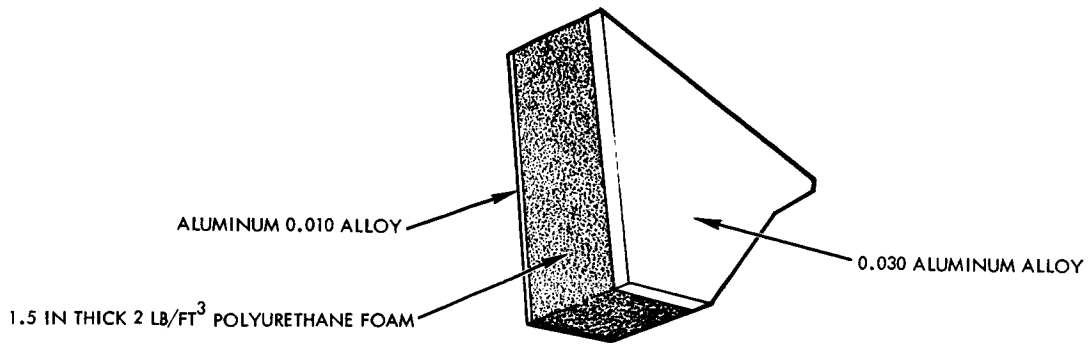

Figure 2-13

METOROID PROTECTION PANELS provide protection required to achieve the no-puncture probability required by the mission success goal and also provide shear rigidity as part of the primary structure

The principal structural elements are four built-up aluminum alloy beams arranged in a double cruciform geometry below the propellant tanks. The eight outboard ends of the beams terminate at fittings whose forward and aft faces respectively provide mechanical interfaces with the equipment module longerons and the eight outboard adapter separation points. (See Figure 2-2.) These fittings transmit the axial loads of the capsule and equipment module directly to the adapter without producing any bending in the propulsion module structure.

Four additional interface fittings are located at the four intersection points of the double cruciform beams. These transmit engine loads and a significant portion of the propellant tank inertia loads directly to the adapter beneath, rather than outboard to the spacecraft periphery. This feature of the design results in a signficant weight and space saving in the spacecraft, since the reduced bending moments permit the use of lighter gages and shallower beams.

Eight peripherally located beams interconnect with and stabilize the outboard ends of the double cruciform beams. Four diagional central beams stabilize the centers of the main beams. (See Figure 2-2.)

The forward beam caps form a plane which supports a two-inch thick aluminum honeycomb sandwich panel platform on which are mounted honeycomb, tank support cylinders. The platform transfers lateral loads

from the tank supports to the eight peripheral beams, which in turn distribute them to the adapter interface fittings. The supports tie directly to the propellant tank skirts at their upper ends and transmit the tank axial and bending loads to the tank support beams via bathtub fittings. This design, similar to that used on the Lunar Module Descent Stage, provides uniform support for the thin-walled pressure vessels. (See Figure 2-14.)

The helium tanks are supported from the tank support platform by thin-gage cylindrical skirts which are laterally stabilized by tubular struts as shown in Figure 2-14.

The engine gimbal ring is supported by two tubular truss assemblies attached to the stabilized mid-points of the cruciform beams. The engine head extends through a cutout in the tank support platform. The two engine gimbal actuators are mounted above the platform between tanks. (See Figure 2-8.)

The lower caps of the beam assembly form four rectangular and four triangular areas. Meteoroid protection is provided in the rectangular areas by fastening an 0.025 aluminum panel between the solar array and

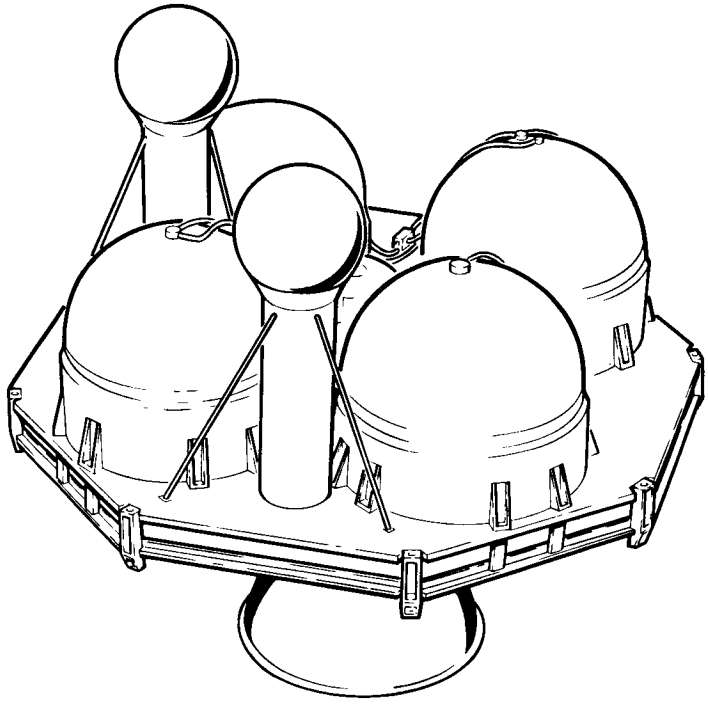

Figure 2-14

TANK SUPPORT SKIRTS provide uniform load distribution from propellant tanks to the propulsion module platform and beam structure. Tension loads are reacted by ten fittings, bolted directly to the grid beams.

the propellant tanks and lines. In the triangular areas, protection is provided by 0.007 aluminum panels fastened to the lower caps backed up by the honeycomb platform.

2.4.3 Release Mechanisms

Release mechanisms are used to release and separate each spacecraft from the launch vehicle, and release the following appendages from the spacecraft:

- High gain antenna
- Medium gain antenna
- Two low gain antennas
- Planetary scan platform

2.4.3.1 Spacecraft Release

In its launch configuration the spacecraft is supported at twelve points by the planetary vehicle adapter, which is in turn attached to the shroud. A bolted joint at each of the attachment points is released by the firing of either of two self-contained, redundant, explosive bolts. Severing either of the bolts releases a split collar around the interfacing attachment bolt, thus initiating release. Details of this mechanism are shown in Figure 2-15. Preloaded compression springs near each attachment point then impart a separation impulse to the spacecraft. See Volume 10 for a more detailed discussion of spacecraft release and separation.

2.4.3.2 Appendage Release

Each of the appendages is designed to be stowed in a position on the spacecraft which will minimize the forces and moments that must be withstood by their supporting structure and attitude-pointing mechanisms during the relatively severe launch environment. Once the planetary vehicle is separated from the launch vehicle, each appendage is released from its stowed position.

The high gain antenna is stowed against two support pads mounted at the apices of three-legged trusses (Figure 2-16). The three legs of the antenna feed are preloaded by a release bolt preventing excessive motion during launch. The oval-shaped medium gain reflector is stowed in a cradle and is also preloaded by its release device as shown in Figure 2-17. The two low gain antennas are simple tubes, preloaded against the spacecraft by the release device as shown in Figure 2-18.

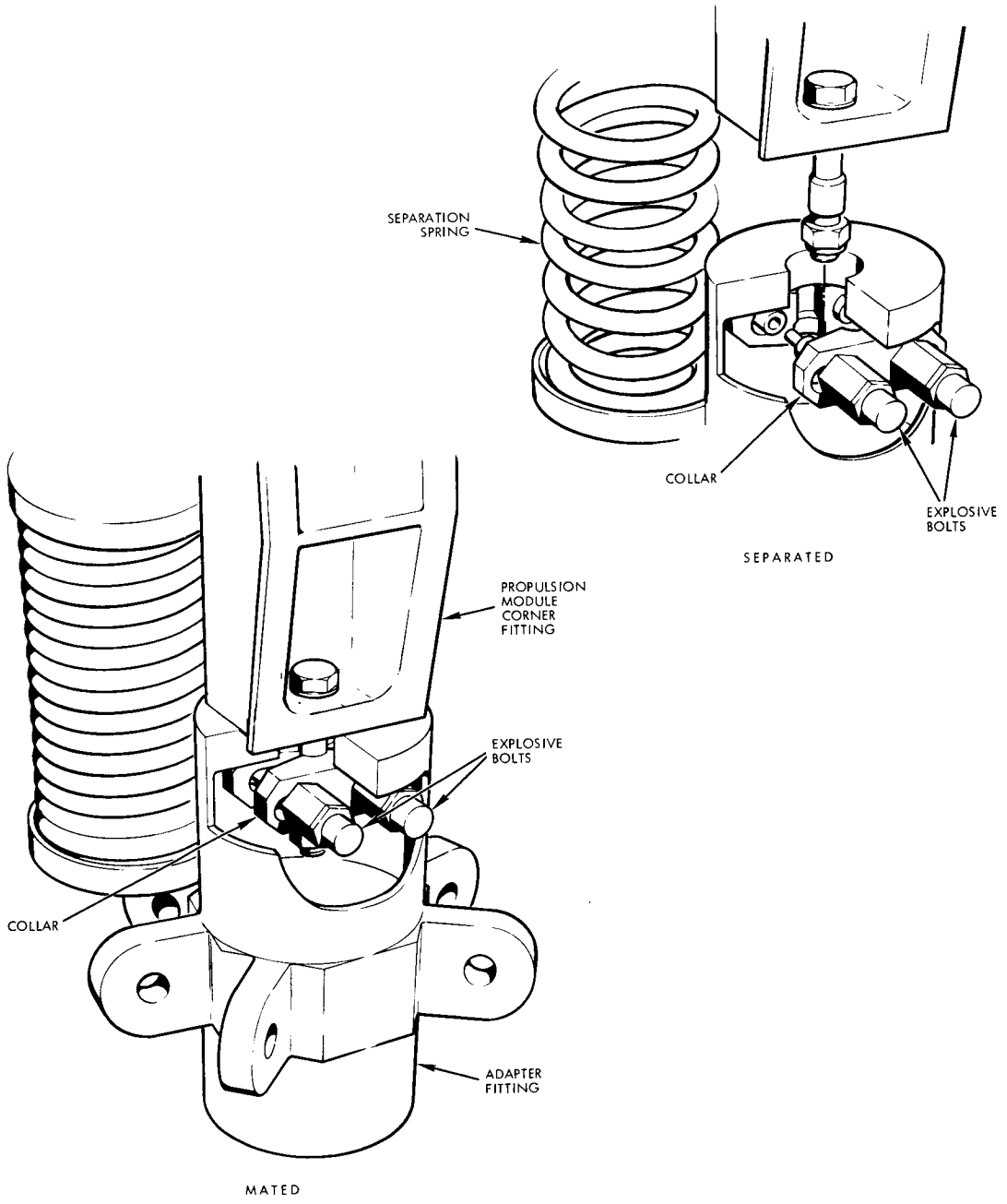

Figure 2-15
SPACECRAFT RELEASE is accomplished by space-qualified, OGO-type, electro-explosive devices installed at twelve release points on planetary vehicle adapter. Springs impart separation velocity after release.

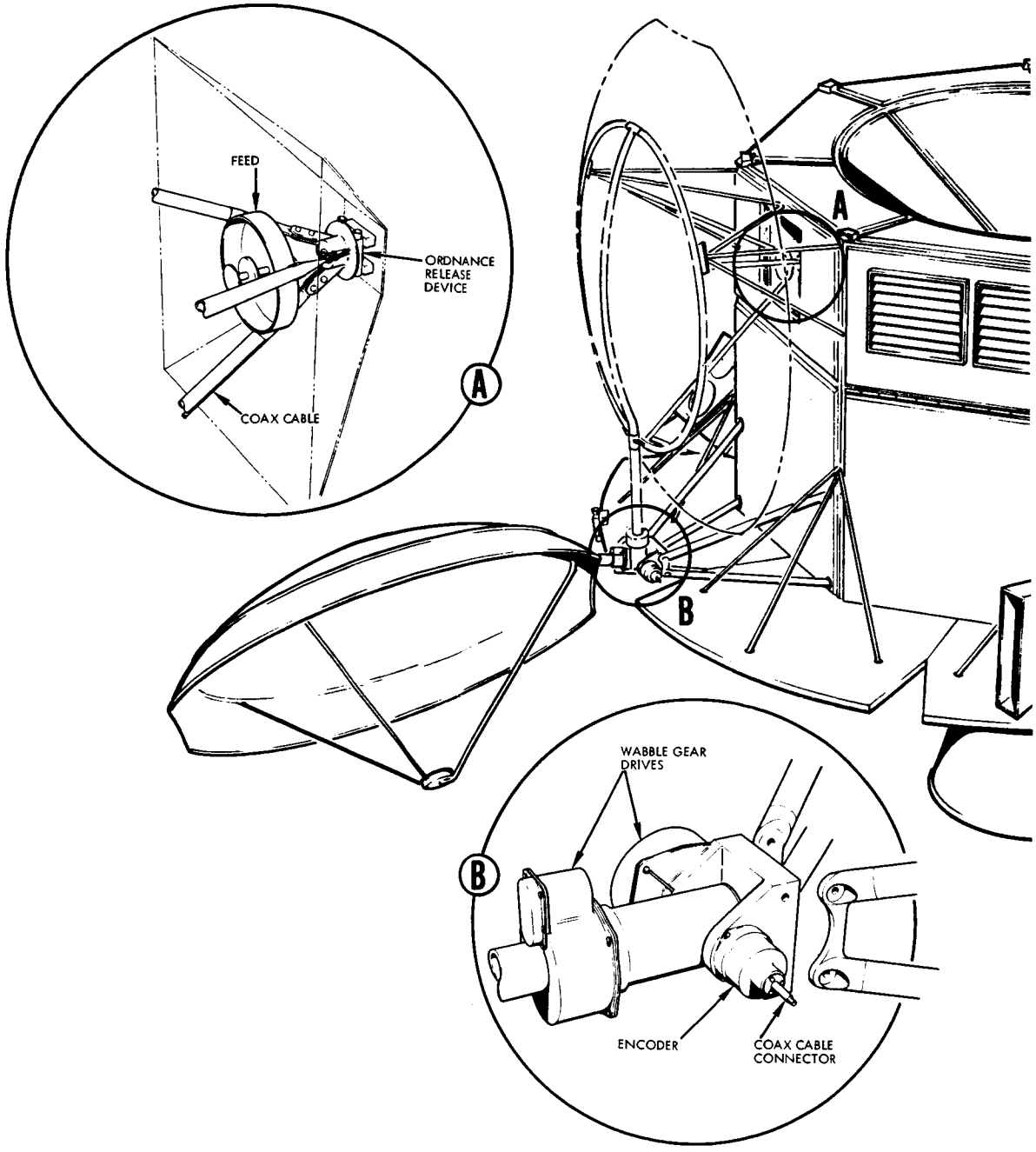

Figure 2-16

HIGH-GAIN ANTENNA is gimbaled about two axes. Electric drive permits attainment of desired lock angles. Non-intersecting axes provide offset to minimize possible shading of solar array. Antenna is pre-loaded against tripods and released by 000-type electro-explosive devices.

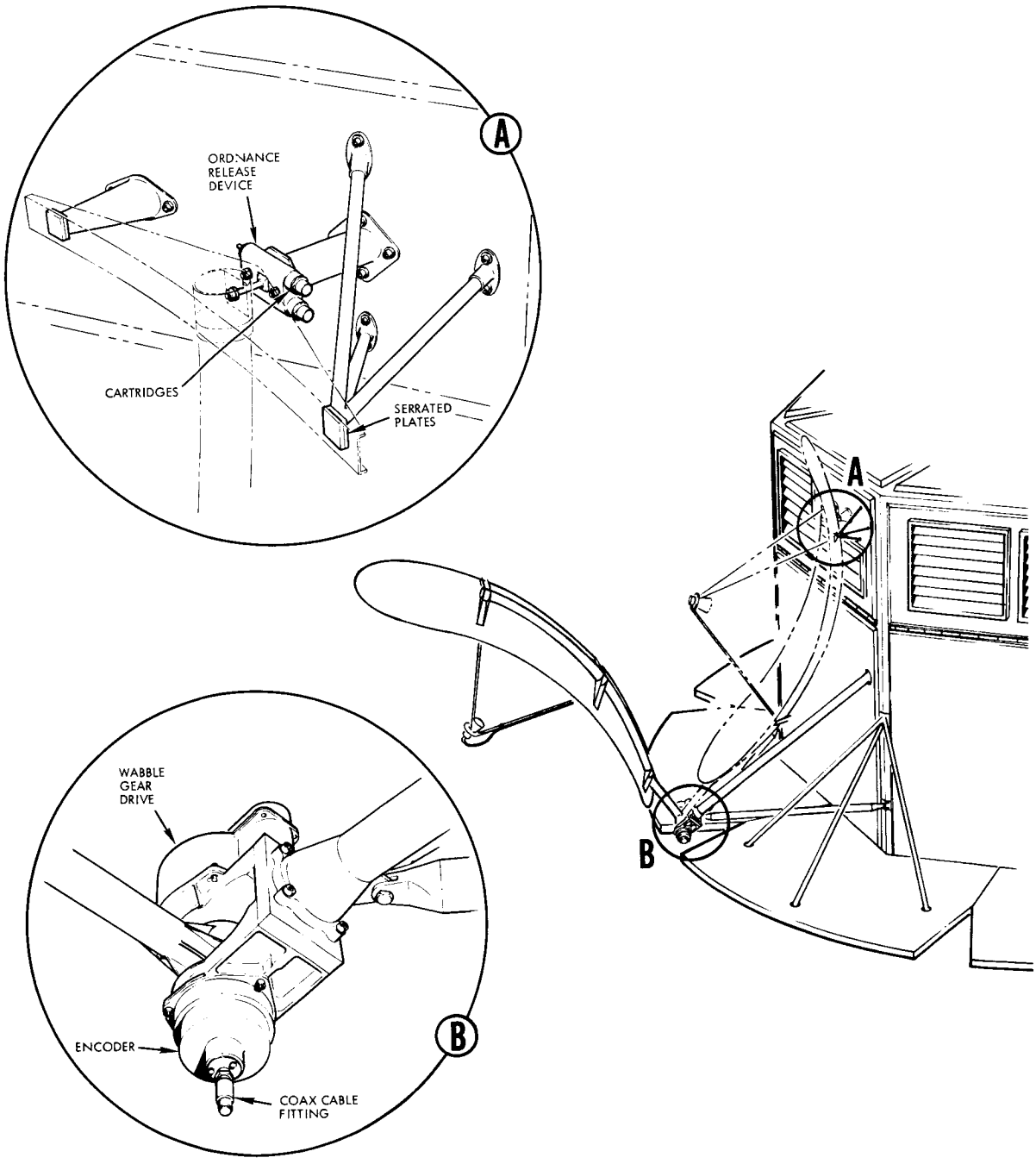

Figure 2-17
MEDIUM GAIN ANTENNA is deployed to operating position by single-axis gimbal drive after explosive release.

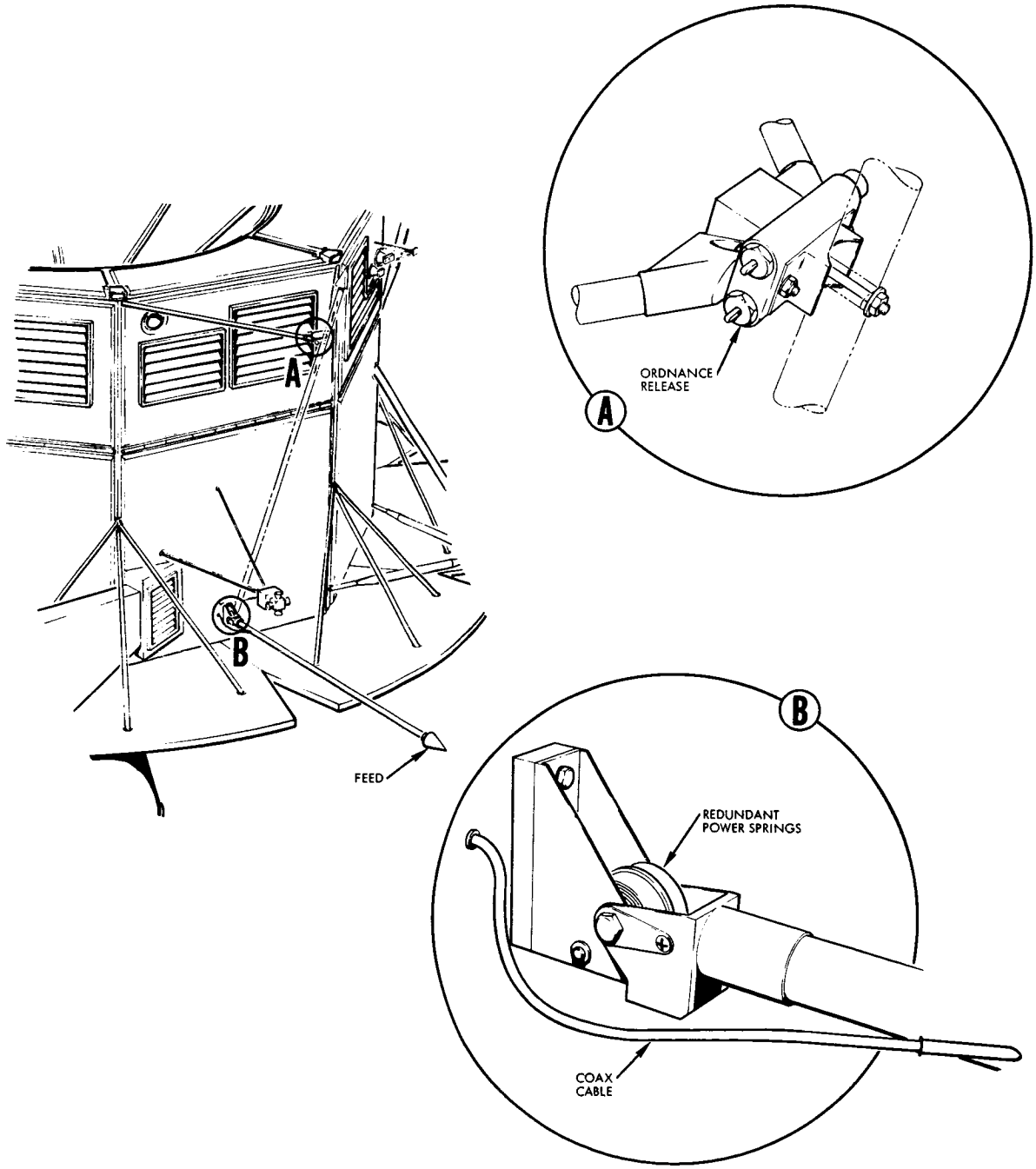

Figure 2-18

LOW-GAIN ANTENNA RELEASE mechanism permits antenna to rotate to final position under impulse provided by torsion springs working against vibration dampers. Details show electro-explosive release device and drive mechanism.

Release of each antenna is effected by a redundant electro-explosive device. This device, shown in Figure 2-19, consists of two squib-actuated pistons. Actuation of either or both releases a yoke assembly which in turn releases the appendage. To avoid spacecraft contamination, the pistons are incorporated in a single housing which contains the squib gases and debris after firing. The design is similar to that used successfully on the OGO program. After release, each appendage is deployed and pointed by a drive system which is part of the appendage itself; these drive systems are described in Volume 4.

The planetary scan platform is stowed against the spacecraft on four compression pads and preloaded by two release devices. It is released by these redundant devices, described above, and is similarly deployed and pointed. (See Figure 2-20.)

2.4.3.3 Boom-Mounted Experiments

The science payload for the recommended spacecraft does not include any deployable, remotely located experiment packages. However, growth of the science payload may require several remotely positioned experiments. Possibilities include a magnetometer weighing approximately 2 pounds, deployed to about 20 feet from the planetary vehicle, and a neutron-albedo sensor weighing approximately 7 pounds requiring a 10 foot displacement from the vehicle.

The recommended type of deployable element is a multi-section hinged boom. It consists of two lengths of aluminum tubing hinged to each other using deployment springs and a latching device at each joint to lock the boom in its extended configuration. (See Figure 2-21.) This design is similar to one used on OGO, and can locate these experiments to within 1 degree with respect to the spacecraft.

2.4.4 Structural Performance Summary

Using the design criteria and safety factors of Section 2.2.2.2, the internal load distribution for the recommended configuration was determined for various flight conditions based on a 16,000 pound propellant load and an 8000 pound capsule. Major structural members were analyzed using the critical loads to verify positive margins of safety and to provide data for

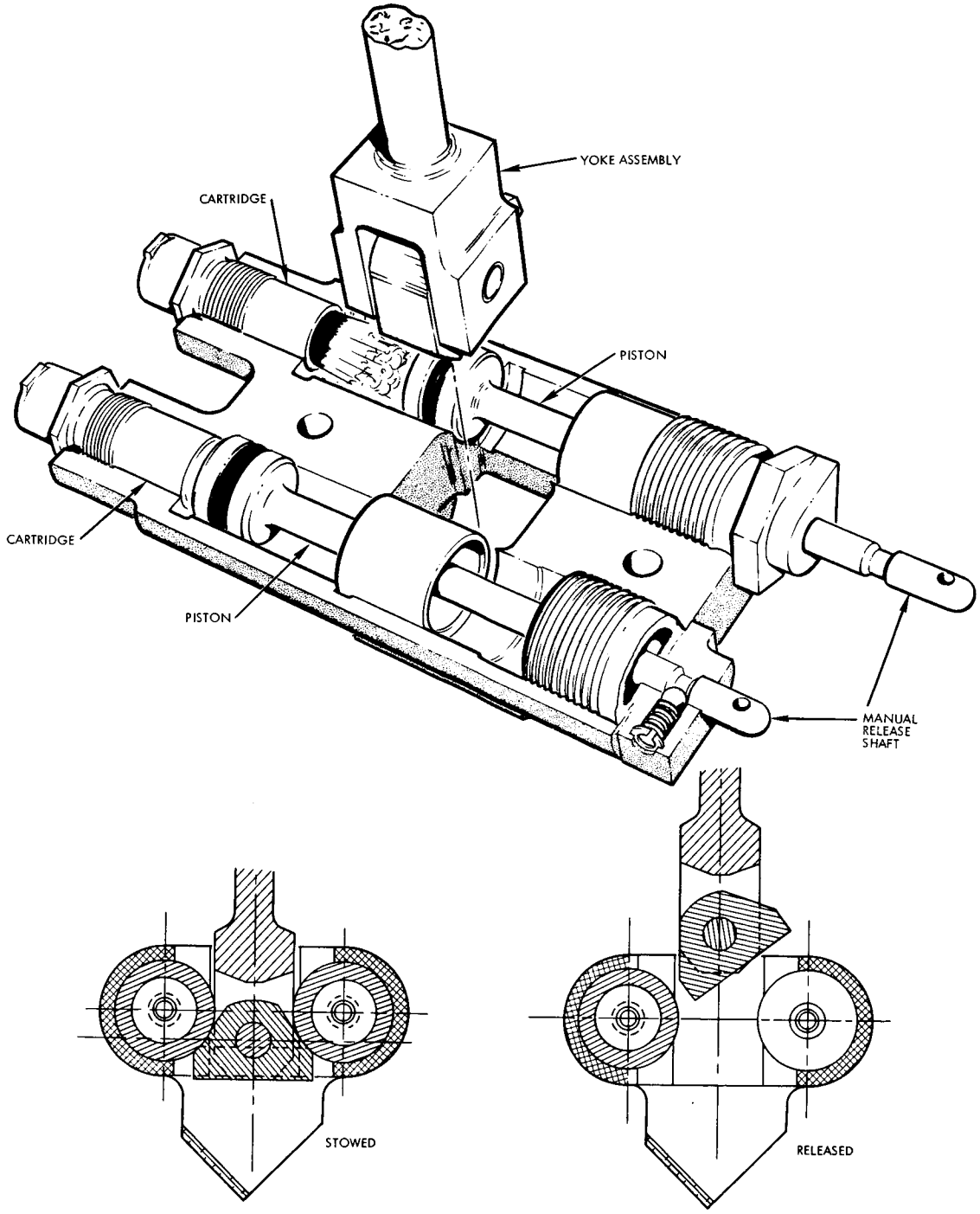

Figure 2-19

APPENDAGE RELEASE DEVICE is electro-explosive and has repeatedly demonstrated its reliability on OGO and other satellites. Redundancy is provided at all appendage release points for additional reliability.

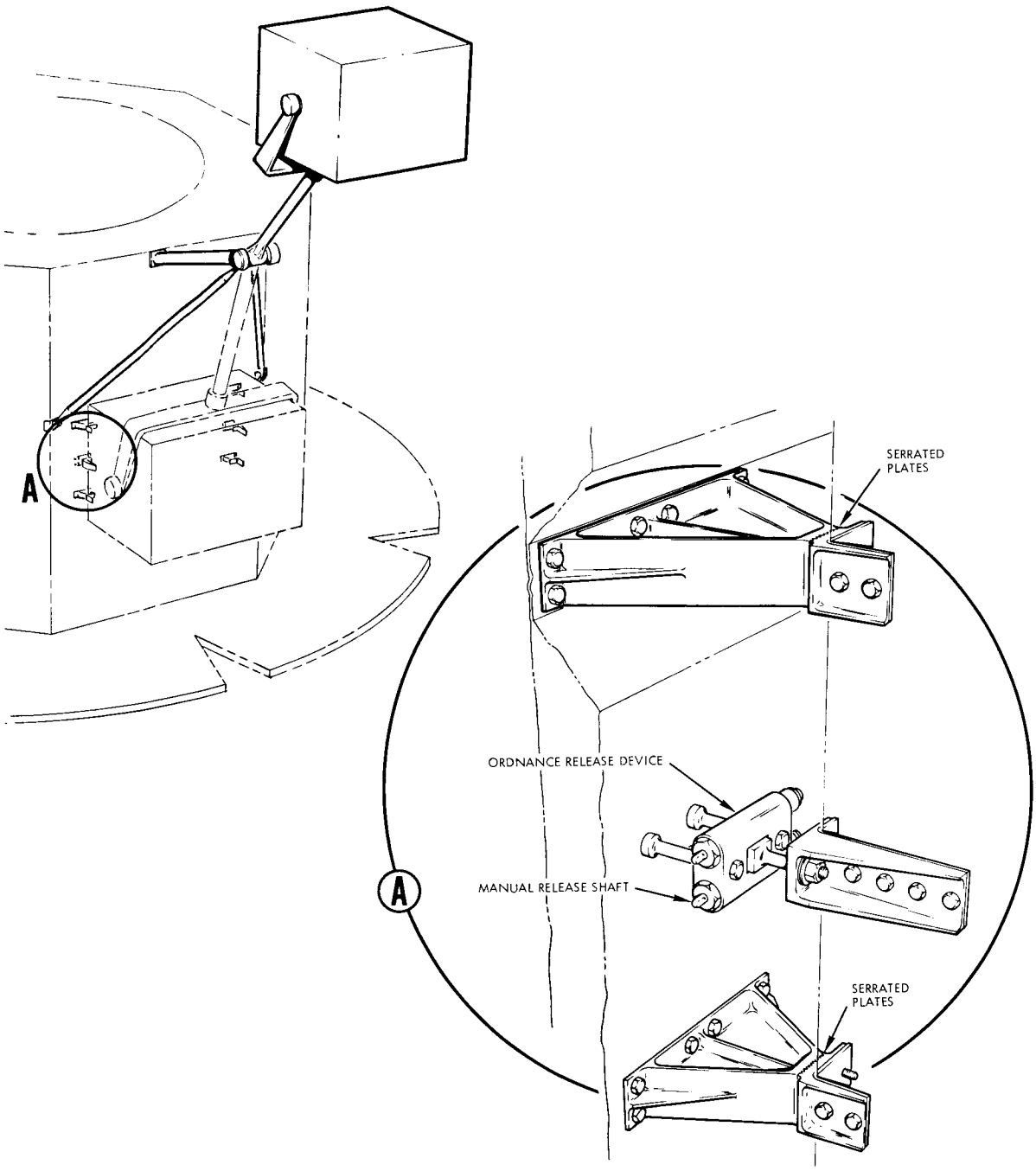

Figure 2-20
PLANETARY SCAN PLATFORM is stowed against spacecraft by means of preloaded bolt and four compression pads. It is released by two OGO-type electro-explosive devices.

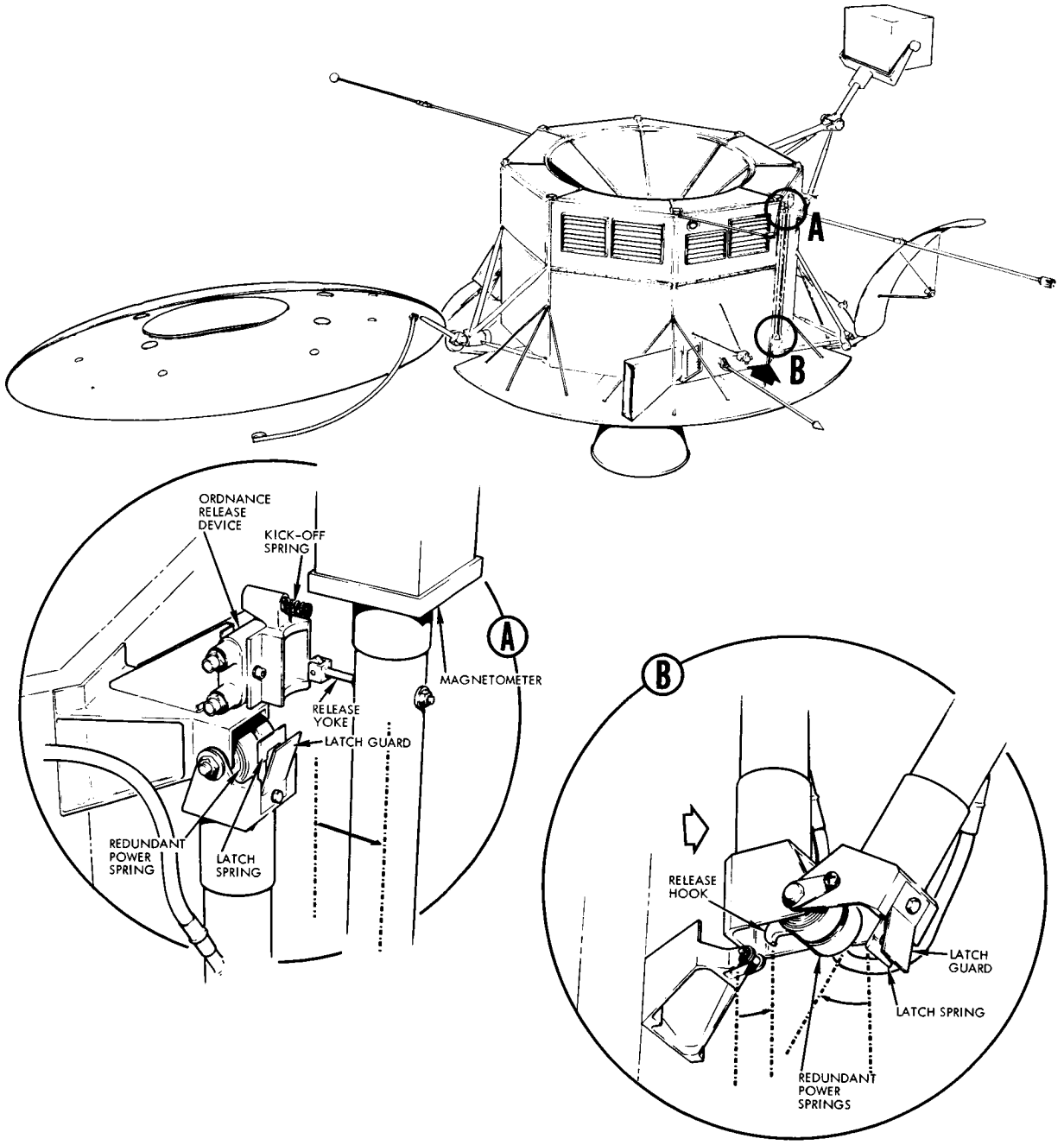

Figure 2-21

MULTI-SECTION HINGED BOOM has been proved in more than two years operation on OGO. This design is still giving trouble free operation in earth or Simple, reliable, it also permits cables to be deployed without difficulty.

a realistic structural weight estimate. The analyses performed were consistent with MIL-HDBK-5A procedures. Table 2-3 lists the major structural members, their critical design conditions, and their margins of safety.

2.5 ANALYSIS AND DESIGN OF METEOROID PROTECTION

The shielding required to prevent destructive meteoroid penetration into the interior of the spacecraft is based on the environments specified in Reference 2. Figures 2-22 and 2-23 depict, respectively, the mean total incident fluxes ($F >$) of cometary and asteroidal particles for the interplanetary and Mars orbit mission phases. Earth-orbiting particles have been neglected in this analysis since the stay is so short.

Baseline parameters selected for the analysis were 650 ft^2 (60.4 M^2) of exposed spacecraft surface area, 224 day (1.93×10^7 sec) nominal interplanetary cruise and specified 2 months (5.18×10^6 sec) of operation in Mars orbit. In addition, protection thicknesses were determined for the six-month Mars orbit design goal. Shielding of the spacecraft by the capsule was neglected since the spacecraft must be capable of performing its mission with the capsule removed. The shielding effect of the annular solar panels is minor and has also been ignored.

Using the incident flux curves of Figures 2-22 and 2-23 and assuming that the standard Poisson distribution applies for determining the probability of any meteoroid impact, design penetrating masses were determined for various probabilities of zero penetration $\left[P_{(O)} \right]$ of the baseline spacecraft. The various thicknesses of aluminum required to prevent penetration by these masses were then determined from the puncture flux (ϕ) equations given in Reference 2, and the relationship between mean circumstance puncturable mass and the flux ratio ($\phi / F >$) developed by Dalton (Reference 4) (Figure 2-24). The resultant thicknesses required for various probabilities of no spacecraft penetration for the entire mission, and its transit and orbit phases are shown in Figures 2-25 and 2-26 for both the specified and design goal mission durations.

The current mission reliability allocation for successful operation in the meteoroid environment is 0.97 (Reference 6). To use this reliability requirement as being equivalent to the probability for no puncture in selecting a shielding thickness would be grossly conservative,

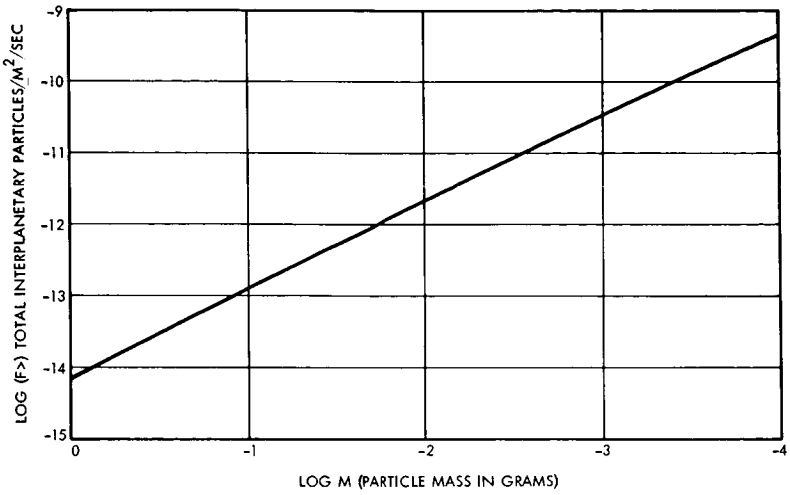

Figure 2-22

PLOT OF METEOROID MASS versus cumulative mean influx of cometary and asteroid particles in interplanetary space.

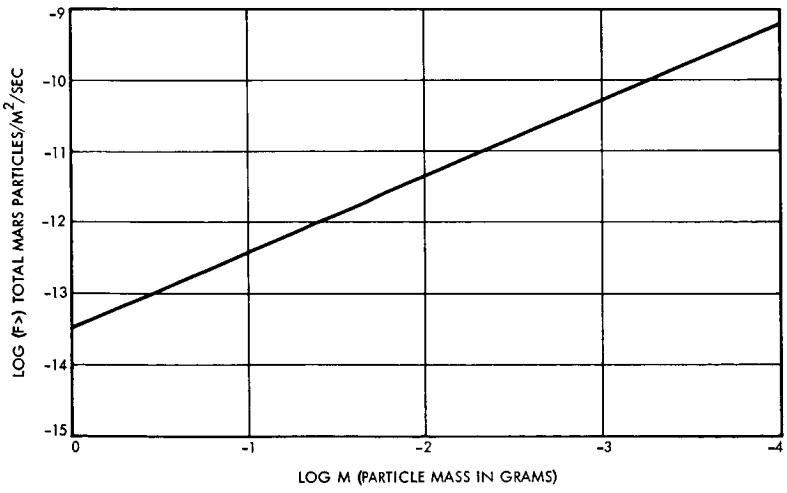

Figure 2-23

PLOT OF METEOROID MASS versus cumulative mean influx of cometary and asteroidal particles near Mars.

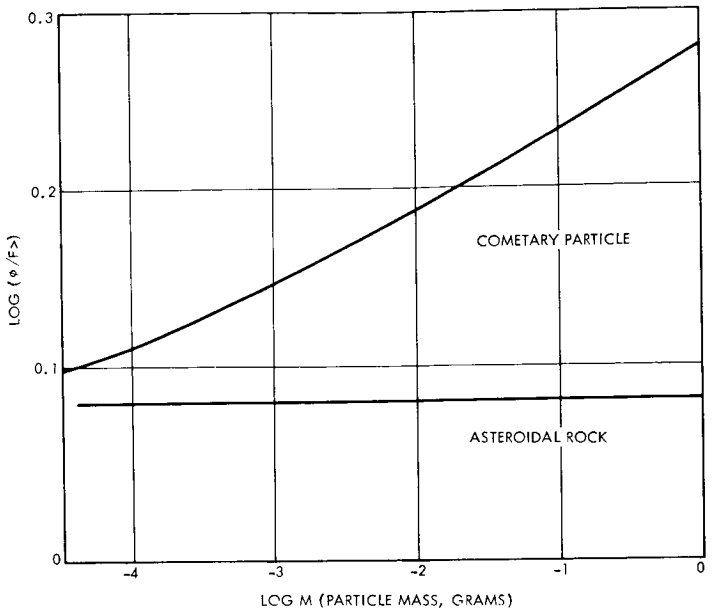

Figure 2-24
PLOT OF RELATIONS between puncture flux enhancement factor and mean circumstance puncturable mass.

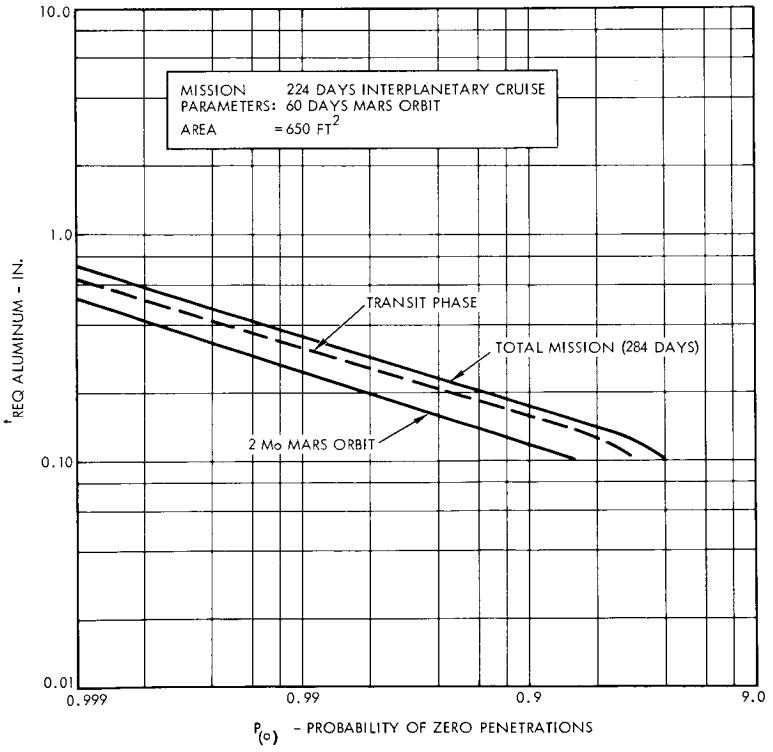

Figure 2-25
PLOT OF PROBABILITY OF NO PUNCTURE versus required thickness of aluminum for mission phases and total mission.

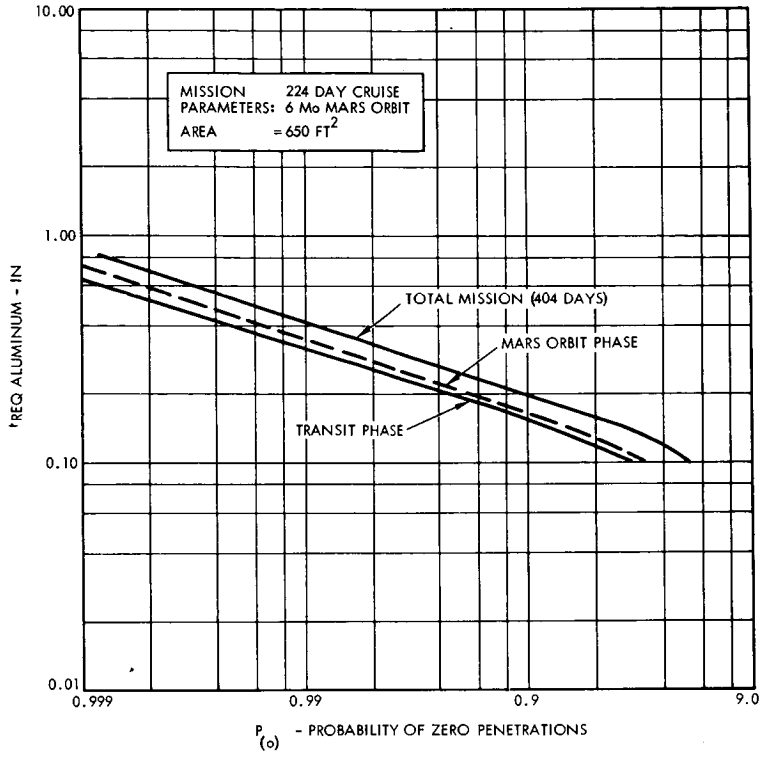

Figure 2-26

PLOT OF PROBABILITY OF NO PUNCTURE versus required thickness of aluminum for mission phases and total mission.

since to do so is equivalent to assuming that any penetration of the shield would lead to mission failure. In addition, such an assumption would impose an undue weight penalty on a spacecraft of such large surface area.

Therefore a mission relaibility analysis was performed which estimated the probability of a meteoroid striking a component after having penetrated the basic shield. Consideration was given to the inherent shielding offered by various components and the fact that many components have redundant or backup modes so that damage to them will not result in a mission failure. Results of this analysis indicate that 0.97 mission reliability is attained if the spacecraft meteoroid shielding is designed to give a $P_{(O)}$ of 0.87. (Resist meteoroids of mass $\leq$ 0.0004 grams.)

From Figure 2-25, it is seen that a $P_{(O)}$ of 0.87 requires the equivalent of a single thickness of 0.16 inches of aluminum. Using the double wall factors recommended by Frost, (Reference 5) it was found that the optimum weight equivalent metoroid shield is a 1.5-inch aluminum faced sandwich, filled with 2 lb/ft^3 polyurethane foam and having an 0.010 inch

Table 2-3. Description and Strength Summary of Major Members in Structural Subsystem

Item	Description	Design Condition	Margin Of Safety
Propulsion Module			
Main Support Beam Caps	2 x 1.5 x 0.065 inch 7075-T6 Tee Extr.	First Stage Burnout	+0.09 (Crippling)
Main Support Beam Web	0.04 inch 7075-T6 Alclad	First Stage Burnout	+0.07 (Buckling)
Secondary Support Beam Caps	2 x 1.5 x 0.08 inch 7075-T6 Tee Extr.	First Stage Burnout	+0.06 (Crippling)
Secondary Support Beam Web	0.05 inch 7075-T6 Alcald	First Stage Burnout	+0.08 (Buckling)
Helium Tank Supports	0.032 Cylindrical Shell 7075-T6 Alclad	First Stage Burnout	+0.02 (Stability)
Propellant Tank Supports	0.50 inch Al. Honeycomb Cylindrical Skirt (0.005 Face Sheets, 2.1 lb/ft^3 Core)	First Stage Burnout	+0.02 (Intercell Buckling)
Engine Support Truss	1.5 inch OD x 0.125 inch 7075-T6 Tubing	Mars Orbit Insertion (Gimbal Angle = 6°)	+0.08 (Stability)
Equipment Module			
Longerons	3 x 2 x 0.125 inch 7075-T6 I-Beam Extr.	First Stage Burnout	+0.16 (Stability)
Meteoroid Panels	1.50 inch Al. Honeycomb Panel (0.010 Outer Face Sheet, 2 lb/ft^3 Foam, 0.030 Inner Face Sheet)	Meteoroid Protection	----------
Propulsion Module Interface Bolts	3/8 inch Dia. x 160 KSI H.T. Bolts	First Stage Shutdown	+0.15 (Tension)
Medium Gain Antenna Support	2 inch OD x 0.028 inch 7075-T6 Tubing	Mars Orbit Insertion	+0.30 (Crippling)
High Gain Antenna Support	2 inch OD x 0.049 inch 7075-T6 Tubing	Vibration During LM Engine Firing	Designed for Stiffness
PSP Support	3 inch OD x 0.049 inch 7075-T6 Tubing	Vibration During LM Engine Firing	Designed for Stiffness

Figure 2-26

To be supplied

Table 2-3. Description and Strength Summary of Major Members in Structural Subsystem

Item	Description	Design Condition	Margin Of Safety
Propulsion Module			
Main Support Beam Caps	2 x 1.5 x 0.065 inch 7075-T6 Tee Extr.	First Stage Burnout	+0.09 (Crippling)
Main Support Beam Web	0.04 inch 7075-T6 Alclad	First Stage Burnout	+0.07 (Buckling)
Secondary Support Beam Caps	2 x 1.5 x 0.08 inch 7075-T6 Tee Extr.	First Stage Burnout	+0.06 (Crippling)
Secondary Support Beam Web	0.05 inch 7075-T6 Alcald	First Stage Burnout	+0.08 (Buckling)
Helium Tank Supports	0.032 Cylindrical Shell 7075-T6 Alclad	First Stage Burnout	+0.02 (Stability)
Propellant Tank Supports	0.50 inch Al. Honeycomb Cylindrical Skirt (0.005 Face Sheets, 2.1 lb/ft^3 Core)	First Stage Burnout	+0.02 (Intercell Buckling)
Engine Support Truss	1.5 inch OD x 0.125 inch 7075-T6 Tubing	Mars Orbit Insertion (Gimbal Angle = 6°)	+0.08 (Stability)
Equipment Module			
Longerons	3 x 2 x 0.125 inch 7075-T6 I-Beam Extr.	First Stage Burnout	+0.16 (Stability)
Meteoroid Panels	1.50 inch Al. Honeycomb Panel (0.010 Outer Face Sheet, 2 lb/ft^3 Foam, 0.030 Inner Face Sheet)	Meteoroid Protection	----------
Propulsion Module Interface Bolts	3/8 inch Dia. x 160 KSI H.T. Bolts	First Stage Shutdown	+0.15 (Tension)
Medium Gain Antenna Support	2 inch OD x 0.028 inch 7075-T6 Tubing	Mars Orbit Insertion	+0.30 (Crippling)
High Gain Antenna Support	2 inch OD x 0.049 inch 7075-T6 Tubing	Vibration During LM Engine Firing	Designed for Stiffness
PSP Support	3 inch OD x 0.049 inch 7075-T6 Tubing	Vibration During LM Engine Firing	Designed for Stiffness

since to do so is equivalent to assuming that any penetration of the shield would lead to mission failure. In addition, such an assumption would impose an undue weight penalty on a spacecraft of such large surface area.

Therefore a mission relaibility analysis was performed which estimated the probability of a meteoroid striking a component after having penetrated the basic shield. Consideration was given to the inherent shielding offered by various components and the fact that many components have redundant or backup modes so that damage to them will not result in a mission failure. Results of this analysis indicate that 0.97 mission reliability is attained if the spacecraft meteoroid shielding is designed to give a $P_{(O)}$ of 0.87. (Resist meteoroids of mass $\leq$ 0.0004 grams.)

From Figure 2-25, it is seen that a $P_{(O)}$ of 0.87 requires the equivalent of a single thickness of 0.16 inches of aluminum. Using the double wall factors recommended by Frost, (Reference 5) it was found that the optimum weight equivalent metoroid shield is a 1.5-inch aluminum faced sandwich, filled with 2 lb/ft^3 polyurethane foam and having an 0.010 inch outer and an 0.030 inch inner face sheet. (A lightweight aluminum honeycomb core is added to reinforce the foam.) This sandwich is used for the majority of meteoroid protection for the recommended spacecraft. In areas where it was impractical to use the basic sandwich, another equivalent of 0.16 inch of aluminum was substituted as, for example, the equipment mounting panels, which are honeycomb sandwiches with 0.035 inch face sheets. Total weight of the meteoroid protection panels on the spacecraft is 563 pounds, not including the weight of primary structure which is used also as meteoroid protection, i.e., equipment panels and the propulsion module platform. It includes, however, the inner face sheets of the equipment module side panels which also act as shear webs for the basic structure and which weigh approximately 100 pounds.

Increasing the required operating life in Mars orbit to six months requires an additional 77 pounds of shielding to achieve the 0.97 mission reliability; use of the present panel design would reduce $P_{(O)}$ to 0.81 and mission reliability to 0.955 (Figure 2-26).

REFERENCES

1. "Voyager Environmental Predictions Document," Jet Propulsion Laboratory, Pasadena, California, 26 October 1966.

2. "Natural Environment Design Criteria Guidelines for MSFC Voyager Spacecraft for Mars 1973 Mission," NASA TMX-53616, June 8, 1967.

3. "Performance and Design Requirements for the 1973 Voyager Mission, General Specification For," Jet Propulsion Laboratory, Pasadena, California, January 1, 1967.

4. C. Dalton, "Near Earth and Interplanetary Meteoroid Flux and Puncture Models," AAS Paper 67-334.

5. V. C. Frost, "Aerospace Meteoroid Environment and Penetration Criterion," Aerospace Report TOR-269 (4560-40).

6. "Voyager Flight Spacecraft—Guidelines, Requirements and Design Characteristics—Preliminary," VVV-293, TRW Systems, Redondo Beach, California, 13 July 1967.

3. PLANETARY VEHICLE ADAPTER

3.1 SUMMARY

The planetary vehicle adapter includes the structure, cabling, and other hardware located between the planetary vehicle, in-flight separation joint and the associated points of attachment to the Voyager shroud. It provides structural support for the planetary vehicle from preflight installation to in-flight separation. In addition, it distributes flight loads into the shroud and contains the means for effecting release of the planetary vehicle from the launch vehicle. Its preliminary specification is shown in Figure 3-1.

The recommended adapter design meets the requirements of Section 3.2 and satisfies the interface requirements of Section 3.3. It consists of the following elements: (See Figure 3-2.)

- Planetary vehicle support truss
- Upper shroud ring
- Lower shroud ring
- Intercostals
- Attachment fittings
- Release and separation devices

In the selected design, all planetary vehicle loads are introduced into the support truss at twelve interface fittings. The four inboard fittings provide direct support to the propulsion module beams, reducing their maximum bending moment by a factor of a six. Though this causes the truss to be heavier than one with only eight interfaces, this is more than compensated for by a reduction in planetary vehicle weight, since one pound of inert spacecraft weight requires 1.2 pounds of propellant to meet mission velocity increment requirements.

The truss distributes planetary vehicle forces to the shroud at eight points. Longitudinal loads are sheared uniformly into the shroud

PRELIMINARY SPECIFICATION

Planetary Vehicle Adapter

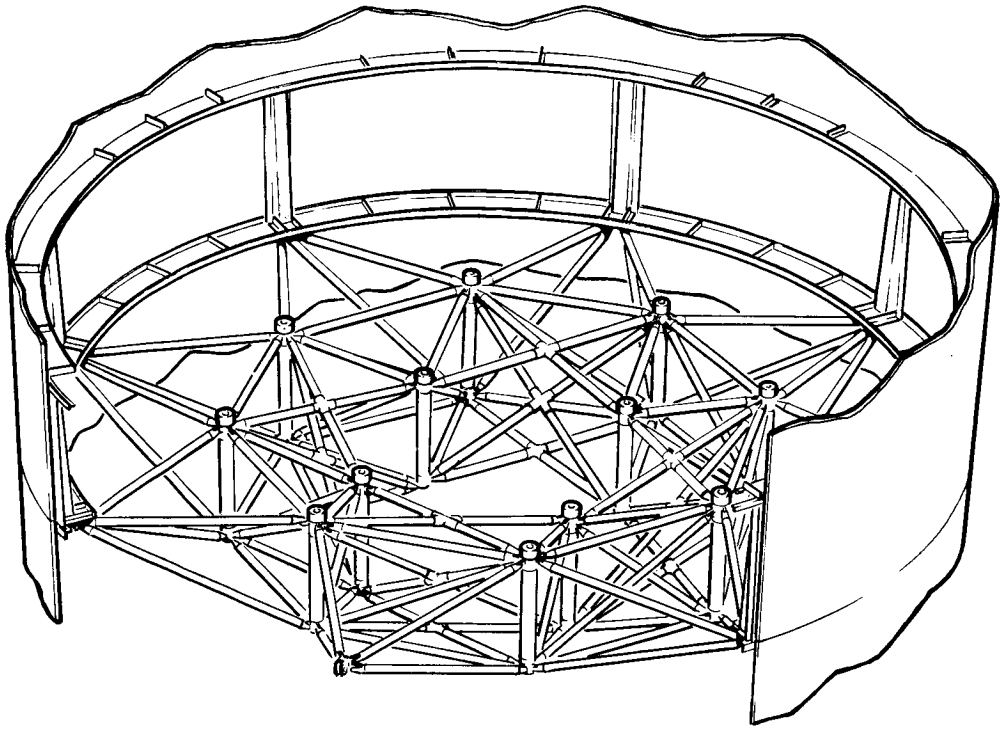

Purpose

Provide the structural support and attachment of the planetary vehicle to the launch vehicle.

Physical Characteristics

The subsystem is comprised of 2 frames, 8 intercostals and support truss and associated fittings and hardware.

Interchangeable and aligned support points.

Electrical distribution and pyrotechnic control for interface/separation fittings.

Performance Characteristics

LOAD FACTORS	LONGITUDINAL		LATERAL	
	Static	Dynamic	Static	Dynamic
Liftoff				
1st stage burnout	5.0	–	±1.0	–
1st stage cut off	–	2.0	–	±1.0

FACTORS OF SAFETY

	Yield	Ultimate
General Structure	1.00	1.25

CONFIGURATION

COMPONENT	OVERALL DIMENSIONS	WEIGHT	MAT'L AND CONSTRUCTION
Intercoastals	257 in diameter x 54 in. deep	41	7075 Aluminum alloy
Truss		474	7075 Aluminum alloy, with machined and bolted joints
Lower frame		30	7075 Aluminum alloy
Upper frame		64	7075 Aluminum alloy
Interface fittings, incl. pyrotechnics and control		44	7075 Aluminum alloy, release mechanism, J box, harness
Total adapter		686 Lb including 33 Lb contingency	

Interfaces

Planetary vehicle - 12 attach points; 8 on 160-inch bolt circle, 4 on 80-inch bolt circle

Shroud - Frames and longerons distribute loads at shroud diameter.

Figure 3-1

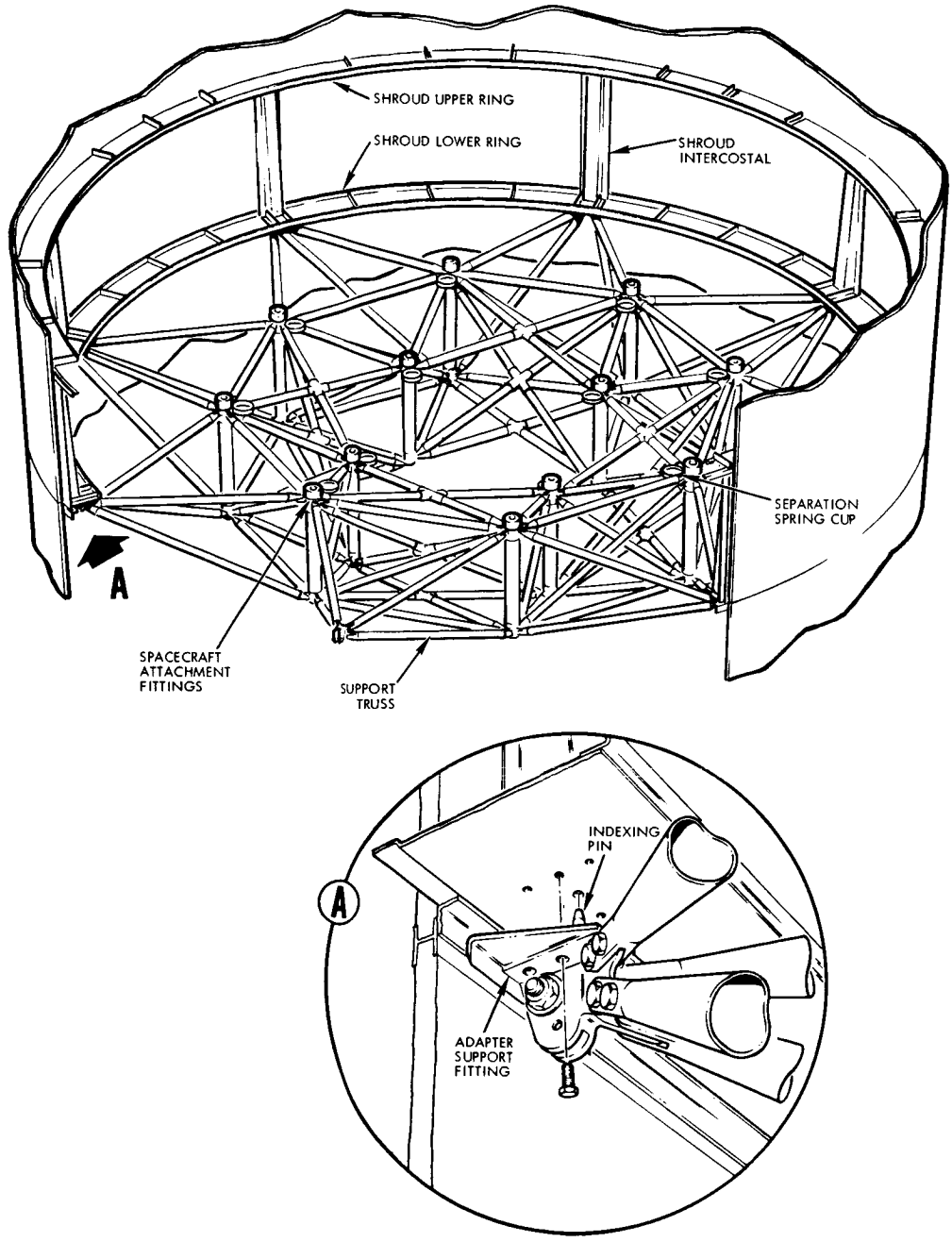

Figure 3-2

PLANETARY VEHICLE ADAPTER/SHROUD ATTACHMENT consists of machined fittings at eight points on the periphery of the adapter truss. They transmit all spacecraft loads into the shroud by means of a support sturcture (consisting of upper and lower rings joined by short intercoastal members) which is fastened to the shroud itself.

structure by intercostals. Moments, due to load offsets, are minimized by the design and are reacted by transverse couples between the ring frames.

The reliability assessment of the planetary vehicle adapter, including its associated planetary vehicle release system, is 0.997. Details of the calculations used to derive this value are presented in Appendix E of Volume 2. The weight breakdown of the planetary vehicle adapter is shown in Table 3-1.

3.2 REQUIREMENTS AND CONSTRAINTS

3.2.1 Mission Constraints

The planetary vehicle adapter supports the planetary vehicle and transfers its loads to the Voyager shroud while subject to Saturn V natural and induced environments. Critical mission accelerations are summarized in Table 2-2.

Operation of the release devices does not cause any contamination of the planetary vehicle. Other applicable mission constraints are included in Section 2.2.1.

3.2.2 Design Requirements

The planetary vehicle adapter is designed to meet the applicable design, environmental, structural, and material requirements of Section 2.2.2, while supporting the maximum-weight planetary vehicle.

3.3 INTERFACE REQUIREMENTS

3.3.1 Cabling and Umbilicals

All interface cabling between the planetary vehicle and launch vehicle is attached to and supported by the adapter. A single umbilical disconnect fitting is provided at the separation plane. No critical electrical alignment will be required at match-mate.

3.3.2 Planetary Vehicle

All planetary vehicle launch loads are transmitted to the launch vehicle through the adapter. In order to prevent deleterious coupling between the planetary vehicle and launch vehicle elements, and to constrain the planetary vehicle within the limits of its specified dynamic

Table 3-1. Planetary Vehicle Adapter Weight Breakdown (Recommended Configuration)

Item		Weight (Lb)
Basic Structure		474.2
Tubular Members		436.6
Joint Fittings		37.6
Electrical Distribution		8.0
Harness		4.0
Junction Box	(1)	4.0
Shroud Modification		134.7
Upper Ring	(1)	53.2
Lower Ring	(1)	18.4
Longerons	(16)	40.6
Fittings	(8)	22.5
Separation System		36.0
Contingency (5%)		32.6
	Total Installed Adapter Weight	685.5

envelope (Figure 2-6), the adapter is optimized for stiffness consistent with minimizing its weight. The natural frequency of the selected design, while supporting the planetary vehicle, should exceed 5 Hz.

The adapter provides an attach pattern at the field joint capable of aligning the planetary vehicle within the required tolerances (see Section 2.3.4). The structural interface between the planetary vehicle and the adapter has a conductive finish on the faying surfaces to provide a low impedance path for planetary vehicle electrical grounding.

3.3.3 Engineering Measurements

Both strain gages and accelerometers will be installed on each planetary vehicle adapter. Loads derived from the strain gage data will be correlated with low frequency accelerations, also measured on the adapter. Low frequency accelerometer and strain gage data will also

be used to establish the mechanical impedance characteristics of the adapter structure for proper test simulation in future spacecraft tests and to verify the design and test criteria specified for the 1973 mission. The accelerometers will also measure random vibration inputs to the spacecraft during liftoff and transonic flight.

3.3.4 Launch Vehicle Shroud

The planetary vehicle adapter transmits its loads to the launch vehicle in a uniform manner and provides the structure required to reinforce the shroud locally. The adapter is attached to the shroud at an interchangeable field joint (Figure 3-2 detail).

The spacecraft is capable of being fueled while mounted within the shroud. The required lines are supported by the adapter.

3.4 DESIGN DESCRIPTION

The recommended adapter design meets the requirements and constraints of Section 3.2 and satisfies the interface requirements of Section 3.3. The design is simple, optimized for strength and stiffness, and requires no complex manufacturing processes.

3.4.1 Planetary Vehicle Support Structure

The planetary vehicle is supported by an aluminum tubular truss structure. The members are 7075 aluminum alloy tubes with tapered end fittings. The D/t ratios of the tubes have been selected to give maximum stiffness with minimum weight. At each joint the tubes are bolted to machined fittings, as shown in Figure 3-2. The calculated natural frequency of the truss, while supporting the maximum weight planetary vehicle is 5.8 Hz.

3.4.2 Shroud Reinforcement Structure

The adapter truss is attached to the shroud reinforcement structure at eight points using titanium alloy fittings as shown in Figure 3-2. The reinforcement structure consists of builtup rings of 7075 aluminum, joined together by eight aluminum intercostals tied to the honeycomb shroud. The intercostals transmit the axial loads into the shroud and distribute the moments into the rings as transverse loads. In addition, the lower ring shears all of the planetary vehicle lateral loads into the shroud through the attachments.

3.4.3 Release and Separation Mechanism

The planetary vehicle is released from the adapter by firing the pair of redundant explosive bolts located at each of the twelve interface points. Details of this device are shown in Figure 2-15. The vehicle is separated from the remaining stage in an over-the-nose mode.

A single mechanical system provides the required separation velocity as well as guidance for the planetary vehicle after release. The velocity impulse is provided by twelve springs, each located near an adapter attach point (see Figure 2-15). Using multiplicity of springs has the advantage of making the net perturbation velocity vector (i.e., nonaxial component) statistically small.

Guidance, during flyout through the shroud, is accomplished by four rollers, mounted at the periphery of the annular solar panels, constrained in four channels mounted to the shroud (see Figure 3-3). These guides constrain any lateral movement of the spacecraft until the shroud is cleared. Complete details of the planetary vehicle separation system and discussion of separation dynamics are in Volume 10.

3.4.4 Structural Performance Summary

The internal load distribution for the configuration was determined by redundant analysis using TRW Computer Program AS113-JPL Stiffness Matrix for the various flight conditions shown in Table 2-2, using a

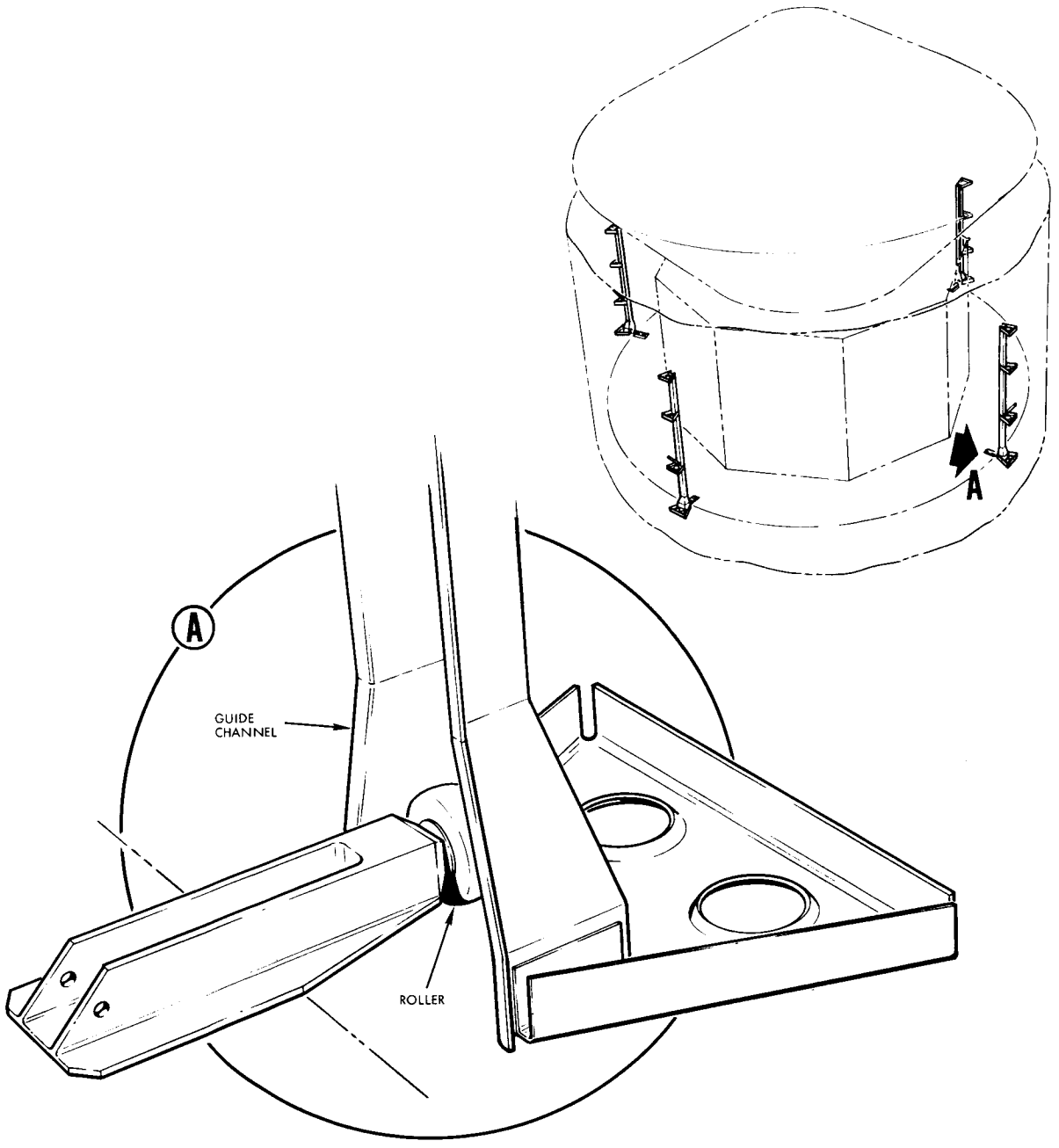

Figure 3-3

PLANETARY VEHICLE SEPARATION is accomplished by twelve springs, which provide the separation impulse. Four rollers, mounted on edges of annular solar panels, ride or rails attached to shroud so that spacecraft is guided safely out of shroud.

30, 000 pound planetary vehicle weight. Major structural members were sized using the critical loads to insure positive margins of safety and to provide data for a realistic structural weight estimate. The analyses performed were consistent with MIL-HDBK-5A procedures.

Table 3-2 summarizes the major structural members analyzed, their critical design condition, and their margins of safety.

Table 3-2. Structural Description and Strength Summary of Major Members of Planetary Vehicle Adapter

Item	Description	Design Condition	Margin of Safety
Truss Adapter			
Tubular Members	7075-T6 Tubing (Various Sizes)	First Stage Burnout	+0.04 (Stability)
Truss Fittings	Machined Fittings (TI-6AL-4V)		+0.10
Separation Bolts	3/8 in. dia., 180 KSI H. T. Bolts		+0.06 (Tension)
Shroud Support Structure			
Intercostal Fittings	Machined Fittings (TI-6AL-4V)		+0.07
Intercostals	3 x 2.5 x 0.072 in. Tapered Hat Section (Tapered 3 to 1 in.) (7075-T6)		+0.31
Aft Ring - outboard cap	1.625 x 1.375 x 0.094 in. 7075-T6 Tee Extr.		+0.00 (Crippling)
Aft Ring Web	0.051 7075-T6 Alclad		+0.03 (Buckling)
Forward Ring - inboard cap	1.5 x 1.0 x 0.04 in. 7075-T6 Tee Extr.		+0.03 (Crippling)
Forward Ring Web	0.025 7075-T6 Alclad	First Stage Burnout	+0.01 (Buckling)

4. PROPULSION

The propulsion subsystem is required to perform four basic maneuvers for the Voyager mission: 1) planetary arrival date separation of the two spacecraft, 2) interplanetary trajectory corrections, 3) insertion into Mars orbit, and 4) trimming of the attained orbit.

The selection of the propulsion system is based on the requirements for all projected missions from 1973 through 1979. The LM Descent Engine, with a minimum of modification in accordance with the statement of work, has been selected for main propulsion and a cluster of C-1 engines for backup propulsion.

4.1 SUMMARY

The LM Descent Engine, as designed for the Apollo Program, provides variable thrust from 1050 to 9850 pounds. As modified for the Voyager mission, it provides two discrete thrust levels: 9850 pounds for Mars orbit insertion and 1700 pounds for all other maneuvers.

For a propulsion system able to perform all planned Voyager missions without further modification, it is necessary to have a propellant capacity that can accommodates the most severe mission requirements with a vehicle that takes advantage of the maximum growth potential. The assumed weight of the planetary vehicle, that incorporates this growth potential, is 30,076 pounds. This includes capsule weights to 8000 pounds and science equipment to 600 pounds. An analysis has been performed (see Section 5.4 of Volume 6) which shows that the propellant capacity needed to accommodate this weight with acceptable safety margins is 16,000 pounds. The propulsion system has therefore been sized for this weight of usable propellant.

The propellant feed system has been designed for minimum weight and maximum simplicity. It is a one-level regulated system without venting. To settle the propellants in a zero-g environment, a bellows tank system has been selected for its light weight and simplicity; it is also a design that has reached a high level of development maturity and is easy to incorporate into the propulsion system.

The possible violation of the contamination constraint due to meteorite-induced tank explosion, discussed in Appendix C, should receive additional study.

The Task B approach to the LMDE head end configuration employed explosive valves for positive sealing and for propellant control. For Task D, the LMDE head end has been reconsidered in the light of improvements resulting from recent development work. Ball valves are retained for control of the high-thrust mode of operation while a quad set of solenoid valves is utilized for the low-thrust mode.

The backup propulsion system consists of a cluster of four C-1 engines which are capable of inserting the planetary vehicle into a degraded orbit. This orbit would be large compared to the orbits defined in the mission specification but would still constitute a successful mission because most experiments could be accomplished.

The Transtage or Agena engine can be physically installed and could be used for the orbit insertion firing.

4.2 SUBSYSTEM DESCRIPTION

This section describes the physical and performance characteristics of the selected propulsion subsystem. The functional interfaces with other spacecraft subsystems are discussed, and a preliminary specification for the propulsion subsystem is presented.

The selected propulsion subsystem configuration and performance characteristics are shown on Figure 4-1, along with a weight breakdown and system schematic.

In this system, the helium pressurant is contained at an initial pressure of 4000 psia in two manifolded tanks. The tanks are sealed for all long-term coast periods by pyrotechnic valves. Pressurant is admitted to the regulators through pyrotechnic valves where it is stepped down to the nominal tank operating pressure of 235 psia.

PRELI

CONFIGURATION

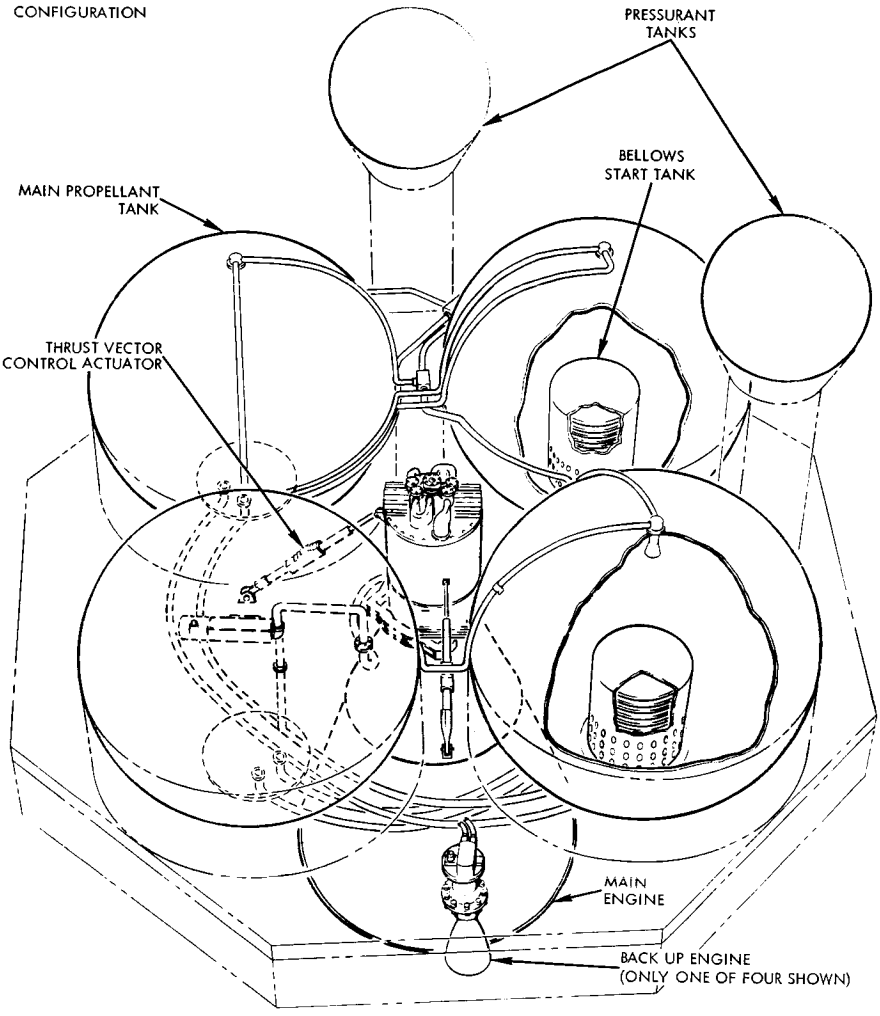

Physical Characteristics

WEIGHTS, LB	
Dry	1565.2
Burnout without helium)	1998.4
Pressurant (helium)	42.2
Usable fuel (50-50 UDMH/N_2H_4)	6153.8
Usable oxidizer (N_2O_4)	9846.2
PRESSURE, PSIA	
Helium storage	4000
Regulator outlet	249
Propellant tank operating	235
Engine inlet	220
Engine chamber	
High thrust	100
Low thrust	18
MISCELLANEOUS	
Maximum engine gimbal angle	± 6°, 2 axis
Nozzle area ratio	47.5:1
Response, signal to 90% thrust	0.25 sec
Engine mixture ratio (oxidizer/fuel)	1.6:1

Purpose

To provide thrust at levels and times as required to accomplish the planetary arrival date separation maneuver, interplanetary trajectory corrections, orbit insertion, and trimming of the attained orbit.

Performance Characteristics

Total impulse:	4.82 x 10^6 lb/sec
Thrust levels	
High:	9850 lb
Low:	1700 lb
Shutdown repeatability:	
High thrust	128 lb-sec
Low thrust	48 lb-sec

PERFORMANCE

Maneuver	Nominal Thrust	Nominal I_{sp}
Planetary arrival date separation	1,700	298
Orbit insertion, start	9,850	305
Orbit insertion, end	10,000	303
Orbit trim	1,700	289

Mission reliability 0.9656

THERMAL REQUIREMENTS

Propellant temperature	Bulk temperature
	ΔT between unlik
	ΔT between like p
Feed system temperature	70 ± 20°F
Engine head end valve temperature	120°F max, 20°F
Engine internal surfaces exposed to solar heat during cycle	200°F max

ENGINE FLOW RATES, LB/SEC

Maneuver	Nominal Thrust
Planetary arrival date separation	1700
Orbit insertion, start	9850
Orbit insertion, end	10,000
Orbit trim	1700

FOLDOUT FRAME

ITEM	QUANTITY	WEIGHT (LB)
PRESSURIZATION SYSTEM		
Pressurant tank	2	264.0
Fill and vent coupling (helium)	1	0.3
Vent coupling (propellant)	2	0.9
Explosive valve, normally closed	11	5.0
Explosive valve, normally open	13	7.0
Filter	3	0.9
Quad pressure regulator	1	12.0
Quad check valve assembly	2	1.8
Burst disc and relief valve assembly	2	1.6
Pressure transducer	3	1.6
Miscellaneous hardware and lines	2	18.0
Temperature transducers		0.5
		312.8
PROPELLANT FEED SYSTEM		
Propellant tank	4	292.0
Start tank assembly	2	50.0
Fill and drain coupling	4	1.8
Prevalve	4	20.0
Start tank control valve	2	10.0
Pressure transducer	2	0.5
Temperature transducer	4	1.0
Miscellaneous hardware		4.3
Fuel lines		13.0
Oxidizer lines		18.0
Filters	4	4.6
Electrical harness		5.0
Junction box		5.0
		425.2

ITEM	QUANTITY	WEIGHT (LB)
ENGINE ASSEMBLY		
Combustion chamber assembly		202.5
Chamber heat shield		8.0
Seal		2.0
Nozzle insulation		26.5
Nozzle extension		36.0
Hardware		5.0
Injector		29.3
Propellant lines and ducts		13.0
Control valve - high thrust		17.0
Control valve - low thrust		13.8
Hardware		0.8
Trim orifices		0.5
Electrical harness		6.0
Junction box		4.0
Hardware - J.B.		3.0
Instrumentation		26.1
Gimbal assembly		5.5
Hardware		4.0
Pintle actuator		405.0
TOTAL DRY WEIGHT		1156.8

SUBSYSTEM SCHEMATIC

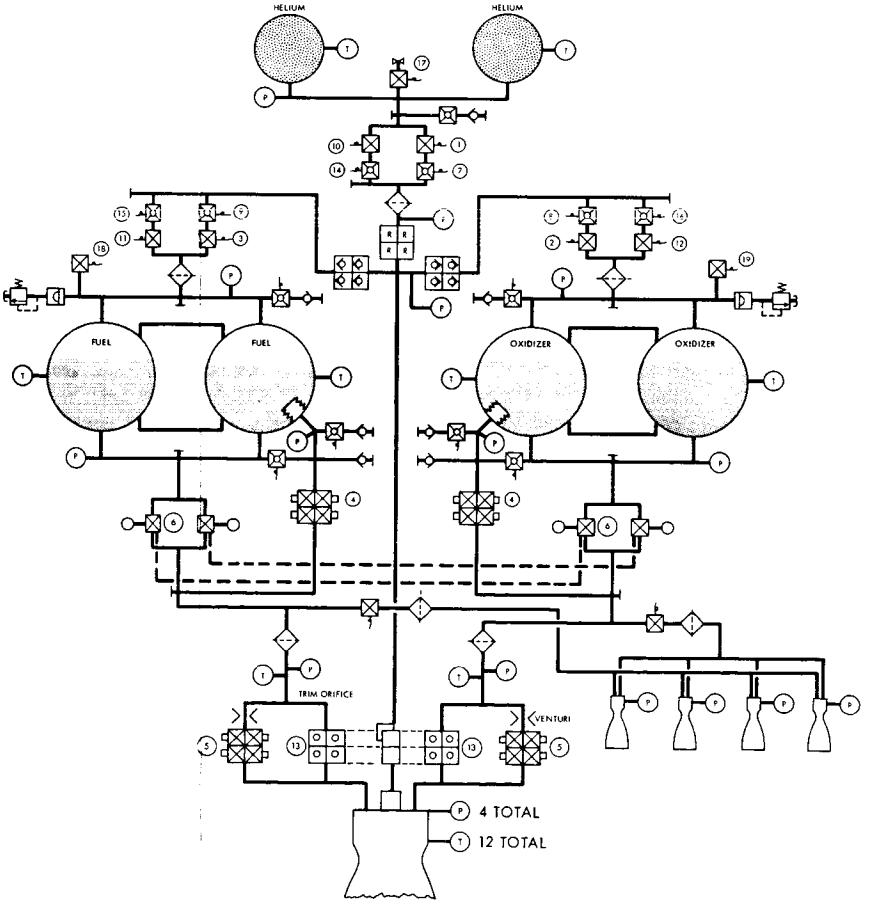

(17) Sequence of operation numbers used in Table 4-4.

Test port

Figure 4-1

The oxidizer and fuel tanks are isolated from each other and from the helium regulator by pyrotechnic valves during all coast periods. When the tanks are being pressurized during the separation and the orbit insertion firings, mixing of the propellants is prevented by quad check valves located in the pressurization lines. For the trajectory correction and orbit trim maneuvers, the propellant quantity used is small compared to the ullage volume, and a blowdown mode of operation is used wherein the tanks are completely isolated from each other and from the pressurant supply system. A burst-disc relief valve combination is provided to protect the propellant tanks in the event of inadvertent overpressurization. Explosive-actuated vent valves are incorporated in the pressurization system to allow venting of the propellant and the helium tanks after completion of all maneuvers.

The propellants are contained in symmetrical pairs of identical fuel and oxidizer tanks. The tanks are manifolded in a parallel flow arrangement and gas-side and liquid-side equalization lines are provided between like propellant tanks.

Alternative tank configurations were not examined in detail since only the configuration of two fuel and two oxidizer tanks operating in parallel feed would fall within the required envelope and meet the vehicle center of gravity excursion constraints. Series feed of the propellants from a tank configuration which paired unlike tanks on the diameter would require a fuel tank offset of approximately one foot to maintain the propulsion subsystem center of gravity on the spacecraft centerline. This would result in increased structure and meteoroid shielding weights to accommodate this increased spacecraft diameter.

A set of parallel redundant prevalves is included in the propellant feed lines for positive sealing of the propellants during coast periods. Corresponding pairs of fuel and oxidizer prevalves are mechanically linked to preclude mixture ratio shift in the event of failure of one of the parallel legs. Positive expulsion bellows tanks are located in one fuel and in one oxidizer tank. Bubble-free propellants from the bellows tanks are supplied to the engine during zero-g starts. After the propellants are settled, the main propellant line prevalves are opened to allow engine

feed on settled propellants and the start tank control valves are closed to stop additional flow from the start tanks.

The LMDE, as configured for Voyager, operates at only two thrust levels: a 1700-pound low thrust level for pre-orbit and post-orbit insertion maneuvers and a 9850-pound high thrust level, which is used only for the orbit insertion maneuver. All starts, including the orbit insertion firing, are made at 1700 pound thrust. In this configuration the LMDE ball valves are retained for operation in the high thrust mode while a pair of small quad redundant solenoid valves is added in parallel with the ball valves for the low thrust operation. A hydraulic actuator using engine fuel manifold pressure is incorporated in the head end assembly for automatically positioning the single-element coaxial injector to the high and low thrust levels. The combustion chamber is identical to the LMDE design. It consists of a continuous titanium shell with a composite phenolic refrasil ablative liner. A columbium nozzle extension skirt is attached at an area ratio of 16:1 and extends to 47.5:1. The nozzle extension is insulated on the outside surface to limit the heat input to the solar cells located on the bottom surface of the spacecraft.

Two views of the propulsion subsystem and the component arrangement are shown in Figure 4-2. As shown in the figure, the four equal-sized propellant tanks are arranged asymmetrically about the engine with the helium tanks distributed asymmetrically to achieve the desired vehicle center of gravity. The engine is mounted in the center compartment formed by four propellant tanks and is suspended at the throat of the combustion chamber on a gimbal ring that is an integral portion of the engine assembly. The gimbal ring is pivoted by means of vehicle-mounted actuators to provide thrust vector control in the pitch and yaw axes during engine firing. The gimbal plane of the engine lies 8 inches below the tank support platform.

Modules containing the pressurization, propellant, and fill and vent components are mounted on the tank support platform. Fuel and oxidizer feed and equalization lines, seen in the view looking forward, connect the tank pairs. These lines are configured with a constant radius of curvature in order to allow insertion into the propulsion

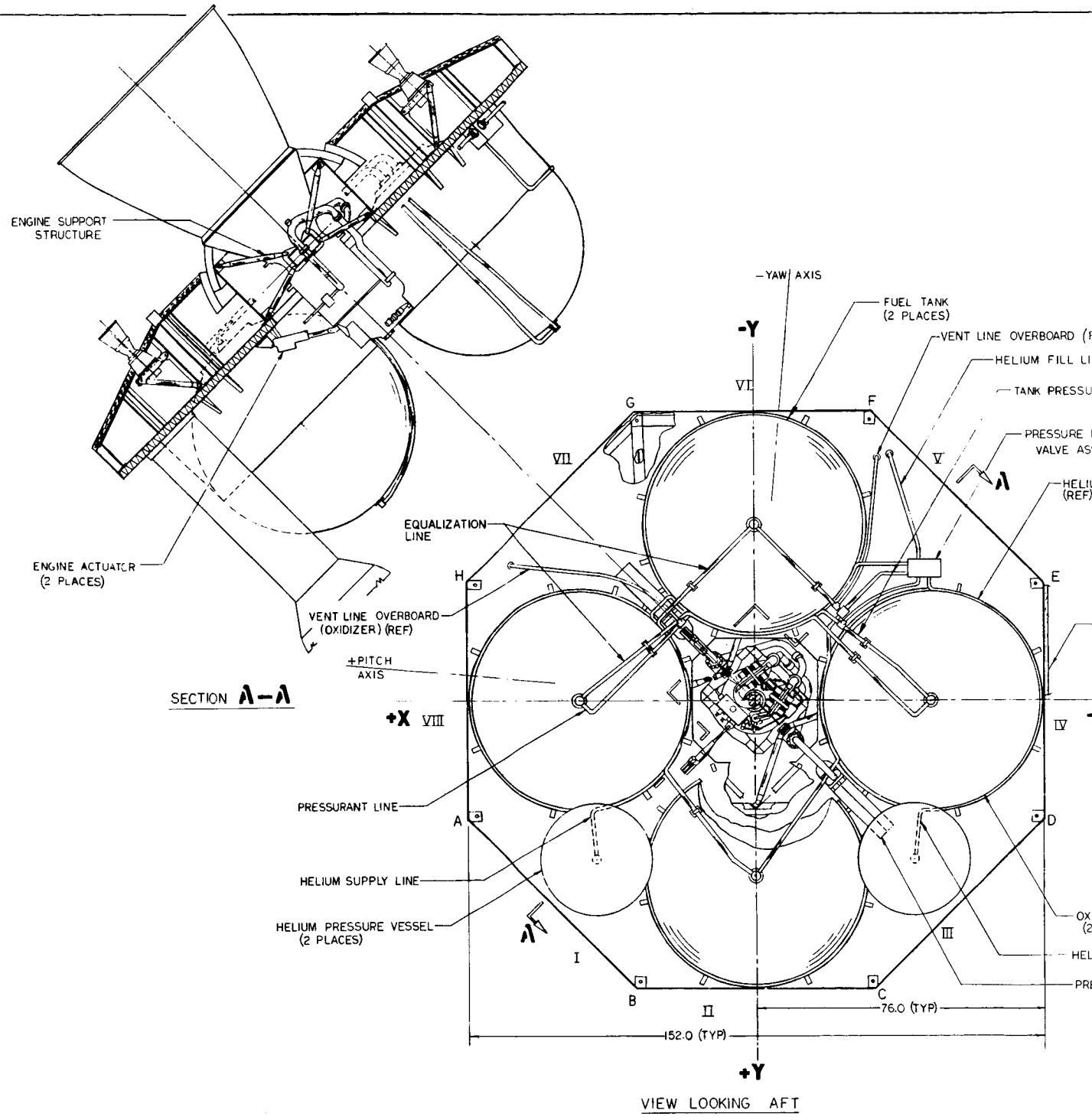

FOLDOUT FRAME

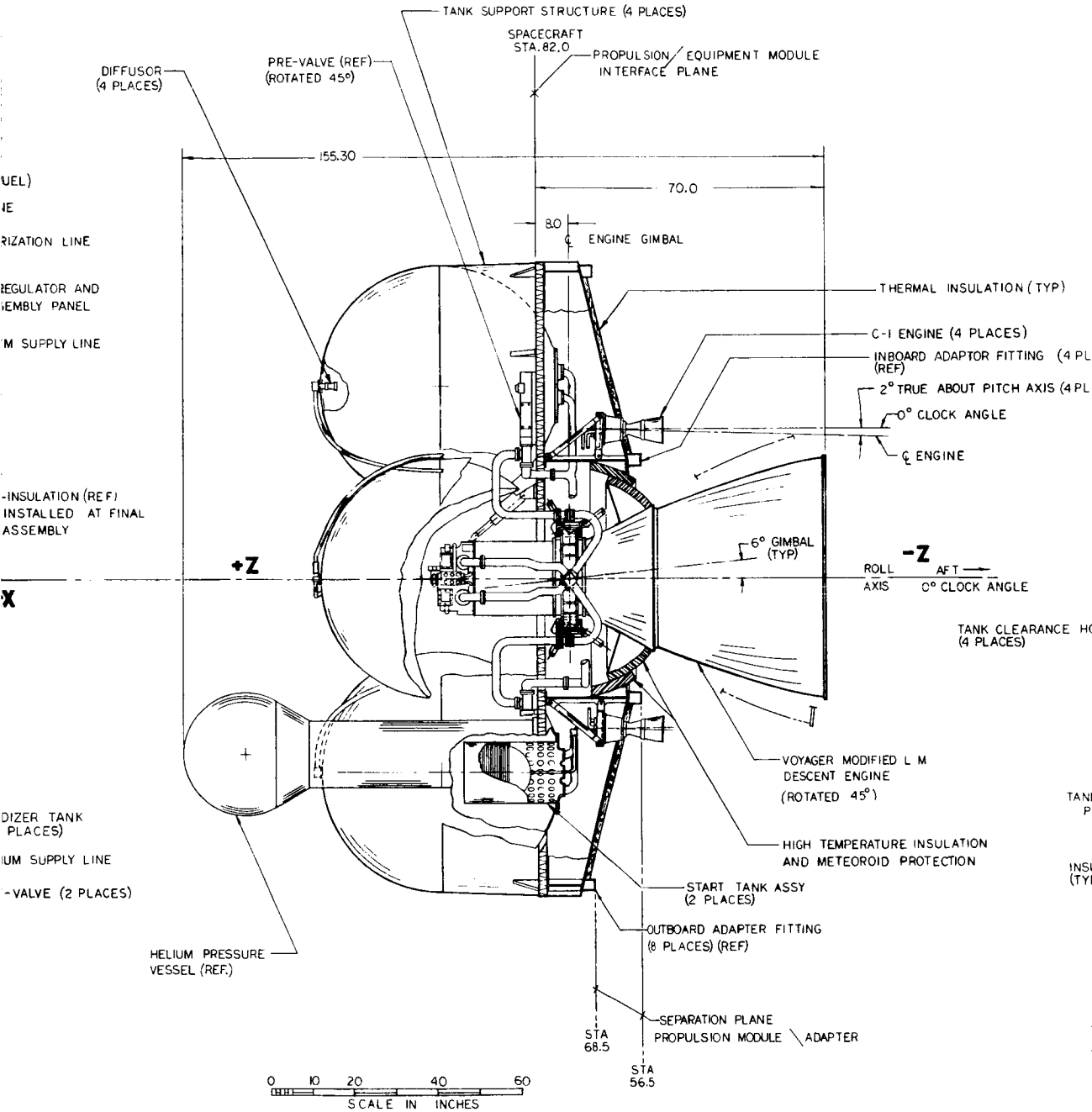

FOLDOUT FRAME

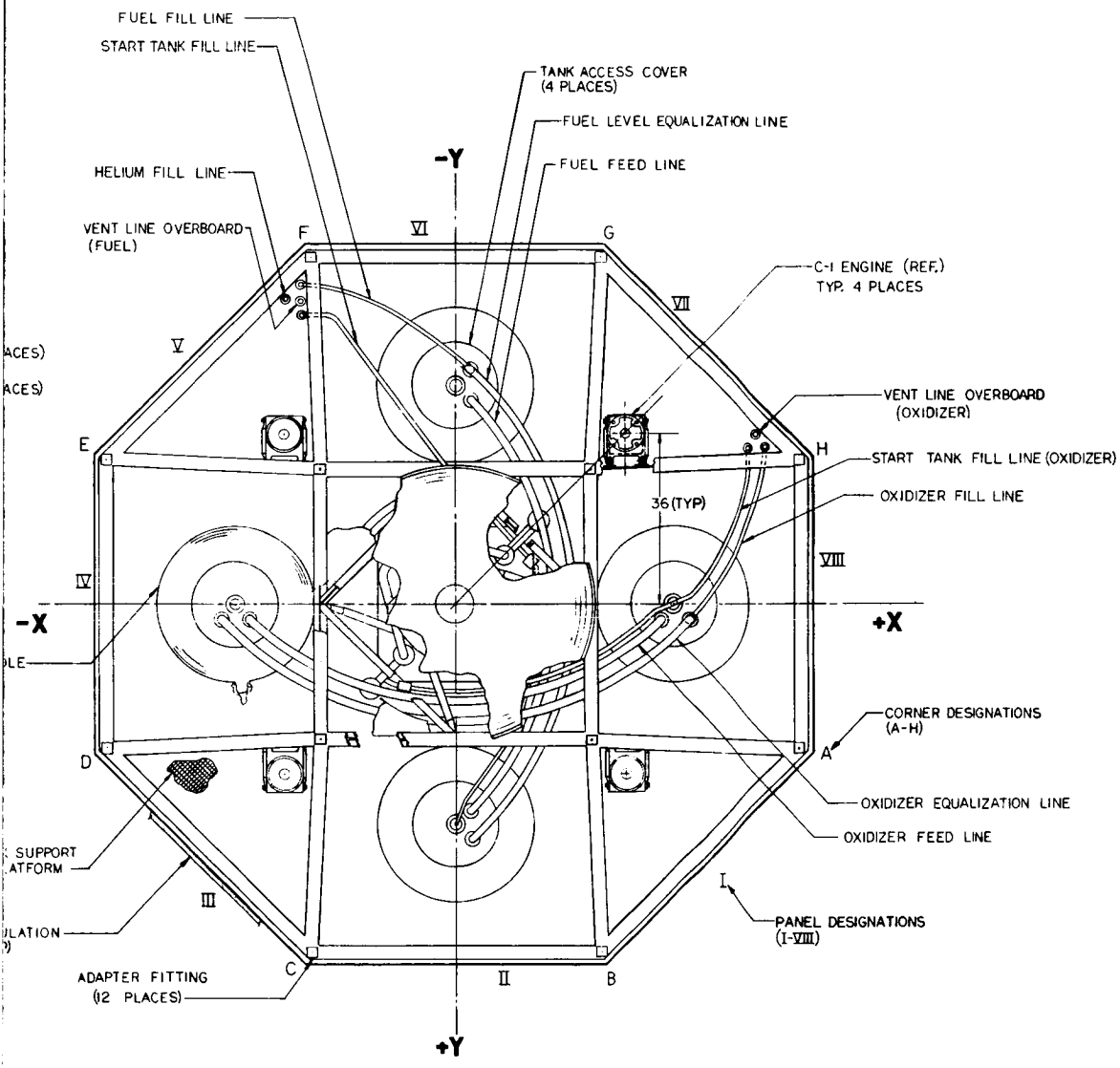

VIEW LOOKING FORWARD

Figure 4-2

module structure. In the view looking aft, the routing of the tank pressurization and equalization lines can be seen.

In this configuration, it is possible to transfer propellant between tanks during zero-g conditions. The problem is greatest after orbit insertion, when only a small fraction of the propellant remains in the tanks. The start transient for the first orbit trim firing has been examined for the worst-case condition, in which all the oxidizer would have migrated into one tank. There will be 4 seconds of propellant-settling firing before the main tanks are connected to the engine and, if sufficient propellant is transferred through the equalization line during these 4 seconds, gas ingestion will not be a problem.

Differential equations representing the tanks and their interconnections were developed and integrated for the first 5 seconds. The results of these calculations are shown in Figure 4-3. The oxidizer side of the system was studied because it is more critical than the fuel because of its higher density. Frictional loss in the connecting lines was computed and found to be important because of the small effective head differential

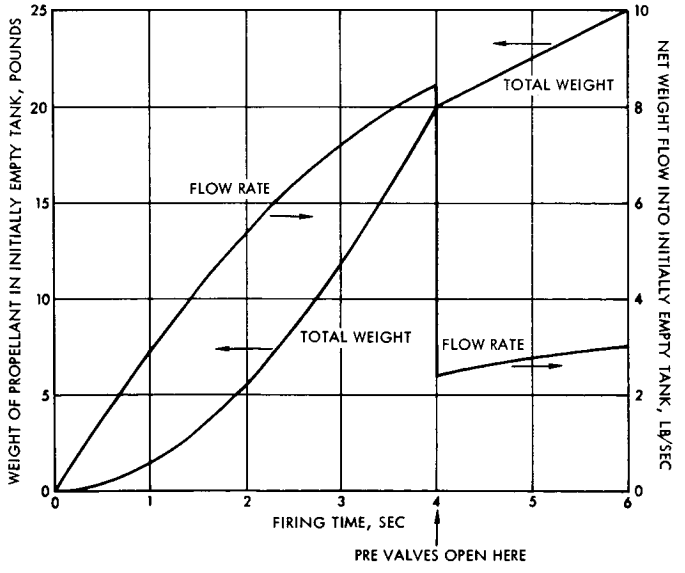

Figure 4-3
PROPELLANT TRANSFER VERSUS FIRING TIME.

between the two tanks. The fluid inertia in the connecting pipes was important during the initial few seconds. As may be seen in Figure 4-2, the propellant weight flow in each line at 4 seconds was 4.2 lb/sec. The total oxidizer transferred to the initially empty tank in this time was 20 pounds, and the propellant height in this tank was 1.4 inches.

At 4 seconds the pre valves are opened, flowing 3.3 lb/sec of oxidizer from each oxidizer tank. At this point there will still be a net flow of 0.9 lb/sec of oxidizer into the initially empty tank. The engine can therefore continue to fire indefinitely without unporting.

The four backup C-1 engines are at the four corners of the structure cruciform. The propellant lines for these engines are routed to a single set of explosive isolation valves mounted on the propellant component modules.

The burn-time requirement of the engine is based on its ability to consume the 16,000 pounds of useful propellant. The breakdown of these 16,000 pounds into the maximum amounts required for each maneuver, determines the engine impulse requirements:

Maneuver	Total Impulse (lb-sec)
Pre-orbit insertion	613,000
Orbit insertion	3,990,000
Orbit trim	217,000

The first maneuver, the velocity increment for the planetary arrival date separation, varies with launch opportunity, and day of launch within the opportunity. The most severe case takes place during 1973 for the earliest arrival dates as shown in Figure 4-4. The velocity increment requirement for this first maneuver was based on 205.3 meters/sec. As can be seen from Figure 4-4, this is a 3-sigma high and therefore a very severe condition. In addition, the determination of burn time was based on a spacecraft with a reasonable expected growth weight to 30,076 pounds. It is very unlikely that this spacecraft will be flown during the first launch. It is therefore apparent that there is a great deal of conservatism built into the engine design velocity increment capability for the first maneuver. This first maneuver from an engine

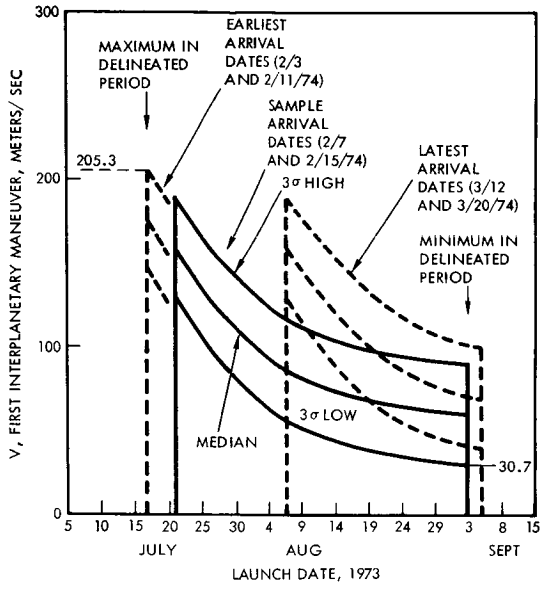

Figure 4-4

VELOCITY INCREMENT REQUIREMENTS, FIRST INTERPLANETARY MANEUVER, VOYAGER, 1973.

standpoint is the most critical since the amount of charring of the ablative material in the thrust chamber determines the allowable burn time for the subsequent orbit insertion firing. Even with this very conservative approach, the present LMDE thrust chamber can accomplish the entire Voyager mission.

The minimum impulse bit and repeatability needs are based on the requirements of the JPL 1973 mission specification, page 45, dated January 1, 1967, Document No. SE 002 BB 001-1B21. The portion applicable to the propulsion subsystem is shown in Table 4-1.

The most stringent condition for the engine, when applying the requirement of Table 4-1, will occur for the minimum weight mission. Assuming a spacecraft configuration that is capable of growth, the minimum weight mission would be the one requiring the least expenditure of propellant. The most stringent condition from the standpoint of minimum impulse bit for the engines will occur when the propellant employed for a maneuver has just about been expended and the vehicle is at the burnout weight.

Table 4-1. Spacecraft Minimum Velocity and Execution Accuracy Requirements

Maneuver	Minimum Velocity Increment (meters/sec)		3σ Error Component Parallel to Specified Velocity Increment, (meters/sec) Larger of the Values:	
	Required	Design Goal	Required	Design Goal
Midcourse	1.0	0.3	0.1 or 3% of the increment	0.03 or 2% of the increment
Orbit in Insertion	1000	---	3% of the increment	1.5% of the increment
Orbit Trim	5.0	1.5	0.5 or 5% of the increment	0.2 or 3% of the increment

It is important also to note that, as indicated on page 46 of the JPL specification, for purposes of determining the propellant quantity allocated for orbit trim, the required velocity increment must be available assuming the capsule has not been ejected. However, for the purposes of determining engine minimum impulse bit and accuracy requirements, the capsule will be assumed to have been ejected in order to gain the lightest weight condition.

To obtain the lightest weight mission in terms of propellant to be expended, the minimum orbit insertion capability required by the JPL specification, page 44, of 1.75 km/sec was used. The weight breakdown of the planetary vehicle used is shown below.

Flight Capsule	5,000.0 lb
Science	400.0
Support Equipment	50.0
Equipment Module	2,084.2
Propulsion Module Inert	2,357.9
Residual Propellant	416.8
Usable Propellant	10,842.5
Gross Weight	21,151.4 lb

The final burnout weight for this vehicle was obtained by removing the total usable propellant of 10,843 pounds from the spacecraft. The resultant 10,309 pounds was used as an input to obtain the burnout weights for orbit insertion of 10,685 and 19,185 pounds for midcourse.

Using the previously mentioned velocity increment requirements and the above burnout weights, the engine required capabilities for minimum impulse bit and repeatability are as shown in Table 4-2.

Table 4-2. Engine Minimum Impulse and Execution Accuracy Requirements

Maneuver	Engine Minimum Impulse Bit Requirements (lb-sec)		3σ Engine Repeatability Requirements (± lb-sec) Larger of the Values:	
	Required	Design Goal	Required	Design Goal
Midcourse	1958	587	196 or 3% of the increment	58.7 or 2% of the increment
Orbit Insertion	1,089,000	---	32,700	16,300
Orbit Trim	2710	814	271 or 5% of the increment	108 or 3% of the increment

At this time not much data on the LMDE shutdown repeatability at low thrust is available since it is not of major significance in the Apollo program. Based on the data available, however, run-to-run variability at the low thrust level of 1700 pounds can meet the design requirements but does not meet the design goal. However, with the use of low thrust, small solenoid valves for the Voyager configuration, a very significant improvement will occur and the design goal should be attainable.

The propulsion subsystem has a storage life capability of 3-1/2 years plus an operational life capability of 2 years. The 3-1/2 year storage capability will provide for delivery 1 year prior to launch and the missing of one launch opportunity. The 2-year operational life will provide the capability for the longest Mars transit time plus a 1-year orbital life.

System integrity is therefore paramount because of the long mission times involved. It is mandatory that the propulsion subsystem be leak-tight both in the gas and the liquid systems. This requirement dictated the need for brazed or welded manifolding and connections to all components. Flanged connections were only used where disassembly capability is required and where it cannot be performed if the joint is brazed or welded.

Pressurant and propellant tanks are designed with the same proof and burst safety factors used as on the Apollo program; 1.33 x maximum operating pressure for proof and 1.5 for burst.

The thrust vector misalignment of the main engine will be no more than 1/8 inch off, or angled at more than 1/2 degree from the centerline of the propulsion module. The nonablative backup engines will improve on this by an order of magnitude.

The main engine roll moment about the spacecraft centerline during firing will not exceed 2 ft-lb when the thrust is directed through the spacecraft center of gravity. The backup engines have large roll moment arms, but with their lower thrust levels should also be able to meet this value.

The design of the propulsion subsystem is based on achievement of the maximum probability of mission success with the alternative of partial success in the event of a noncatastrophic component failure. This was achieved by the use of a conservative design philosophy limited to the utilization of well-established technology. Wherever possible, well-developed components of demonstrated reliability were utilized. In component selection, highly reliable, single components have been used rather than redundant items of lower reliability. If components of this type were not available, then passive redundancy was utilized to increase the reliability level. Active redundancy was used where no reasonable alternative existed. Active redundancy is exemplified by incorporation of the C-1 engines as a backup for the main engine. Active sensing of main engine failure is accomplished by use of an on-board, thrust-integrating accelerometer. If no thrust indication is recorded 3 seconds after the start signal has been sent to the main engine, the backup engine explosive-isolation valve is fired and the backup engines are turned on.

Spacecraft attitude control, during backup engine operation, will be obtained by pulsing one of the diagonally-paired engines for pitch and yaw control. Roll attitude will still be stabilized by the four 3-pound, cold gas, ACS thrusters.

During orbit insertion, the main engine fires for about 300 seconds. The backup engines, however, are required to operate continuously for about 9000 seconds. Pulsing for attitude control amounts to a loss in impulse. The loss of impulse is made up by extending by a few percent the engine firing time.

In order to maximize the probability of success of the Voyager program, sufficient instrumentation and telemetry equipment have been provided to check in-flight operation of all principal propellant supply and engine components. This information will also be used to benefit subsequent Voyager missions.

In keeping with the established spacecraft design ground rules, the explosively actuated valves of the propulsion subsystem, their circuitry, and the shielding of the circuits conform to AFETR-P80-2. Safeing of the explosive valves is accomplished in the pyrotechnic distribution subsystem of the spacecraft.

The primary thermal constraints on the engine are on those surfaces which impose a heat load on the spacecraft solar array. The engine nozzle extension will be the main contributor. Since the total heat input to the array is a function of the radiated engine heat plus the heat input received from the sun, two temperature limits on the engine resulted because of the decreasing solar flux during the interplanetary trajectory. The external skirt insulation blanket was designed so that its outer surface temperature will not exceed 750°F for the Mars orbit insertion maneuver. The maximum combustion chamber exterior wall surface temperature will not exceed 400°F for any maneuver.

4.3 PROPULSION INTERFACES

The propulsion subsystem interfaces with other subsystems are illustrated in Figure 4-5. All electrical power to the various electrically operated components of the propulsion subsystem is derived in proper sequence from the power distribution subsystem which also safes and

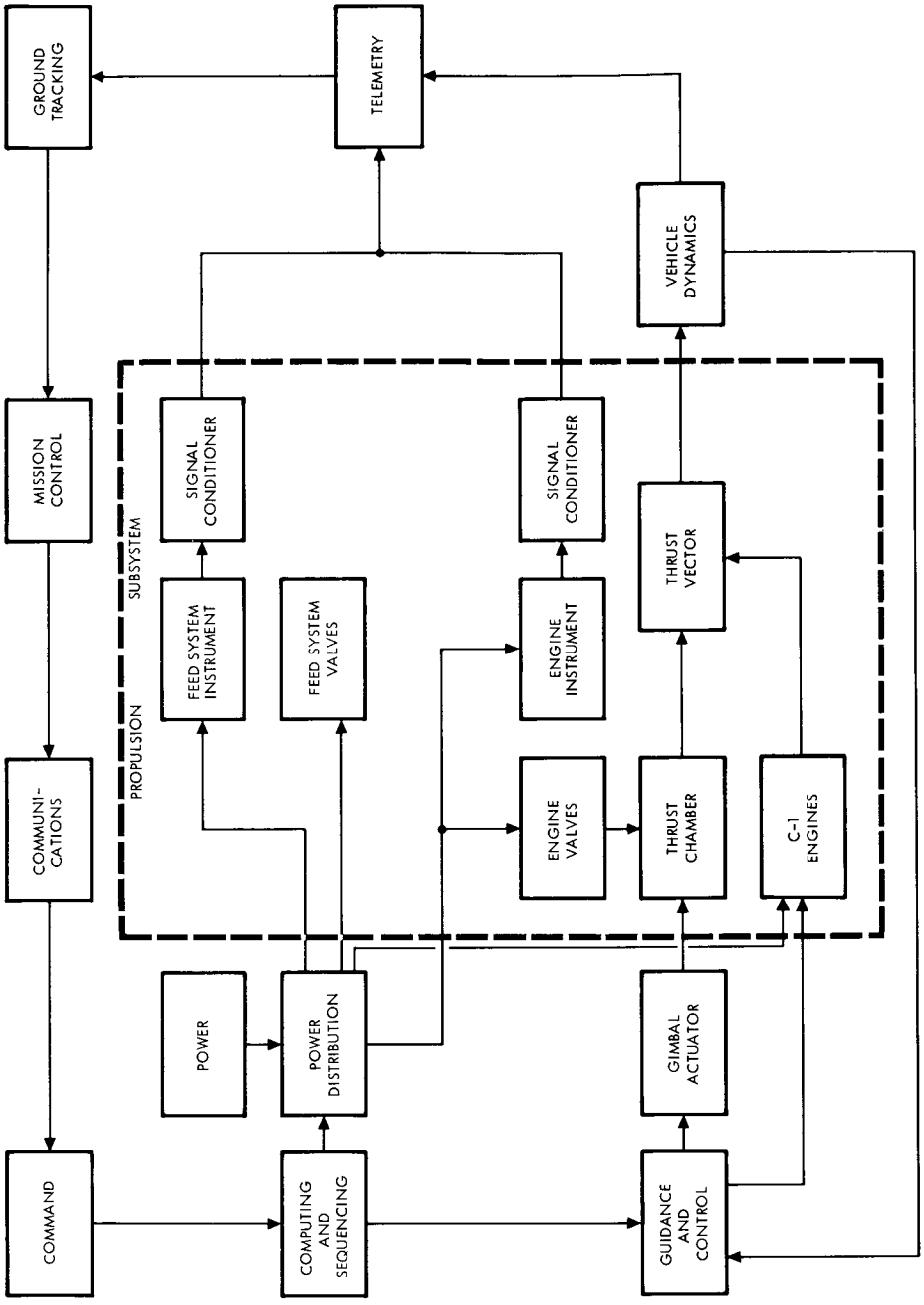

Figure 4-5
PROPULSION SUBSYSTEM CONTROL INTERRELATIONSHIP.

arms the pyrotechnic valves. The outputs of the sensors which monitor the operation of the propulsion subsystem are fed to the telemetry subsection for transmission. The interface with the structure subsystem is represented by the mechanical attachments through which vehicle structural and thrust loads are transmitted. The thermal interface between the propulsion subsystem and the equipment module is comprised of both engine heating of the spacecraft and the thermal control required of the spacecraft to keep the propulsion subsystem components and the propellant tankage within acceptable temperature limits.

The propulsion subsystem propellant tanks are attached to the propulsion module structure through an intermediate tank support skirt. The pressurant tanks are similarly mounted. The engine gimbal ring is supported by a truss system that is attached to the propulsion module structure. All components such as, valves, regulators, etc., are in modules mounted on the tank support platform. The propellant lines are configured in arcs joining the tank bottoms below the tank support structure. Since these lines penetrate the main structure at several points, the lines are specifically shaped to permit easy assembly and disassembly of the propellant feed system manifolding.

The propulsion subsystem requires that the thermal subsystem maintain the propellant and component temperatures within the limits specified in Figure 4-1. On the other hand, the operation of the propulsion subsystem imposes thermal loads on the spacecraft by conduction and radiation from the engine and the exhaust plume. These thermal inputs result in the need to insulate the nozzle extension and are discussed in Section 4.4.1.

4.3.1 Electrical Power Distribution

The operation of the propulsion subsystem requires that sufficient electrical power be provided at specifically defined intervals during the flight of the spacecraft. In the design of the propulsion system, electrical components requiring a precisely regulated power source have been avoided. However, the use of solenoid-actuated valves precludes the acceptance of very wide voltage changes by the power source.

The electric power required by the propulsion subsystem, exclusive of instrumentation requirements, can be met by the nominal spacecraft

system power at 37 to 50 volts. Since most available electrically actuated valves are designed for a nominal 28 volt operation, adapting these items to the higher spacecraft voltage will require rewinding of the actuator coils. This process will not affect functional operation of the valves so that major requalification of these components will not be necessary.

The electrical interface between the propulsion subsystem and the spacecraft power source is a junction box attached to the propulsion module structure from which all cabling proceeds to the propulsion components. Power switching of the components is accomplished upstream of the junction box in the spacecraft power distribution subsystem.

The majority of the components require power for a comparatively short period of time as shown in Table 4-3. The major exceptions are the engine propellant valves, which draw power for the entire period when the engine is thrusting.

With the exception of the instrumentation, no power is required by the propulsion subsystem until the Mars-arrival separation maneuver. The valve actuation time intervals are average values and may be varied without significant effect on the operation of the system. The engine-on times are based on the most severe requirements of the 1973 through 1979 missions as dictated by the impulse requirements listed in paragraph 4.2.1, and the appropriate engine thrust levels.

Table 4-3. Propulsion Subsystem Component Power Requirements (Exclusive of Instrumentation)

Component	No. of Units	Duration of Operation (Nominal)	Power Required Per Unit (Watts)
Explosive Valve	24	0.01 sec	0.1
Start Solenoid Quad Valve Package	2	3 sec	200
Low Thrust Quad Solenoid Valve Package	2	Engine ON	200
Motor Actuated Prevalves	4	3 sec	25
High Thrust Ball Valve Package	1	Engine ON	65

The power schedule and sequence of operation for the propulsion subsystem is shown in Table 4-4. The numbers in parenthesis correspond to those shown in the system schematic of Figure 4-1.

In keeping with the goals of providing completely automatic operation of the Voyager spacecraft, telemetry requirements for the propulsion subsystem are based on recovery of sufficient diagnostic information to assess the degree to which this subsystem has performed satisfactorily and also to provide decision-making information for ground command of subsystem operation, when required. All of the telemetered functions can be acceptably sampled at low rates when the propulsion subsystem is inactive since their values are not expected to change abruptly during the major portion of the lifetime of the vehicle. For these slowly changing parameters and for the simple event indications, a nominal 48 seconds between samplings is adequate. In order to provide meaningful assessment of propulsion subsystem performance, measurements must be made of rapid transients. The changes in engine-chamber and feed system pressures are primary examples and require 0.35 second between samples to provide meaningful data. Table 4-5 lists the propulsion subsystem operating parameters to be telemetered during firing of the engine. In the event of a catastrophic failure of the propulsion system, there is a high probability that the vehicle, and hence, the antenna may be damaged so that further data will not be recovered from the spacecraft. Should this occur, without real time data transmission, it is unlikely that cause of failure could be determined.

The relationship between the propulsion subsystem and those subsystems exercising a command relationship to the propulsion subsystem are also illustrated in Figure 4-5. Command functions are introduced into the propulsion subsystem as electrical signals to actuate the various propulsion subsystem components and command the two gimbal actuator assemblies.

4.3.2 Reliability Assessment

The analysis of Voyager propulsion subsystem reliability is presented in Volume 2, Appendix E3. A computerized mission phase failure mode and effects analysis was used to assess the effects of

Table 4-4. Propulsion Subsystem Power Schedule and Sequence of Operation

Event	Sequential Step	Command	Nominal Time of Event (sec)	Subsystem Power Level Required During Each Sequential Step (watts)
Planetary Arrival Date	1	Open pressurization valve (1)*	-10	
	2	Open propellant tank isolation valves (2)(3)	-9	
Separation Maneuver	3	Open start tank control valves (4)	-3	400
	4	Open low thrust engine control valves (5)	0	800
	5	Open feed system pre-valves (6)	4	1000
	6	Close start tank control valves	7	600
	7	Shutoff power to propellant pre-valves (valves remain open)	8	400
	8	Close low thrust engine control valves	374	0
	9	Close feed system pre-valves	375	200
	10	Shutoff power to propellant pre-valve	379	0
Seal Pressurization System		Fire valves (7)(8)(9)		
Interplanetary Trajectory Correction Maneuver	1	Open start control tank valves	-3	400
	2	Open low thrust engine control valves	0	800
	3	Open feed system pre-valves	4	1000
	4	Close start tank control valves	7	600
	5	Shutoff power to feed system pre-valves (valves remain open)	8	400
	6	Close low thrust engine control valves	As req'd	0
	7	Close feed system pre-valves	-	200
	8	Shutoff power to feed system pre-valves	-	0
Orbit Insertion	1	Open pressurization valve (10)	-10	
	2	Open propellant tank isolation valves (11)(12)	-9	
	3	Open start tank control valves	-3	400
	4	Open low thrust engine control valves	0	800
	5	Open feed system pre-valves	4	1000
	6	Close start tank control valves	7	600
	7	Shutoff power to feed system control pre-valves (valves remain open)	8	400
	8	Open high thrust engine control valves (13)(injector pintle automatically moves to the high thrust position)	9	465
	9	Close to low thrust engine control valves	10	65
	10	Close high thrust engine control valves	412	0
	11	Close feed system pre-valves	413	200
	12	Shutoff power to feed system pre-valves	417	0
Seal Pressurization System		Fire valves (14)(15)(16)		
Orbit Trim Maneuvers		Orbit trim maneuvers are carried out in the same sequence and with the same power requirements as those of the trajectory correction maneuvers		
Depressurization		Fire valves (17)(18)(19)		

*Numbers in parenthesis correspond to valve numbers on the propulsion subsystem one page specification, Figure 4-1.

Table 4-5. Propulsion Subsystem Telemetry Measurements

Item	Accuracy (%)	Quantity	Range (psia)	Time Between Samples During System Operation (Sec)
Pressure				
Pressurization System				
Helium Tank	2	1	0-4500	48
Regulator Inlet	2	1	0-4500	48
Regulator Discharge	2	1	0-300	48
Propellant Tank Inlet Pressure	2	2	0-300	48
Feed System				
Oxidizer Tank Discharge	2	1	0-300	48
Fuel Tank Discharge	2	1	0-300	48
Oxidizer Start Tank Discharge	2	1	0-300	48
Fuel Start Tank Discharge	2	1	0-300	48
LMDE				
Engine Feed System Interface Oxidizer	2	1	0-300	0.35
Engine Feed System Interface Fuel	2	1	0-300	0.35
Injector Inlet Oxidizer	2	1	0-300	0.35
Injector Inlet Fuel	2	1	0-300	0.35
Chamber Pressure	2	2	0-200	0.35
C-1 Engines				
Chamber Pressure	2	4	0-200	0.35

Table 4-5. Propulsion Subsystem Telemetry Measurements (Cont)

Item	Accuracy (%)	Quantity	Range of	Time Between Samples During System Operation (Sec)
Temperature				
Pressurization System				
Helium Tank	5	2	0-150	48
Feed System				
Propellant Tank, Main Oxidizer	5	2	0-150	48
Propellant Tank, Main Fuel	5	2	0-150	48
Propellant Inlet to Engine, Oxidizer	5	1	0-150	48
Propellant Inlet to Engine, Fuel	5	1	0-150	48
Engine				
Thrust Chamber Case (2 Skirt, 2 Outer Skirt, 2 Head End, 3 Combustion Chamber, 2 Throat, 1 Actuator)	5	12	-65 to 1000	48
Events				
Pressurization System				
Explosive Valve Actuation	15			48
Engine				
Pintle Actuator Position	2			48
Quad Solenoid Valve Current*	2			48
Quad Solenoid Valve Position	16			48
Pre-Valve Position	8			48
Pre-Valve Current*	1			48
Pilot Operated Ball Valves Position	8			48
Pilot Operated Ball Valves Current*	2			48

*Monitored in distribution control unit

alternative component failures on mission success. The results of this analysis indicate that the selected propulsion subsystem, has an estimated mission reliability for orbiting Mars and completing the orbit trim maneuvers of 0.9656.

The applicable reliability equation is:

$$R_{Propulsion} = \left[R_{Feed\ and\ Propellant}\right] \left\{1 - \left[1-R_{LM}\right] \left[1 - \left(R_{C-1} \cdot P_o\right)\right]\right\} = 0.9656$$

$R_{Propulsion}$ = Reliability of the propulsion subsystem

$R_{Feed\ and\ Propellant}$ = Reliability of the pressurization feed and propellant acquisition equipment

R_{LM} = Reliability of LMDE

R_{C-1} = Reliability of four C-1 engines

$P_o = 75\%$ = Estimated percentage of orbital objectives accomplished if C-1 engines are used for orbit insertion.

4.4 MAIN ENGINES

The studies of the Voyager spacecraft engine design fall into two major categories. The first is concerned with the capability of the LM Descent Engine to perform the Voyager mission; and the second, with the use of the LM engine in conjunction with C-1 engines.

The major effort in the engine area was examination of the LMDE to determine what thrust levels should be used, the needed nozzle extension design, and what modifications would be required to ensure that the engine would meet the requirements of the Voyager mission. This section discusses the implication of Voyager mission requirements and vehicle interfaces on the LM Descent Engine design, and the tradeoff studies which were used to select operating parameters and to define hardware modifications to the engine.

The engine duty cycle required for the nominal Voyager mission consists of:

- A planetary arrival date separation maneuver which will require a maximum total impulse of 613,000 lb-sec.
- Up to two interplanetary trajectory maneuvers. The maneuvers will require low, but precise, impulse bits.
- An orbit insertion maneuver. This maneuver will consume the major portion of the system propellant and will require a maximum total impulse of up to 3,990,000 lb-sec.
- Up to four orbit trim maneuvers during the operational life of the mission. These maneuvers will require a total of 217,000 lb-sec of impulse.

The maximum thrust level selected is 9850 pounds. This thrust level was chosen for the orbit insertion maneuver because it minimizes burn time, results in maximum propulsion system performance, and is a level for which there is considerable previous test experience.

The low thrust level for the other maneuvers was selected as 1700 pounds. This selection was based on a compromise between engine life, specific impulse, and the ability to meet the minimum impulse bit

The design of the radiation cooled nozzle extension for the LMDE was modified by adding external insulation to keep radiation to the solar array at an acceptable level.

The valving and thrust control recommended represents a minimum modification to the existing engine. The continuously variable thrust control actuator was replaced by a simpler two-position actuator, and a small quad redundant solenoid valve package was incorporated for controlling propellant flow during the low thrust maneuver.

4.4.1 Configuration Selection

This section presents the work which was performed in adapting the Lunar Module Descent Engine to the Voyager mission requirements. In most respects the LM Descent Engine can be used without significant modification. Hardware modifications which are either desired or

required for the Voyager application include changes to the engine throttling capability and changes in the configuration of the head end assembly and the nozzle extension. The considerations which were employed in studying these aspects of the engine are presented below.

The Apollo lunar descent mission requires that the engine be continuously throttleable from 1050 to 6300 pounds thrust in addition to a single operating point at 9850 pounds thrust. In contrast, the Voyager mission requires only a two thrust-level capability. High thrust to minimize burn time and "gt" losses during orbit insertion and low thrust to meet the minimum impulse bit and repeatability requirements.

In selecting optimum thrust levels for Voyager, the following items were considered:

- Engine Burn Time. Since the life of the ablative chamber is limited, it is desirable to minimize burn time and hence to maximize the thrust in each phase. In any event, the current combustion chamber design places definite limits on firing time capability, and thrust levels must be selected so that they are consistent with these limits.

- Minimum Impulse Bit and Repeatability. For the trajectory and orbit correction maneuvers, small impulse bits and good shutdown repeatability are required. These requirements tend to drive the optimum thrust level toward the lower end of the descent engine thrust scale as impulse reproducibility improves with decreasing engine thrust setting.

- Engine Performance. In order to maximize the payload capabilities of the vehicle, it is desirable to operate the engine in thrust regions where the delivered specific impulse is maximum. Specific impulse for the LMDE increases with increased thrust level.

In addition to the above, the selected thrust level should lie in a region where current test data exist and where currently available test facilities can be used. These factors tend to set the high thrust level at 9850 pounds, where most of the currently available data are concentrated, and tend to limit the low thrust level to above 1500 pounds since the high altitude facilities at the Capistrano Test Site and at WSTF are not capable of operating simultaneously at 9850 pounds thrust and below 1500 pounds thrust.

The results of engine qualification tests at these levels are shown below in Table 4-6.

Table 4-6. LMDS Engine Qualification Test Results

Engine Serial No.	Burn Time (sec)	Thrust (lb) Initial	Thrust (lb) Final	Specific Impulse (sec) Initial	Specific Impulse (sec) Final
1024	20	1500	1500*	299.3	287.5
	390	9750	- 9800	304.3	302.2
1025	8	1500	1500	301.7	289.5
	20	1500	1500	296.5	284.3
	390	9720	9850	305.1	302.5
1034	20	1500	1500	298.9	293.3
	390	9730	9850	304.3	301.8

*No change over the run period.

The burn time required to de liver 3,990,000 lb-sec of impulse for the orbit insertion maneuver is 405 seconds. Since the single continuous-burn capability of a fully-charred engine is 770 seconds, it can amply accommodate operation at the 9850 pound thrust level for the orbit insertion maneuvers. The specific impulse above 6000 pound thrust is practically flat and, therefore, the selection of a higher thrust level is unaffected by engine performance. Finally the shutdown impulse reproducibility for the orbit insertion maneuver, as given in Table 4-2, is an order of magnitude larger than the reproducibility demonstrated by the current LMDE. Therefore, the 9850-pound selection for the high thrust level meets all vehicle operational requirements.

For the low thrust mode, the most stringent requirements from the standpoint of burn time and impulse repeatability are posed by the arrival date separation, and trajectory correction maneuvers, which require a single-burn total impulse of up to 613,000 lb-sec. The lowest LMDE thrust level of 1050 pounds will require a firing time duration of 584 seconds. The engine is currently qualified to a duty cycle which includes a single firing of 870 seconds duration, and is therefore, perfectly capable of operation for 584 seconds. However, due to heat soakback following

the 584 second firing, the combustion chamber ablative liner will char through to the encasing titanium wall, and will have to be restarted in this condition for the full-thrust orbit insertion maneuver. Although the engine has been restarted after fully charring in ground tests, and will be restarted in space after fully charring in early Apollo flights, it is nevertheless desirable to operate the engine in such a manner that full thrust restart on a completely charred chamber is not necessary. This can be accomplished by increasing the 1050 pound low thrust level. Increased thrust level also results in an increase in specific impulse. The limiting characteristic for increasing thrust would be the impulse repeatability.

Thermal analysis of the combustion chamber was performed to define the extent of charring which results from operation at various thrust levels followed by heat soakback in space. A one-dimensional thermal model of the combustion chamber, developed in support of the original descent engine design, was used. It should be noted that this computer program is conservative at low thrust levels because of the way that the variation of heat transfer with chamber pressure is handled. The results of the thermal analysis are shown in Figure 4-6 which represents the char depth after soakback vs time of operation at three thrust levels. It was assumed for these calculations that, prior to the firings, the thrust chamber had a char depth of 0.34 inch as a result of engine acceptance. As can be seen from the figure, the firing time which results in complete liner charring following soakback increases as the thrust is decreased.

In Figure 4-7, the data from Figure 4-6 are replotted in terms of total engine impulse capability as limited by full charring of the chamber liner. Also shown in Figure 4-7 are the total separation maneuver impulse requirements for the 30,076 and the 20,107 pound planetary vehicle configurations for the '73 and subsequent missions. On the basis of these data, the lower limit of operation for the low thrust mode is 1700 pounds. At this thrust a very large margin in chamber life exists for missions subsequent to 1973, which require 110 m/sec velocity increment or less. It is very likely that a 20,107 pound vehicle will be flown in the 1973 mission, and again this results in a sizable margin. However,

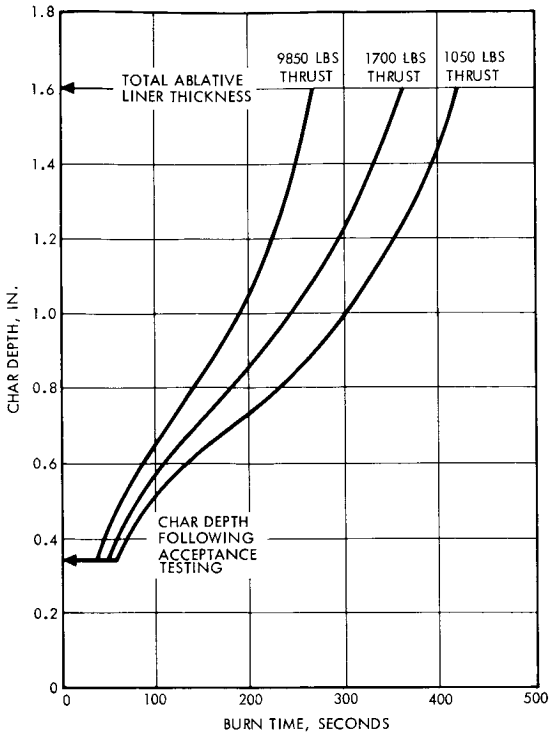

Figure 4-6

CHARR DEPTH FOLLOWING SOAKBACK AT VARIOUS THRUST LEVELS.

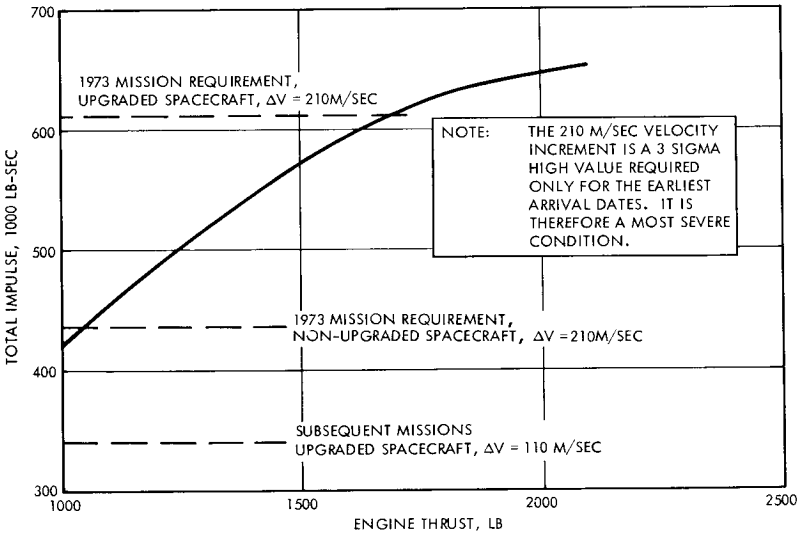

Figure 4-7

ENGINE IMPULSE CAPABILITY AS LIMITED BY COMPLETE CHARRING FOLLOWING SOAKBACK, as compared to Mars arrival date separation maneuver impulse.

even if an 30,076 pound vehicle is used in the 1973 flight, the 1700-pound thrust level is still compatible with the burn time requirements, and will result in just charring to the combustion chamber wall. Thus, it represents the minimum at which the low thrust level can be set.

While the thermal considerations discussed above set the minimum thrust level, impulse bit and repeatability considerations set the maximum. As far as minimum impulse bit is concerned, almost any small value can be delivered by adjusting the valve on time to a sufficiently low value. The basic problem then becomes the question of shutdown repeatability.

At this time not many data on the descent engine shutdown repeatability as a function of thrust are available as shutdown repeatability at the low thrust levels is not of major significance in the Apollo program. The available run-to-run and engine-to-engine variability from the descent engine program are plotted in Figure 4-8 and are compared to the most stringent design goals and design requirements. It should be noted that these data are for the current descent engine configuration, and that a

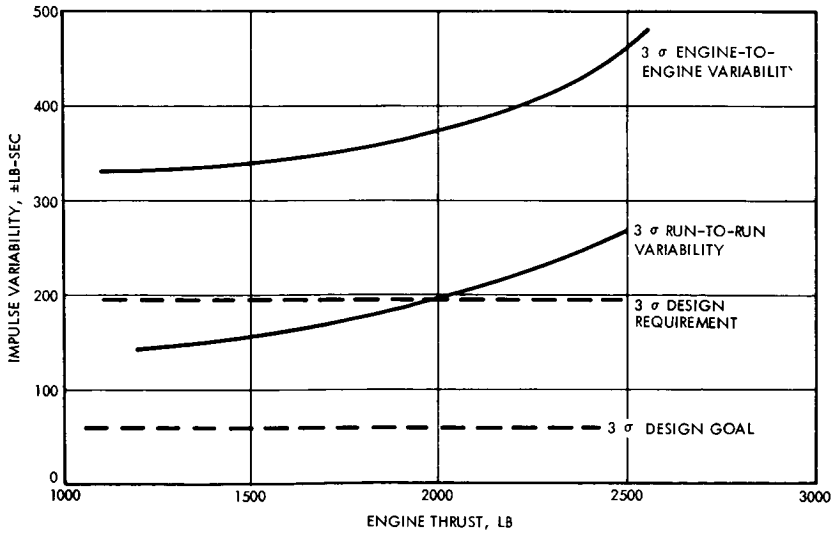

Figure 4-8

MEASURED SHUTDOWN IMPULSE VARIABILITY OF LMDE, with Apollo Head End Assembly Configuration.

sizable portion of the shutdown variation represented by these curves is due to instrumentation scatter. Figure 4-8 shows that the run-to-run variability of the engine in its current configuration can meet the design requirements at thrust levels less than 2000 pounds, but falls short of the design goal. The engine-to-engine variability is considerably above the design requirements at all levels.

Preliminary data correlations indicate that the majority of the shutdown variations arise from variations in the quad ball valve action time. As discussed in the following section, the ball valves will be replaced for the low thrust mode by fast acting solenoids with greatly improved action time reproducibility. Thus, a significant improvement in shutdown impulse repeatability will be realized.* Nevertheless, in order to minimize shutdown impulse variation, it is desirable to operate at 1700 pounds or the lowest thrust level permitted by the thermal constraints.

The selection of 1700 pounds as the low thrust level utilizes the engine where the specific impulse is higher than at lower levels. As compared to 1050 pounds thrust, operation at 1700 pounds thrust increases the specific impulse so that, during the first maneuver, about 100 pounds less propellant is needed. Any increase in thrust above the 1700 pound level results in negligible further specific impulse gains.

Based on the LMDE data, the Voyager predicted performance at nominal interface temperatures and pressures as specified in Figure 4-1 is as follows:

Maneuver	Nominal Thrust Level (lb)	Nominal I_{sp} (sec)
Planetary Arrival Date Separation	1,700	298
Orbit Insertion, Start	9,850	305
Orbit Insertion, End	10,000	303
Orbit Trim	1,700	289

*A program is currently in progress (MSFC Contract No. NAS 8-20864) which will demonstrate the minimum impulse and repeatability capabilities of the engine with MMH as adapted to Voyager.

The Task B approach to the engine head end configuration employed explosive valves for positive sealing and for propellant control. This was based on expected advancements in the state of the art of large, normally-open explosive valves and of the LMDE ball valves at the time of Task B. For Task D, the LMDE head end was reconsidered in the light of advancements on the engine during the additional years of development. During this time the sealing capability of the ball valves has undergone significant improvement while the large normally-open explosive valves are still in the experimental stage. The ball valves were therefore retained for control of the high-thrust mode of operation while a quad set of small solenoid valves were utilized for the low-thrust mode as shown in Figure 4-1 schematic. The present LMD pintle actuator could be replaced with a simpler two-position actuator, as was used in the Task B approach. However, the controlled actuator can also be eliminated entirely and the injector designed so that it automatically positions itself at high and low thrust positions as shown in Figure 4-9. The latter design was selected because, by eliminating a control component, it resulted in a lighter engine and an increase in reliability. It also eliminated a possible leak path through the actuator. The change from the present LMDE results in the following benefits:

- Improvement of shutdown impulse repeatability, as discussed in Section 4.4.1
- Simplification of the thrust control system
- Simplification of thrust command signal requirements
- Elimination of the currently required throttle actuator reference voltages
- Simplification of engine calibration and adjustment process
- Reduction of the operating requirements on the ball valves to a single start and shutdown
- Weight saving of 17.5 pounds.

In its present configuration, the descent engine uses a radiation-cooled columbium nozzle extension from an area ratio of 16:1 to 47.5:1. Vehicle thermal studies indicate that the nozzle extension heating rates

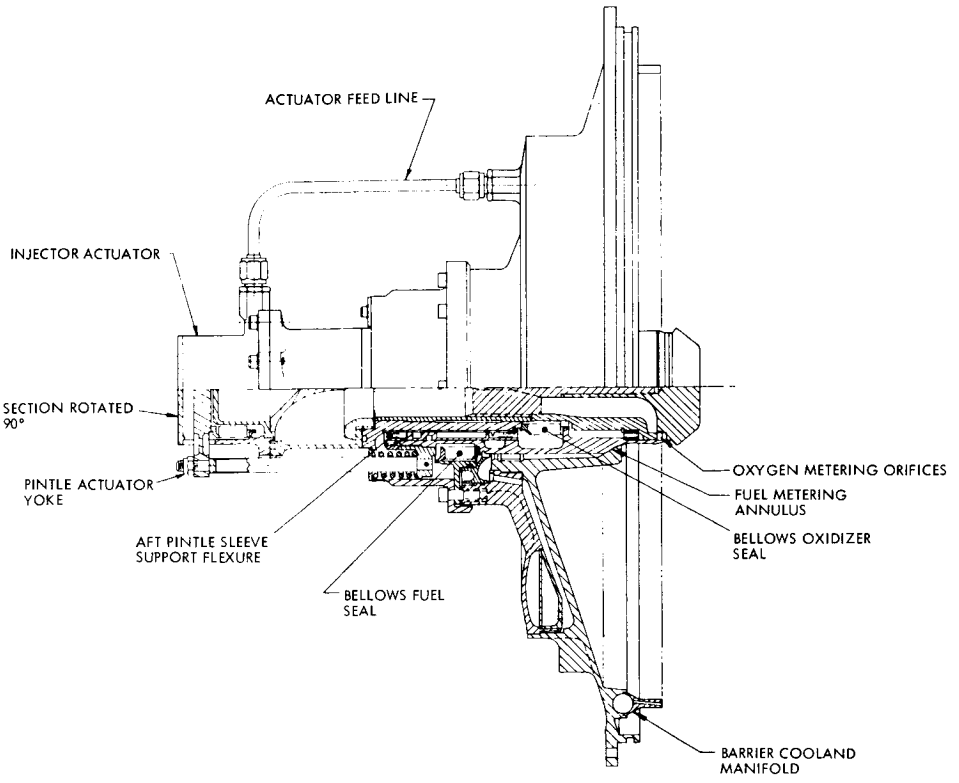

Figure 4-9

INJECTOR ASSEMBLY CROSS-SECTION shows the fuel-metering annulus in the closed position. The injector sleeve is supported by its flexural bushings rathes than sliding bearings to avoid cold welding. The pintle actuator drives the injector sleeve through yoked rods.

on the solar arrays located on the bottom surface of the vehicle are unacceptably high. Using a reflective shield around the nozzle extension, which would still allow radiation from the outside surface of the nozzle extension while protecting the solar arrays, is not acceptable because of space limitations. Thus, two means of limiting the heat load to the solar cells are available. One is to make the nozzle extension ablative and the other is to insulate the external surface of the extension and allow for radiation cooling from the inside surface only.

Provision of an ablative extension is attended by two problems. One is the large weight penalty. Even with optimistic designs, an ablative extension from 16:1 to 47.5:1 would weigh about 90 pounds. To carry the additional weight, the engine gimbal and thrust mount assembly might also have to be redesigned. The second problem derives from the difficulty and expense of fabricating a relatively thin 60-inch diameter ablative extension. Hence, it is preferable to insulate the existing radiation-cooled extension if practicable.

Thermal analyses indicate that the most critical heat load to the solar cells occurs as a result of the arrival separation maneuver, when the vehicle is near earth and the steady-state temperature of the array is already high due to solar radiation. The insulation of the nozzle extension, therefore, has to be designed for this condition. The most severe thermal stress on the nozzle extension, on the other hand, occurs during the full-thrust firing when gas side heat transfer coefficients are the highest. With sufficient insulation to limit the solar array temperature to a maximum of 300°F at the end of the separation maneuver, the maximum internal wall temperature of the columbium wall is 2520°F. This temperature occurs at an area ratio of 18:1 and compares with 2430°F for the current uninsulated extension. The relatively small increase in temperature is due to the fact that the current extension is partially buried within the LM descent stage structure and can not radiate freely to space. Insulation of the extension, therefore, does not alter its thermal environment as much as might be expected, and only a relatively small temperature increase results.

Operation at 2520°F is well within the capabilities of the columbium, but is very close to the 2600°F upper temperature limit of the aluminide coating used for oxidation protection of the columbium. In order to provide additional margin, the aluminide coating will be replaced by a silicide coating which has a 2700°F temperature limit capability. The silicide coating is currently used by TRW on the Multi-Mission Bipropellant Engine, which uses N_2O_4 and monomethyl hydrazine as propellants.

The nozzle insulation material is a molded fiberfrax cone fabricated in three sections mounted directly on the extension surface. The aft section will be conical vacuum-formed to the exact contour of the nozzle extension, with the small opening of sufficient diameter to be slipped over the extension for a flush fit. This section will be fastened to the aft stiffener on the nozzle extension. The other two sections will be formed as a split ring and assembled flush to the forward end of the extension, where they will be held in place by a metal band. This insulation package will be designed with sufficient flexibility and structural strength to withstand launch, boost and mission environments. The predicted operating

temperatures are well within the temperature capability of the fiberfrax insulation which can be used up to 3200°F for short periods of time.

4.4.2 Selected Voyager Engine Configuration Description

The modified LM Descent Engine proposed for Voyager is shown in Figure 4-10 and a specification in Figure 4-11. The major components of the engine and their significant design features are listed in Table 4-7. The injector, the combustion chamber, the nozzle extension, the thrust mount, and the gimbal assembly are the same as used on the LM Descent Engine. The injector pintle actuator, the control valve and the flow control system are simplified to provide two-thrust-level operation in place of continuous throttling.

Engine performance in terms of specific impulse varies both with thrust and with the condition of the engine during any part of the duty cycle. The change in performance during the duty cycle is due to erosion of the chamber throat and the consequent reduction in chamber pressure and nozzle expansion ratio.

The performance estimates quoted below are based on LM Descent Engine test data with N_2O_4 and 50/50 UDMH/hydrazine as propellants. A test program to evaluate performance with MMH as the fuel is in progress, and data from these tests will be used when they become available.

For a typical mission, the initial low-thrust maneuver is at 1700 pounds thrust. The initial nominal specific impulse will be 298 seconds. During this maneuver, the chamber walls will be charred, however, there will be essentially no degradation in performance since no throat area change takes place. Hence, the engine will deliver an average I_{sp} of 298 seconds for all maneuvers prior to orbit insertion.

At the start of orbit insertion, at 9850 pounds thrust, the initial specific impulse will be a nominal value of 305 seconds. During the orbit insertion maneuver, erosion in the chamber throat will decrease the effective area ratio of the nozzle resulting in a decrease in specific impulse. Predicted change in performance during the orbit insertion maneuver is 2 to 3 seconds at full thrust. A secondary effect of throat erosion is the decrease in chamber pressure, which in turn increases the pressure drop

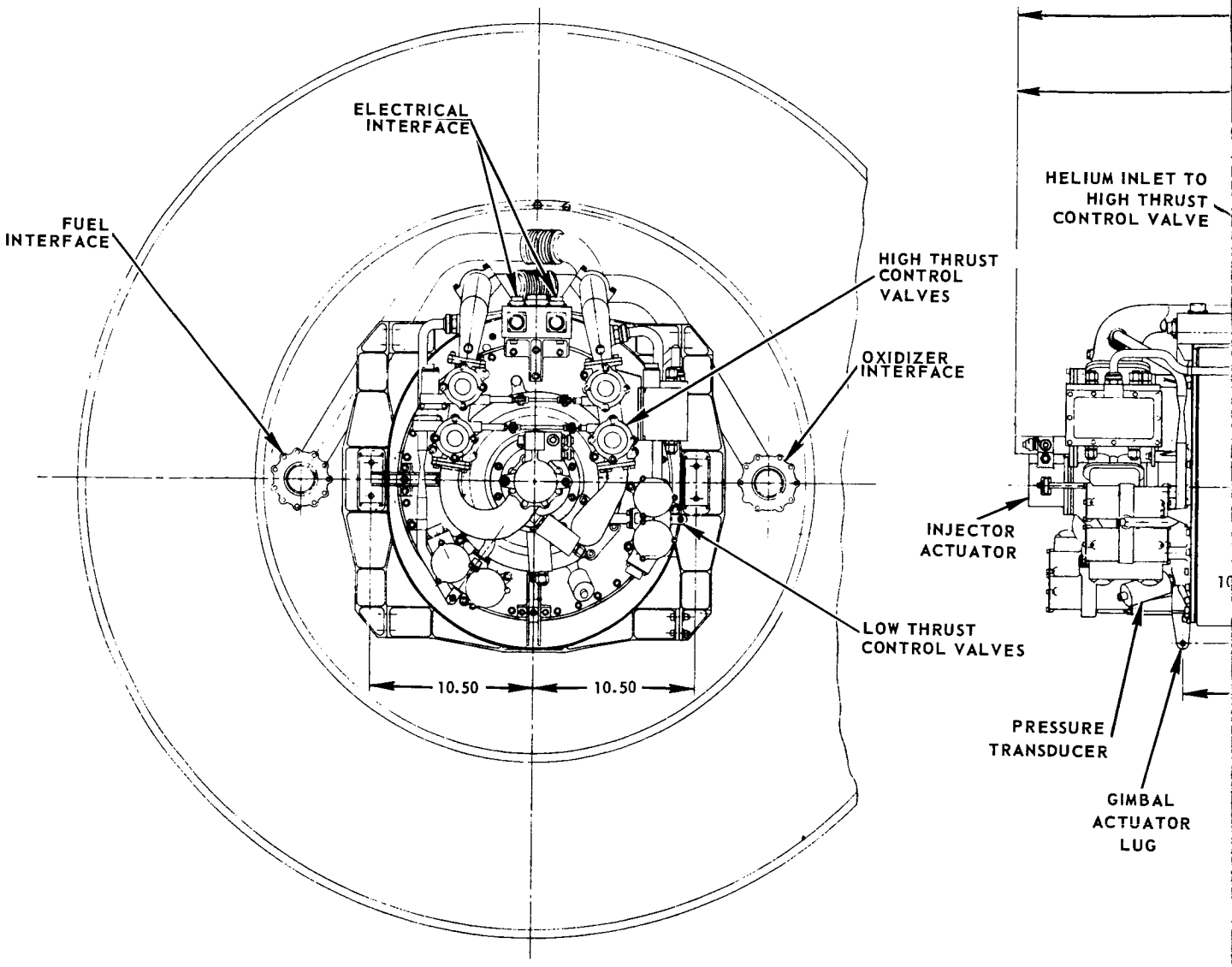

FOLDOUT FRAME

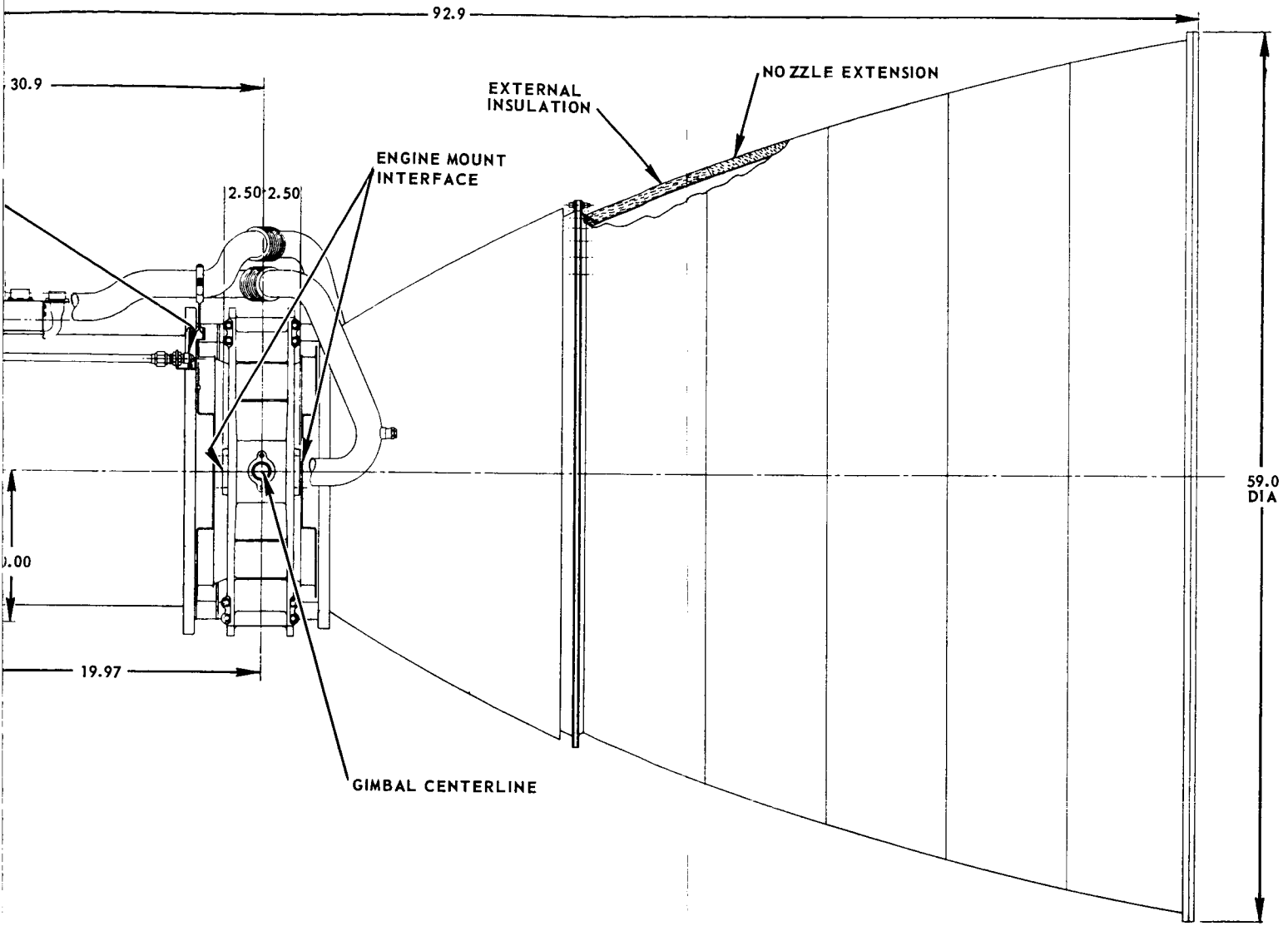

Figure 4-10
VOYAGER ENGINE

FOLDOUT FRAME

PRELIMINARY SPECIFICATION

Main Engine Component Specification

Purpose

To provide thrust at levels compatible with the spacecraft and burn time compatible with the needed velocity increments for each required mission maneuver.

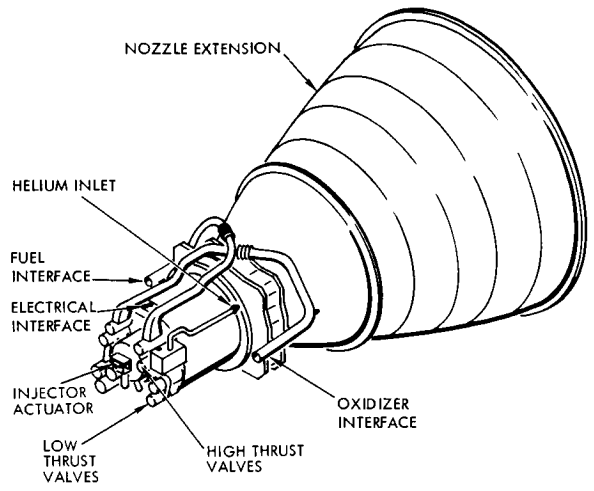

Performance Characteristics

Thrust	
High	9850 lb
Low	1700 lb
Specific Impulse, Nominal, Start of Duty Cycle	
High thrust	305 sec
Low thrust	298 sec
Inlet pressure	
High thrust	220 psia
Low thrust	230 psia
Chamber pressure	
High thrust	100 psia
Low thrust	18 psia
Mixture ratio	1.60
Restart capability	unlimited
Shutdown repeatability	
High thrust	± 128 lb sec
Low thrust	± 98 lb sec

Physical Characteristics

Nozzle area ratio	47.5:1
Nozzle length, in.	62.0
Chamber area ratio	2.9:1
Throat area, in.	54.37
Throat dia, in.	8.32
Exit area $in.^2$	2577
Exit dia, in.	59
Chamber inside dia, in.	14.2
Chamber inside length, in.	14.7
Characteristic length, in.	40
Gimbal angle, 2 axis	± 6.0 degrees
Materials: Nozzle extension - Columbian	
Insulation on extension - Fibrefrax	
Chamber shell - Titanium	
Lines - Stainless steel	
Gimbal ring - Aluminum	
Weight	408 lb

Figure 4-11

controlling the main propellant flow. This results in a flow increase and an increase in engine thrust up to about 10,000 pounds. Since the amount of velocity increment will be controlled by an integrating accelerometer, the change in thrust level will not adversely effect the maneuver. After the orbit insertion maneuver, all orbit trim maneuvers will be performed with an ablated chamber. Low thrust performance with the ablated chamber will be 289 seconds.

The center of gravity of the engine is located within a theoretical cylinder 0.50 inches in diameter and 6.0 inches in length which is concentric with the geometric longitudinal axis of the thrust chamber and is bisected by the gimbal plane when the engine is on the 0 degree gimbal position. The center of gravity will remain within this defined location throughout the operational life of the engine.

The moments of inertia are presented below. The roll torques developed by the engine as a result of the shift in thrust vector alignment will be less than 25 inch-pounds.

Table 4-7. Major Engine Components and Design Features

Injector

- Central coaxial element
- Single movable sleeve to control injector momentum
- Lightweight titanium fabrication

Injector Pintle Actuator

- Automatic positioning by force balance
- Direct mechanical coupling to injector movable element

Control System – Low Thrust

- Fixed cavitating venturis with trim orifices
- Quad redundant solenoid operated, poppet valves

Control System – High Thrust

- Trim Orifices
- Quad redundant, helium pressure, pilot valve operated, mechanically linked ball valves

Thrust Chamber Assembly

- Insulated ablative combustion chamber encased in a one piece titanium shell for maximum performance with minimum weight
- Insulated, oxidation resistant coated columbum nozzle extension
- Aluminum box beam gimbal with fabroid spherical bearings mounted at the engine throat plane
- Single electrical interface for entire electrical system

Moment Plane	Amount (lb-sq. in.)
I_X	60,174
I_Y	233,460
I_Z	233,519

The initial thrust vector alignment will be such that the thrust vector line will be within 0.125 inch of the engine reference line at the gimbal plane, and the included angle between the engine reference line and geometric thrust vector line will not exceed 0.5 degree.

The thrust vector line is defined by a line joining the centroids of the chamber throat and the exit plane of the chamber at an expansion ratio of 16:1.

The engine reference line is a line passing through the center of the gimbal axes and is perpendicular to the gimbal plane and the head end flange plane.

Upon completion of the required mission duty cycle the thrust vector line will be within 0.25 inch of the engine reference line at the chamber thrust plane.

The flow control schematic of the Voyager engine is shown in Figure 4-12. To improve reliability, the low-thrust solenoid valves are used in a quad arrangement.

Two separate propellant flow paths are provided for high and low thrust operation. For low thrust, propellants are provided upon command by solenoid actuated, quad-redundant poppet valves. Propellants pass through fixed cavitating venturis and the poppet valves to the injector. The single moving element of the injector is kept in the low thrust position by spring forces.

Low-thrust starts are accomplished by means of propellant supplied from the start tanks through the low-thrust solenoid valves. Switchover from the start tank to the main propellant tanks is accomplished by means of the pre-valves and the bellows tank solenoid valves in the propellant feed system, shown in Figure 4-1.

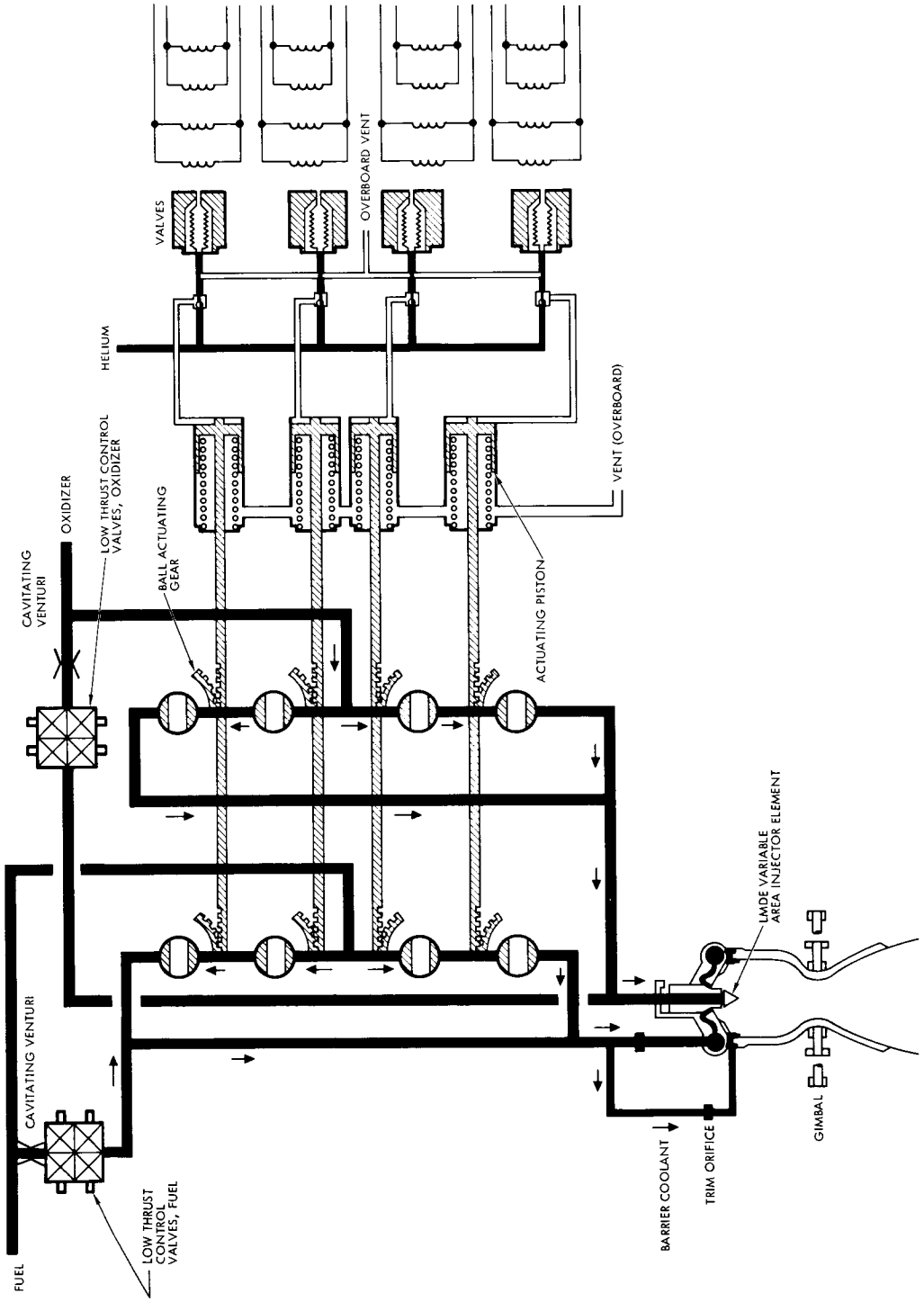

Figure 4-12
VOYAGER HEAD END ASSEMBLY FLUID FLOW SCHEMATIC shows the propellant flow paths and the mechanical operation of the high thrust ball valves. The gear segments are connected to the balls and rotate them to open or closed positions.

outer and an 0.030 inch inner face sheet. (A lightweight aluminum honeycomb core is added to reinforce the foam.) This sandwich is used for the majority of meteoroid protection for the recommended spacecraft. In areas where it was impractical to use the basic sandwich, another equivalent of 0.16 inch of aluminum was substituted as, for example, the equipment mounting panels, which are honeycomb sandwiches with 0.035 inch face sheets. Total weight of the meteoroid protection panels on the spacecraft is 563 pounds, not including the weight of primary structure which is used also as meteoroid protection, i.e., equipment panels and the propulsion module platform. It includes, however, the inner face sheets of the equipment module side panels which also act as shear webs for the basic structure and which weigh approximately 100 pounds.

Increasing the required operating life in Mars orbit to six months requires an additional 77 pounds of shielding to achieve the 0.97 mission reliability; use of the present panel design would reduce $P_{(O)}$ to 0.81 and mission reliability to 0.955 (Figure 2-26).

REFERENCES

1. "Voyager Environmental Predictions Document," Jet Propulsion Laboratory, Pasadena, California, 26 October 1966.

2. "Natural Environment Design Criteria Guidelines for MSFC Voyager Spacecraft for Mars 1973 Mission," NASA TMX-53616, June 8, 1967.

3. "Performance and Design Requirements for the 1973 Voyager Mission, General Specification For," Jet Propulsion Laboratory, Pasadena, California, January 1, 1967.

4. C. Dalton, "Near Earth and Interplanetary Meteoroid Flux and Puncture Models," AAS Paper 67-334.

5. V.C. Frost, "Aerospace Meteoroid Environment and Penetration Criterion," Aerospace Report TOR-269 (4560-40).

6. "Voyager Flight Spacecraft—Guidelines, Requirements and Design Characteristics—Preliminary," VVV-293, TRW Systems, Redondo Beach, California, 13 July 1967.

Table 4-8. Pressure Budget for Low Thrust (1700 pounds) Operation

Station	Component	Oxidizer Pressure (psia)	Oxidizer Pressure Drop (psi)	Fuel Pressure (psia)	Fuel Pressure Drop (psi)
Engine interface		234.5		234.5	
	Inlet lines		0.5		0.5
	Cavitating venturi and trim orifice		137.8		201.8
	Solenoid valves quad-redundant		8.0		4.0
Inlet to injector		88.2		28.2	
	Injector		69.7		9.7
Head end chamber pressure		18.5		18.5	
	Chamber losses		0.5		0.5
Throat total pressure		18.0		18.0	

Table 4-9. Pressure Budget for High Thrust (9850 pounds) Operation

Station	Component	Oxidizer Pressure (psia)	Oxidizer Pressure Drop (psi)	Fuel Pressure (psia)	Fuel Pressure Drop (psi)
Engine interface		220		220	
	Trim orifice		4		9
	Propellant lines		2		2
Inlet to injector		214		209	
	Injector trim orifice		—		80
	Valve		1		1
	Injector		110		25
Head end chamber pressure		103		103	
	Chamber loss		3		3
Throat total pressure		100		100	

4.4.3.2 Injector Pintle Position Control

Since the continuous throttling capability of the LM Descent Engine is not required for the Voyager mission, various methods of simplifying the engine thrust control system to accommodate the two-level thrust requirement were investigated. The first method considered was to attach a direct-acting two-position actuator to drive the injector sleeve. This actuator could be powered either by a separate pneumatic pressure source or by fuel pressure taken from the fuel inlet manifold. This method results in a significant mechanical simplification over the electro mechanical actuator and linkage of the LM engine. However, both the pneumatic and fuel-powered actuators require control valves and electrical and mechanical interfaces. The fuel-powered actuator also requires an overboard dump.

To circumvent these disadvantages, a third method of positioning the injection sleeve, which uses the hydraulic pressure generated by the fuel, was examined. As can be seen in Figure 4-9, the actuator piston is directly yoked to the injector sleeve. When the engine is off, the spring maintains the sleeve in the low thrust position. When the engine is started with the quad solenoid valve, fuel flow rate is controlled by the cavitating venturi in the fuel line. At the low flow rate, the manifold pressure acting on the actuator piston is inadequate to overcome the spring force, and the net force of 150 pounds keeps the sleeve in the low thrust position. For high thrust operation, the main valves are opened causing the fuel manifold pressure to increase to essentially full tank pressure. This pressure results in a force of 310 pounds which is sufficient to drive the actuator position to the high thrust stop. A one page actuator specification is shown in Figure 4-13.

Although there is no requirement to decrease the throttle setting during a firing, this could be achieved by opening the quad solenoid valves prior to shutting down the main propellant valve. When the main propellant valves close, flow is controlled by the cavitating venturi. As the flow decreases, the manifold pressure drops and the spring returns the injector sleeve to the low thrust position.

PRELIMINARY SPECIFICATION

Injector Pintle Actuator

Purpose

To position injector pintle at high or low thrust position automatically

Performance Characteristics

Pressure	20-235 psia
Proof pressure	540 psia
Burst pressure	810 psia
Actuation forces	
Low thrust	150 lb
High thrust	310 lb
External leakage, gas	5 cc/hr GN_2 (max)

Physical Characteristics

Fluids:	Aerozine -50 or MMH
Weight:	4.0 lb

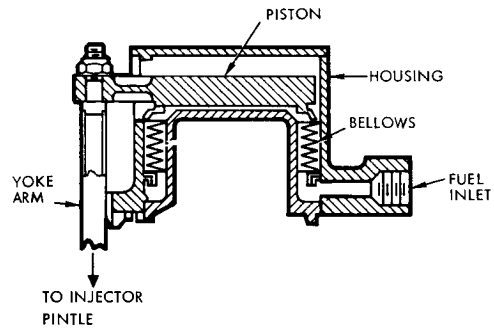

Figure 4-13

4.4.3.3 High Thrust Control Valve

The high thrust control valve for the Voyager spacecraft engine is essentially identical to the LMDE bipropellant valve (TRW Part No. C104619), except the actuation medium used is helium rather than fuel. This unit is manufactured by the Whittaker Corporation of Chatsworth, California. The assembly is configured to straddle the LM injector arm while mounted directly on the engine faceplate.

The design is a quad-redundant ball-type valve utilizing helium as the actuation medium controlled by two-position three-way solenoid pilot valves. In the normally closed position each of the four actuator pistons is vented through individual pilot valves and is held closed by two concentric springs. Energization of the pilot valve solenoid seals the vent and directs the helium to the actuator piston, moving the piston and rotating simultaneously the fuel and oxidizer rotors to the open position. Actuation of the rotors is accomplished by means of a rack and pinion gear located in the gear cavities adjacent to each rotor cavity. Valve closure is accomplished by de-energizing the pilot solenoid, sealing the supply

pressure, and venting the helium to the ambient environment. The piston return springs then move the piston to the "off" position, rotating the ball and shutting off the main propellant flow passages. Switches are provided to give an electrical signal in both the closed and open positions.

The high thrust control valve was designed within the confines of the general Apollo directive of minimum weight and power consumption commensurate with maximum reliability. To this end every effort has been made to optimize valve performance by the use of the best materials and design practices for each detail subcomponent. The physical and performance characteristics of this assembly are shown in Figure 4-14.

4.4.3.4 Low Thrust Control Valve

The low thrust propellant control valves consist of two quad-redundant packages, one each for on-off control of the fuel and oxidizer low thrust flow paths. Each of the two valve packages are located close to the injector manifold inlet ducts to minimize the downstream fill volume. The valves are manufactured by the Parker Aircraft Corp., Los Angeles, California.

The four individual valves comprising each of the two quad assemblies are essentially the Parker-qualified propellant valves used throughout the LM system except that for the Voyager application the latching solenoid is replaced by a single solenoid actuator. The basic design consists of a pair of isolation bellows sized to precisely balance the pressure forces imposed by fluids from either direction. This feature, permitting flow in either direction, allows compact packaging of the four units. A one page specification is shown in Figure 4-15.

Important design features include:

- Total elimination of sliding fits and seals assures repeatable operation and eliminates sticking
- A precision, Parker-manufactured bellows, which pressure balances the valve, reducing operating forces to very low levels that permit direct solenoid operation at high speed
- Teflon valve seats with zero propellant leakage
- Materials fully compatible with N_2O_4 and Aerozine 50 or MMH

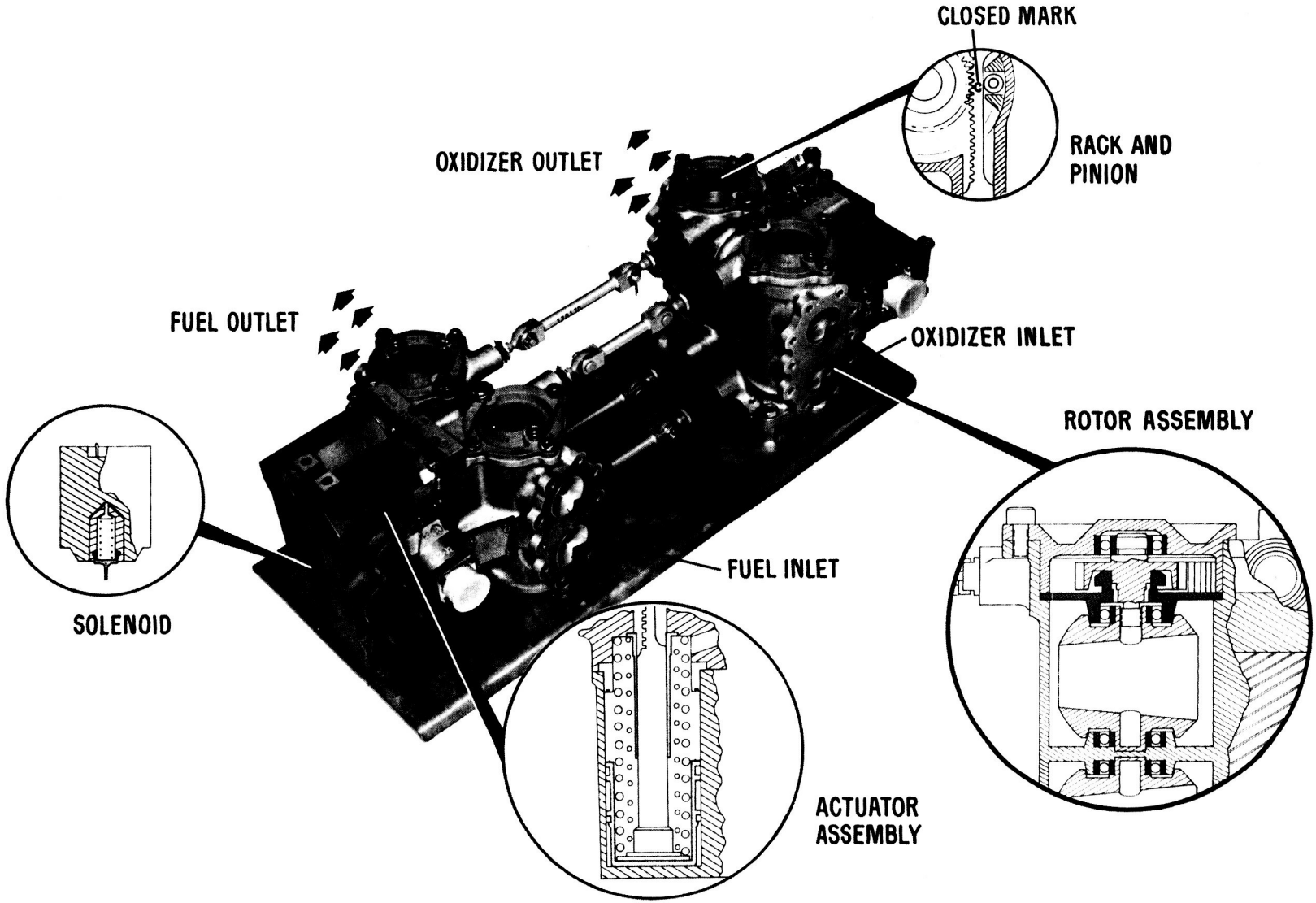

Figure 4-14

HIGH THRUST CONTROL VALVE shows the overall configuration of the quad redundant ball valve and details of its construction. Voyager uses gas actuation instead of fuel to eliminate the fuel-leakage path, a prevalve, and overboard dump lines and their possible freezing problem. Gas leakage is prevented by explosive valves already in the system.

PRELIMINARY SPECIFICATION

Low Thrust Control Valve

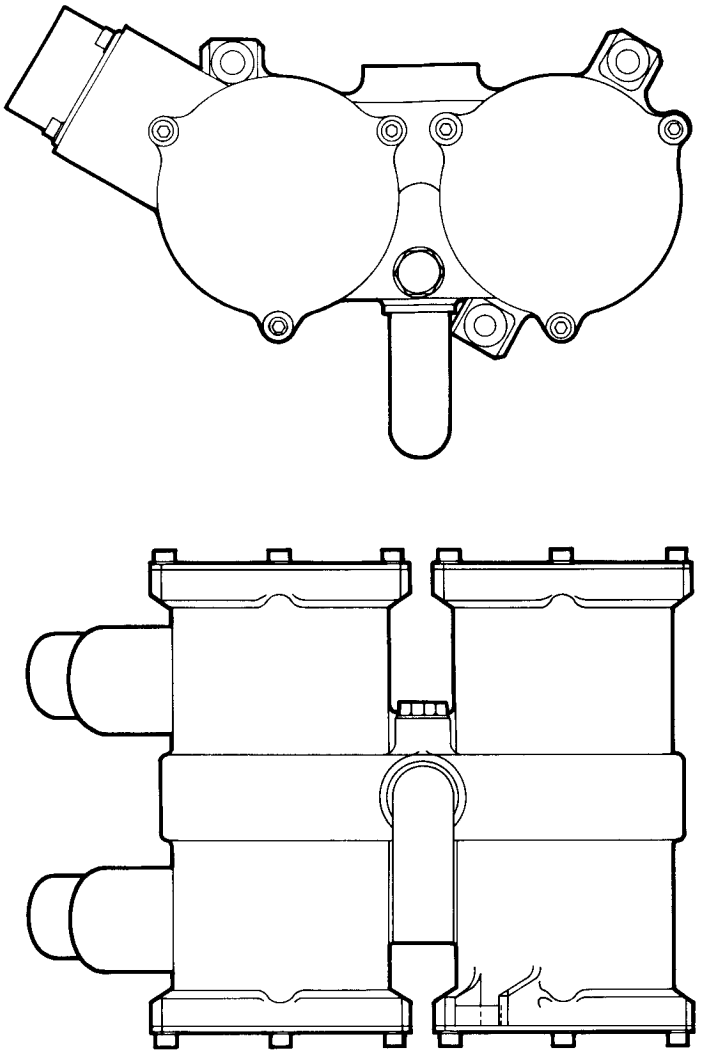

Purpose

To control propellant flow for the low thrust mode of operation

Physical Characteristics

Fluids	Storable propellants; N_2O_4, Aerozine or MMH
Weight	5 pounds total
Accessories	Position switches and back EMF suppression are included

Performance Characteristics

Pressure	
Proof pressure	270 psi max
Burst pressure	810 psi
Flow capacity	3.6 lb sec N_2O_4 with 25 psi max drop per valve, 2.2 lb sec Aerozine with 16 psi max/valve
Power	50 watts max per solenoid
Response	30 ms maximum at 235 psig, 24 VDC
Internal leakage, gas	5 cc/hr GN_2 max
Backflow relief	Relief pressure 200-250 psid Reseat pressure 150-200 psid
Life	1000 dry actuations 10,000 wet actuations with propellants

Figure 4-15

- Leakproof, all-welded construction eliminating static seal problem
- Dual redundant electrical receptacles.

The valve is normally held closed against a seat by a spring force supplied by the bellows. The poppet is pressure-balanced to inlet and outlet pressure by making the bellows effective area equal to the mean seating area. In the closed position, a flat-faced armature is held against a stop by a preload applied by a Belleville flexure guide. An isolation bellows keeps the solenoid and armature components dry and free from exposure to propellants.

To open the valve, current is applied to a bipole solenoid. The transient current and flux of the magnetic circuit increase until the developed solenoid force equals the force holding the poppet against the valve seat. As the force continues to build up, the armature mechanically pulls the poppet away from the seat to allow fluid to flow.

When the coil is de-energized, the transient axial force of the solenoid decreases to a level at which the compressed bellows and Belleville flexure force the poppet closed.

A relief valve is incorporated to allow back flow through the assembly. The device consists of a spring-restrained ball poppet seated against teflon with a design cracking pressure of between 200 and 250 psi differential.

4.4.3.5 Thrust Chamber Assembly

The thrust chamber assembly shown in Figure 4-16, consisting of the combustion chamber, nozzle extension, thrust mount and gimbal assembly, and insulation, is identical to that currently used on the LMDE except for the addition of external insulation on the nozzle extension.

The thrust mount and gimbal assembly consists of a rectangular beam frame and four trunnion subassemblies. Two of the trunnions are bolted to the chamber through Zee-rings mounted on the chamber skirt extensions fore and aft of the chamber throat. The Zee-rings are thermally insulated from the chamber while maintaining the primary structural attachment. The opposed two trunnions provide the structural attachment for the spacecraft.

The rectangular gimbal frame consists of four aluminum I-cross section beams bolted together at the corners. A center well in each beam houses a trunnion, bearing, and shaft. The assembly is designed for all structural and vibrational loads and will permit engine gimballing of ±6 degrees in both the pitch and yaw planes. The spherical gimbal bearing consists of a stainless steel ball and race separated by a composite liner of Teflon and glass fibers impregnated with a phenolic resin. The bearing bolts and spacer are titanium alloy.

The attachment points for the actuators used to gimbal the engine are located on the forward side of the injector. The details of these attachment points can be modified to accommodate interface requirements.

The combustion chamber consists of a composite abaltive chamber liner and exit cone bonded together into a titanium case. This proven design concept shown in Figure 4-17 of a composite structure permits complete charring of the ablative liners, with all structural loads being carried by the titanium shell, and results in minimum weight consistent with high performance and maximum reliability.

The ablative liner in the forward chamber section and in the throat consists of an inner liner of relatively heavyweight, highly erosion resistant silica-phenolic material oriented at 60 degrees to the axial centerline of the chamber. This inner liner is overwrapped with a lightweight ablative insulation of needle-felted silica cloth impregnated with phenomic resin and sealed with an outer liner of high-density, silica-phenolic cloth.

The ablative exit cone consists of an inner liner of the heavyweight ablative material and an outer liner of lightweight ablative insulation. These liners are both formed in a convolay or rosette pattern with 32 equally spaced, high strength quartz tie-plies, providing a mechanical bond between the liners.

The titanium case is fabricated from two forgings rough machined and welded together at the throat plane and then final machined with all skirts and flanges integral with the shell. The shell has been qualified at three times maximum operating pressure of 116 psi at 800°F.

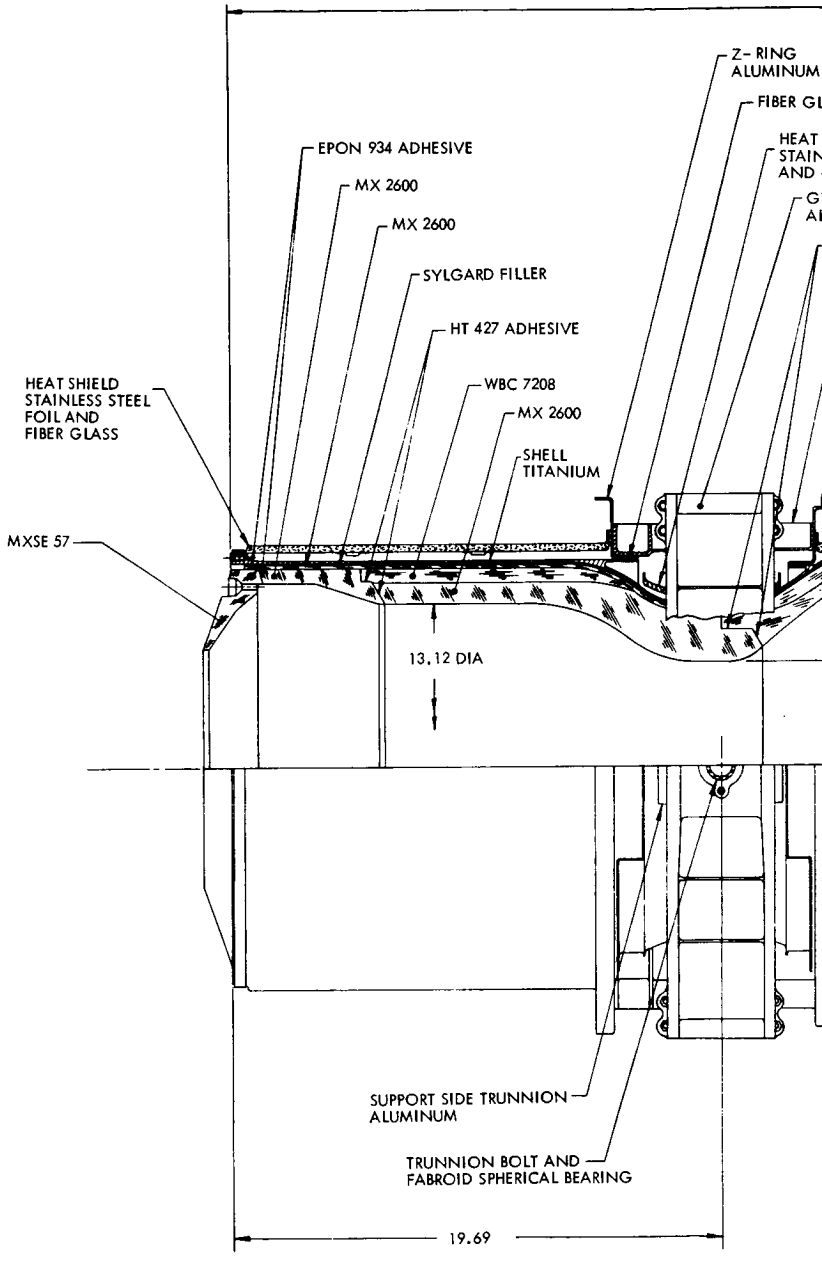

Figure 4-16

THRUST CHAMBER ASSEME
insulation on the outside o
from excessive heat radiatio

FOLDOUT FRAME

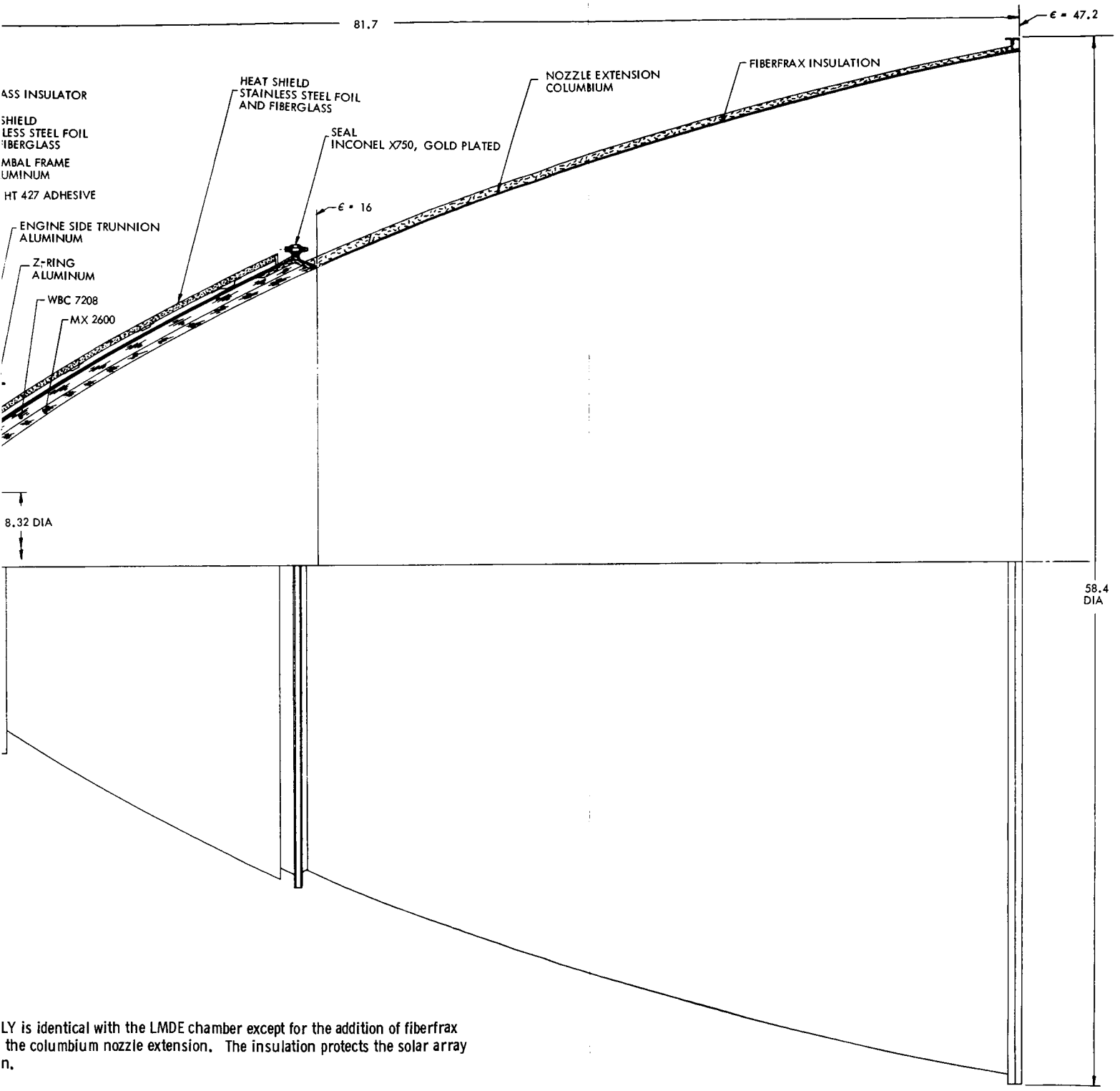

LY is identical with the LMDE chamber except for the addition of fiberfrax
the columbium nozzle extension. The insulation protects the solar array
n.

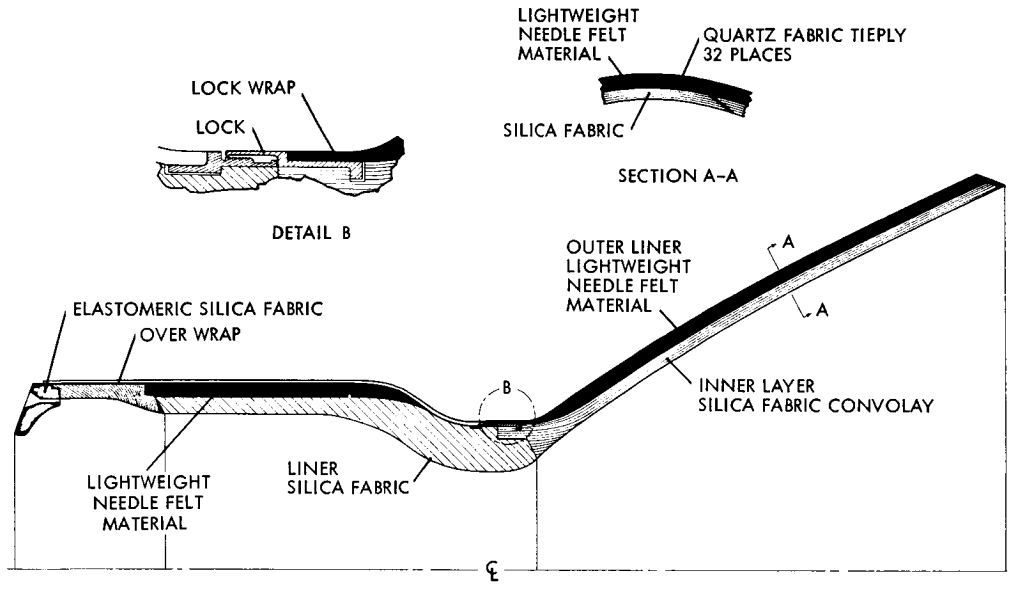

Figure 4-17
LIGHTWEIGHT CHAMBER LINER, identical to the LMDE liner.

The thrust chamber assembly is completely insulated for backwall temperature control. The combustion chamber insulation consists of two layers of stainless steel foil separated by a layer of fiber glass mat. It is fabricated in individual sections to cover the chamber, throat and exit cone.

The chamber liner has an integrally wrapped threaded lock ring at the aft end, and the exit cone liner has a lock ring with protruding tangs at the forward end. When these two components are assembled into the titanium case, the rings engage, forming a positive mechanical lock at the throat plane. This joint is further supported by high-temperature epoxy-phenolic adhesive. The assembled ablative liners are supported and bonded in the titanium case by a silicone elastomeric resin.

The nozzle extension is fabricated of columbium alloy and is coated for oxidation resistance. The extension is step-tapered for minimum weight consistent with all design requirements.

A leak-proof joint is effected between the nozzle extension and the titanium case with a gold-plated Inconel K-type spring seal. Additional

sealing assurance is attained by applying a thin layer of the "uncured" oxidation resistant coating to the nozzle extension flange immediately prior to assembly.

4.5 BACKUP ENGINE

In accordance with the Voyager philosophy of using redundancy to improve mission reliability, a backup engine system was considered for the single main engine. The approach used was to determine if existing small engines could be clustered around the main engine and thereby provide the desired redundancy.

The first step in the investigation was to determine if the C-1 engine cluster could impart sufficient velocity increment to the vehicle in time to ensure orbit insertion in the event the main engine failed to ignite. The analysis, discussed in Appendix D, indicates that the C-1 engine cluster using all of the available propellants, could place the vehicle in a highly elliptical orbit of typically 1000 x 80,000 kilometers. Once it had been determined that the C-1 engine cluster could provide a backup for the main engine, various alternate modes of operation were examined to determine the impact on system reliability.

4.5.1 C-1 Engine Description

The C-1 engine is a fixed-thrust, pressure-fed, bipropellant liquid engine designed to meet attitude control, orbit maneuvering, and ullage-management requirements common to spacecraft and upper stage vehicles. The engine assembly is shown in Figure 4-18.

The C-1 engine considered for the Voyager application consists of a bipropellant valve assembly, a Radiamic thrust chamber and an externally insulated, radiation-cooled nozzle extension. The bipropellant valve assembly is a Moog torque motor valve. The injector, which is a vortex type, is bolted to the chamber jacket assembly. The chamber liner is welded to the injector.

The thrust chamber utilizes a refractory alloy liner with an outer, regeneratively cooled jacket. Fuel enters the jacket at the injector end of the engine and flows to the nozzle throat from which it is returned to the

PRELIMINARY SPECIFICATION

C-1 Engine

Purpose

Four C-1 engines will be used as a back up subsystem to perform any of the propulsion maneuvers in the event of a main engine failure.

Performance Characteristics

Engine life:	10,000 sec	Minimum Impulse Bit 3 lb-sec
Thrust:	100 ± 5 lb	
Specific impulse	292 sec	
Supply Conditions		
Pressure	195 ± 15 psia	
Mixture ratio	1.6 ± 3 percent	
Temperature:	+40 to +100°F	
Electrical		
Operating voltage:	20 to 33 VDC	
Nominal voltage	26 VDC	
Power	13 watts	

Physical Characteristics

Weight (dry)	6.25 lb
Overall length	17.29 in.
Area ratio	60:1
Propellants	
Oxidizer	N_2O_4
Fuel	MMH or A-50

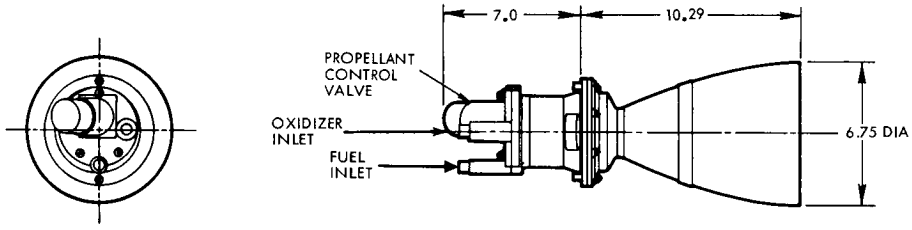

Figure 4-18

injector through an inner set of coolant passages. The refractory liner is of 90 percent tantalum, 10 percent tungsten alloy with a silicide coating.

The nozzle radiation cooled extension is a composite structure with C-103 columbium alloy in the forward section and 6A1-4V titanium alloy used for the aft section.

4.5.2 Operational Implications Related to Use of C-1 Engine

Assuming that the four C-1 engine cluster configuration is used in conjunction with the main engine, certain system implications must be considered.

Both the C-1 and main engine must be qualified for the same propellant and must operate at the same mixture ratio.

The use of the C-1 engines as a backup for the main engine is not a passively redundant scheme. Sensing devices, to ascertain failure modes, and preprogrammed switching circuits will be required.

The C-1 engine must be mounted with the thrust axis nominally parallel to the vehicle axis. Canting the engine to point the thrust axis

through the vehicle c.g. would result in a prohibitive cosine loss to the axial impulse. This mounting constraint introduces two potential problem areas related to vehicle guidance, the first resulting from thrust imbalance between engines and the second resulting from an abrupt engine failure during a maneuver. The variation in thrust between the four engines can be countered with the 3-pound thrust ACS engines located on the extremities of the vehicle. However, this would consume a prohibitive quantity of gas. Hence, it is necessary to either modulate the thrust duty cycle or gimbal the engine furthest from the c.g. sufficiently to offset the thrust imbalance.

The C-1 engine will have to either employ an ablative nozzle extension or else insulate the present radiation cooled extension to preclude overheating the solar array on the base of the spacecraft. The ablative extension will be heavier than would insulating the nozzle extension as was the case for the main engine. Therefore, insulation will be applied to the C-1 engine nozzle extension in a manner identical with that used for the main engine.

4.5.3 Alternate Methods of Using the C-1 Engine

Two alternate methods of using the C-1 engines to enhance the overall reliability of the propulsion system were considered. The first approach considered was to use the four C-1 engine cluster as a backup subsystem in the event the main engine was unable to perform any of the propulsion maneuvers but the critical orbit insertion maneuver in particular. The second would be to divide the maneuvers between the C-1 engine cluster and the main engine so that the C-1 engines perform the midcourse and orbit trim and the main engine performs the orbit insertion.

The first approach has the advantage of keeping an isolated standby system available as a backup in the event the primary system fails for any maneuver. In this manner the C-1 engines also cannot degrade the basic system reliability by providing additional leakage paths during the transit period.

The second approach sacrifices the advantages of redundancy in that a fresh backup is not available for any maneuver and the orbit insertion maneuver in particular. However, the impulse and the thrust required for the midcourse maneuvers are well within the capability of the C-1 engine. It might also be noted that the C-1 engines could be configured to have

engine-out capability in this mode, which would provide additional reliability margin. However, in this mode they could no longer act as a backup to the main engine during the critical orbit insertion maneuver. The main engine, however, in this mode starts the orbit insertion maneuver with a fresh chamber with considerable design margin.

4.5.4 Reliability Implications Related to Use of the C-1 Engines

A quantitative comparison was made of propulsion systems which use the two alternate methods of using the C-1 engines to a baseline system which used the main engine to perform the entire mission. The results of the analyses indicate that a modest improvement in propulsion system reliability is achieved by adding the C-1 engine cluster as a backup. This modest improvement results because the major part of the subsystem unreliability is in the feed system components, and changes to the relatively reliable engine have little effect on subsystem reliability. The alternate method was deemed less desirable because of the possibility of a Surveyor type of failure when using multiple engines.

4.5.5 Selected Method of Incorporation

The facts that the C-1 engines can be easily installed, are relatively low in weight (approximately 65 pounds for four engines including additional propellant needed because of the additional inert weight), and can be installed in the propulsion system in a manner that would not degrade the reliability of the system during normal operation are reasonable arguments for the use of the C-1 engines. The problem related to thrust imbalance between C-1 engines because of spacecraft center of gravity shifts can be solved by either modulating the thrust duty cycle of the engines or mounting them so that they can be gimballed. Modulating the thrust duty cycle to compensate for thrust imbalance requires shutdown of the engine furthest from the vehicle center of gravity about once every 12 seconds for a period of about 0.15 second for pre-orbit insertion and orbit insertion maneuvers. Since this mode is easily integrated into the guidance and control system and the installation of the engines is far simpler for this control method, it is the recommended choice. Required firing times are about 9000 seconds.

Roll attitude will still be stabilized by the four 3-pound cold gas ACS thrusters.

The basic principle of attitude control in presence of disturbance torques by means of modulating the C-1 engine(s) does not differ from limit-cycle operation during cruise flight mode under a constant solar-radiation pressure torque. Therefore, stability and control of spacecraft attitude can be treated in the same manner as in the cruise flight. Some change will be made in the time constants of lead-lag networks and overall control loop gains to accommodate a fast control response in the C-1 engine pulsing valve drive. This is required for 0.02 g excited propellant sloshing dynamics, and to minimize the possible coupling effects of the C-1 engine on-off frequency with those of other subsystems on spacecraft dynamics.

The recommended configuration is to mount the four C-1 engines with their nominal thrust axes parallel to the vehicle centerline and to isolate them from the main feed system by explosive valves. The C-1 engines would then be held in reserve so that any time during the mission that a main engine failure occurred, the C-1 engines would be available to take over as a fresh backup.

4.6 PRESSURIZATION AND PROPELLANT FEED SYSTEM

In attempting to establish the pressurization and feed system most suitable for the Voyager mission, a number of systems were evaluated. In all cases the orbit injection firing is conducted utilizing a high pressure regulated system and all trajectory corrections and orbit trim maneuvers are done in a blowdown mode. Variations in the manner in which expulsion is accomplished during the first planetary arrival date separation maneuver required several candidate systems to be evaluated.

The candidate systems, which are described in detail in the following sections, can be summarized briefly as follows:

- An ullage blowdown system in which the planetary arrival date separation firing is conducted without activating any of the pressurization system components and instead utilizing the pressurization available by expanding the prepressurized ullage space

- An ullage makeup system in which during the planetary arrival date separation maneuver, unregulated helium is bled through an orifice from the main storage bottles into the tank ullage so as to reduce the engine inlet pressure variation

- A single level regulation system utilizing a single pressure regulator package to deliver constant pressure to the propellant tanks and which is used for both the planetary arrival date separation and orbit insertion maneuvers

- A two pressure level regulated system utilizing two sets of pressure regulators; one set to deliver relatively low pressure for the planetary arrival date separation maneuver and another set to provide high pressure which is used during the orbit insertion maneuver

The single level regulation system is the selected configuration pending further resolution of the meteorite induced tank explosion hazard, which could lead to a violation of the contamination constraint as discussed in Section 4.6.2.2.

4.6.1 Candidate Systems

4.6.1.1 Blowdown Systems Descriptions

Two variations of the blowdown mode of pressurization for the planetary arrival date separation maneuver were studied. Up to three firings were considered during this phase of the mission, where 2150 pounds of propellant may be required to obtain a ΔV capability of up to 210 m/sec with a 30,076 pound upgraded spacecraft. The 210 m/sec includes 205.3 m/sec for the worst case planetary arrival date separation maneuver shown in Figure 4-4 and 4.7 m/sec for a trajectory correction during this first burn. The variations, described below, are the propellant tank ullage blowdown system shown in Figure 4-19 and the ullage makeup system shown in Figure 4-20.

Ullage Blowdown. This pressurization and feed system will provide sufficient initial ullage in the propellant tanks to perform the arrival date separation firing by expansion of the ullage gas without supplying additional pressurant from the storage bottle.

Interplanetary trajectory correction maneuvers will take place during the arrival date separation maneuver and 30 days prior to Mars encounter. All trajectory corrections will also be accomplished in a blowdown mode.

The majority of the total propellant load will be used during the high thrust level orbit insertion firing which will be conducted in a regulated high pressure (235 psia tank pressure) mode. This is accomplished by actuating the two normally closed isolation squib valves upstream of the

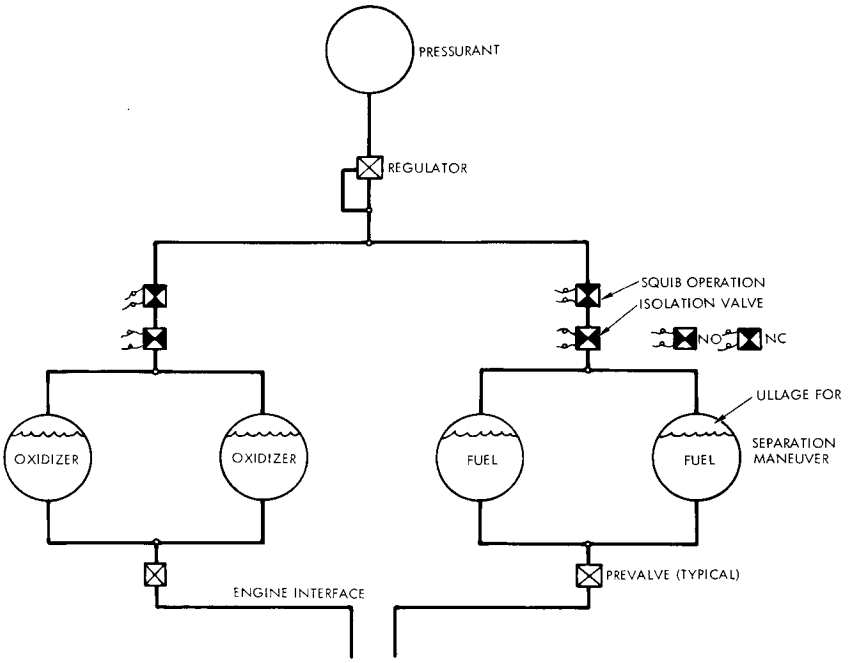

Figure 4-19
ULLAGE BLOWDOWN PRESSURIZATION SYSTEM. This schematic is simplified, omitting such items as fill and drain lines, fittings, transducers, since these were not considered in the tradeoff.

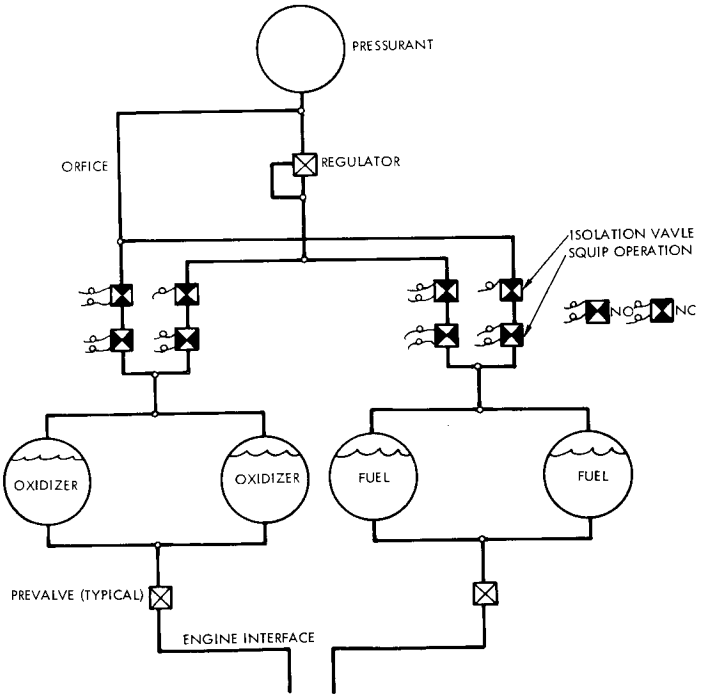

Figure 4-20
ULLAGE MAKEUP PRESSURIZATION SYSTEM, a blowdown system where gas is added to maintain essentially constant tank pressure to reduce the engine inlet pressure variations. If engine flow rates vary, however, the constant makeup gas supply could result in tank overpressurization.

propellant tanks. This allows the helium to flow from the storage bottle through the pressure regulator into the propellant tanks. The use of additional components such as helium tank isolation valves and propellant line check valves is discussed later since it is the intent of these diagrams to show system operation in its simplest form. The prevalves are opened prior to engine firing. After the completion of the orbit insertion firing, the normally open propellant tank squib valves, engine control valves, and the prevalves are closed. The tanks are vented to 125 psia, and the remaining orbit trim firings conducted in the ullage blowdown mode. At this time the propellant tank ullage is in the order of 85 percent, resulting in negligible pressure decay for the orbit trim expulsion.

The propellant tanks were sized to allow the expulsion of 2150 pounds of propellant (7.3 ft^3/tank) during the arrival date separation maneuver. At the start of the maneuver, the tank pressures will be 235 psia and during the maneuver will decay to 125 psia. Relatively large tank ullages are required. The tank ullage requirements are a function of injector pressure drop ratio, as shown in Figure 4-21. For estimating ullage requirements from this curve, the injector pressure drop ratio may be taken as numerically equivalent to the ullage pressure blowdown range. An ullage of approximately 17 percent is indicated for a 235 to 125 psia tank pressure decay.

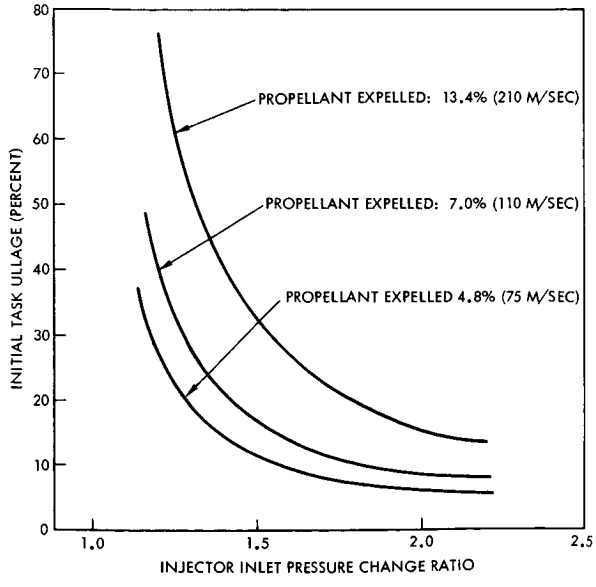

Figure 4-21

INITIAL ULLAGE VERSUS INJECTOR INLET PRESSURE CHANGE RATIO shows the effect of initial ullage volume in the propellant tanks of a blowdown system on the injection pressure change during engine operation for different quantities of propellant expelled. With an initial tank ullage pressure of 235 psia and a desired minimum pressure of 125 psia for satisfactory engine operation, an ullage of approximately 17 percent is required when the propellant expelled is 13.4 percent of the total propellant.

Ullage Makeup. To circumvent the principal disadvantage of the ullage blowdown system, the resultant inlet pressure variation seen by the engine, a pressurization scheme was considered in which high pressure unregulated helium flows directly from the helium storage bottle to the propellant tanks. Metering is accomplished by an orifice whose size is chosen to approximate the volumetric flow rate from the propellant tanks to the engine. The orifice is sized to maintain the 125 psia minimum tank pressure used for low thrust engine firings. The tank pressure for the planetary arrival date separation maneuver using this system varies by approximately 18 psi. As can be seen from Figure 4-20, one branch, consisting of a squib-operated normally closed and a normally open valve, is used to initiate and terminate the pressurization for the maneuver. After the maneuver, sufficient ullage would be available in the propellant tanks to perform the trajectory correction firings in the propellant tank ullage blowdown mode.

Since the initial tank pressures would be affected by the propellant temperature-vapor pressure relationship, control of propellant mixture ratio, and hence propellant outage, will be a problem with this system.

The high-thrust orbit insertion firing would be conducted at a regulated pressure of 235 psia by activating the normally closed valves in the other branch. Engine shutdown is accomplished by closing the normally open valves. The tanks are then vented to 125 psia and the orbit trim firings can again be conducted in the blowdown mode.

4.6.1.2 Regulated Systems Descriptions

Single Level Regulated System. The single regulated pressure level feed system is shown schematically in Figure 4-22. This system differs from the two systems described previously in that the pressurant required for the planetary arrival date separation maneuver as well as the orbit insertion maneuver is supplied through the main pressure regulator assembly providing a constant tank pressure. As before, the subsequent trajectory correction and orbit trim firings are conducted in the ullage blowdown mode since the propellant expended during these maneuvers is very small. This system required a two leg propellant tank isolation valve arrangement, as shown in Figure 4-22, to provide active pressure

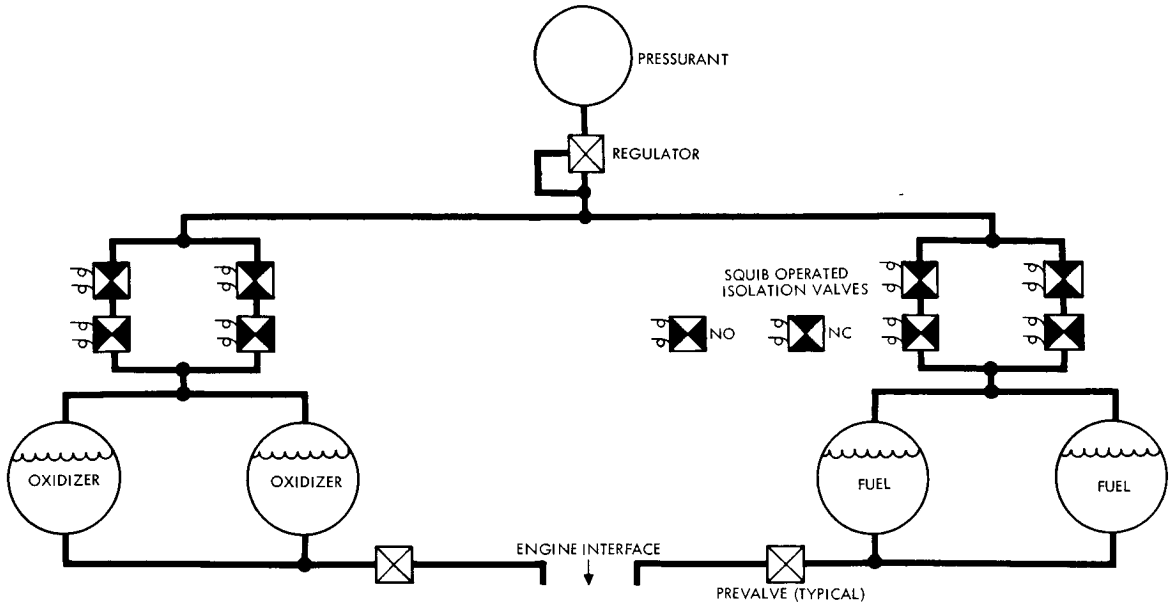

Figure 4-22
SINGLE LEVEL REGULATED PRESSURIZATION SYSTEM SCHEMATIC.

regulation and subsequent isolation for separation and orbit insertion firings only. This system is the most conventional and is typical of most operational systems. The excess pressure is dropped with cavitating venturis for low thrust firings. The cavitating venturi also keeps flow rate constant if a valve in the low thrust quad valve fails to open.

In each of the previous systems considered, the long coast phases are conducted with tanks at relatively low pressure and correspondingly low stress level. With this system the propellant tanks would remain near full working pressure for the entire mission duration. The post-orbit-insertion venting cycle used in the previous systems to reduce the tank-pressures for low thrust engine operation would not be required.

Two-Level Pressure Regulated Systems. The two-level regulated pressure system, through separate regulator circuits, provides a regulated low pressure level for the low thrust separation firing and a high pressure level for the high thrust orbit injection firing. As with all the other candidate systems, the subsequent midcourse correction and orbit trim firings are all conducted in an ullage blowdown mode. Two basic arrangements are shown. One, in Figure 4-23, is the same as the single level pressure regulated system with the addition of a low pressure regulator bypassing the main regulator. Regulator isolation valves, as

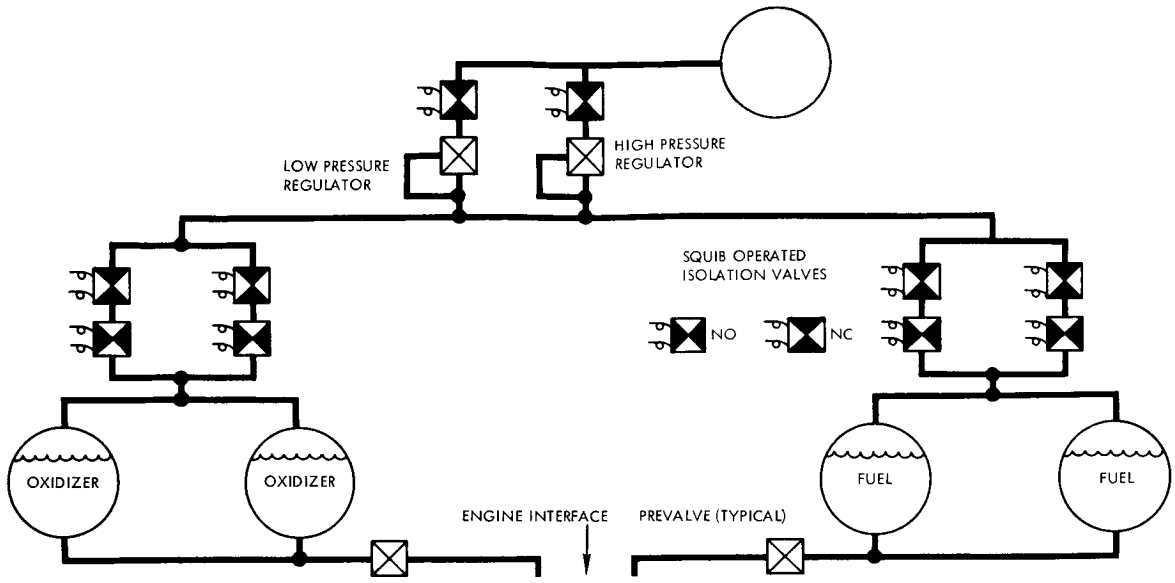

Figure 4-23
TWO LEVEL REGULATED PRESSURIZATION SYSTEM SCHEMATIC.

shown, are required to enable selection of the desired regulator branch. With this arrangement any combination of the propellant tank isolation branches and regulator branches can be used. An alternative arrangement, Figure 4-24, with somewhat less flexibility and somewhat increased plumbing requirements is also shown. This arrangement is identical to the unregulated ullage makeup system with a low pressure regulator in place of the orifice.

4.6.2 Evaluation Criteria

The basic criteria established for system evaluation and comparison are reliability, physical size and weight, development risk, and operational flexibility. Where possible, quantitative values associated with the criteria are compared and discussed. In less tangible areas, flexibility of operational modes, design options, and associated factors are discussed as they relate to development risk, probability of mission success, and/or potential planetary contamination. Factors which apply equally well to all candidate systems are not developed in detail since, although they may represent important design considerations, they do not have an important bearing on the logic of the selection process.

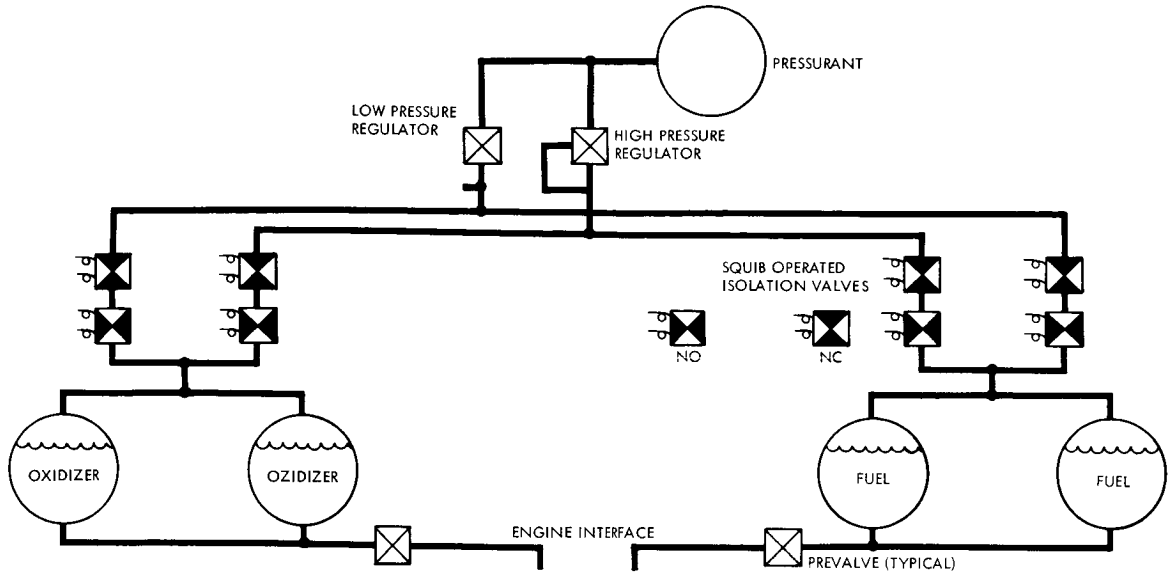

Figure 4-24

PRESSURIZATION SYSTEM SCHEMATIC. Two level regulated (alternative arrangement).

4.6.2.1 Operational Considerations

Before the basic systems described in the previous section can be considered for operational use some thought must be given to the operational modes, flexibility of operation, and reliability and, in addition, to how these can be enhanced by system modifications incorporating redundancy or options in system operation. Consideration must also be given to practical functions such as overpressure relief and venting.

For the candidate systems, quad redundancy was used in the main regulator (used for the orbit insertion firing) and the propellant tank pressurization line check valves. Only parallel redundancy was incorporated into the propellant tank outlet pre-valves since they are slow acting and have very high sealing forces. The engine valves provide component series redundancy. Redundancy has not been utilized for squib valves as they have demonstrated high reliability when used with redundant bridge wires. Quad redundancy was used for those components with a history of somewhat higher failure rate such as the pressure regulators, or with those components where quad redundant component packages are well developed and widely used such as the check valves. In the two pressure level regulated system a flow limiting orifice is used as backup for the regulators overpressure failure mode in the low pressure branch. This

eliminates two regulators from the package since parallel redundancy rather than quad redundancy can be used. The use of this orifice is made possible by the limited pressure range that the pressure bottle will expand through when flowing through the low pressure regulator circuit. A conventional burst disc-overpressure relief valve arrangement is provided for the propellant tanks. This system is provided only to prevent tank rupture in the event of a malfunction in the pressurization system.

For all candidate systems, except the single level pressure regulated system, the propellant tanks are to be vented to the low pressure level compatible with low thrust operation for the orbit trim firings after the completion of the orbit injection maneuver. Venting is accomplished through the use of pressure switches and squib valves. The tanks are vented in series to prevent gross mixing of propellant vapors in the vicinity of the spacecraft during the venting operation. To take advantage of the settled propellant, the venting of the oxidizer tank is initiated by the engine shutdown signal. When the predetermined pressure is reached as determined by the oxidizer tank pressure switch, the oxidizer tank vent line will be sealed off and venting of the fuel tank initiated. This line will also be sealed with an explosive valve when the desired pressure is reached as indicated by the fuel tank pressure switches. Propellant orientation will be maintained during the venting operation through the use of aft facing jets for vented efflux.

4.6.2.2 The Meteoroid Hazard

Although suitable tank shielding can provide a reasonable probability of mission success, preliminary calculations indicate difficulty in meeting the 3×10^{-5} Mars contamination probability allotment for any mode of spacecraft contamination of Mars even if this were assigned to the allowable probability of propellant tank rupture due to meteoroid impact.

An attempt was made to provide a quantitative assessment of the likelihood of propellant tank failure due to meteoroid impact and the effect of tank pressure induced stress on the probability of failure. This evaluation is presented in Appendix C. The study indicates that reducing tank pressure from the nominal high thrust level of 235 to a

value suitable for low thrust firings in the order of 125 psia during the coast phases would reduce the probability of tank puncture and subsequent rupture by a factor of about four. The greatest danger of tank rupture is presented by meteoroids of the order of 0.001 gram. Larger ones occur too infrequently and smaller ones have insufficient kinetic energy to induce the impact overpressure after puncturing the tank wall. For a mission time of 15 months and an equivalent unshielded tank area of 10 square meters the probability of encounter with a 1-milligram meteoroid is 10^{-2}. At the 3×10^{-5} probability level assigned to the tank rupture failure mode from the overall planetary contamination allotment of 10^{-4}, the corresponding meteoroid size is one gram. Encounter of a meteoroid of this size would be devastating under any condition.

Since the weight penalty associated with shielding would be severe and the effectivity uncertain, the most suitable technique to reduce the probability of meteoroid induced tank rupture appears to be to lower the tank stress level to a value that will not result in crack propagation and subsequent rupture. This stress level is in the order of 10 to 15 percent of ultimate for the 6Al-4V titanium alloy used in tank construction. Reducing the stress level can be accomplished by reducing tank pressure, i.e., venting to a pressure level of 60 psia for the coast periods or by designing the tanks to an allowable stress level in the order of 20,000 psi for the coast mode pressure level. Either approach involves a substantial weight penalty.

4.6.3 Candidate Evaluation

Estimates of relative pressurization system weight, nominal duty cycle reliability and tank sizes for the candidate systems are compared in Table 4-10. In view of the points raised in the previous section in micrometeoroid effects on propellant tank rupture, data are included for the regulated systems incorporating propellant tank venting to the 60 psi level after each firing.

Of the basic systems the ullage blowdown system is characterized by high weight, larger tankage requirements, and subsequently a larger spacecraft size and weight, and the highest calculated reliability. The

Table 4-10. Comparison of Nominal Pressurization System Parameters

System	Tank Pressures (psi)			Weight (lb)	Reliability	Tank Sizes (in.)	
	High Thrust	Low Thrust	Coast			Propellant	Pressurant
Ullage blowdown	235	235-125	125	534	0.998569	59.8	31
Ullage make-up	235	150-125	125	447	0.998543	57.5	30
Single level regulated	235	235	235	445	0.998540	57.5	30
Above, with venting	235	235	60	1157	0.998538	57.5	41
Two level regulated	235	125	125	453	0.998450	57.5	30
Above, with venting	235	125	60	712	0.998448	57.5	35

remaining systems, without venting, are all comparable in weight since they have the same gas requirements and differ only by a few control components. The one level regulated pressure system is the lightest. This system is also the most reliable in operation. The low pressure coast systems do have some advantage from the tank rupture standpoint but not enough to comply with the present contamination constraint requirements.

If a venting system which maintains the tank pressure at 60 psia in all coast periods is employed, the resultant weight penalties are in the order of 480 pounds for the single level pressure regulated system and 180 pounds for the two-level pressure regulated system. The weight penalty for the ullage makeup system is about 180 pounds since it operates at essentially the same pressures as the two-level pressure regulated system. Clearly the low pressure systems have a distinct weight advantage where venting is employed since less pressurant is lost after each firing. The use of the ullage blowdown system or the venting approach are mutually exclusive.

Large tank weight penalties would be involved if the low working stress approach is used to minimize the probability of tank rupture with meteoroid impact. The low pressure coast systems would incur a weight penalty of about 580 pounds. Since the tanks for the ullage blowdown system are approximately 20 percent larger than the low pressure systems, the weight would be larger (700 pounds). For the single level pressure regulated system, the weight penalty would be 1100 pounds, approximately twice that of the low pressure systems.

A further comparison of a more qualitative nature is presented in Table 4-11 in the form of a summary of advantages and disadvantages. The variation in engine inlet pressure inherent in the blowdown system is a disadvantage since it affects engine operation. Although the engine is capable of running satisfactorily over some range of feed pressures, the bulk of the engine development and qualification testing to date has been performed at fixed feed pressure.

The potential for higher propellant outages as previously discussed is a disadvantage for the ullage makeup system. This system also lacks

Table 4-11. Pros and Cons for Candidate Systems

	Pros	Cons
Ullage blowdown	Pressurization system inactive prior to orbit insertion firing	• 2:1 variation in engine feed pressure • Increased spacecraft size and weight
Ullage blowdown with makeup	Relative simplicity	• 0.7:1 variation in engine feed pressure • Potential overpressurization • Potentially high propellant outages
Single level pressure regulated Without venting With venting	Simple, conventional system if venting is not required	• High pressure coast mode or weight and complexity penalty due to venting
Two level pressure regulated Without venting With venting	Pressure levels tailored to thrust levels	• Slightly increased complexity • Lightest weight if venting required

flexibility since the flow orifice is only suitable for a very limited range of flow rates. If the engine propellant flow was less than expected, over-pressurization of the propellant tanks could occur.

The single level pressure regulated system is the lightest, simplest, and most reliable of the candidate systems. The main disadvantages of this system stem from the potential weight penalties associated with attempting to meet the Mars contamination constraint. Since none of the systems will meet the current contamination allotment it appears that this area should be the subject of further reassessment. Until this situation is clarified the simple single level pressure regulated system is recommended as the primary choice for continued detailed preliminary design. If a technique such as the low pressure venting or low stress level propellant tank design is considered necessary, the use of the low pressure bypass regulator resulting in the low pressure regulated system can be reconsidered as a weight saving measure since this would then represent the next most desirable system.

With tanks sized for the 16,000 pounds of propellant and using a single-level regulated system, it would be possible to operate the system in an ullage blowdown mode for early missions where a lighter weight capsule is used and propellant is correspondingly off-loaded resulting in increased ullage. Figure 4-25 shows the ullage blowdown ratio that would result for various degrees of propellant off-loading and first firing velocity increment requirement. Typical 1973 loadings are 11,000 to 12,000 pounds of propellant. This results in a blowdown pressure range of 1.3 to 1.4 for the most severe planetary arrival date separation firing. Thus, it would be possible to gain flight experience while operating the system in its simplest mode and while preserving the growth capability for later up-graded missions.

4.7 PROPELLANT ACQUISITION

The Voyager Phase 1A Task B study recommended the use of positive displacement bellows tanks located inside of the main propellant tanks to provide propellants to the engine for starting under zero-g conditions. The acceleration produced by the engine while operating with propellants from the bellows tanks was used to settle

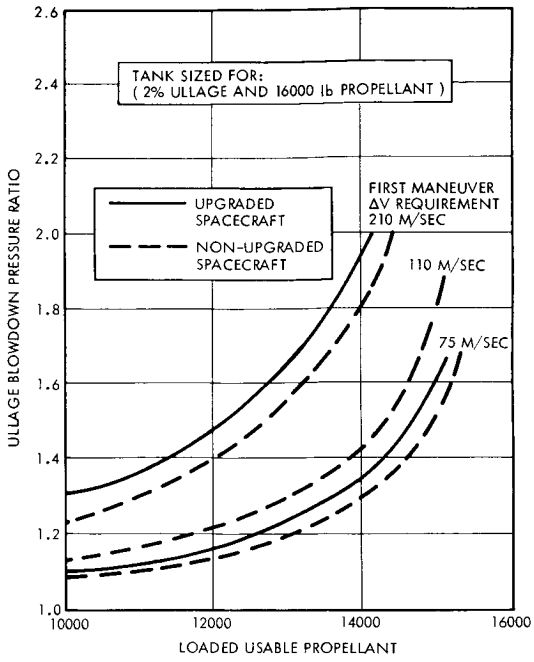

Figure 4-25
DEPENDANCE OF ULLAGE BLOWDOWN RATIO UPON PROPELLANT LOAD

the propellants in the main tanks. Switchover from the bellows tanks to the main tanks was achieved through a combination of squib valves and hydraulic balancing of the feed lines. In the current study several alternate propellant acquisition methods including three small thruster systems (two using gaseous nitrogen and one using monopropellant hydrazine), a screen propellant retention system, and the bellows start tank system were investigated.

The results of this study indicate that the bellows start tank system, as combined with the current engine and feed system configuration, still offers the most advantages and minimum developmental risk. In comparison to the bellows system, gaseous nitrogen systems have a weight disadvantage in excess of 200 pounds and a monopropellant system is significantly more complex. The gaseous nitrogen thruster systems may also be deficient in their ability to remove gas bubbles from the propellant feed lines due to the low vehicle accelerations they produce. A screen system offers a major advantage in that it is very light weight and is a passive system. However, potential problems of mass transport due to thermal gradients and of helium gas coming out of solution behind the

screen need to be solved and fabrication and repair techniques need to be developed. Also a satisfactory feasibility demonstration would have to be accomplished before screens could be considered as the primary propellant settling system for the Voyager vehicle. This system, because of its light weight, is proposed as a potential product improvement over the bellows start tank.

The propellant acquisition system must ensure that essentially bubble-free propellants are supplied to the engine during start up for each of the eight vehicle maneuvers. This requirement was translated into a total settling impulse which was used to size each of the systems considered.

The total impulse required for the settling maneuver was based on the settling process shown in Figure 4-26. This process consists of:

1) An initial flow of the propellants in the form of a cylindrical sheet down the tank walls;

2) Formation of a geyser as the propellants rush to fill the bottom of the tank

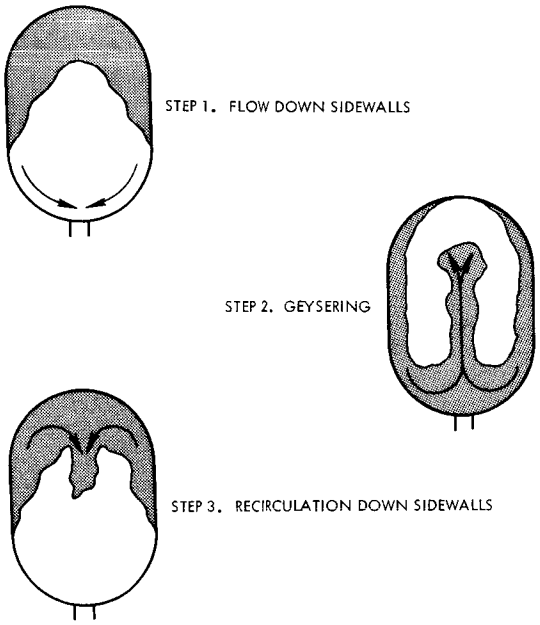

Figure 4-26
STEPS INVOLVED IN SETTLING THE PROPELLANT assuming all of the propellant is at the end of the tank opposite to that needed for engine start. The process illustrates what happens in a bare tank without baffles or other geyser suppression means.

3) A recirculation of the geyser and subsequent flow down the tank wall with a quiet closing of the propellants at the bottom of the tank.

For this process, the time required to settle the propellants is calculated as shown in Appendix A and is slightly more than twice the time for free fall of propellants under the acceleration field produced by the settling system thrusters.

Figure 4-27 shows the duration of the most severe settling maneuver of the mission in seconds versus vehicle acceleration. This occurs

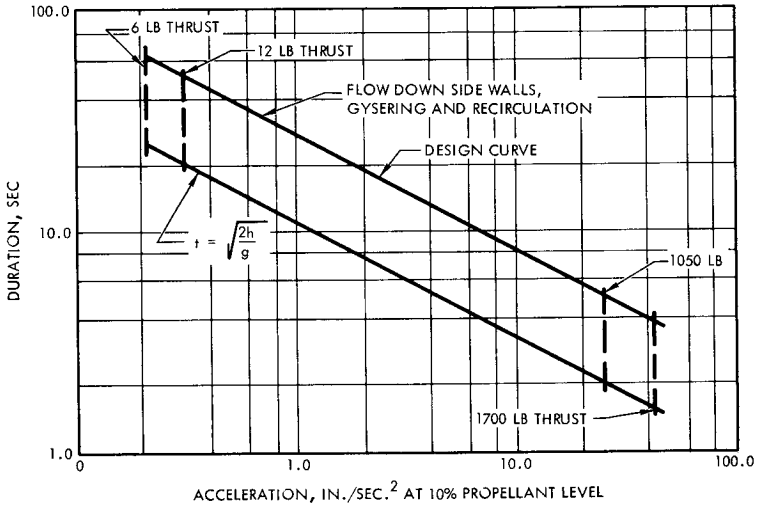

Figure 4-27

FIRING DURATION NEEDED TO SETTLE PROPELLANTS, showing acceleration at applicable thrust levels under consideration. The design curve shown is conservative since means can be incorporated to surpress the geysering.

during start-up with 10 percent propellant available in the tanks. This is typical for a start-up prior to an orbit correction maneuver. For purposes of comparison and for sizing all of the systems it was very conservatively assumed that system impulse would be based on all eight starts occurring with only 10 percent propellant in the tanks.

Additional requirements which were assumed as ground rules for the thruster settling system to establish a basis for comparison were that:

- Each alternate should contain sufficient redundancy to compensate for failure of a single thruster.
- The system weight includes sufficient additional attitude control system (ACS) gas and the needed additional tank weight to contain it to compensate for a failed thruster in the settling system.

4.7.1 Candidate Systems

The following paragraphs describe the hardware and the operation for each of the candidate propellant acquisition systems. Weights and other physical characteristics have been determined consistent with the requirements discussed previously in this section.

4.7.1.1 Combined Settling and Attitude Control System

In this system, propellant settling is accomplished by increasing the gas capacity and using the already on-board attitude control system (ACS) shown in Figure 4-28. In the high thrust mode the ACS is capable of delivering with its four aft facing thrusters, a total thrust of 12 pounds.

Performance Characteristics

Thrust	3 lb
Regulated pressure:	630 psia
Specific impulse:	60 lb sec
Total impulse capability:	12,300 lb sec
Nozzle chamber pressure	
High thrust:	420 psia

Physical Characteristics

Propellant:	Ambient nitrogen
Total subsystem wieght:	487 lb
Gas weight:	205 lb
Initial storage pressure:	3000 psia
Solenoid valve power requirements:	20 watts each peak
Valve heater power requirements:	3 watts each

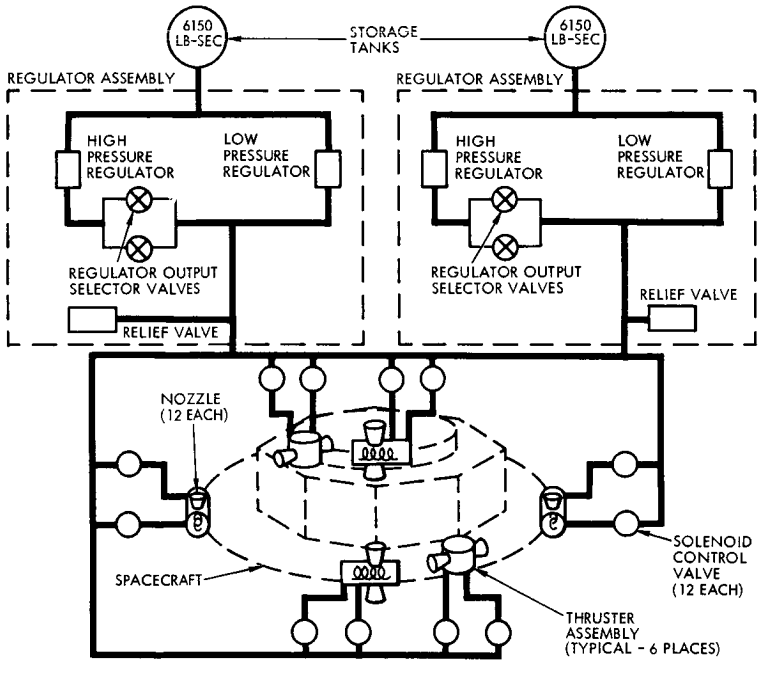

Figure 4-28
SETTLING SYSTEM USING ATTITUDE CONTROL SYSTEM for settling the propellants. Additional gas must be carried in the ACS.

Referring back to Figure 4-27, the nominal firing duration to settle propellants would be approximately 45 seconds for a thrust of 12 pounds.

To determine the total impulse and consequently the weight of the system, it is necessary to consider the case where one of the thrusters fails in the open position. Should this occur it is necessary to pulse two opposing thrusters fed from the same gas supply. One thruster cannot be used to oppose the failed open thruster because the ACS system logic can only provide pure torque by the firing of two thrusters. This mode of operation would deplete all of the gas from the supply with the failed thruster and one third of the supply from the second gas source or two thirds of the total gas supply. Hence, in order to complete the mission with the remaining one third of the initial gas supply, the original quantity of gas must be three times that required for the nominal mission. It should be noted that in the case where one thruster has failed, the maneuver will be performed with only two of the 3-pound thrusters at a thrust of 6 pounds. The settling time with 6-pound thrust as shown in Figure 4-27 is 65 seconds. Hence, the total impulse required per start for the case with the failed thruster is

$$I_t = 6 \text{ lb} \times 65 \text{ sec} = 390 \text{ lb-sec}$$

Using a specific impulse for unheated gaseous nitrogen of 60 seconds, the weight of nitrogen required per maneuver would be

$$W_g = \frac{390 \text{ lb-sec}}{60 \text{ sec}} = 6.5 \text{ lb}$$

For eight maneuvers, and assuming the factor of 3 to compensate for the failed thruster mode of operation, the total gaseous nitrogen required would be

$$W_g = 6.5 \times 8 \times 3 = 156 \text{ lb}$$

The weight of the ACS system without provision for propellant settling is 140 pounds. This weight includes 31 pounds for thrusters, valves, plumbing, and the pressure regulator; 60 pounds for the gas

storage tank and 49 pounds of gas. The additional weight required to perform propellant settling is 347 pounds; 156 pounds of additional gas and 191 pounds of additional gas storage tank.

For purposes of comparing systems, an additional correction was included to account for the velocity increment added to the spacecraft during the propellant acquisition maneuvers. This correction corresponds to the weight of the main liquid propellants which would be required to add the same velocity increment. This weight is essentially equal to the weight of the gas used in the nominal mode of operation times the ratio of the specific impulse between the gaseous nitrogen and the main liquid propellant. In this case the correction would be

$$\Delta W_g = 52 \text{ lb} \times \frac{60 \text{ sec}}{298 \text{ sec}} = 10.5 \text{ lb}$$

Hence, the total weight chargeable to the combined propellant acquisition system is 336.5 pounds.

4.7.1.2 Separate Gaseous Nitrogen Settling System

In an attempt to reduce the weight penalty associated with the use of the ACS for propellant settling, a completely separate gaseous nitrogen system, shown in Figure 4-29, was studied. With this system the gas required results in a failure mode factor of 2.34 rather than the factor of 3.0 associated with the combined ACS settling systems. In the case of a failed open thruster, one of the settling system propellant tanks will be depleted and some additional propellant will be consumed by the ACS system in order to maintain the spacecraft attitude. In order to reduce the amount of ACS gas required to balance a failed open settling thruster, the moment arm of the settling system thruster was made 1/3 that of the ACS thruster. The system was sized for this failure mode assuming the failure also occurred during the first firing as was done for the combined ACS settling system.

The required impulse and weight of nitrogen per start are 390 lb-sec and 6.5 pounds, respectively. These values are identical with those determined previously for the combined system.

Performance Characteristics

Thrust:	3 lb
Regulated pressure:	630 psia
Specific impulse	
Minimum:	60 sec
Total impulse capacility:	6,240 lb-sec
Chamber pressure	420 psia

Physical Characteristics

Propellant	nitrogen
Total subsystem weight:	252 lb
Gas weight:	104 lb
Initial storage pressure:	3000 psia
Solenoid valve power requirements:	20 watts each peak
Valve heater power requirements:	3 watts each

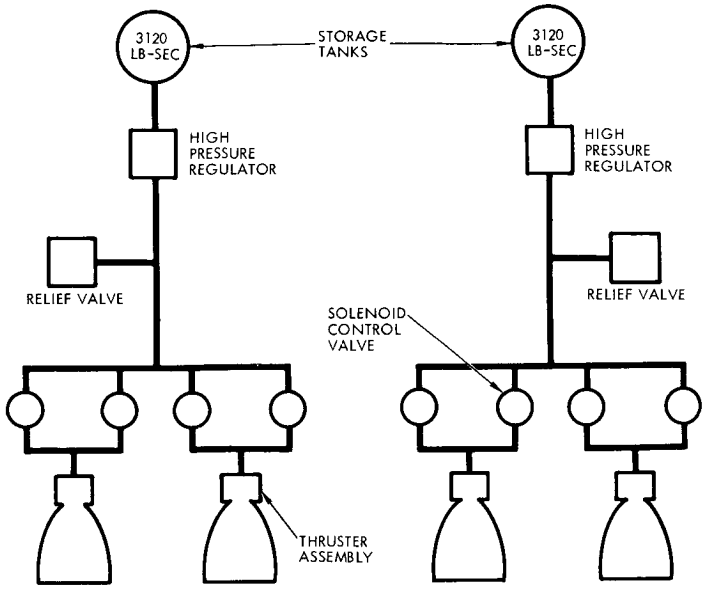

Figure 4-29

GAS SETTLING SYSTEM INDEPENDENT OF THE ATTITUDE CONTROL SYSTEM. The advantage is the reduced gas loss during a valve open malfunction.

The gaseous nitrogen required for each settling system is

$$8 \text{ starts} \times 6.5 \text{ lb} = 52 \text{ lb/tank}$$

A failure mode depletion of one tank will result in the need for twice this amount or 104 pounds. The ACS gaseous nitrogen required to null one settling thruster failed open is $1/3 \times 17.5$ pounds. The total gas involved in settling is then $104 + 17.5 = 121.5$ pounds. The failure mode factor for this system is therefore $121.5/52 = 2.34$.

The total additional ACS weight is 39 pounds including 17.5 pounds of gaseous nitrogen and 21.5 pounds of tankage.

The total weight of the separate gaseous nitrogen system is 252 pounds including two tanks at 128 pounds, 104 pounds of propellant and 20 pounds of plumbing, thrusters, regulators, and valves.

As was done in the previous section, the correction to account for the velocity increment added to the spacecraft during the propellant acquisition maneuver is:

$$\Delta W_g = 52 \text{ lb} \times \frac{60 \text{ sec}}{298 \text{ sec}} = 10.5 \text{ lb}$$

The total weight chargeable to the separate gaseous nitrogen acquisition system is therefore 252 + 39 - 10.5 = 280.5 pounds.

That both of the gaseous nitrogen system weights are quite large is certainly not unexpected when the specific impulse of the respective propellants is considered, i.e., 60 seconds for gaseous nitrogen as compared to over 200 seconds for hot gas systems. The amount of gaseous nitrogen required in the combined ACS settling system configuration results in a weight penalty of 2 to 6 times the weight of hot gas systems. While the separate gas system weight penalty is about 4 to 6 times the weight of such systems.

The gas systems are also deficient in their ability to remove bubbles from the feed system as illustrated in Figure 4-30. The thrust required to remove bubbles was calculated assuming that the Bond number must be equal to or greater than 0.83 and that the gross vehicle weight was approximately 30,000 pounds. As shown in Figure 4-30, the low thrust systems are an order of magnitude lower in thrust than that required to remove bubbles from the 2-inch feed lines.

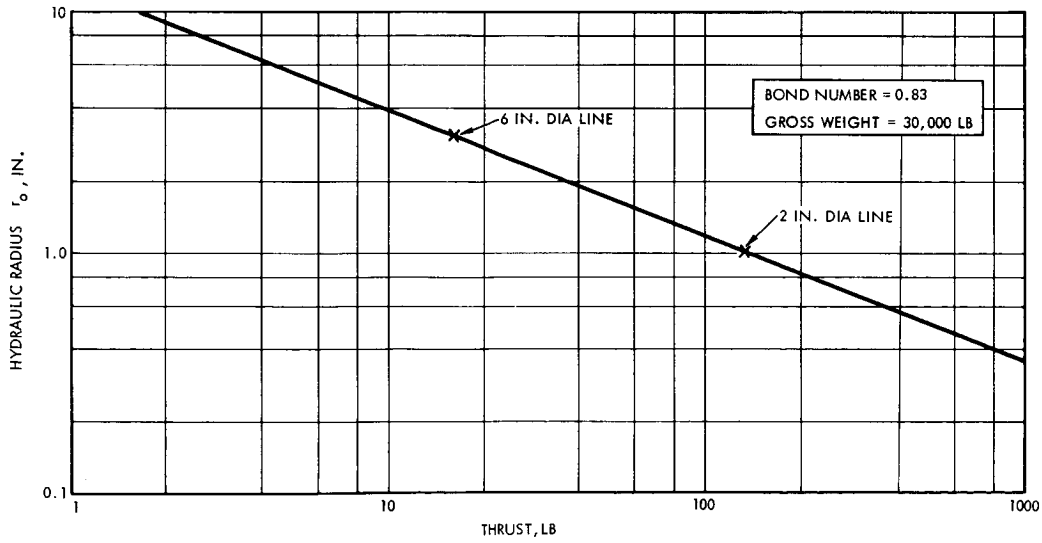

Figure 4-30

THRUST REQUIRED FOR BUBBLE REMOVAL in propellant manifolds as a function of hydraulic radius for the critical Bond number of 0.83. Appreciable thrust levels are needed to remove bubbles in the 2-inch-diameter propellant feed lines on Voyager.

4.7.1.3 Monopropellant System

The second alternate considered is a monopropellant hydrazine system shown in Figure 4-31. As shown, the monopropellant alternate is two completely redundant systems, as was the previously discussed gaseous nitrogen system. Each of the redundant systems consists of a

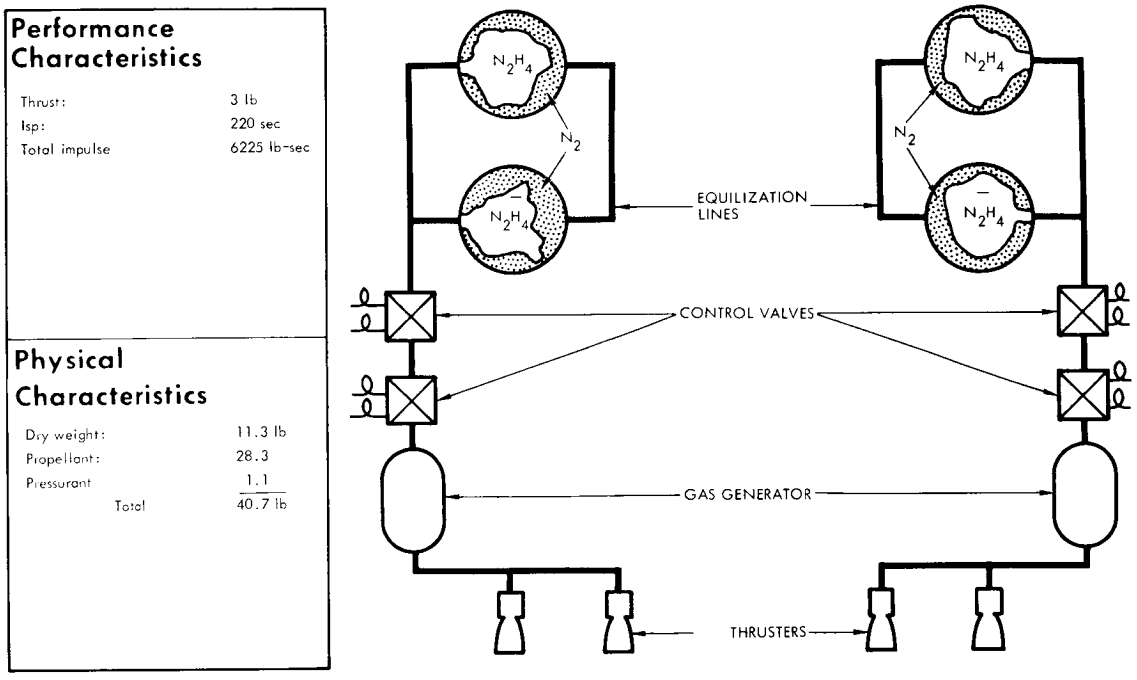

Figure 4-31

HYDRAZINE THRUSTER SYSTEM FOR SETTING MAIN ENGINE PROPELLANTS. A separate gas generator avoids the possible freezing associated with thrusters exposed to the space environment.

pair of propellant tanks with positive expulsion bladders, fill and drain valves, instrumentation, two series redundant propellant valves, and a pair of 3-pound thrust monopropellant thrusters. In the event either of the systems fail to operate, the other system is capable of completing the propellant acquisition maneuver requirements.

In order to reduce the low temperature problems and to improve system reliability, gas generators supply hot gas to the thrusters. This approach eliminates the potential propellant freezing problem associated with line runs containing hydrazine to outboard thrusters. The lines instead contain hot gas. Two valves in series are used to assure positive propellant shutoff. The available thrust for propellant acquisition with one system not operating would be 6 pounds. Referring

to Figure 4-27 the burning time required is 65 seconds. The total impulse per start per system would be identical to the previous systems or 390 lb-sec. With a typical monopropellant engine specific impulse of 220 seconds, eight starts with both systems functioning would require a propellant weight (W_p) of:

$$W_1 = \frac{390 \times 2 \times 8}{220} = 28.3 \text{ lb of propellant}$$

Since the engines must operate in pairs, because of the valve configuration, it is not possible to produce a single malfunction situation which would require attitude control gas.

The weight of the system is 40.7 pounds of which 28.3 pounds is propellant, 1.1 pounds is pressurant and 11.3 pounds is tankage, plumbing, valves, and thrusters. The correction for the velocity increment added is 28.3 x 220/298 = 20.9 pounds. Hence, the weight chargeable to the system is 19.8 pounds.

The advantages of this system lie principally in its light weight, flexibility, and growth potential. Though the system was sized at 12 pounds total thrust to be comparable with the cold gas systems, additional thrust for bubble removal could be attained by increasing thrust to 130 pounds but at the expense of the resultant increase in the system weight.

The use of hydrazine in small lines routed to the thrusters is a potential low temperature problem which is avoided by application of the gas generators. However, special thermal control may be required to maintain the lines and components upstream of the shutoff valves above the freezing temperature of hydrazine (35°F), which is a disadvantage when compared to the lack of temperature limitations of the other candidate systems.

The addition of a monopropellant system to the spacecraft requires all of the control, ground equipment, and cost associated with the design and testing of a new system. The complexity resulting from the utilization of an additional propellant (hydrazine) is certainly a major disadvantage.

4.7.1.4 Screen System

The screen system maintains the propellant in a "settled" condition free of bubbles by means of preferential transfer of liquid, rather than gas, across a very fine mesh screen. This concept is based on the ability of an 18 mesh absolute screen to maintain a positive differential pressure of at least 2 psi without breaking the surface tension forces at the liquid-gas interface on the screen surface. For added reliability two screens are used. The volume between the two screens, shown in Figure 4-32, is such that even if gas were transferred across the primary

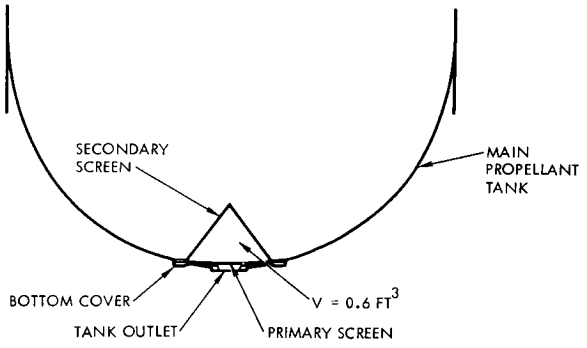

Figure 4-32
RETENTION SCREEN for acquiring the propellant uses two screens to insure gas-free propellant. If any bubbles manage to pass through the top screen they will be trapped within the screened-off compartment.

screen during propellant settling for each of the eight low thrust starts, no gas would transfer across the secondary screen during the last start. The volume required in the oxidizer tanks is:

$$\frac{8 \text{ starts} \times 3.9 \text{ sec} \times 3.5 \text{ lb/sec}}{2 \text{ tanks} \times 90.5 \text{ lb/ft}^3} = 0.605 \text{ ft}^3$$

which is the same as the fuel volume required for an equal volume engine mixture ratio. The settling time of 3.9 seconds was derived from Figure 4-27 using a 1700 pound thrust level. With a required volume of 0.605 cubic foot and the cone base diameter of 16 inches, shown in Figure 4-32, the cone height is:

$$h = \frac{0.605}{\pi} \frac{3}{(2/3)^2} = 1.3 \text{ ft} = 15.6 \text{ inches}$$

The cone surface area is then:

$$A = \pi \left(\frac{8}{12}\right) \sqrt{\left(\frac{8}{12}\right)^2 + (1.3)^2} = 3.1 \text{ ft}^2$$

The area of the base of the cone is

$$A = \pi \left(\frac{8^2}{12}\right) = 1.4 \text{ ft}^2$$

The total cone weight is

$$4.5 \text{ ft}^2 \times \frac{1 \text{ lb}}{4 \text{ ft}^2} = 1.125 \text{ lb/cone}$$

Assuming a 100 percent factor for welding and for supports, the total weight of the screen system is 4 x 2.25 = 9.0 pounds.

The pressure drop across either screen during propellant flow must not exceed the 2 psi value which would break the surface tension forces and thereby allow flow of gas into the propellant feed system. The maximum drop across the primary screen was calculated based on the maximum flow rates at the high thrust mode of operation. Under these conditions it is 0.25 psi across the primary screen and 0.8 psi across the secondary screen at 21 pounds N_2O_4 per second flow rate. This maximum expected drop is less than 1/2 of the 2 psi which would break the surface tension forces implying a more than adequate safety margin.

The use of screens for propellant orientation has the advantage of low weight and simplicity. However, before screens can be used, questions concerning the ability of the system to function properly in the Voyager environment must be answered. Also, some practical problems concerning fabrication and procedures related to producing such a system are apparent. The most serious of the problems is that if for any reason gas does get into the feed system, it will be trapped there forming very large bubbles which will be subsequently ingested into the engine, potentially causing damage or at least performance degradation. In spite of sophisticated analysis, the confidence level in this system will be low until such time as it is proven in long-term space missions.

In a screen system it is possible that there will be mass transport of propellant caused by evaporation of liquid on the warmer end of each tank followed by condensation at the cooler end. If this were the case, liquid trapped behind the screens on the warmer end would be removed by evaporation to the cooler region, leaving only vapor and pressurant gas between the screens and the feed lines if the cooler end was opposite to the screen location. The thermal gradient causing this transport has been roughly predicted and used to estimate the worst case mass transfer in Appendix B. As discussed in the appendix, the anticipated free convection of the liquid (due to acceleration caused by solar pressure) will tend to limit temperature differentials and thereby limit mass transfer due to gaseous diffusion of propellant through the ullage to the cold end of the tank. When the spacecraft is in orbit it is expected that the heat loads will be primarily from the equipment modules located in the forward end of the spacecraft. With the temperature gradient in this direction, the mass transport due to diffusion is in the favorable direction and would assist in maintaining propellants behind the screen.

A second problem is helium gas bubbles coming out of solution between the screen and the tank wall. Because helium is soluble in the propellants, dissolved gas will normally be present in the liquid. The solubility increases with temperature, so that with decreasing temperature helium will come out of solution. Due to the anticipated temperature profile within the tank during the Voyager mission, the propellant will cool behind the screen, making that a probable location for the formation of pressurant gas bubbles. These bubbles would be trapped behind the screen by the surface tension forces and would enter the engine through the feed line during starting.

The available data on helium solubility in the propellants varies widely depending on the data source. Using the data of Chang and Gokcen,* for a temperature decrease of 50°F from near-earth to near-

*Chang, E. T. and N. A. Gokcen, "Thermodynamic Properties of Gases in Propellants and Oxidizers, I. Solubilities of He, N_2, O_2, AR, and N_2O_3 in Liquid N_2O_4, "J. of Phys. Chemistry, 70 2394 (1966).

**R. R. Liberto, Titan II Storable Propellant Handbook, Report No. 8111-933U03, AFFTC TR-61-32, Bell Aerosystems Company, Buffalo, N. Y.

Mars, the net volume of helium which would come out of solution is approximately 1 percent of the N_2O_4 volume being considered. If this same calculation is performed using the data of the Titan II Handbook,** the net volume of helium which would come out of solution is 27 percent. The problem of which solubility data to use is recommended for further study. The LMDE has demonstrated the capability of ingesting at least a 5 percent volume fraction, however, 27 percent may well be a problem.

The question of fabrication techniques and quality control is secondary to the thermodynamic questions. Testing of a screen system to verify integrity and effective mesh size is a matter of measuring the differential pressure at which the surface tension forces are overcome. The integrity of the screen can be verified by this means following the various vibration and other environmental tests to which the vehicle is subjected. Repairing a faulty screen detected at any time following tank fabrication would require removal of the tank cover and screen assembly, which is no more difficult than repairing any of the other candidate systems.

4.7.1.5 Bellows Settling System

The start tank design of the bellows settling system used in this study is similar to existing hardware on Agena and the Saturn V-IVB stage. Bellows start tanks can be designed to provide many displacement cycles and therefore are amenable to functional checkout and possible propellant dumping at the launching facility, a necessary condition for Voyager. The proposed design employs a double metal bellows containing enough propellant for eight starts. The bellows, supported agsinst side loads and pressure instability, is mounted on the propellant tank cover as shown in Figure 4-33.

The normal mode of operation, as shown in Figure 4-34, is to open the start tank control valves, open the engine low thrust control valves, and then at the expiration of the 39 seconds settling time open the feed system pre-valves. Opening the pre-valves allows settled propellant to flow to the engine. The start tank control valves are then closed to prevent continued flow from the start tank. The engine continues to fire on settled propellant.

PRELIMINARY SPECIFICATION

Bellows Tank Assembly

Purpose

To supply gas free propellant for settling main tank propellants

Performance Characteristics

Operating pressure:	270 psia max
Proof pressure:	306 psia
Burst pressure:	408 psia
Rated flow: Oxidizer (N_2O_4):	3.5 lb sec
Fuel (aero 50)	2.2 lb sec
Service life:	150 cycles

Physical Characteristics

SIZE:

Container outside diameter 16.5 in. max
Double bellows inside diameter 12.5 in. min
Bellows container length 19.25 in.
Container support length 5.8 in.
Liquid volume, useable: 2096 in.^{3} min

MATERIALS:

Double bellows: 17-7 PM S.S
Contianer and supports: Titanium

WEIGHT:

Inside bellows tank:	4.45 lb
Outside bellows tank:	5.04
Lower dome and rim:	5.46
Upper dome and rim:	4.82
Container:	4.00
	23.86 lb

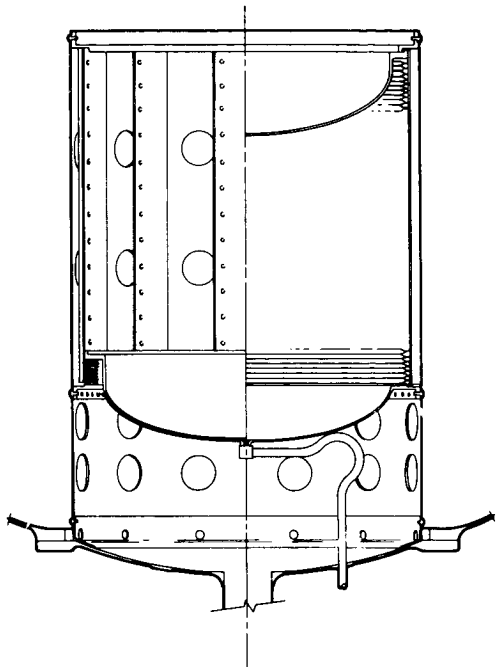

Figure 4-33

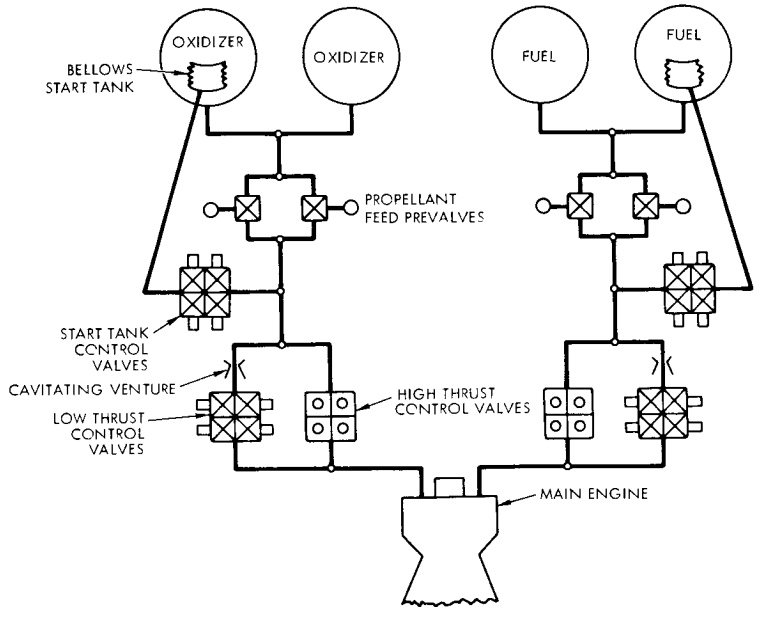

Figure 4-34
FEED SYSTEM incorporating a bellows start tank.

The function of the start tank system components are as follows:

- Start tanks: Provide propellant to the engine by means of positive expulsion during the settling operation
- Start tank control valves: Eliminate leakage during coast and prevent flow into the propellant feed line during engine operation
- Feed system pre-valves: Prevent flow from the main tank during the settling operation

The bellows system weights are as follows:

Propellant Weight

Duration	3.9 sec for 1700 lb thrust
Number of starts	8
Total usable propellant	3.9 sec x 5.70 lb/sec x 8 = 178 lb
Unusable propellant	4 lb
Total propellant	182 lb

Component Weights

Bellows tanks	47.8 lb
Two quad solenoids	10.0
Two fill disconnects	0.6
Instrumentation	2.0
Brackets, supports, etc.	2.0
	64.4 lb

Total weight of bellows tank system including all propellant 246.4 lb

This system utilizes all of the propellant at the same specific impulse as the main engine, therefore the velocity increment correction for the start tank system includes all of the usable propellant, i.e., 178 pounds. The total weight chargeable therefore to the bellows settling system is only the inert weight plus the unusable propellant or 68.4 pounds. All of the usable propellant in the bellows tank can be utilized by leaving the start tank solenoid valve open throughout the duration of the last orbit trim maneuver.

The problems associated with the bellows start tank system center around the possibility of loss of propellants from the tank, rendering the system incapable of future operation. This loss can occur by means of seal leakage, leakage through valves, a failure of the quad redundant start tank solenoid valves to close, and leakage or rupture of the bellows start tanks. These potential leakages are minimized by welded or brazed joints, by valve redundancy, and by the double-wall bellows tank. The bellows are located inside the main propellant tanks, and are therefore not subject to external forces which otherwise could be potentially damaging.

Quad redundancy is utilized such that the calculated reliability of the bellows start tank system is equivalent to the reliability of the redundant gas and monopropellant systems.

Potential fabrication problems, though always present, are minimized by previous industry experience with similar tanks as used on the S-IVB and in the Agena.

The major advantages of the bellows start tank system are the potential for high settling acceleration, low weight and high available impulse. Virtually all of the propellant required for settling is available for application to the vehicle velocity increment at the same specific impulse as the main propulsion. The acceleration level provided is more than adequate to remove large gas bubbles from the propellant feed lines. Because of the inherent weight savings possible, it might be advantageous to consider the screen system as a potential product improvement means for propellant setting.

4.7.2 Evaluation Criteria

The criteria used to select one of the alternative propellant acquisition systems were primarily weight, development maturity, and the degree to which the system would add complexity to the Voyager spacecraft. Because all of the systems considered have approximately equal high reliabilities the criterion of reliability did not enter strongly into the selection. System cost was not used in the evaluation since technical considerations were considered overriding; however, if two systems were to be found equal on a technical basis, cost would have been used

for the final selection criterion. Since each system was designed for eight engine starts which is in excess of the nominal mission requirements, system growth potential also was not used in the evaluation process.

4.7.3 Candidate System Evaluation

The principal characteristics of each of the propellant acquisition systems described in the previous sections are summarized for convenience in Table 4-12. The term "comparative weight" represents the total system weight minus that weight of each system propellant which contributes to the spacecraft velocity. This weight also includes an additional attitude control system weight required to compensate for a failed open thruster.

Examination of the system weights shows that the use of a gaseous nitrogen system is not competitive from a weight standpoint even though the reliability is high and state of the art in such systems is very well developed.

A screen system, while offering the least weight penalty and with the major advantage of being a totally passive system, cannot be selected because of insufficient development maturity.

The monopropellant and bellows start tank systems are competitive in reliability. The degree of experience available with monopropellant systems is about equal to that with start tank and the monopropellant system will be lighter in weight. The monopropellant system does introduce the complexity associated with the addition of a complete new propulsion system with a third liquid propellant to the Voyager spacecraft. A solution to the possible monopropellant freezing problems which might be encountered is the use of a monopropellant hot gas reactor exhausting through out-board nozzles. This modification of the monopropellant system does not have any extensive development history. For these reasons the bellows start tank propellant acquisition system has been selected for the Voyager application.

Table 4-12. Propellant Acquisition System Parameters

Parameter	Gas Systems		Bellows Tank System	Screen System	Monopropellant System
	Combined	Separate			
Thrust, lb	3	3	1700	1700	3
Specific Impulse, sec	60	60	298	298	220
Propellant	N_2	N_2	N_2O_4/A-50	N_2O_4/A-50	N_2H_4
Total Impulse lb-sec	0.9×10^4	0.6×10^4	53×10^4	NA	0.6×10^4
Propellant weight, lb	156	104	178	NA	28.3
Comparative weight, lb	336.5	280.5	68.4	9.0	19.8
Reliability	$0.9^4 77$	$0.9^4 5$	$0.9^4 56$	unknown	$0.9^4 8$

4.8 PROPELLANT SUPPLY SYSTEM COMPONENTS

The approach used in component selection and design was to select existing components with design margin for the Voyager mission and which were qualified for space flight use. The Lunar Module Descent stage (LMDS) since it is designed for operation with the LMD engine provides the bulk of the components which are compatible with the required pressure levels and flow rates. In some areas additional design or requalification is required to meet the long term leakage requirements unique to the Voyager interplanetary mission. These areas are discussed in connection with the individual components in the sections that follow.

4.8.1 Pressurant Tanks

Conventional spherical titanium (6Al-4V) tanks are used for pressurant storage. Two skirt-mounted spheres are used to maintain the spacecraft center of gravity near the vehicle axis. Preliminary sizing studies indicated that two 30 inch spheres will contain the required pressurant at a storage pressure of 4000 psi. A survey of manufactures indicates several high pressure spheres are currently being fabricated in the 28 to 34 inch range. Most of these could be used with an adjustment in storage pressure to provide the required pressurant quantity. Development of a custom storage tank is, however, a straightforward engineering task requiring a modest investment in additional tooling. The final choice between the use of an existing tank or the development of a custom tank will be based on a more detailed cost evaluation.

A preliminary specification of the pressurant storage tank is shown in Figure 4-35.

4.8.2 Pressurant Fill and Vent Coupling

The pressurant fill and vent couplings are used to remotely charge and, if necessary, empty the helium storage tanks and for venting of the propellant tanks during the fill operation and subsequent pressurization of the propellant tank ullage space. The remotely actuated disconnect internal to the shroud is used in conjunction with

PRELIMINARY SPECIFICATION

Pressurant Storage Tank

Purpose

To contain the pressurant required for propellant expulsion

Performance Characteristics

Number required:	2
Operating pressure:	4000 psi Max
Proof pressure:	8000 psi
Burst pressure:	12,000 psi
Minimum gas capacity:	21 lb
Weight	132 lb
Material:	6Al-4V titanium
Service life:	50 cycles
Allowable leakage	10 sec 1ir (He)

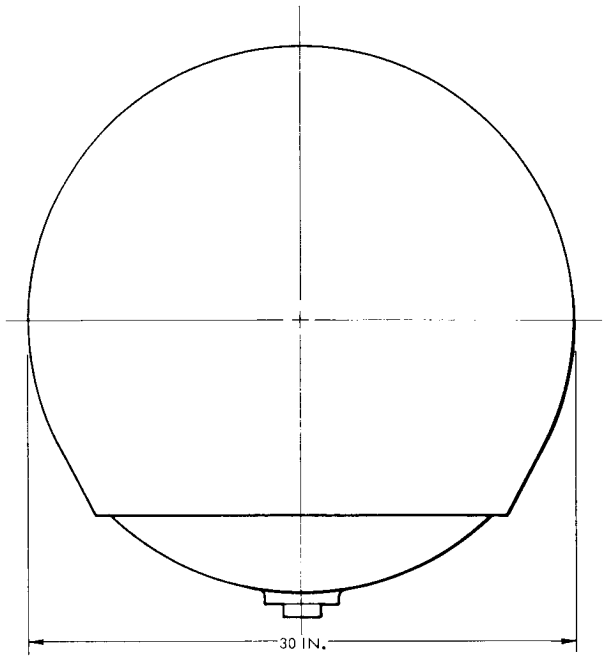

Figure 4-35

an explosive valve for sealing of the line. See Figure 4-36 for a brief specification of this component.

4.8.3 Isolation and Vent Valves

Electro-explosive valves are used to isolate the propellant and pressurant tanks to prevent leakage during the long coast periods, and after the propulsive phases of the mission are completed to allow complete depressurizing of these tanks. The components used on the LMDS for these isolation functions will be incorporated into the Voyager system. Both normally closed and normally open valves are required. A normally closed valve is required in each propellant tank circuit for the final depressurization. A preliminary specification for the electro-explosive valves is presented in Figure 4-37.

4.8.4 Pressurant Filters

Pressurant filters are used to remove potentially damaging particulate contamination from the pressurization system to protect sensitive components such as the pressure regulator. The filters are located

PRELIMINARY SPECIFICATION

Remote Actuated Pressuant Fill and Vent Coupling

Purpose

To permit loading and venting of pressurant.

Performance Characteristics

Number required	1
Line size	1/4 in.
Operating pressure	4000 psi
Proof pressure	8000 psi
Burst pressure	12,000 psi
Actuation pressure	220 psi
Allowable leakage external disconnected	10 scc/hr (He)
Service life	400 cycles
Weight (spacecraft item)	0.3 lb
Similar to	LMDS

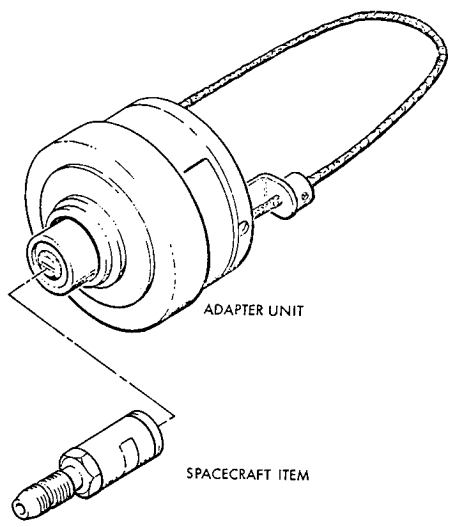

Figure 4-36

PRELIMINARY SPECIFICATION

Pressurant Isolation and Vent Valves

Purpose

To provide positive sealing of the pressurant and gas side of the propellant tanks during non propulsive mission phases.

Performance Characteristics

Number required:	6 normally open 9 normally closed
Line size:	1/2 in.
Operating pressure:	0-4000 psi
Proof pressure:	8,000 psi
Burst pressure:	12,000 psi
Pressure drop at rated flow:	ΔP 3 psi at 0.7 lb/sec (He)
Allowable, internal:	3 scc/hr (He)
external:	1 scc/hr (He)
Service life:	1 cycle
Weight:	0.8 lb
Power required:	1 amp 1 watt - no fire 4 amp - all fire Dual bridgwire
Similar to:	Pyronetics
Used on:	LMDS

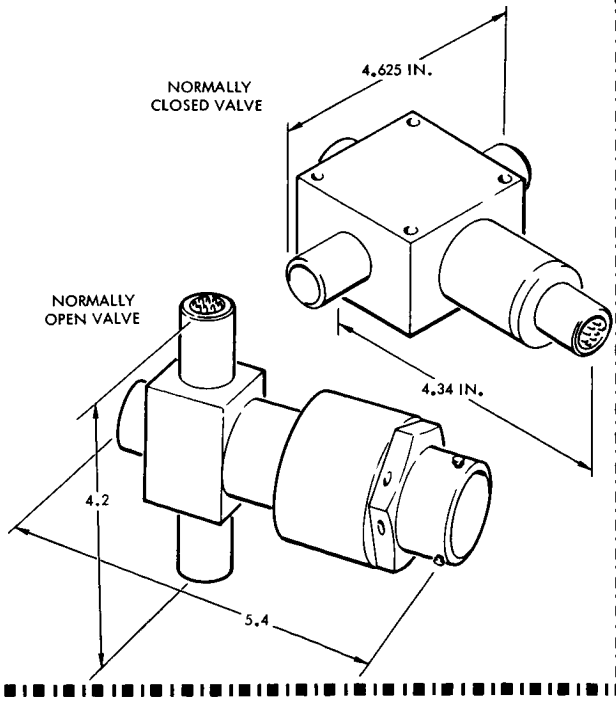

Figure 4-37

immediately downstream of the electroexplosive valve packages since valves of this type are often a source of contaminates. A preliminary specification is shown in Figure 4-38.

4.8.5 Quad Pressure Regulator Package

The regulator package admits the pressurant to the propellant tanks at the required pressure level. It is arranged in a quad redundant package in order to increase the reliability of the basic regulator.

A preliminary specification for the quad pressure regulator is presented in Figure 4-39. The LMDS regulator is not currently designed for use in a quad arrangement and hence may not be directly applicable. Each regulator element will, however, be similar in concept and construction featuring single stage piloted operation.

4.8.6 Quad Check Valve

The check valves are used to prevent mixing of propellants or propellant vapors in the common pressurization lines during conditions of low pressurant flow which may occur during start or shutdown.

The quad check valves qualified for use on the LMDS are directly applicable and will be adopted for Voyager use. A preliminary specification is shown in Figure 4-40.

4.8.7 Propellant Tank

Conventional spherical titanium (6Al-4V) pressure vessels are used to contain the propellants in the desired configuration and permit expulsion of propellant to the engine at the required pressure levels. These are skirt-mounted and will have an access port for installation of the start tank assembly. The technology for tankage of this type has been thoroughly developed on the Apollo program. Stress corrosion of titanium tanks containing nitrogen tetroxide was a serious problem. However, it was solved for Apollo by controlling the amount of nitrous oxide in the propellant. One-year stress corrosion tests sponsored by TRW Systems has proved that this solution is also applicable to the Voyager mission. See Figure 4-41 for a preliminary component specification.

PRELIMINARY SPECIFICATION

Pressurant Filter

Purpose

To maintain the system free of damaging particulate contamination particularly that which may be introduced by actuation of the electro explosive valves.

Performance Characteristics

Number required:	3
Line size:	1/2 in.
Particle rating	
Nominal:	5 micron
Absolute	15 micron
Operating pressure:	0-4000 psi
Proof pressure:	8000 psi
Burst pressure:	12,000 psi
Pressure drop at rated flow:	3 psi at 4.25 lb/sec (He)
Allowable leakage external:	1 scc/hr (He)
Service life:	3000 cycles
Weight:	0.53 lb
Used on:	LMDS

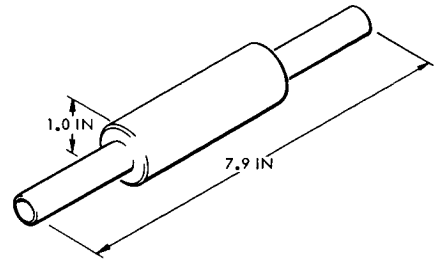

Figure 4-38

PRELIMINARY SPECIFICATION

Quad Pressure Regulator Package

Purpose

To admit the pressurant to the propellant tanks at the predetermined pressure level.

Performance Characteristics

Number required:		1
Line size:		1/2 in.
Operating pressure	Inlet:	4000 - 315 psia
	Outlet:	249 ± 24 psia
	Lockup:	254 psia
Proof pressure	Inlet:	8000 psi
	Outlet:	500 psi
Burst pressure:	Inlet:	12,000
	Outlet:	750
Rated flow		5.2 to 0.52 lb/min (He)
Allowable leakage:	Internal at lockup	40 scc/hr (He)
	External	32 scc/hr (He)
Service life:		3000 cycles
Weight:		6.5 lb
Similar to:		LMDS

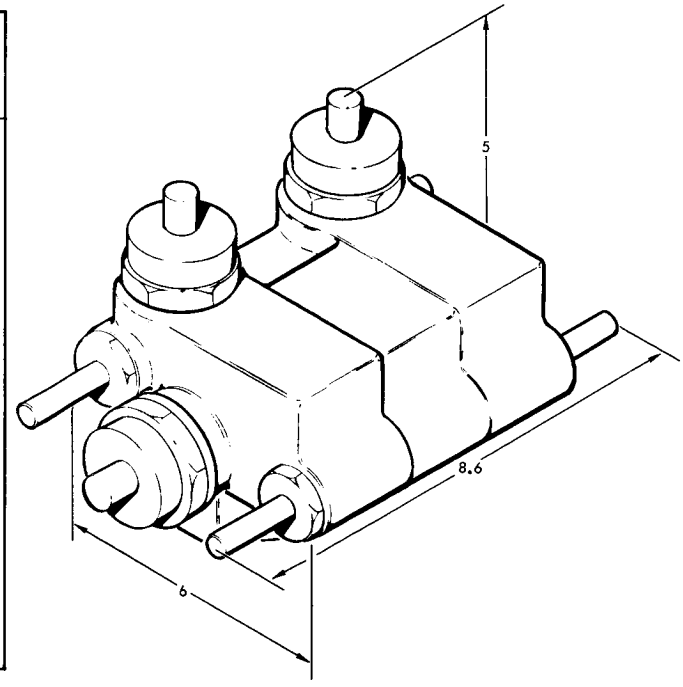

Figure 4-39

PRELIMINARY SPECIFICATION

Quad Check Valve

Purpose

To prevent propellant or vapor mixing in the common pressurization lines.

Performance Characteristics

Number required:	2
Line size, in.:	1/2 in.
Operating pressure:	270 psi maximum
Proof pressure:	540 psi
Burst pressure:	810 psi
Pressure drop at rated flow:	3.0 psi at 2.3 lb/sec (He)
Allowable leakage Internal: External:	 10 scc/hr (He) 2 scc/hr (He)
Service life:	8000 cycles
Weight:	0.9 lb
Cracking pressure, each valve:	2.0 psi
Reseat pressure:	1.0 psi
Similar to:	James, Pond and Clark No. P1-754
Used on:	LMDS

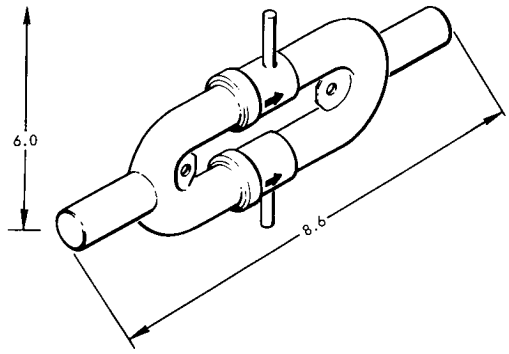

Figure 4-40

PRELIMINARY SPECIFICATION

Propellant Tank

Purpose

To contain the propellant supply and permit pressurized expulsion.

Performance Characteristics

Number required:	4
Internal volume:	57.0 ft^3
Operating pressure:	270 psi max
Proof pressure:	360 psi
Burst pressure:	405 psi
Service life:	150 cycles
Weight:	100 lb
Material	6Al-4V titanium
Allowable leakage:	10 scc/hr (He)
Propellants	N_2O_4; A50 or MMH

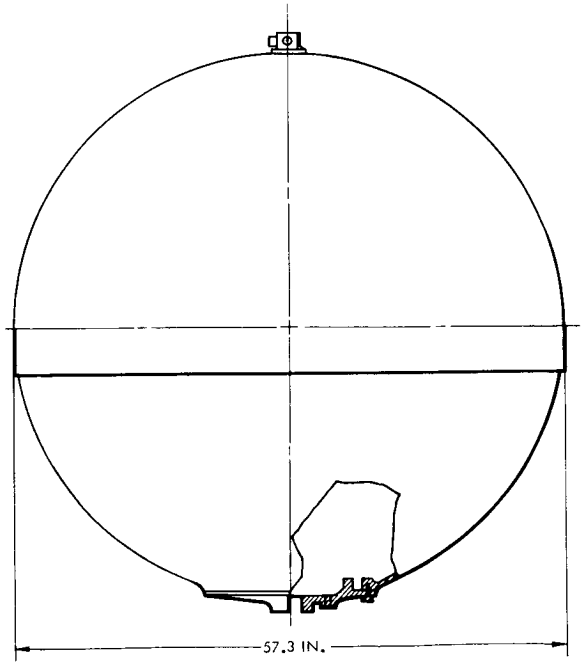

Figure 4-41

4.8.8 Propellant Fill and Drain Coupling

Propellant fill and drain coupling, consisting of a spacecraft half and a ground support half, is required for remote propellant loading and, if necessary, unloading. An interlock prevents opening of the valve in the disconnected position. Explosive valves are used for final sealing of the line prior to flight. A specification for this component is shown in Figure 4-42.

PRELIMINARY SPECIFICATION

Remote Actuated Pressurant Fill and Vent Coupling

Purpose

To permit loading and draining of the main propellant and start tanks.

Performance Characteristics

Number required:	4
Line size:	0.5 in.
Operating pressure:	270 psi maximum
Proof pressure:	540 psi
Burst pressure:	810 psi
Actuating pressure:	220 psia
Allowable leakage, external disconnected:	10 scc/hr (He)
Service life:	400 cycles
Weight (spacecraft item)	0.45 lb
Similar to:	LMDS

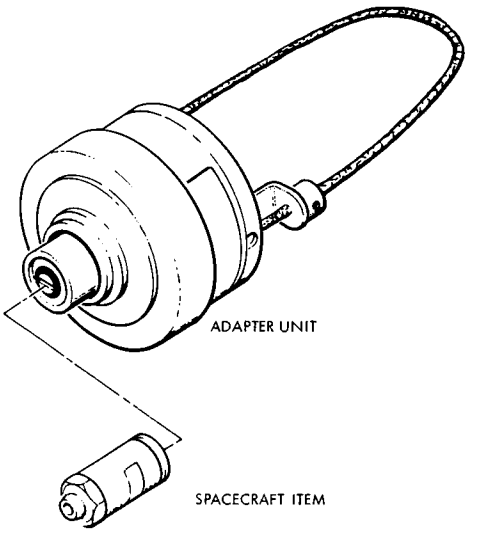

Figure 4-42

4.8.9 Propellant Tank Overpressure Relief Valve

The propellant tank overpressure relief valve consists of a burst disc backed up by a relief valve. In normal operation the burst disc remains intact providing a positive seal against pressurant leakage. Should an abnormal condition involving excessive tank pressure occur, the burst disc will rupture without fragmentation, at approximately 15 psi above the maximum tank working pressure. The relief valve will crack if the pressure continues to rise an additional 7 psi and then

reseat when the pressure drops to approximately 10 psi below the cracking pressure.

It is anticipated that the LMDS overpressure relief valve can be used directly on Voyager. A preliminary specification is provided in Figure 4-43.

PRELIMINARY SPECIFICATION

Propellant Tank Overpressure Relief

Purpose

To protect the propellant tank against damage due to overpressure.

Performance Characteristics

Numbered required:	2
Line size:	1/2 in.
Operating pressure:	
Burst disc rupture:	270 ± 12
Relief valve crack:	275 ± 4
Relief valve reseat:	265
Proof pressure:	540 psi
Burst pressure	810 psi
Rated flow:	10 lb/min (He)
Allowable leakage, burst disc intact:	1 scc/hr (He)
relief valve:	10 scc/hr(He)
Service life (after burst disc rupture)	3000 cycles
Weight:	0.8 lb
Used on:	LMDS

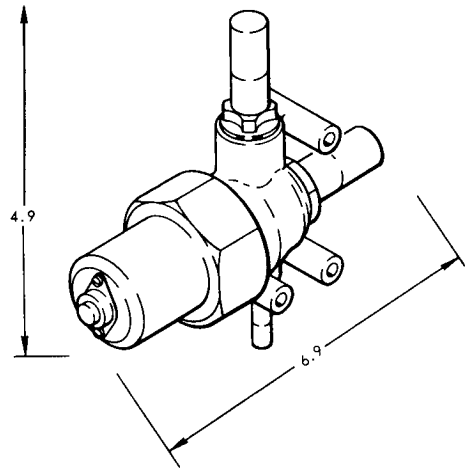

Figure 4-43

4.8.10 Propellant Supply Pre-valve

The propellant supply pre-valve is a component that has no counterpart in the LMDS feed system. This valve is used in the start sequence to change the flow from the start tanks to the main tanks and also to provide positive sealing for the long mission coast phases. Since the engine valves provide the proper propellant phasing for engine start, rapid and reproducible actuation is not a requirement for the pre-valves. The valve incorporates the following features; high seating force, restrained teflon seat, no wiping action across the seat, and fail closed. Linked pairs (fuel and oxidizer) are used to maintain propellant mixture ratio in the event of a failure.

In order to attain the high seat pressure necessary to eliminate pre-valve leakage, a motor-driven poppet valve has been identified as the type of valve to be used. The motor, in addition to stroking the valve, applies the needed seating pressure after closure. A valve of this type was developed and flight qualified for the Atlas missile pressurization system.

A two-stage solenoid actuated valve is also being examined as an alternate. This approach simplifies the requirement established for valve closure in the event of power failure. See Figure 4-44 for a preliminary specification of this component.

PRELIMINARY SPECIFICATION

Propellant Supply Prevalve

Purpose

To permit propellant flow from the main tanks phased after propellant settling has occured and to provide positive sealing of the tank outlet lines during the long coast periods.

Performance Characteristics

Number required:	2 pair (ox-fuel mechanically linked)
Line size:	2.0 in.
Operating pressure:	270 psi max
Proof pressure:	540 psi
Burst pressure:	810 psi
Pressure drop at rated flow:	3.1 psi at 6 lb/sec A-50 5 psi at 10 lb/sec N_2O_4 or MMH
Allowable leakage Internal: External:	 10 scc/hr (He) 2 scc/hr (He)
Service life:	100 cycles
Weight, max:	5.0 lb
Actuation time:	3.0 sec
Powered required:	100 w at 32 VDC each pair
Similar to:	Robertshaw - Fulton
Used on:	Atlas

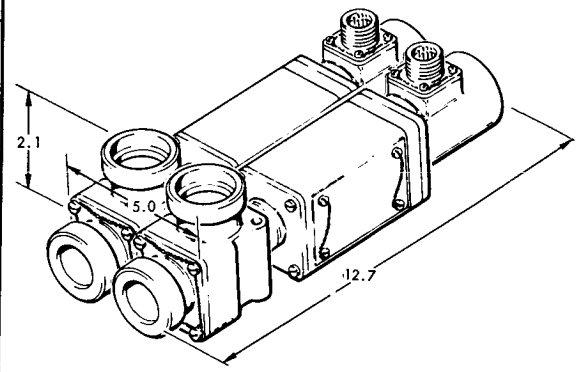

Figure 4-44

4.8.11 Bellows Assembly

The design of the bellows tank, as presented in the propulsion studies Volume I of Task C, has been updated to include additional propellant and a redundant outer bellows. This design is illustrated in Figure 4-33. The additional propellant required is the result of

increased settling thrust and of an updated analysis of the settling duration.

The addition of the redundant outer bellows to improve reliability does pose some problems. The interspace volume between the bellows must be designed such that if a failure occurs (leakage) the liquid accumulated in the interspace will not cause further bellows failure when the tank is collapsed during subsequent starts. Failure could be caused by excessive pressure build-up in the interspace due to compression of the accumulated liquid leakage as the tank collapsed during a normal expulsion sequence. The proposed design eliminates this problem by maintaining a negligible interspace volume.

The bellows tank support is designed to act as a guide for the upper dome as it travels towards the fixed lower dome during the expulsion operation. In addition the support provides stability to the bellows such that relatively high internal pressures can be applied without causing permanent deformation of the bellows.

The base support will be attached to the tank access cover providing simple installation or removal of the tank assembly.

4.8.12 Start Tank Control Valve

The start tank control quad solenoid valve is identical to the one utilized on the main engine described in Section 4.4.3 and shown in Figure 4-14. The application of this valve to the start tank system requires no changes because of identical operating pressures, flow rates, actuation times, and power requirements.

4.9 TRANSTAGE AND AGENA FIT

The Task D guidelines requested that the Agena and Transtage engines be considered in the Voyager spacecraft from the standpoint of mechanical fitting into the selected spacecraft configuration after it had been designed for the modified LMDE. No consideration was given to the possible need for changes in the propellant pressurization and feed system. In doing this work the items that were considered are:

- Engine mount location
- Clearance of engine gimbal and head end assembly

- Propellant line interface and line routings
- Engine support
- Interference with the spacecraft allowable envelope
- Electrical interface

4.9.1 The Agena Engine

The Agena rocket engine (Bell Model 8533-478016 "D"), as shown in Figure 4-45, was considered from a mechanical fit standpoint as a replacement for the main propulsion engine for the Voyager spacecraft. A layout study was performed to determine the location needed for the engine mount, propellant interfaces, and the engine support structure.

The results of the layout study indicate that the Agena engine head end will fit within the spacecraft, as shown in Figure 4-46. The expansion nozzle, however, extends beyond the spacecraft allowable envelope.

4.9.1.1 Engine Mount Location

The engine mount was located so that the gimbal location coincides with the LMDE gimbal position. The engine gimbal position could be moved forward about 3 inches before major structural mounting redesign would be required of the propulsion module main supporting structure. However, this forward movement of 3 inches would not be sufficient to move the exit nozzle bell to within the spacecraft allowable envlope. An Agena engine with a smaller nozzle area ratio is required.

4.9.1.2 Clearance of Engine Gimbal and Head End Assembly

Since the Agena head end assembly is within the Voyager engine head end assembly envelope no interference exists in the radial and in the forward directions. At present the Agena gimbal angle capability is ±3.5 degrees which does not provide the ±6 degrees required by the spacecraft. To allow the Agena engine to gimbal the ±6 degrees requires that the accessories packaged around the chamber be repackaged to allow more clearance around the chamber. This would require, for example, relocating the turbine exhaust ducting and turbine housing.

4.9.1.3 Propellant Line Interface and Line Routing

The propellant line interfaces are different than the LMDE assembly. This requires propellant line rerouting. As there is adequate clearance of approximately 3 inches for the fed system lines around and above the head end assembly, no problems are anticipated in this area. Line size transitions (fuel from 1-1/2 to 1-3/4 inch and oxidizer 2.0 to 2-1/4 inch) can be made at the engine feed system interface.

4.9.1.4 Engine Support

The engine supports, which distribute the loads from the engine to the spacecraft main structure, are similar in concept to the LMDE assembly. The truss structure is different in the length and the angles of the truss members.

4.9.1.5 Interference with the Spacecraft Allowable Envelope

The Agena engine, as modified for the Voyager application, has an increased exit nozzle length and diameter. It presently extends beyond the allowable envelope and would require a slightly shorter nozzle.

4.9.1.6 Electrical Interface

The electrical interfaces of the Agena engine are within the evelope provided for the LMDE assembly. No problems are anticipated with mechanical fit in this area even though the number and sizes of the connectors are not the same as the LMDE installation. The connectors are small and can be easily relocated.

4.9.2 The Transtage Engine

The Transtage rocket engine (Aerojet Model No. AJ 10 138), shown in Figure 4-47, was also considered from a mechanical fit standpoint as a replacement for the main propulsion engine for the Voyager spacecraft. A layout study was performed to determine the needed location of the engine mount, propellant interfaces, and the engine support structure.

The results of the layout study, shown in Figure 4-48, indicate that the Transtage engine will fit within the spacecraft allowable envelope.

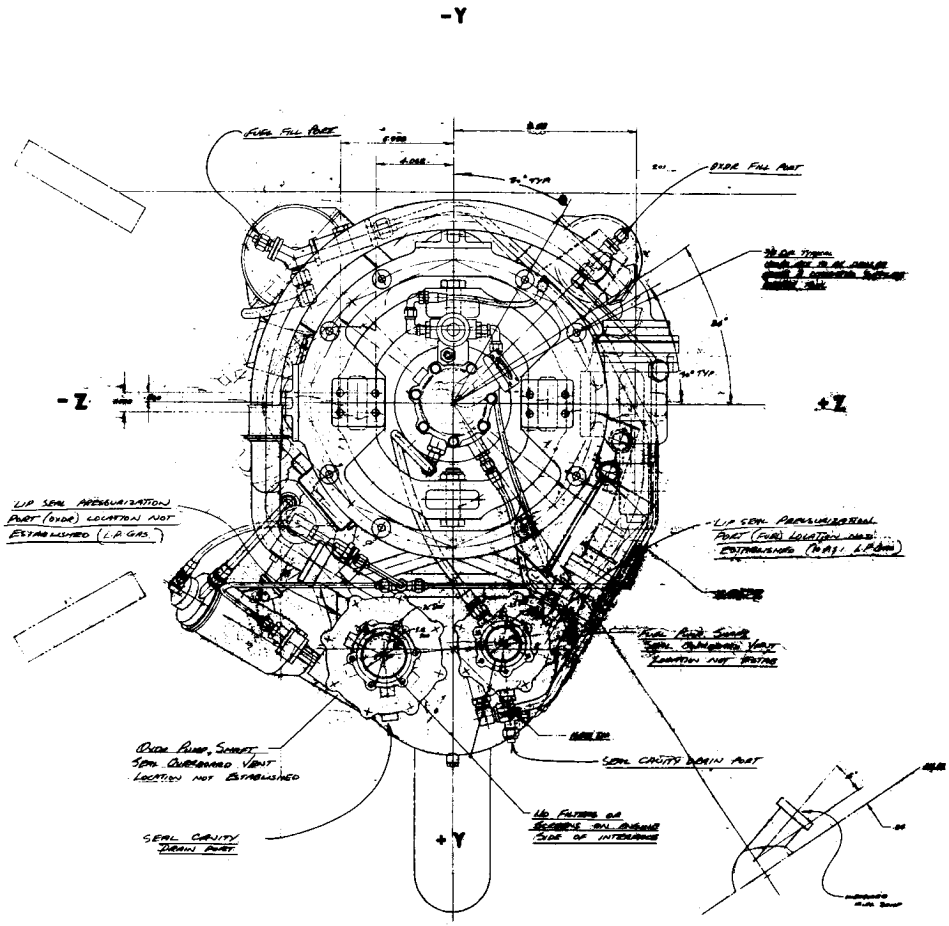

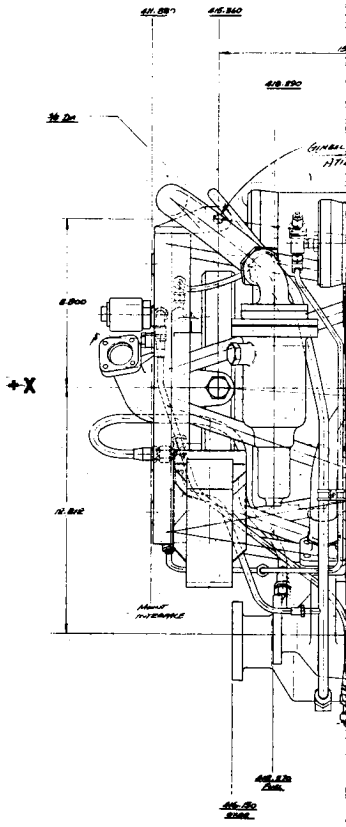

FOLDOUT FRAME

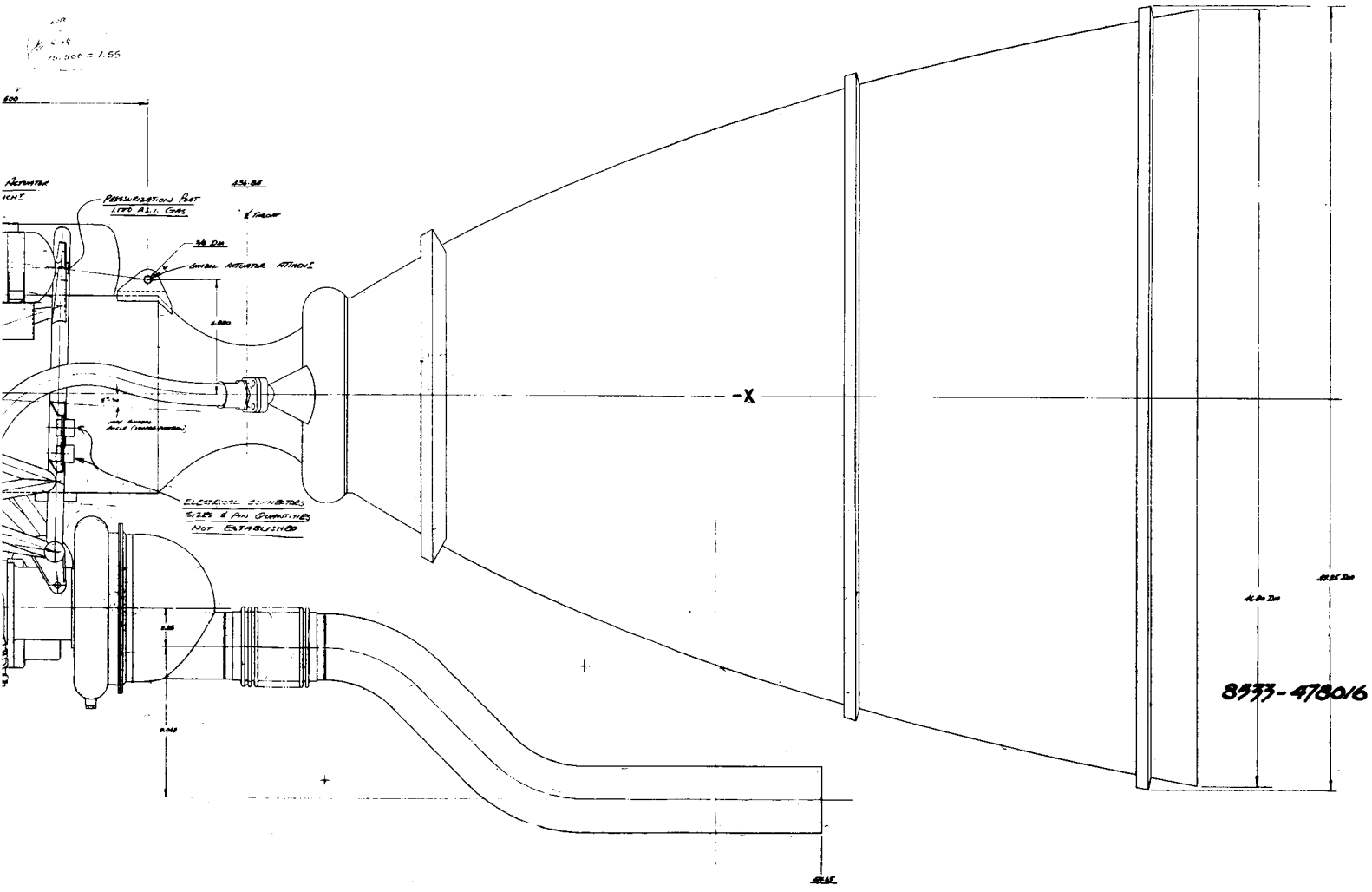

Figure 4-45

FOLDOUT FRAME

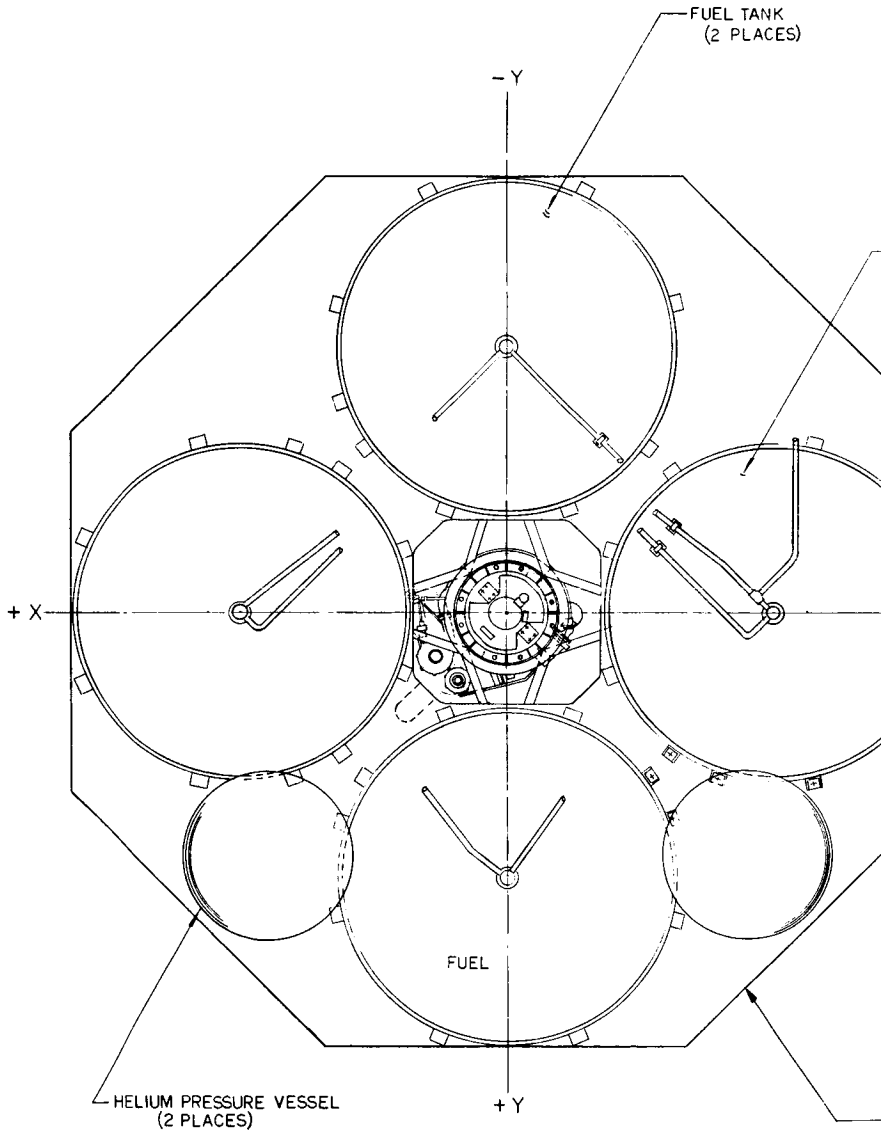

AD7-173 $\frac{1}{10}$

FOLDOUT FRAME 1

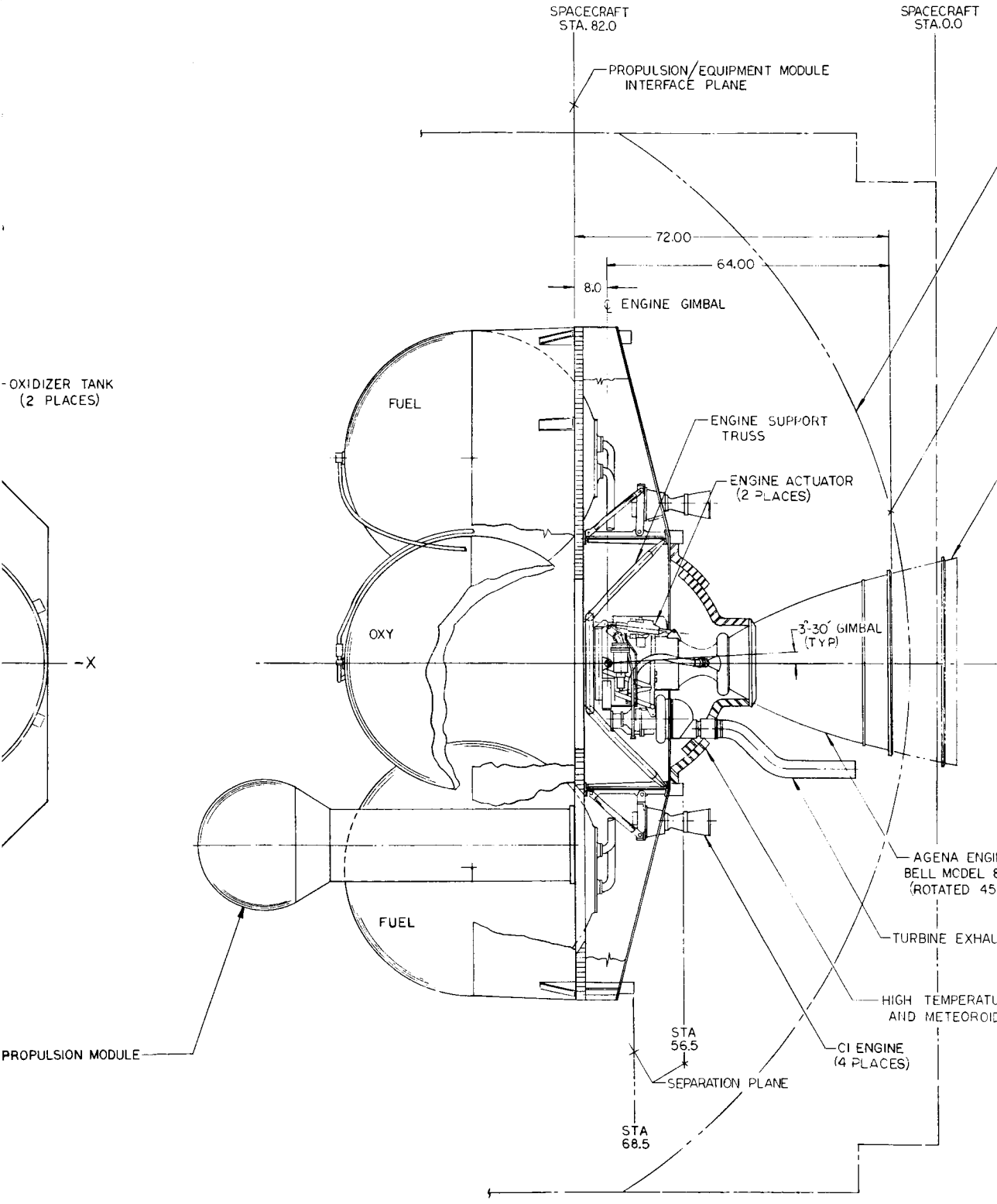

FOLDOUT FRAME 2

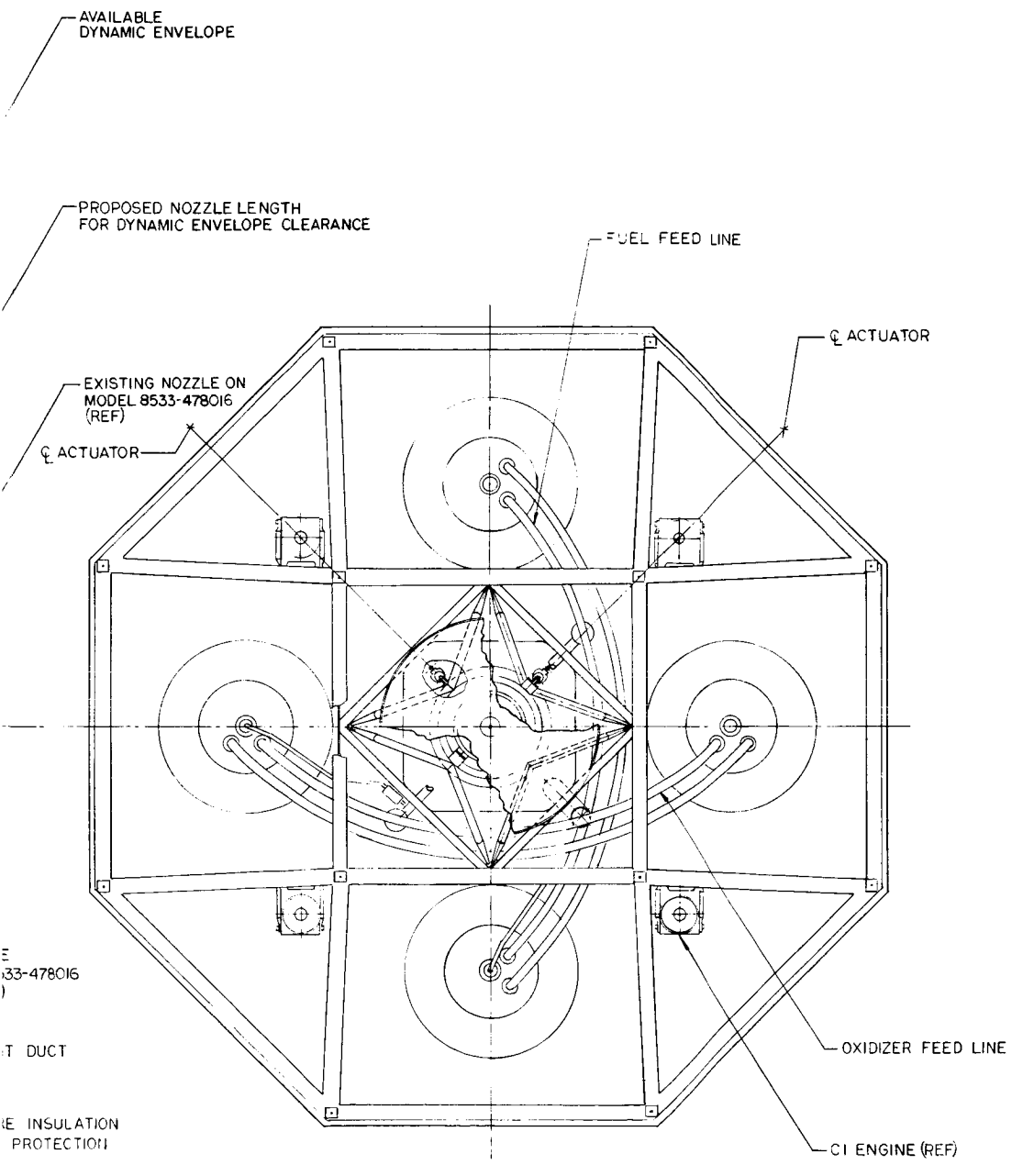

VIEW LOOKING FWD.
(INSULATION OMITTED)

0 10 20 30 40 50
SCALE IN INCHES

Figure 4-48

FOLDOUT FRAME 3

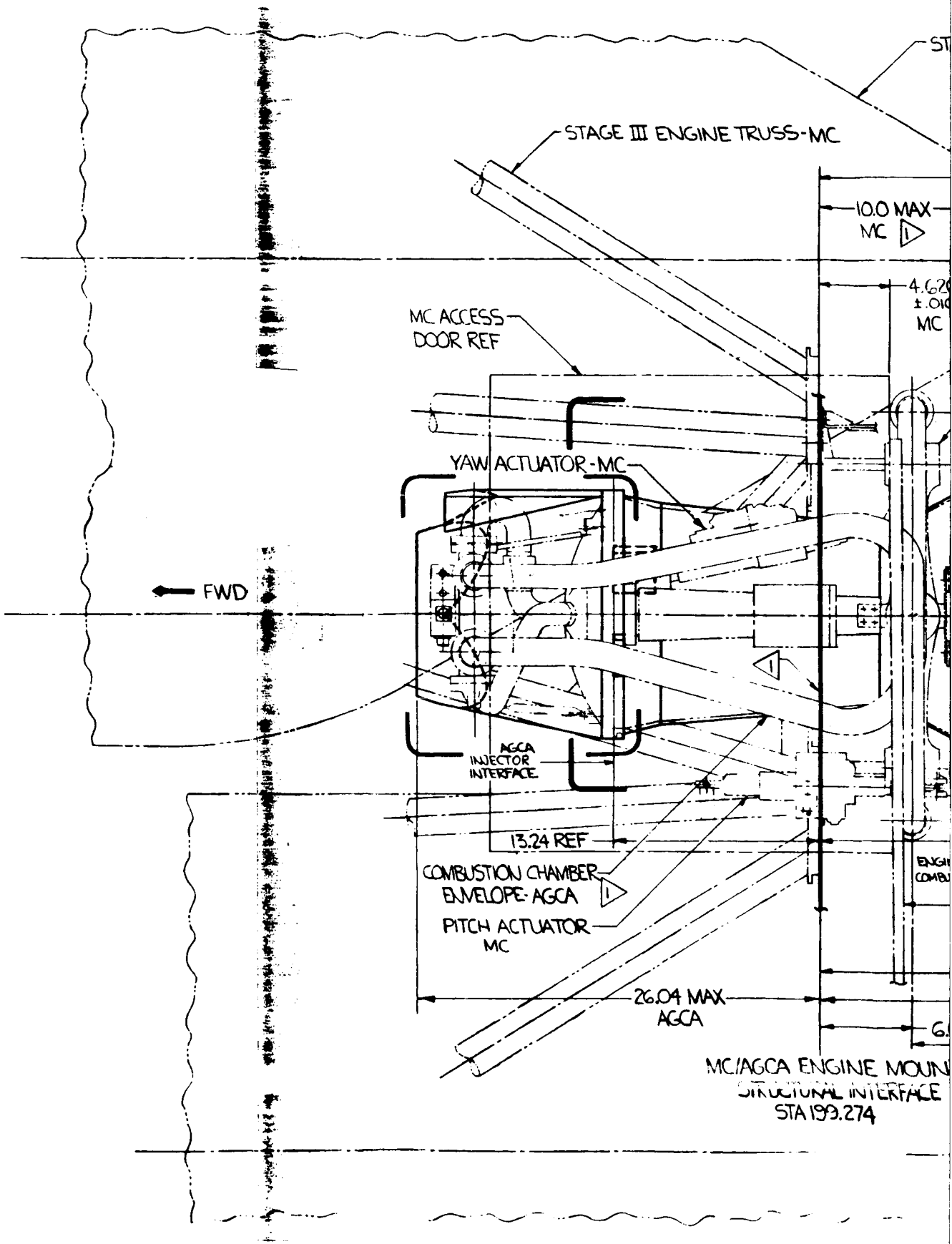
STAGE III ENGINE TRUSS-MC
10.0 MAX
MC
MC ACCESS
DOOR REF
YAW ACTUATOR-MC
FWD
AGCA
INJECTOR
INTERFACE
13.24 REF
COMBUSTION CHAMBER
ENVELOPE-AGCA
PITCH ACTUATOR
MC
26.04 MAX
AGCA
MC/AGCA ENGINE MOUN
STRUCTURAL INTERFACE
STA 199.274

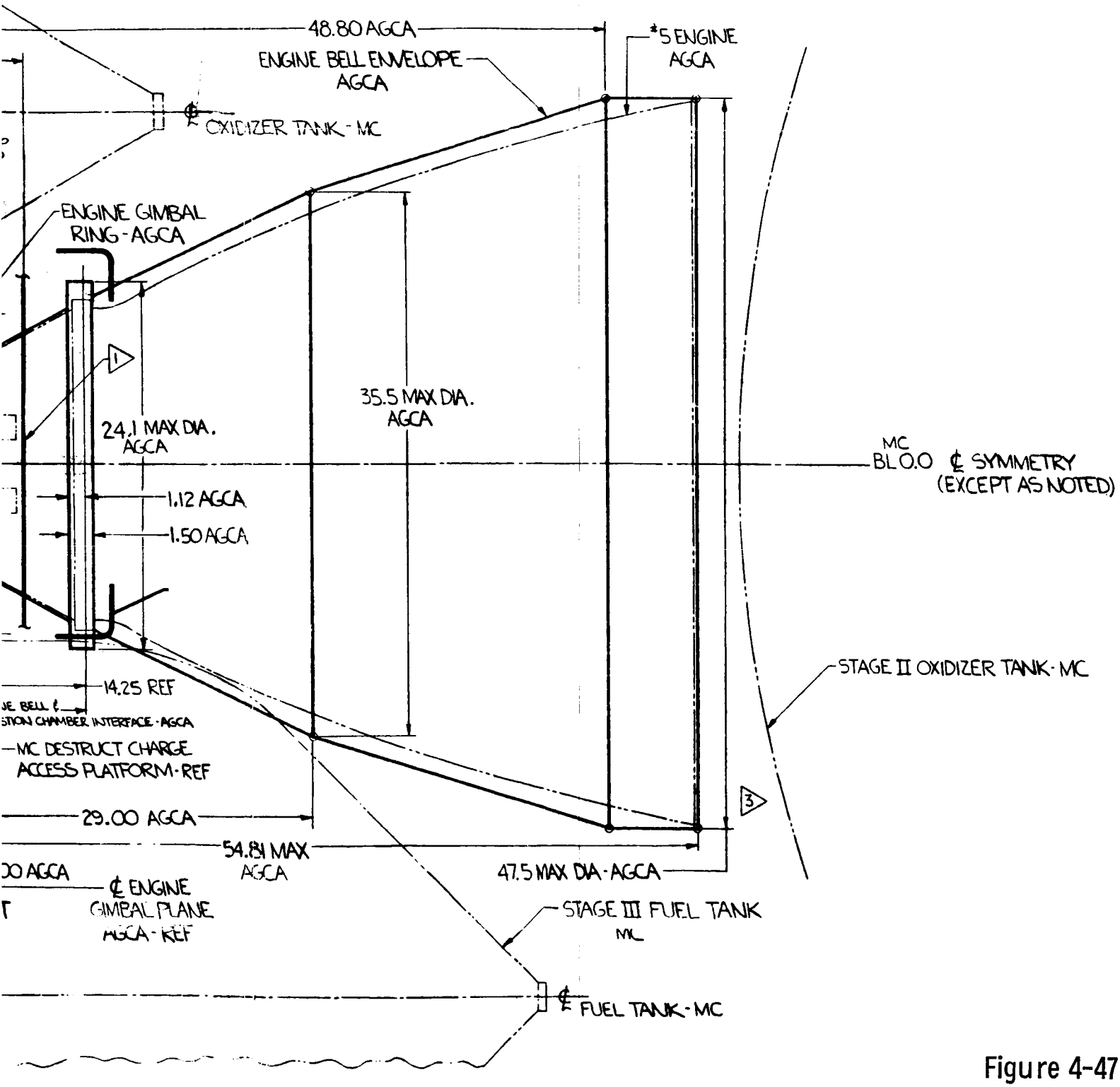

Figure 4-47

FOLDOUT FRAME

4.9.2.1 Engine Mount Location

The Transtage engine is mounted 10 inches aft of the baseline LMDE gimbal position. Movement of the engine forward would result in the engine feed lines around the gimbal ring interfering with the engine support trusses. These lines may be seen in the drawing just aft of the nozzle attachment ring. Further aft positioning would go beyond the available spacecraft dynamic envelope. In the selected gimbal position the required ±6-degree gimbal angle capability can be provided.

4.9.2.2 Clearance of Engine Gimbal and Head End Assembly

Since the Transtage head end assembly is within the Voyager engine envelope the clearance is adequate in the radial and forward directions. The Transtage gimbal angle capability of ±6 degrees meets the spacecraft requirements.

4.9.2.3 Propellant Line Interface and Line Routing

The propellant line interface requires rerouting of the feed line as in the case of the Agena engine. There is approximately 4.0 inch clearance for the feed system lines around and above the head end assembly; no problems are anticipated in this area. Line size transitions can be made at the engine and feed system interface.

4.9.2.4 Engine Support

The engine supports which distribute the loads from the engine to the spacecraft main structure are similar in concept to the LMDE assembly. The truss structure is different in the length and the angles of the truss members.

4.9.2.5 Interference with the Spacecraft Allowable Envelope

Since the Transtage engine is within the Voyager engine envelope at the exit nozzle the engine will be within the spacecraft allowable envelope.

4.9.2.6 Electrical Interface

The electrical interfaces of the Transtage engine are shown in Figure 4-48 and are within the envelope provided for the LMDE assembly.

No problems are anticipated with mechanical fit in this area even though the number and sizes of the connectors are not the same as the LMDE installation. The connectors are small and can be easily relocated.

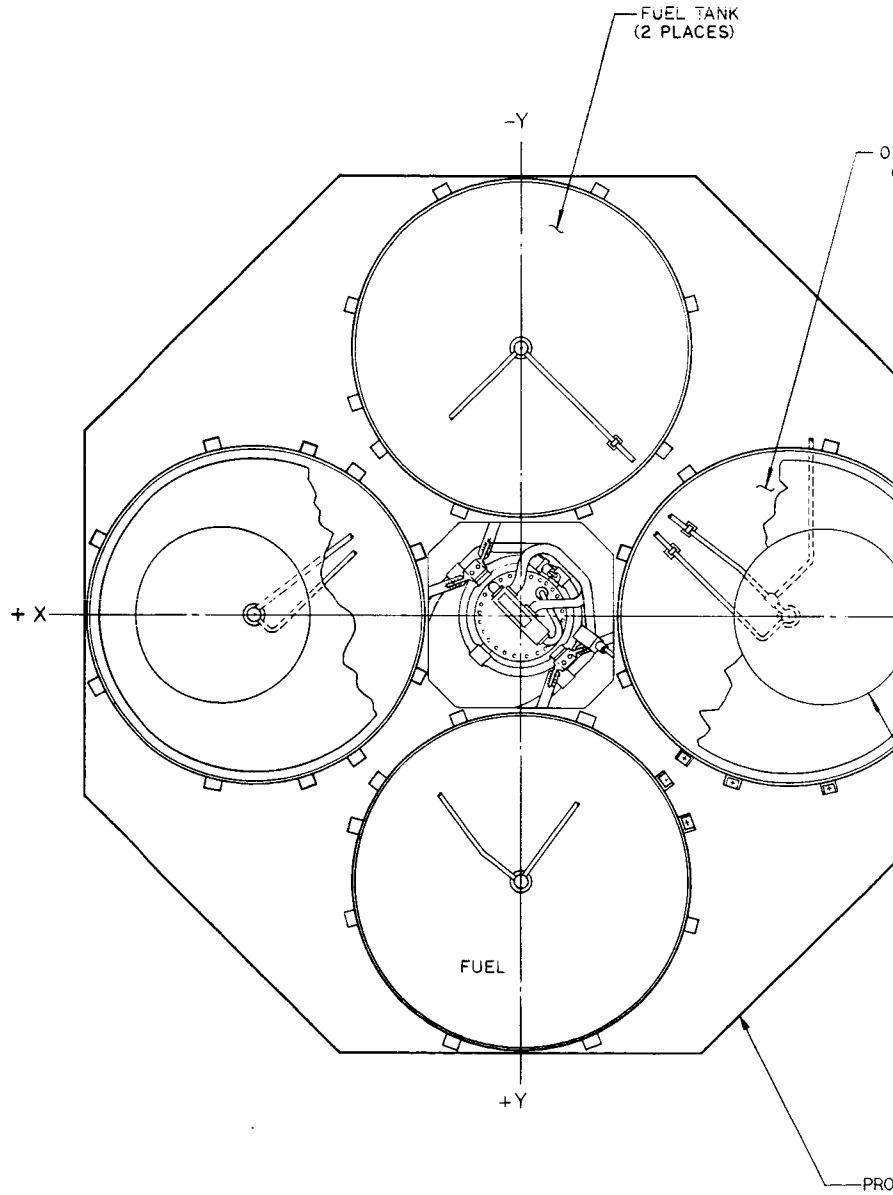

AD7-174

FOLDOUT FRAME 1

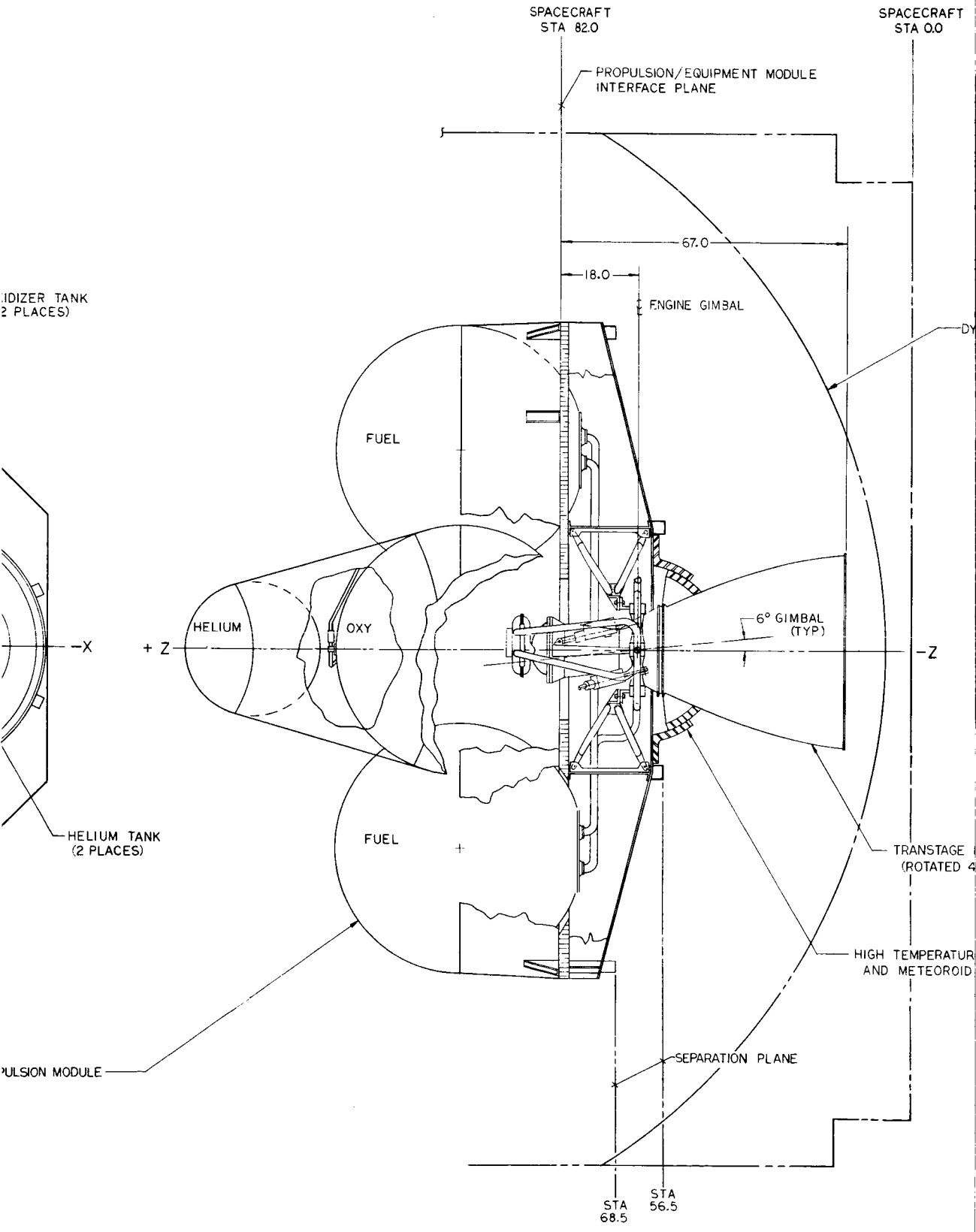

FOLDOUT FRAME 2

NAMIC ENVELOPE

ENGINE
5°)

E INSULATION
PROTECTION

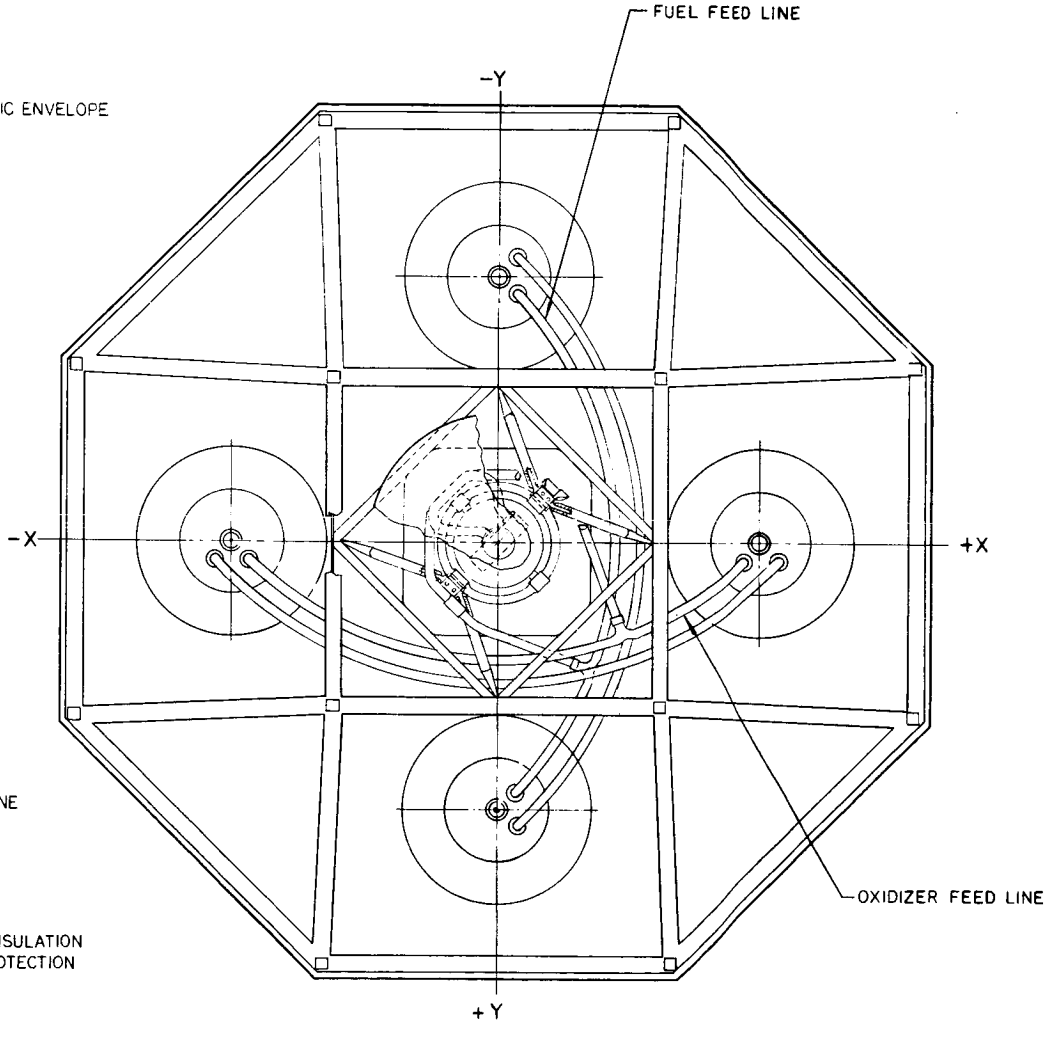

VIEW LOOKING FWD
(INSULATION OMITTED)

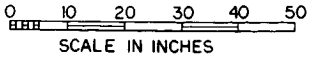

Figure 4-48

FOLDOUT FRAME 3

5. TEMPERATURE CONTROL SUBSYSTEM

5.1 SUMMARY

The temperature control subsystem provides the appropriate thermal environments for all sections of the spacecraft during all phases of the Voyager mission by combining passive and active techniques (Figure 5-1). It makes use of multilayer insulations, high temperature insulations, louvers, special surface finishes, thermostatically controlled heaters, and varying degrees of structural coupling.

A functional diagram for the temperature control subsystem is shown in Figure 5-2. This system utilizes an insulated enclosure concept, whereby the external spacecraft surfaces are covered with insulation except for radiating areas. Excess heat is radiated from these areas to space. The radiation is controlled by louvers as required to maintain the internal spacecraft temperature within desired limits. Various surface coatings and finishes are used to achieve proper heat transfer between the spacecraft elements. Thermostatically controlled heaters are utilized for local control of critical components.

The multilayer insulation on the outside of the spacecraft limits heat gain to or loss from the spacecraft so that the heat to be dissipated is almost all internally generated and remains within the control range of the louvers. Radiative heat transfer from the hot LM engine or the hot C-1 engines to the spacecraft is also limited by the multilayer insulation covering the base of the propulsion module. The LM engine is covered on the outside with multilayer insulation from the injector to the nozzle extension. This insulation limits radiation heat transfer from the hot engine to the spacecraft equipment and structure. The nozzle extension of the LM engine and the C-1 engines are wrapped with high temperature insulation to limit nozzle radiation to the base-mounted solar arrays. The deployment mechanisms are covered with multilayer insulation to minimize heat exchange with the sun, space, and the solar array. They are also isolated from the adjacent structure by low conductivity attachment fittings.

The louvers serve to regulate the temperature of the equipment and guidance and control panels by adjusting the amount of internally

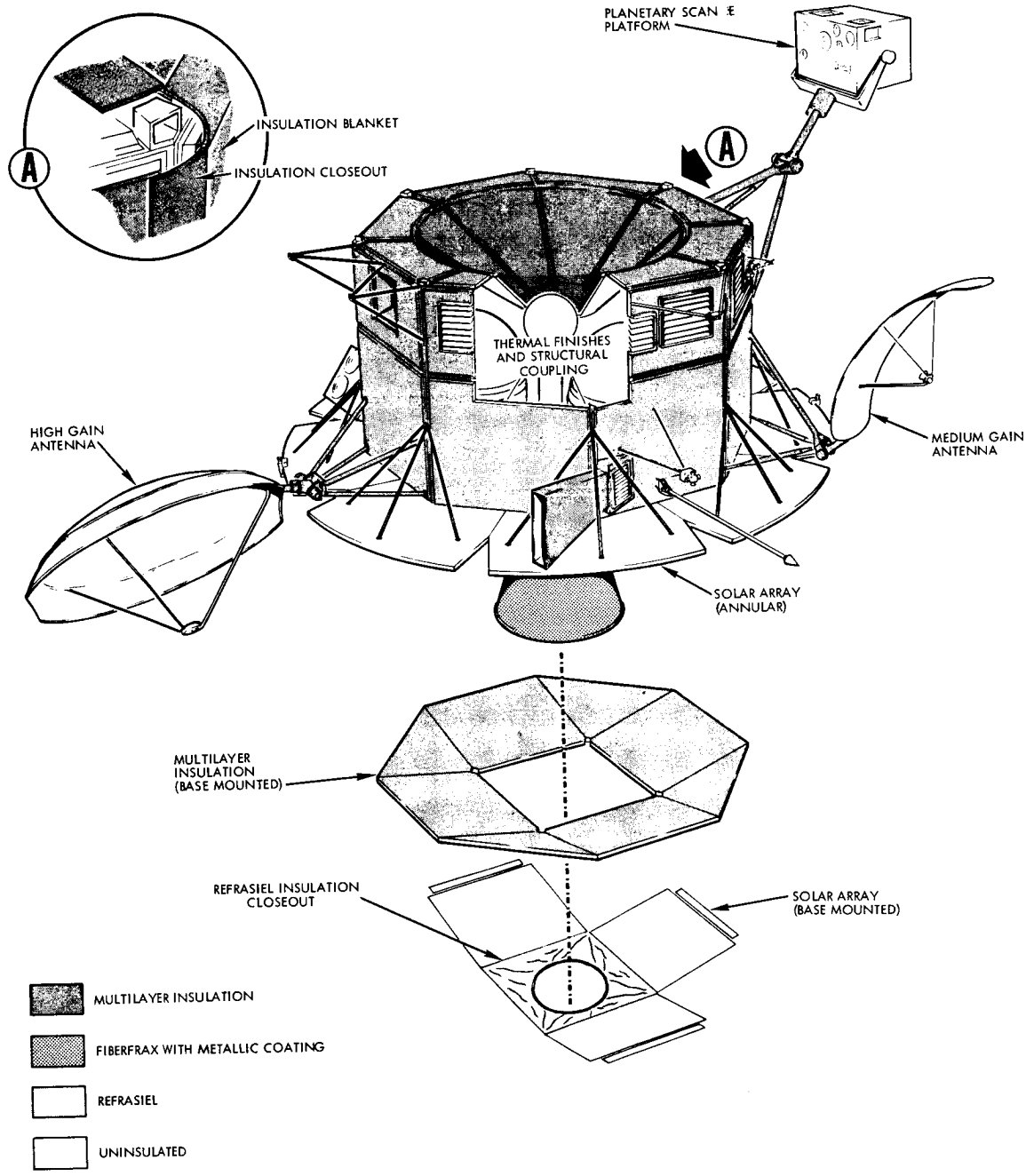

Figure 5-1

SPACECRAFT TEMPERATURE CONTROL SUBSYSTEM consists of multi-layer insulation, which covers spacecraft exterior except for louvers, . . . louvers, which control radiation of internally generated heat, . . . special finishes and low-conductivity joints, which limit thermal coupling, . . . thermostatically controlled heaters, which maintain temperatures for critical components.

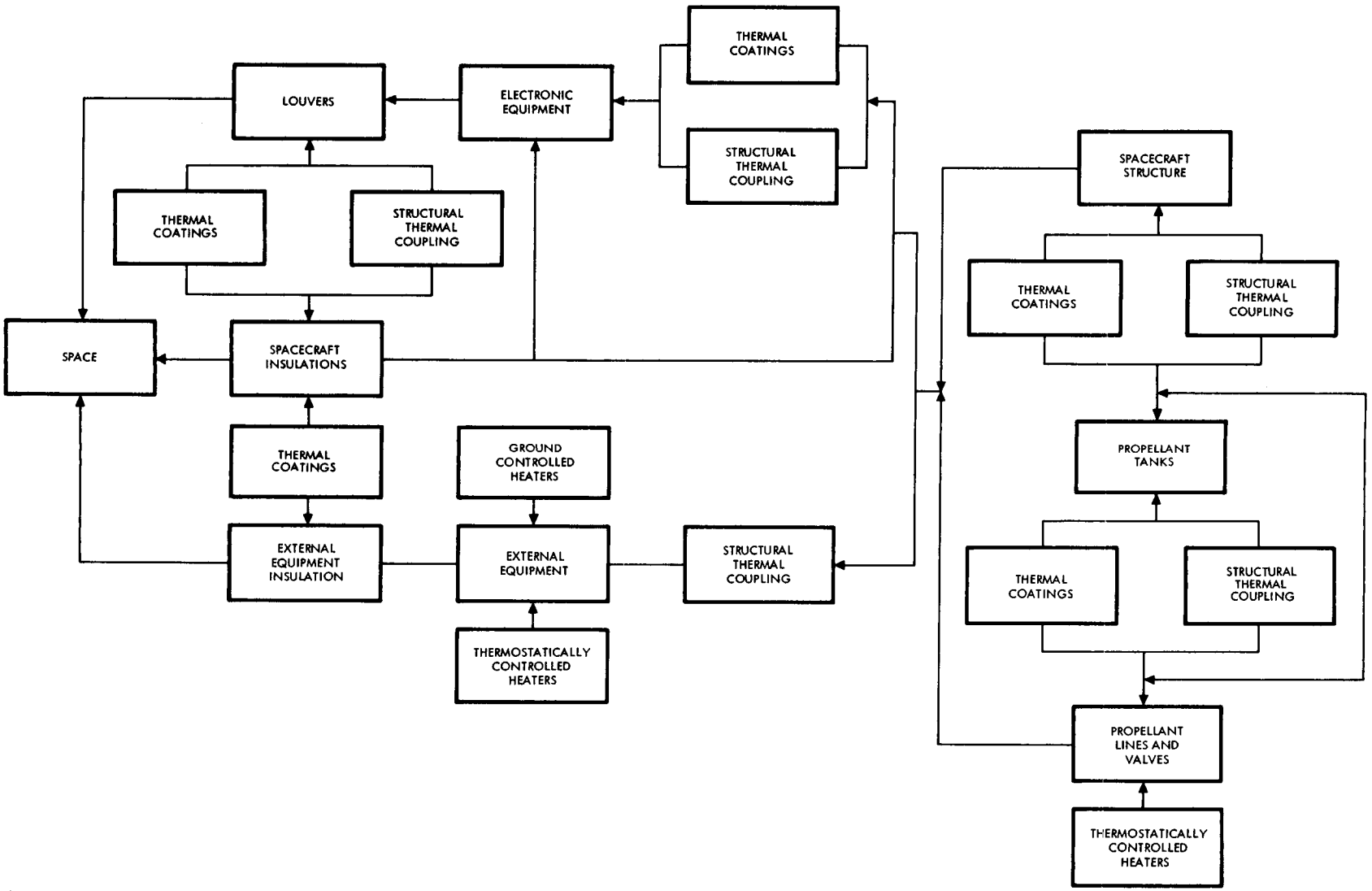

Figure 5-2

TEMPERATURE CONTROL SUBSYSTEM. Block diagram illustrates thermal relationships between the various components and space.

dissipated power radiated to space. The electronic components are mounted on equipment panels and each equipment panel has a radiating area sized to dissipate that panel's maximum heat load. The louvers open so that heat from the solar array is reflected to space rather than into the spacecraft. The system of louver-covered radiating surfaces affords active temperature control to provide a suitable temperature environment for internally-mounted equipment during mission life. In addition to accommodating relatively large, predictable, local and distributed changes in internal and external thermal environments during the mission, the louver system also has the capability of accommodating uncertainties in spacecraft thermal loads such as those occasioned by uncertainty in degraded valves of surface properties, heat leaks, and failure-mode power dissipation.

The radiating areas directly behind the louvers and on the backs of the solar panels are coated with a high emissivity coating. The high emissivity coating on the back of the solar array provides low solar cell temperatures for electrical efficiency and on the radiating areas assures maximum equipment panel radiation to space with the louvers open.

The internal surfaces of the main compartment are finished with high emissivity materials to enhance radiative heat transfer between large areas of the spacecraft to create a uniform environment. Faying surfaces of the component-mounting interfaces remain bare metal for good thermal and electrical contact. On external surfaces, the surface finishes provide controlled radiation to space.

The planetary scan platform support structure is insulated with multilayer insulation (Figure 5-1). Inside the planetary scan platform, surface finishes thermally couple the science components. One of the infrared detectors requires a cryogenic refrigerator which must be developed to meet this detector's specific operational requirements.

5.2 REQUIREMENTS AND CONSTRAINTS

5.2.1 Mission Constraints

5.2.1.1 General

During the Voyager mission, the spacecraft is subjected to varying environmental extremes as presented in Figure 5-3. The Voyager spacecraft is fully attitude-stabilized, utilizing celestial reference. Except for special maneuvers, the spacecraft is oriented so that its base or aft surface is normal to solar radiation. The temperature control subsystem is required to provide a desirable thermal environment for the entire spacecraft for all phases of the Voyager mission.

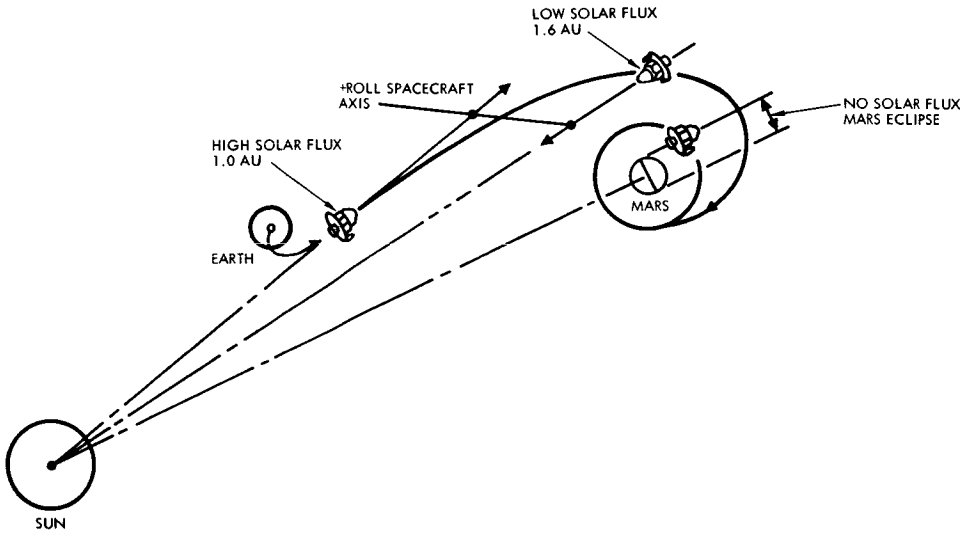

Figure 5-3

HOT AND COLD CONDITIONS DURING MISSION dictate design requirements for temperature control subsystem. Solar input varies from 442 BTU/ hr. Ft^2 near Earth to 159 near Mars and zero during Mars eclipse.

5.2.1.2 Planetary Quarantine

Provisions are made to avoid contamination of the capsule by temperature control subsystem materials or actions after opening the capsule biological barrier in preparation for capsule-spacecraft separation at Mars approach.

The spacecraft does not require heat sterilization. As a result, the temperature control subsystem has not been designed to be compatible with heat sterilization. When encapsulated in the shroud section, the spacecraft will be exposed to a 100°F gaseous environment, 12 percent ethylene oxide, 88 percent Freon, for about 10 hours followed by a nitrogen purge. The multilayer insulation contains sufficient perforations to allow all insulation layers to be exposed to the decontamination gases. All components of the temperature control subsystem are compatible with this operation.

5.2.1.3 Prelaunch and Launch Environment

The temperature control subsystem is required to maintain the spacecraft and its components within their allowable temperatures during the prelaunch and launch. The prelaunch includes all final assembly, checkout, and test procedures and the activities resulting in commitment to launch. The launch includes the final space vehicle countdown and launch.

When encapsulated in the fairing, the spacecraft is cooled by a flow of dry nitrogen within the fairing. The insulation is perforated to permit venting of the nitrogen during boost.

5.2.1.4 Space Environment

The temperature control subsystem must provide adequate temperature control for the space environment encountered during:

- Near-earth steady state
- First interplanetary trajectory correction transient
- Transit from earth to Mars
- Near-Mars steady state
- Mars orbit insertion transient
- Mars eclipse transient

The system must also function properly for the following spacecraft orientations:

- Attitude stabilized (reference to sun and Canopus)
- Not attitude stabilized, during earth eclipse, initial stabilization, midcourse correction, retro-propulsion firing, Mars orbit trim and capsule orientation, and mars eclipse (maximum 2.6 hours)

The following environmental factors are sources of external heat:

- Solar thermal radiation
- Mars albedo
- Mars infrared emission
- Earth radiation

5.2.2 Design Requirements

5.2.2.1 Mechanical Loads

The louver assemblies and multilayer insulation attachments are designed to withstand the accelerations and acoustical vibrations that occur during the boost phase of the Voyager mission. The multilayer insulation is capable of withstanding the inertia forces imposed on it during the boost phase.

5.2.2.2 Installation

All components of the temperature control subsystem, with the exception of the multilayer insulation, are installed in the spacecraft during normal assembly procedures. The multilayer insulation is installed on the spacecraft after assembly and checkout of the spacecraft have been completed. Replacement of thermal components can be made without special adjustment or calibrations.

5.2.2.3 Temperature Control

The temperature control subsystem is required to maintain the spacecraft and its components within their allowable temperature ranges. It is required to use materials that are compatible with the spacecraft environment and that are compatible with the other subsystems on the spacecraft.

5.2.2.4 Reliability

The temperature control subsystem is required to have maximum reliability consistent with optimum design. The system reliability is to be compatible with the spacecraft life. Passive temperature control techniques are to be used wherever possible to maximize reliability.

5.2.2.5 Materials

The temperature control subsystem makes use of materials that are already flight-proven in spacecraft application. The materials conform to the following requirements:

- Materials have acceptable permanent, induced and transferred magnetic field.
- Materials are stable in space environment and compatible with decontamination processes.
- The insulation contains no materials that are nutrients for fungus.
- The degradation of thermal properties, as a result of exposure to space environment, has been accounted for.
- Thermal contacts will not use dissimilar materials. The only place where this will vary is in the bimetallic louver actuators.
- In areas where the electronic equipment is mounted using thermal filler, the fillers used to obtain desired thermal conductance will not produce electrolytic corrosion.

5.3 INTERFACES

5.3.1 Electrical Subsystems

5.3.1.1 Internal Equipment

Most of the electrical subsystem components requiring temperature control are located inside the equipment module on the equipment panels. The temperature control subsystem is required to keep the components within their operating and nonoperating temperature limits as given in Section 5.4.2. The subsystem is also required to dissipate the excess heat from the internal components as given in Section 5.4.2. Mounting of the electrical components must be compatible with the various electrical subsystem requirements.

5.3.1.2 External Equipment

External electrical equipment requires temperature control to maintain it within its operating and nonoperating temperatures and to dissipate the waste heat as given in Section 5.4.2. The temperature control subsystem must not interfere with equipment performance or its deployment.

5.3.2 Structures Subsystem

5.3.2.1 Equipment Module

Insulation design and attachment must be compatible with the equipment module structural design. The design of joints, fittings, and attachments require that the desired thermal conductivity be consistent with structural integrity. Mechanical joints, fittings, and attachments between the equipment module and adjoining external equipment are designed to impede heat flow. All mechanical joints between the structure and associated equipment module panels and between the equipment and propulsion modules are designed to enhance desired heat flow. Many different thermal finishes are required to provide good passive temperature control. All coatings must be compatible with the materials used in the design.

5.3.2.2 Propulsion Module

Insulation design and attachment must be compatible with the propulsion module structural design. The design of joints, fittings, and attachments require that the desired thermal conductivity be consistent with structural integrity. Solar panel attachments are designed so that compacting of multilayer insulation blankets is minimized. Generally good conduction is required between the equipment and propulsion modules; between upper platform surface and propellant and helium tanks. The joints, fittings, and attachments between the base-mounted solar arrays and the propulsion module, and between the engine and propulsion module are designed to impede heat flow.

The LM engine is covered on the outside with multilayer insulation from the injector to the engine nozzle at an area ratio of 16/1. This insulation is 1/2 inch thick and consists of alternating layers of aluminum foil and fiberglass paper to limit radiative heat transfer from the hot engine to the spacecraft equipment and structure. The inside of the LM engine is covered with ablative insulation from the combustion chamber to the engine nozzle at an area ratio of 16/1. The nozzle extension from area ratio 16/1 to the exit plane is covered by an insulation having a hemispherical infrared emissivity of 0.2 or less. The purpose of the insulation and surface finish control is to limit radiation to external equipment and structure. The engine actuators are thermally isolated from the propulsion module structure. The C-1 engine nozzle extensions are insulated in the same manner as the LM engine nozzle extension.

5.3.3 Capsule

The capsule/equipment module interface is designed to limit heat leak between the capsule and the spacecraft. The capsule rejects heat by means of a radiator to space. Some of this heat may be incident on the spacecraft.

5.3.4 Planetary Scan Platform

The planetary scan platform houses the scientific instruments and related electronics. The temperature control of the scan platform drive and deployment mechanisms is required to ensure operation. The scientific instruments and their electronics are mounted in the planetary scan platform must be maintained within their specified temperature limits.

5.4 SUBSYSTEM DESIGN AND PERFORMANCE

5.4.1 Thermal Model

The thermal model of the Voyager spacecraft provides an analytical tool for evaluation of the thermal design. It utilizes the TRW Thermal Analyzer Program (TAP). TAP is an n-dimensional asymmetric finite difference routine where the thermal parameters are entered as their electrical analogies for solution on high speed digital computers. The thermal model divides the spacecraft into analytical nodes. Each of the

nodes, representing a segment of the spacecraft, is connected to its adjacent node by thermal resistance to account for conduction and radiative heat transfer.

The thermal model (Figure 5-4) represents the recommended Voyager spacecraft. It includes the following:

- Solar array
- Tankage (i.e., fuel tanks, oxidizer tanks, helium tanks, nitrogen tanks)
- Equipment module structure
- Meteroid protection shields
- Multilayer insulation
- Electronic equipment mounting plates
- Bimetallic louver assemblies
- Externally mounted equipment (i.e., high-gain, medium-gain antennas, and PSP)
- Engine and nozzle

For the mission conditions where the capsule is attached, Figure 5-4, the capsule is represented as a surface boundary above the equipment module top meteroid shield.

5.4.1.1 Spacecraft Steady-State Temperatures

Steady-state temperatures were obtained for two extreme solar flux environments (Figure 5-3) during transit to Mars, near-Earth and near-Mars. The near-earth steady state is representative of the first leg of Voyager flight. The sun-exposed surfaces of the solar array, antennas, planetary scan platform and nozzles receive a constant solar flux of 442 Btu/hr-ft^2, yielding an equilibrium heat balance among sun, spacecraft, and space. The solar vector is colinear with the LM engine nozzle axis. During the near-earth steady-state it is anticipated that the maximum temperatures will be reached, and electronic power dissipation was assumed to be a maximum. Temperatures were obtained for two conditions: (a) capsule attached (b) capsule separated. In the latter condition, the capsule is uniformly dissipating from 1.7 to 7 kw from its lower surface, Figure 5-5, which is directly above the spacecraft. Since extreme conditions are desired, one analysis was performed with the capsule dissipating 1.7 kw and another with it dissipating 7 kw.

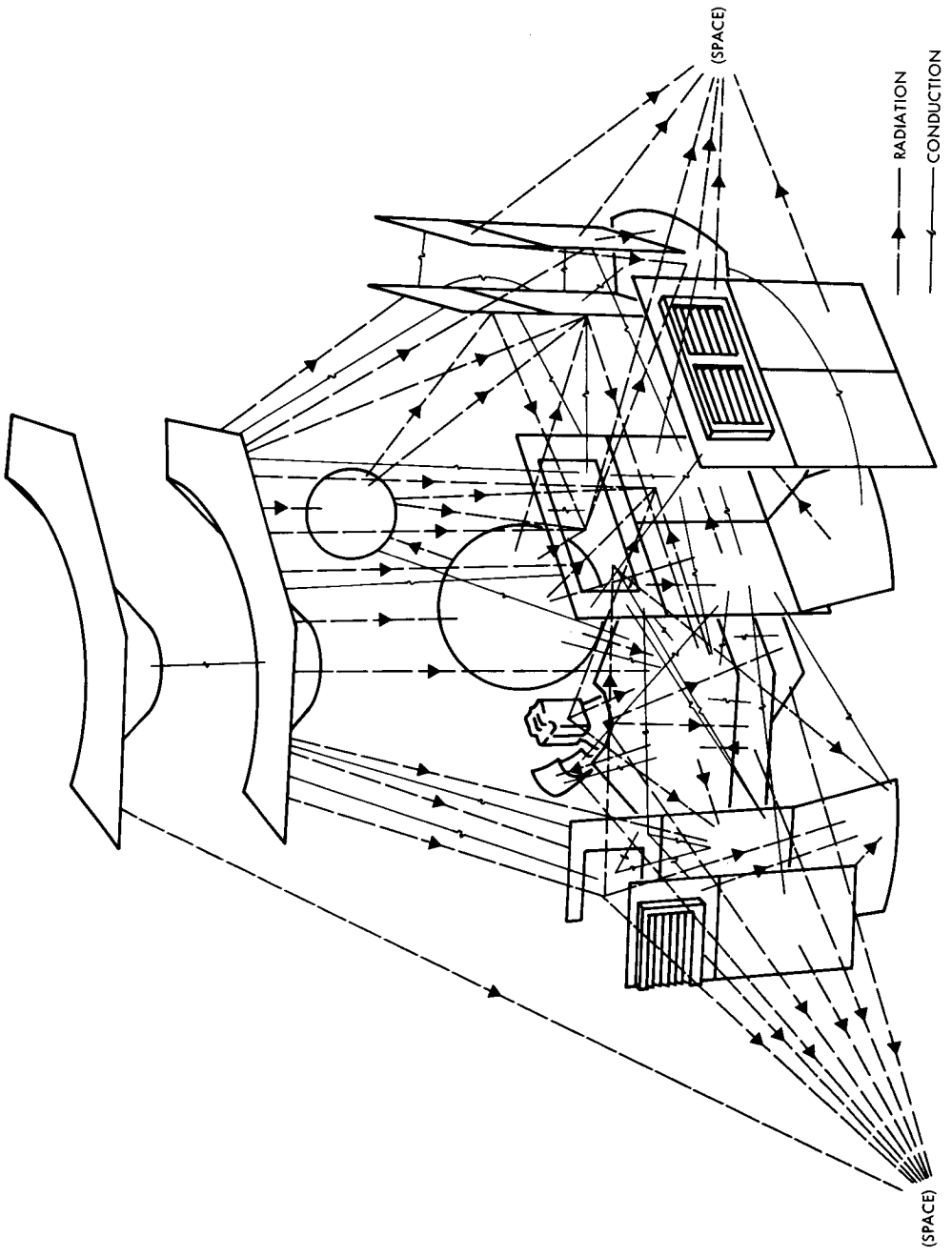

Figure 5-4
SPACECRAFT THERMAL MODEL divides the spacecraft into analytical nodes and provides a tool for evaluation of the thermal design.

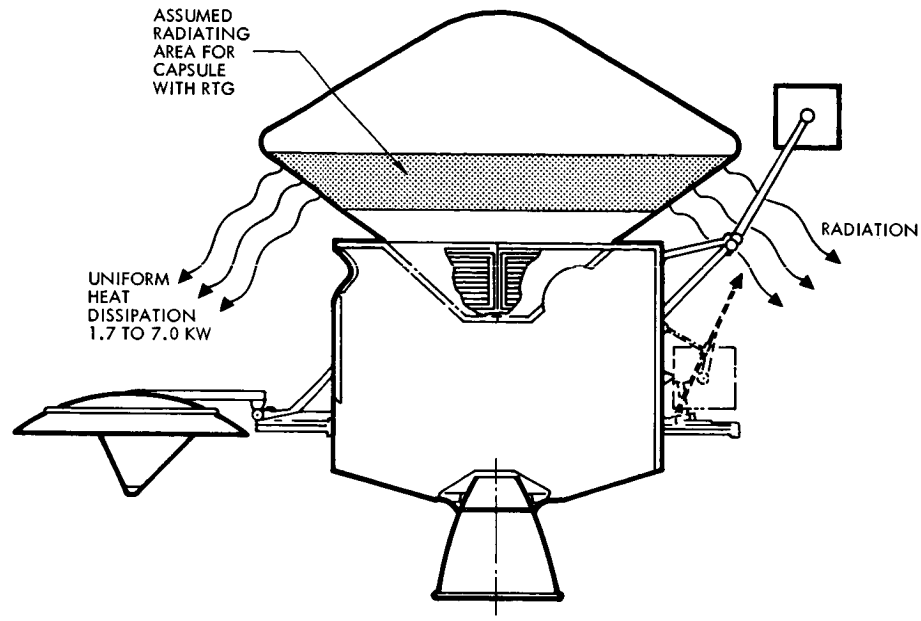

Figure 5-5
CAPSULE RADIATING AREA dissipates from 1.7 to 7 Kw, part of which is incident on the spacecraft.

Near-Mars steady-state is representative of the portion of the mission in the vicinity of Mars before orbit insertion. For this period, the solar array, antennas, planetary scan platform, and nozzles receive a constant solar flux of 159 Btu/hr-ft^2, and computations are made until thermal equilibrium is reached. The analyses were performed with the capsule separated, and with the capsule attached, dissipating 1.7 and 7 kw. Near-earth and near-Mars steady-state temperatures are presented in Table 5-1.

5.4.1.2 Mars Eclipse Transient

The coldest temperatures in the Voyager mission result from a 2.6-hour Martian eclipse. The near-Mars steady-state temperatures correspond to initial conditions for eclipse. Temperatures decrease during eclipse, since the spacecraft receives no solar heat. The spacecraft areas most severely affected during eclipse are those normally sun-oriented. The solar array, nozzle extension, low-gain antenna, and planetary scan platform experience the largest temperature drops during eclipse (Figure 5-6).

Table 5-1. Steady Temperature for Near-Earth and Near-Mars Isolation and all Within Acceptable Limits

Node No.	Description	Near-Earth, Steady-State Temperature (°F)			Near-Mars, Steady-State Temperature (°F)		
		Without Capsule	With Capsule Dissipating 1.7 kw	With Capsule Dissipating 7 kw	Without Capsule	With Capsule Dissipating 1.7 kw	With Capsule Dissipating 7 kw
1-4	Solar array (annular)	125	128	132	-7	-3	5
5-8	Solar array (base)	246	246	246	86	86	86
9-12	Insulation, forward	-145	-123	-95	-196	-171	-131
13-16	Meteoroid shield, forward	83	87	91	71	76	82
17-20	Insulation, aft	-99	-90	-80	-170	-160	-141
21-24	Meteoroid shield, aft	79	83	88	61	68	74
25	Compartment top	-250	-	-	-252	-	-
26	Compartment top, Meteoroid shield	83	88	83	70	77	83
29	Insulation (bottom)	91	91	92	69	69	70
30	Tank platform	81	84	89	63	69	75
31-32	Heat shield	211	211	211	46	46	46
37-38	Propellant tanks	80	83	89	63	69	75
39-40	Oxidizer tanks	80	83	89	63	69	75
41-42	Helium tanks	82	86	90	71	76	81
43-44	Nitrogen tanks	81	84	88	72	76	81
45	Medium-gain antenna	65	67	69	-51	-49	-44
46	High-gain antenna	46	49	51	-68	-65	-60
47	Planetary Scan Platform support arm	-160	-145	-160	-216	-199	-173
48	Planetary Scan Platform box	119	122	126	-21	-12	3
49	Feed line (oxidizer tanks below platform)	86	85	90	63	69	75
50	Crossover line (oxidizer tanks below platform)	86	86	90	63	69	75
51	Feed line (fuel tanks, below platform)	86	85	90	63	69	75
52	Crossover line (fuel tanks, below platform)	86	85	90	63	69	75
53	Fuel line above platform	80	83	89	62	69	75
54	Oxidizer line above platform	80	83	89	62	69	75
56	Nozzle	237	237	237	77	77	77
57	Engine	80	83	89	62	69	75
58	Engine strut	80	83	89	62	69	75
62-65	Equipment baseplates behind louvers	76	78	79	74	76	77
67	Planetary Scan Platform insulation	-184	-180	-180	-246	-243	-242
68-71	Equipment baseplates	135	138	142	117	121	126
80	Capsule	-	-43	76	-	-74	62

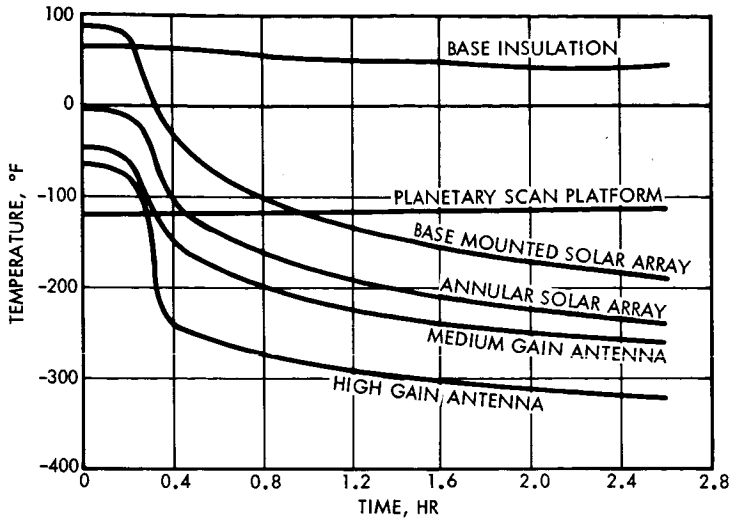

Figure 5-6
THE COLDEST TEMPERATURES DURING THE VOYAGER MISSION occur at the end of the 2.6 hr Martian eclipse.

5.4.1.3 Engine Firing Transient

Thermal radiation from the LM engine to the spacecraft surfaces can affect the performance of those surfaces. An analysis was performed for the first interplanetary trajectory correction and for the Mars orbit insertion. Results from the steady-state near-earth and steady-state near-Mars analyses are taken as initial conditions. The first interplanetary trajectory correction is an upper bound hot condition near-earth. Certain critical areas (base-mounted solar array, annular solar array, high-gain antenna, and planetary scan platform receive a solar heat flux of 442 Btu/hr-ft^2, in addition to radiant energy from the engine plume and nozzle. A detailed description of engine plume heating is given in Volume 10, Section 4.

The results (Figure 5-7 and Figure 5-8) of the analysis indicate that all of the critical components, with the exception of the base-mounted solar array, are well within their respective temperature limits. The base-mounted solar array experiences a brief temperature excursion to 300°F.

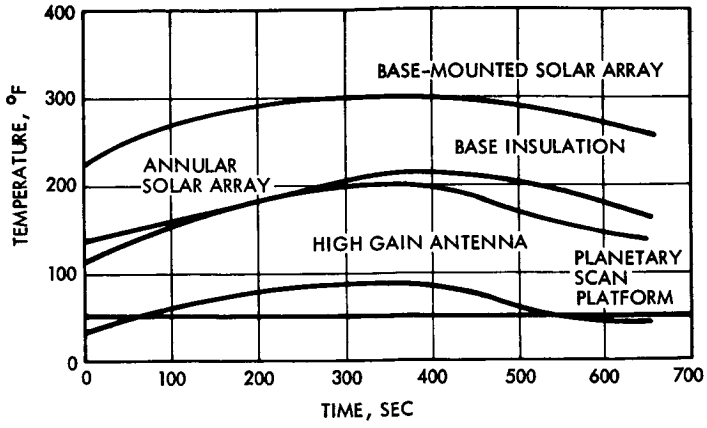

Figure 5-7

FIRST TRAJECTORY CORRECTION provides maximum temperatures for the spacecraft and its components.

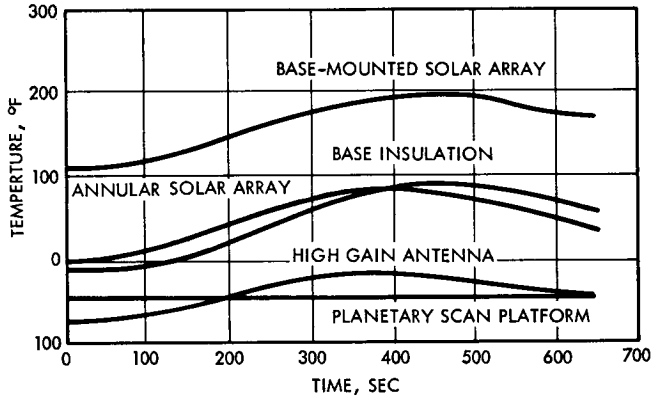

Figure 5-8

MARS ORBIT INSERTION TEMPERATURES do not exceed those of first trajectory correction burn in spite of higher thrust during orbit insertion. This is due to lower solar flux near Mars.

5.4.1.4 Louvers

Thermal modeling of the louver system and electronic equipment temperatures was restricted to a broad temperature analysis. Individual components were lumped into four heat-dissipating capacitors. Each of the capacitors represented one of the aluminum honeycomb panels upon which equipment is mounted. A portion of the internally-generated heat from the equipment is transferred to the spacecraft

interior by radiation. The remaining heat is radiated to space from the honeycomb mounting panels. A detailed analysis of the louvers and electronic equipment is presented in Section 5.4.2.

5.4.1.5 Propellant Temperatures

Temperature results from the thermal model indicate that the following thermal design criteria can be met during the mission, including Martian eclipse:

- Propellants maintained above their freezing point
- Differences in fuel and oxidizer temperatures within $5^{\circ}F$
- Differences in temperature between like fuel and propellant tanks within $2^{\circ}F$

Propellant feed and crossover lines are maintained within their temperature limits.

5.4.1.6 Thermal Model Description

The thermal model represents the entire structure of the spacecraft as shown in Figure 5-4.

All material properties are handled as constants in the thermal model except for louver thermal properties. Louver emissivity is varied as a function of panel mounting temperature as discussed in Section 5.4.2. Material property constants are presented in Table 5-2.

The thermal model is subdivided as follows:

- Annular solar array
- Base-mounted solar array
- Four side panels of meteroid shield
- Four side panels of multilayer insulation (aluminized mylar)
- Equipment bay top meteroid shield
- Equipment bay top multilayer insulation (aluminized mylar)
- Spacecraft base multilayer insulation (aluminized mylar)
- Tank support platform

- Engine heat shield (refrasil insulation)
- Two titanium fuel tanks
- Two titanium oxidizer tanks
- Two titanium helium tanks
- Two titanium nitrogen tanks
- Two stainless steel feed lines, one oxidizer, and one fuel
- Two stainless steel crossover line, one oxidizer, and one fuel
- Medium-gain antenna
- High-gain antenna
- Planetary scan platform box and support arm
- LM engine
- Engine strut
- Columbian nozzle extension with fiberflax insulation and spun metal exterior surface

Table 5-2. Material Property Constants*

Description	Thermal Conductivity (Btu/hr-ft-^{o}F)	Solar Absorptivity	Thermal Emissivity	Ratio $\alpha s/\epsilon t$
Solar array	-	0.71	0.81	0.88
Multilayer mylar insulation	0.002 (K/L)	0.17	0.78	0.22
Meteroid shielding	0.0019	-	0.81	-
Honeycomb equipment mounting panel	75	-	0.81	-
Engine nozzle extension	-	0.89	0.2	-
Engine heat shield	0.042	0.15	0.5	0.3
High gain and medium gain antennas	-	0.4	0.81	0.5
Planetary scan platform	-	0.33	0.24	0.19

*With the exception of the emissivity of the aluminum mounting panels, all spacecraft materials are assumed to have constant properties.

- Four aluminum honeycomb equipment mounting panels
- Bimetallic louver system

Radiation heat transfer modes for the spacecraft are as follows:

- Radiation between meteroid shield side panels and tankage
- Radiation between annular solar array and multi-layer insulation side panels
- Radiation between nozzle extension and base-mounted solar array and base insulation
- Radiation between nozzle extension and high-gain antenna
- Radiation between base insulation and tank support platform
- Radiation from all exterior surfaces to space
- Radiation from variable emissivity equipment mounting plates to space

All interior surfaces are coupled by high emissivity and high conductivity, thereby holding interior spacecraft temperature gradients to a minimum.

All interconnecting spacecraft sections are tied together by conduction, including conduction across multilayer insulation and across and parallel to to meteroid shielding.

The basic spacecraft thermal model is represented by approximately 70 nodes and approximately 380 thermal resistances. Standard electrical analogy techniques are incorporated in the TRW Digital Thermal Analyzer Program used to solve the thermal model.

Steady State Equation

$$T_i = T_i\,(1 - \delta) + \left\{ \frac{\delta\left[(q_{xi}) + (q_{ci}) + (q_{ri})\right]}{\frac{1}{\sum R_i}} \right\}$$

where

δ = arbitrary convergency constant to prevent divergence of iterative solution

T_i = temperature of i-th mode

qxi = net heat transfer from external source or by external heat dessipation for the i-th node

qri = net heat transfer by radiation for the i-th node

qci = net heat transfer by conduction for the i-th node

Transient Equation

$$T_i(\theta + \Delta\theta) = T_i(\theta) + \left(\frac{\Delta\theta}{c_i}\right)\left\{\left[q_x(\theta)\right]_i + \left[q_c(\theta)\right]_i + \left[q_r(\theta)\right]_i\right\}$$

where

q_x = net heat transfer from an external source or by external heat dissipation

q_r = net heat transfer by radiation

q_c = net heat transfer by conduction

c_i = capacitor of i-th mode

θ = time

$\Delta\theta$ = computing increment of time

T_i = temperature of i-th mode

i = node number

5.4.2 Temperature Control, Equipment Module

5.4.2.1 System Definition

In considering temperature control of the equipment module, it must be remembered that thermal interactions exist between the equipment module, the propulsion module, and the capsule. These interactions were described in Section 5.4.1.

5.4.2.2 Equipment Module Components and Locations

The equipment module consists of electrical and mechanical components both internal and external to the structure. A list of the equipment module components is given in Tables 5.3 and 5.4. The locations of electrical components mounted on equipment panels are shown in Figures 5-9 through 5-14. Mechanical components such as the control subsystem components are mounted inside the equipment module. Figure 5-15 shows the guidance and control components locations. Electrical and mechanical components such as the antennas, drive motors and thrusters are mounted external to the equipment module. The components can be located by referring to Figure 5-16.

5.4.2.3 Equipment Module Temperature Control Techniques

Temperature control of the contents of the compartment is achieved by the following:

- Insulation of equipment module external surfaces
- Minimize heat transfer between the equipment module and the capsule and between the equipment module and external equipment
- Distribution of internally located heat generating components
- Radiant and conductive interchange within the enclosure
- Thermal louvers to radiate excess heat

External insulation, shown schematically in Figure 5-17, cover equipment module external surfaces except the louver areas. The prime function of the insulation is to minimize heat loss to space and to limit heat gains when irradiated by the sun. Because the heat sources within the equipment module are localized, rather than evenly distributed, a high performance insulation is required to prevent remotely located passive equipment from getting too cold during eclipse. Multilayer insulation is used.

Attachment of external equipment to the equipment module creates potential heat leaks. Design of mechanical attachments, utilizing thermal insulating materials, minimizes the heat transfer.

Table 5.3. Equipment Module Components on Equipment Panels

Panel Location	Component	Number of Items	Weight (each) (lb)	Dimensions (inches) L	W	H	Volume (each) (in^3)	Maximum Electrical Power (watts) Average	Peak	Allowable Operating Temperature Limit (°F) Max	Min	Allowable Nonoperating Temperature Limit (°F) Max	Min	Computed Steady State Temperatures Max (°F)	Min (°F)
	Power Subsystem														
VIII	Power Control Unit	1	20	10	10	5	500	100	120	120	-20	200	-50	119	69
VIII	Shunt Element Assembly	1	6	25	6	3	450	100	110	150	-20	200	-50	112	62
VIII	400 Hz Inverter	1	10	7	7	5	245	0.5	12	120	-20	200	-50	102	53
I	Battery	3	59	13.3	8.5	7.5	850	70	70	90	50	90	-50	87	52
III	DC-DC Converter Temperature Control	1	5	6	6	3.5	126	10	20	120	-20	200	-50	114	56
III	DC-DC Converter - Data Storage and Telemetry	1	5	6	6	3.5	126	15	20	120	-20	200	-50	119	58
IV	DC-DC Converter - S-Band Radio	1	5	6	6	3.5	126	30	40	120	-20	200	-50	120	68
IV	DC-DC Converter - Guidance and Control	1	5	6	6	3.5	126	10	20	120	-20	200	-50	114	56
V	DC-DC Converter - Capsule Supply	1	5	6	6	3.5	126	30	40	120	-20	200	-50	120	63
V	DC-DC Converter - PSP Assembly	1	5	6	6	3.5	126	20	30	120	-20	200	-50	114	56
VII	DC-DC Converter - Command and Sequencing	1	5	6	6	3.5	126	10	20	120	-20	200	-50	114	56
VII	DC-DC Converter	1	5	6	6	3.5	126	10	20	120	-20	200	-50	102	50
	S-Band Radio Subsystem														
IV	Antenna Drive Electronic S-Band Electronics	1	9.2	7	6	12	505	18.6	18.6	130	-20	200	-20	120	58
IV	S-Band Receiver	4	14	7.25	5	3	109	2.0	2.0	110	30	175	-25	103	53
IV	Receiver Selector	1	1.0	3.5	5.0	1.62	28.4	0.9	0.9	110	30	175	-25	108	58
IV	Low Gain Antenna Selector, one watt transmitter and power monitor	1	1.0	3.5	5.0	1.62	28.4	0.3	0.3	110	30	175	-25	103	53
IV		1	3.0	7.25	5.0	1.62	58.7	15	15	110	30	175	-25	109	59
IV	Modulator Exciter	2	3.0	7.25	5.0	1.62	58.7	2.1	2.1	110	30	175	-25	104	54
IV	Power Amplifier Monitor and Power Supply	2	7.8	12	4.2	3.0	151	165	165	210+	-20	250+	-25	220	120
IV	Transmitter Selector	1	1.0	3.5	5.0	1.62	28.4	0.9	0.9	110	30	175	-25	108	58
IV	Circulator Switch Assembly and Control Unit	1	7.5	10	6	6	360	-	1 amp x 50 μs	110	30	175	-25	101	51
IV	Diplexer	4	1.0	7.5	4.0	2.5	75	-	-	110	30	175	-25	101	51
IV	Baseband Assembly	1	1.0	3.5	5	2.5	43.8	1.0	1.0	110	30	175	-25	106	56
IV	Preamplifier Radio Link	1	0.5	2	2	1	4	0.25	0.25	110	30	175	-25	103	53
IV	UHF Receiver	2	2.0	7	6	1	42	7.5	7.5	110	30	175	-25	110	66
IV	UHF Demodulator	2	0.4	7	6	1	42	1.0	1.0	110	30	175	-25	110	66
	Command and Sequencing Subsystem														
VII	Command Unit	2	2.6	7	7	1.8	89	6.5	6.5	110	30	175	-25	108	64
VII	Primary Computer and Sequencer	1	20.0	8	8	7.5	480	20	20	110	30	175	-25	108	64
VII	Backup Computer and Sequencer	1	18.0	8	8	6.5	415	20	20	110	30	175	-25	104	62
	Data Handling and Storage Subsystem														
III	Spacecraft and Capsule Recorder	4	20	12	10	8	650	20	30	110	30	170	-25	107	68
III	Engineering and Science Recorder	2	18	12	10	8	600	15	22	110	30	175	-25	106	67
III	Telemetry Data Handling Unit	1	11	10	8	6	580	6	12	110	30	175	-25	104	65
	Guidance and Control Subsystem														
G&C I & II	Inertial Reference Assembly	2	25	12	8	7	672	40	54.1	130	30	180	-22	112	62
VII	Guidance and Control Electronics Assembly	1	13.0	7	11	6	462	25	38	130	-30	200	-30	108	60
I & IV	Limb and Terminator Crossing Detector	2	0.6	1.5	2.5	2.5	9.5	0.2	0.2	130	30	160	-20	90	52
G&C I & II	Canopus Sensor	2	7.0	4	12	4	192	6	6	130	-30	160	-30	94	54
	Electrical Distribution Subsystem														
VIII	Pyro Control Assembly	1	25	15	7	7	490	2	500 ω 50 μs	150	10	160	-10	102	52
VIII	Distribution Control Unit	1	12	10	7	7	490	5	5	150	10	160	-10	104	54
III	Junction Box	1	7	9	6	6	324	-	-	160	10	160	-10	101	56
IV	Junction Box	1	7	9	6	6	324	-	-	160	10	160	-10	101	51
V	Junction Box	1	3	4	5	6	120	-	-	160	10	160	-10	103	58
VII	Junction Box	1	7	9	6	6	324	-	-	160	10	160	-10	102	57
VIII	Junction Box	1	7	9	6	6	324	-	-	160	10	160	-10	101	51

+Baseplate temperature limit

Table 5-4. Equipment Module Components not on Equipment Panels

Sub-system	Component	Number of Items	Weight (each) (lb)	Dimensions (inches)			Volume (each)	Maximum Electrical Power (watts)		Allowable Operating Temperature Limit (°F)		Allowable Nonoperating Temperature Limit (°F)		Computed Steady State Temperatures	
				L	W	H	(in^3)	Average	Peak	Max.	Min.	Max.	Min.	Max. (°F)	Min. (°F)
	Power Subsystem														
Power	Solar Array Panel (annular)	8	21.4				21 ft^2	139	-	250	-260	250	-260	132	-240
Power	Solar Array Panel (rect.)	3	16.2	50	60	1	21 ft^2	105	-	250	-260	250	-260	246	-190
	S-Band Radio Subsystem														
S-Band	Low Gain Antenna	2	3.0	-	-	-	-	-	-	360	-350	360	-350	65	-262
S-Band	Low Gain Antenna Feed	2	3.25	16.5 ft. long		-	-	-	-	360	-350	360	-350	65	-260
	High Gain Antenna Assy														
S-Band	High Gain Antenna Support Structure	1	52.1	-	-	-	-	-	-	250	-250	250	-350	51	-321
S-Band	Reflector and Associated Structure	1		9.5 ft. diameter			-	-	-	250	-250	250	-350	51	-321
S-Band	Feed Assembly	1	6.4	-	-	-	-	-	-	250	-250	250	-350	51	-321
S-Band	High Gain Antenna Drive	1	30	16	12	20	3840	8	37	250	-250	250	-350	*51	-230
	Medium Gain Antenna Assembly														
S-Band	Medium Gain Antenna Support Structure	1	12.4	-	-	-	-	-	-	360	-350	360	-350	60	-320
S-Band	Reflector and Associated Structure	1		-	-	-	-	-	-	360	-350	360	-350	60	-320
S-Band	Feed Assembly	1	5.2	-	-	-	-	-	-	250	-250	250	-350	60	-320
S-Band	Medium Gain Antenna Drive	1	17.0	16	12	12	2302	7	25	250	-250	250	-250	60	-230
	Relay Link Subsystem														
Relay Link	Relay Link Antenna	1	8.0	-	-	-	-	-	-	360	-350	360	-350	65	-300
	Guidance and Control Subsystem														
G&C	Coarse Sun Sensor	2	3.0	1.5	1	1	1.5	0.3	0.3	130	30	160	-20	130	30
G&C	Fine Sun Sensor	2	0.20	2	3.0	2	12	0.7	0.7	130	30	160	-20	120	0
G&C	Pressure Vessel	2	35.7	17.1" Dia.			20500	-	-	250	-250	250	-250	88	72
G&C	Solenoid Valve - Low Pressure	16	0.6	-	-	-	-	-	25	250	-65	250	-65	90	50
G&C	Transducer - Low Pressure	2	0.7	-	-	-	-	-	-	140	0	200	0	90	50
G&C	Transducer - High Pressure	2	0.1	-	-	-	-	-	-	140	0	200	0	90	55
G&C	Fill Valve	2	0.20	-	-	-	-	-	-	140	0	200	0	90	50
G&C	Plumbing Set	2	1.00	-	-	-	-	-	-	250	-200	250	-200	90	50
G&C	Thruster Assembly	4	0.6	-	-	-	-	-	-	250	-200	250	-200	140	-102
G&C	Outlet Transducer	12	51.0 Total							140	0	200	0	90	50
G&C	H.P. Regulator	2	2.5							140	0	200	0	90	50
G&C	L.P. Regulator	2	1.2							140	0	200	0	90	50
	Temperature Cont. Subsystem														
TC	Louver Assembly	8	18	60	36	1	216	-	-	250	-200	250	-200	180	-10
TC	Strip Heater and Thermostats	9	2	-	-	-	-	2	2	250	-200	250	-200	80	-200
TC	Insulation	23	102 Total	97	62	1	6014	-	-	300	-400	300	-400	90	-250
	Data Handling and Storage Subsystem														
DH	PSP Multiplexer	1	2.0	4	5	0.5	10	0.5	1.0	110	30	175	-125	85	35
DH	PSP Remote Photoimaging Multiplexer	1	2.0	4	5	1.0	20	2.0	3.0	110	30	175	-125	85	35

Table 5-4. Equipment Module Components not on Equipment Panels (Continued)

Sub-system	Component	Number of Items	Weight (each) (lb)	Dimensions (inches) L	W	H	Volume (each) (in^3)	Maximum Electrical Power (watts) Average	Peak	Allowable Operating Temperature Limit (°F) Max.	Min.	Allowable Nonoperating Temperature Limit (°F) Max.	Min.	Computed Steady State Temperatures Max. (°F)	Min. (°F)
	Electrical Distribution Subsystem														
ED	Equipment Module Main Harness	1	69	-	-	-	-	-	-	160	10	160	-10	90	50
ED	Equipment Module Science Harness	1	45	-	-	-	-	-	-	160	10	160	-10	90	50
ED	Panel I Harness	1	15	-	-	-	-	-	-	160	10	160	-10	90	50
ED	Panel III Harness	1	15	-	-	-	-	-	-	160	10	160	-10	90	50
ED	Panel IV Harness	1	15	-	-	-	-	-	-	160	10	160	-10	90	50
ED	Panel VII Harness	1	15	-	-	-	-	-	-	160	10	160	-10	90	50
ED	Panel VIII Harness	1	15	-	-	-	-	-	-	160	10	160	-10	90	50
ED	Inflight Jumper	1	1.0	2	2	2	8	-	-	160	10	160	-10	90	50
ED	Ordnance Harness and Test Connector	1	5.0	-	-	-	-	-	-	160	10	160	-10	90	50
ED	Capsule Disconnect	1	1.0	-	-	-	-	-	-	160	10	160	-10	90	50
ED	Science Boom Harness	1	5.0	-	-	-	-	-	-	160	10	160	-10	90	50
ED	PSP Science J-Box	1	13.0	9	4	12	432	-	-	160	10	160	-10	90	50
ED	PSP Science Harness	1	7.0	-	-	-	-	-	-	160	10	160	-10	90	50
	Structure Subsystem														
Struct	Equipment Panel Structure	6	26.5	62	36	1	2232	-	-	250	-250	250	-250	90	50
Struct	Meteoroid Protective Panel	19	496 (total)	62	96.5	1.5	-	-	-	250	-250	250	-250	90	50
Struct	PSP Tiedown Assembly	1	1.5	-	-	-	-	-	-	250	-250	250	-250	130	-230
Struct	High Gain Antenna - Tiedown Assembly	1	1.0	-	-	-	-	-	-	250	-250	250	-250	130	-230
Struct	Low Gain Antenna - Tiedown Assembly	2	1.0	1" odx. 035" x 35"			-	-	-	250	-250	250	-250	130	-230
Struct	Medium Gain Antenna - Tiedown Assembly	1	2.0	1" odx. 035"		15" 35" 50"	-	-	-	250	-250	250	-250	130	-230
Struct	Low Gain Antenna Deployment Mechanism	2	1.0	-	-	-	-	-	-	250	-250	250	-250	130	-230
Struct	Low Gain Antenna Boom	2	3.0	103" x 1.2500 x 0.050 wat				-	-	250	-250	250	-250	130	-230
Struct	Primary Struct Assembly	1	196	-	-	-	-	-	-	250	-250	250	-250	100	-10
Struct	Solar Array Support Structure	1	35.0	-	-	-	-	-	-	250	-250	250	-250	246	-240
Struct	High Gain Antenna Support Structure	1	21.4	2.0" OD. x .049 x 60"				-	-	250	-250	250	-250	130	-230
Struct	Medium Gain Antenna Support Structure	1	10.5	1.0" OD x .035 x 100"		35" 50"		-	-	250	-250	250	-250	130	-230
Struct	PSP Support Structure	1	32.0	-	-	-	-	-	-	250	-250	250	-250	130	-230
Struct	PSP Deploy. Mechanism	1	5.0	-	-	-	-	-	-	250	-250	250	-250	130	-230
Struct	PSP Drive Assembly (Yoke)	1	7.0	-	-	-	-	-	-	250	-250	250	-250	130	-230
Struct	PSP Drive Assembly (Main Shaft)	1	7.0	-	-	-	-	-	-	250	-250	250	-250	130	-230
	PSP Assembly														
Science	Low Resolution Camera	1	-	2.5	2.5	-	212	25	25	85	35	85	35	84	35
Science	Medium Resolution Camera	3	50	12	6	6	432	50	50	85	35	85	35	84	35
Science	High Resolution Camera	1	50	15	7	7	735	20	20	85	35	85	35	84	35
Science	Broadband IR Spectrom.	1	20	14	12	11	1848	2.1	2.1	105	-20	105	-20	84	35
Science	IR Radiometry Unit	1	20	10	7	7	490	20	20	105	-20	105	-20	84	35
Science	UV Spectrometry Unit	1	30	24	8	8	1536	20	20	105	32	105	32	84	35
Science	Protective Shutter Group	1								120	0	120	0	84	35
Science	Mars Sensor	1	12.0	-	-	-	200			113	0	113	0	84	35
Science	PSP Drive Electrical Assembly	1	8.75	7	6	10	468	12	12	250	-250	250	-250	250	-250
Science	PSP Structure	1	-	-	-	-	-	17.9	17.9	250	-250	250	-250	250	-250
	Command and Sequencer Subsystem									250	-250	250	-250		
C&S	PSP Drive Decoder Unit	1	2.0	4	5	0.5	10	0.5	0.5	110	30	160	30	85	35

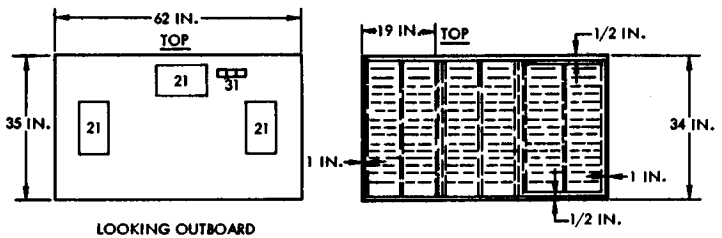

(3) DOUBLE 19 IN. x 34 IN. LOUVERS 13.5 SQ. FT.
EFFECTIVE LOUVER AREA 10.7 SQ. FT.

ITEM NO.	COMPONENT NAME	COMPONENT DIMENSIONS (IN.) L	W	H	COMPONENT BASE AREA ($IN.^2$)	MAXIMUM UNIT STEADY STATE HEAT DISSIPATION (WATTS)	Q/A BASE $\left(\frac{WATTS}{IN.^2}\right)$	COMPONENT TEMPERATURE LIMIT MAX. (°F)	MIN. (°F)	LOUVER AREA REQUIRED ($IN.^2$)	CONTACT CONDITION REQUIRED $\left(\frac{BTU}{HR - FT^2}\right)$	RESULTANT LOUVER Q/A $\left(\frac{WATTS}{IN.^2}\right)$	LOUVER TEMPERATURE (°F)	BASE PLATE TEMPERATURE (°F)	COMPONENT TEMPERATURE (°F)	BASE PLATE THICKNESS (IN. TOTAL)
21	BATTERY	13.3	8.5	7.5	115	70+	0.61	90	50	575	25	0.122	69	75	87	0.064
21	BATTERY	13.3	8.5	7.5	115	70+	0.61	90	50	575	25	0.122	69	75	87	0.064
21	BATTERY	13.3	8.5	7.5	115	70+	0.61	90	50	575	25	0.122	69	75	87	0.064
31	LIMB AND TERMINATOR CROSSING SENSOR	1.5	2.5	2.5	*	0.2	N/A	130	30	N/A	N/A	N/A	69	75	90	0.032
	*NOT MOUNTED DIRECTLY TO BASE PLATE +NEAR END OF BATTERY CHARGING N/A NOT APPLICABLE															
	TOTAL				345 (2.4 SQ. FT.)	210.2				1725 (12 SQ.FT.)		0.122				

Figure 5-9

EQUIPMENT PANEL NO. 1, Power subsystem.

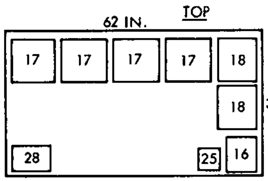

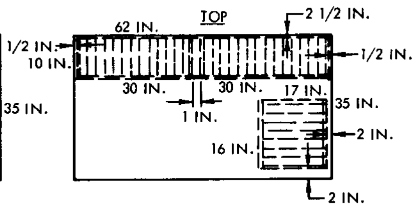

(2) SINGLE 10 IN. x 30 IN. LOUVERS } = 6.07 SQ FT
(1) SINGLE 17 IN. x 16 IN. LOUVER }

EFFECTIVE LOUVER AREA = 4.58 SQ.FT.

ITEM NO.	COMPONENT NAME	COMPONENT DIMENSIONS (IN.)			COMPONENT BASE AREA (IN.^{2})	MAXIMUM UNIT STEADY STATE HEAT DISSIPATION (WATTS)	Q/A BASE (WATTS / IN.^{2})	COMPONENT TEMPERATURE LIMIT		LOUVER AREA REQUIRED (IN.^{2})	CONTACT CONDITION REQUIRED (BTU / HR - FT^2)	RESULTANT LOUVER Q/A (WATTS / IN.^{2})	LOUVER TEMPERATURE (°F)	BASE PLATE TEMPERATURE (°F)	COMPONENT TEMPERATURE (°F)	BASE PLATE THICKNESS (IN. TOTAL)
		L	W	H				MAX. (°F)	MIN. (°F)							
16	TELEMETRY DATA HANDLING UNIT	10	8	6	80	6	0.075	110	30	27	10	0.22	89	100	104	0.032
17	SPACECRAFT AND CAPSULE RECORDER	12	10	8	120	20	0.166	110	30	90	10	0.22	89	100	107	0.032
17	SPACECRAFT AND CAPSULE RECORDER	12	10	8	120	20	0.166	110	30	90	10	0.22	89	100	107	0.032
17	SPACECRAFT AND CAPSULE RECORDER	12	10	8	120	20	0.166	110	30	90	10	0.22	89	100	107	0.032
17	SPACECRAFT AND CAPSULE RECORDER	12	10	8	120	20	0.166	110	30	90	10	0.22	89	100	107	0.032
18	ENGINEERING AND SCIENCE RECORDER	12	10	8	120	20	0.126	110	30	69	10	0.22	89	100	106	0.032
18	ENGINEERING AND SCIENCE RECORDER	12	10	8	120	20.	0.126	110	30	69	10	0.22	89	100	106	0.032
25	DC/DC CONVERTER DATA HANDLING	6	6	3.5	36	15	0.420	120	-20	70	10	0.22	89	100	119	0.032
28	J-BOX	9	6	6	54	—	—	160	10	—	10	0.22	89	100	101	0.032
	TOTAL				890 (6.20 SQ. FT.)	121				595 (4.15 SQ.FT.)		0.22				

Figure 5-10

EQUIPMENT PANEL NO. 3, Data Handling and Storage subsystem.

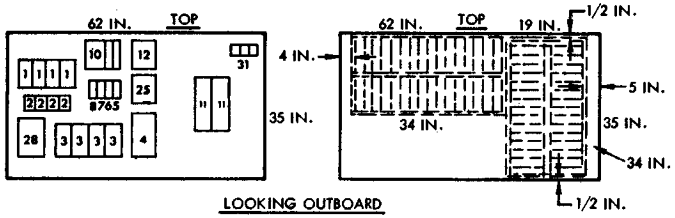

(2) DOUBLE 19 IN. X 30 IN. LOUVERS = 9.000 SQ. FT.

EFFECTIVE LOUVER AREA = 7.10 SQ. FT.

ITEM NO.	COMPONENT NAME	COMPONENT DIMENSIONS (IN.) L	W	H	COMPONENT BASE AREA (IN.^{2})	MAXIMUM UNIT STEADY STATE HEAT DISSIPATION (WATTS)	Q/A BASE (WATTS / IN.^{2})	COMPONENT TEMPERATURE LIMIT MAX. (°F)	MIN. (°F)	LOUVER AREA REQUIRED (IN.^{2})	CONTACT CONDITION REQUIRED (BTU / HR - FT^2)	RESULTANT LOUVER Q/A (WATTS / IN.^{2})	LOUVER TEMPERATURE (°F)	BASE PLATE TEMPERATURE (°F)	COMPONENT TEMPERATURE (°F)	BASE PLATE THICKNESS (IN. TOTAL)
1	S-BAND RECEIVER	7.3	3	5	21.9	2.0	0.092	110	30	9.0	10	0.22	89	100	103	0.032
1	S-BAND RECEIVER	7.3	3	5	21.9	2.0	0.092	110	30	9.0	10	0.22	89	100	103	0.032
1	S-BAND RECEIVER	7.3	3	5	21.9	2.0	0.092	110	30	9.0	10	0.22	89	100	103	0.032
1	S-BAND RECEIVER	7.3	3	5	21.9	2.0	0.092	110	30	9.0	10	0.22	89	100	103	0.032
2	PREAMPLIFIER	2	2	1	4	0.25	0.063	110	30	1.1	10	0.22	89	100	103	0.032
2	PREAMPLIFIER	2	2	1	4	0.25	0.063	110	30	1.1	10	0.22	89	100	103	0.032
2	PREAMPLIFIER	2	2	1	4	0.25	0.063	110	30	1.1	10	0.22	89	100	103	0.032
2	PREAMPLIFIER	2	2	1	4	0.25	0.063	110	30	1.1	10	0.22	89	100	103	0.032
3	DIPLEXER	7.5	4	2.5	30	—	—	110	30	—	10	0.22	89	100	101	0.032
3	DIPLEXER	7.5	4	2.5	30	—	—	110	30	—	10	0.22	89	100	101	0.032
3	DIPLEXER	7.5	4	2.5	30	—	—	110	30	—	10	0.22	89	100	101	0.032
3	DIPLEXER	7.5	4	2.5	30	—	—	110	30	—	10	0.22	89	100	101	0.032
4	CIRCULATOR SWITCHING ASSEMBLY	10	6	6	60	—	—	110	30	—	10	0.22	89	100	101	0.032
5	BASE BAND ASSEMBLY	3.5	2.5	5	8.8	1.0	0.114	110	30	5.0	10	0.22	89	100	106	0.032
6	TRANSMITTER SELECTOR	3.5	1.6	5	5.6	0.9	0.160	110	30	4.0	10	0.22	89	100	108	0.032
7	RECEIVER SELECTOR	3.5	1.6	5	5.6	0.9	0.160	110	30	4.0	10	0.22	89	100	108	0.032
8	LOW GAIN ANTENNA SELECTOR	3.5	1.6	5	5.6	0.3	0.053	110	30	1.4	10	0.22	89	100	103	0.032
9	MODULATOR EXCITER	7.3	1.6	5	11.7	2.1	0.18	110	30	9.6	10	0.22	89	100	109	0.032
9	MODULATOR EXCITER	7.3	1.6	5	11.7	**		110	30	—	10	0.22	89	100	104	0.032
10	1-WATT TRANSMITTER	7.3	5	1.6	36.5	15.0	0.41	110	30	70	25	0.22	89	100	109	0.064
11	POWER AMPLIFIER ASSEMBLY	12	4.2	3	50.4	165.0	3.3	210+	-20	396	25	0.41	178	198	286	0.125
11	POWER AMPLIFIER ASSEMBLY	12	4.2	3	50.4	**	—	210+	-20	—	25	0.41	178	198	220	0.125
12	ANTENNA DRIVE ELECTOR	7	6	12	42	18.6	0.45	130	-20	84	10	0.22	89	100	120	0.032
31	LIMB AND TERM SENSOR	1.5	2.5	2.5	*	0.2	N/A	130	30	N/A	—	N/A	89	100	90	N/A
25	DC/DC CONVERTER	6	6	3.5	36	30.0	0.84	120	-20	144	20	0.22	89	100	120	0.064
28	J-BOX	9	6	6	54		—	160	10	—	10	—	89	100	101	0.032
	TOTAL				601.1	243.0				758.4						

* NOT MOUNTED TO BASE PLATE DIRECTLY ** ONLY ONE OPERATES AT A TIME + BASE PLATE ALLOWABLE N/A NOT APPLICABLE

Figure 5-11

EQUIPMENT PANEL NO. 4, S-band and Relay Link subsystem.

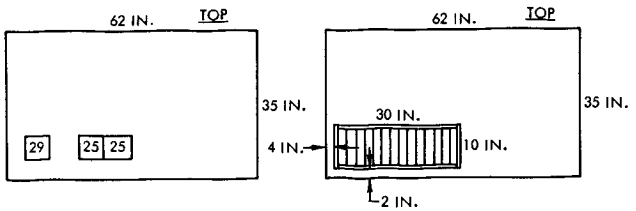

(1) SINGLE 10 IN. x 30 IN. LOUVER = 2.09 SQ. FT.
EFFECTIVE LOUVER AREA = 1.56 SQ. FT.

ITEM NO.	COMPONENT NAME	COMPONENT DIMENSIONS (IN.) L	W	H	COMPONENT BASE AREA ($IN.^2$)	MAXIMUM UNIT STEADY STATE HEAT DISSIPATION (WATTS)	Q/A BASE $\left(\frac{WATTS}{IN.^2}\right)$	COMPONENT TEMPERATURE LIMIT MAX. (°F)	MIN. (°F)	LOUVER AREA REQUIRED ($IN.^2$)	CONTACT CONDITION REQUIRED $\left(\frac{BTU}{HR - FT^2}\right)$	RESULTANT LOUVER Q/A $\left(\frac{WATTS}{IN.^2}\right)$	LOUVER TEMPERATURE (°F)	BASE PLATE TEMPERATURE (°F)	COMPONENT TEMPERATURE (°F)	BASE PLATE THICKNESS (IN. TOTAL)
25	DC/DC CONVERTER GUIDANCE AND CONTROL	6	6	3.5	36	10	0.28	120	-20	46	10	0.22	89	100	114	0.032
25	DC/DC CONVERTER PLANETARY SCAN PLATFORM	6	6	3.5	36	20	0.56	120	-20	92	20	0.22	89	100	114	0.032
29	J-BOX (SCIENCE)	4	5	6	36	–	–	160	10	–	10	–	89	100	103	0.032
	TOTAL				108 (0.75 SQ. FT.)	30				138 (0.96 SQ.FT.)		0.22				

Figure 5-12

EQUIPMENT PANEL NO. 5, Science Electrical Power subsystem.

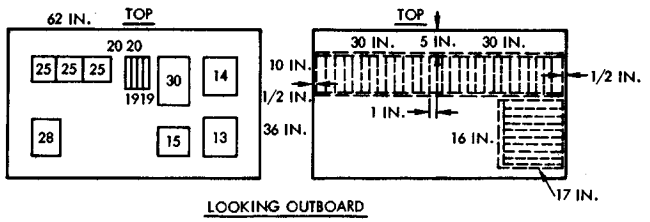

2 SINGLE 10 IN. x 30 IN. LOUVERS
1 SINGLE 10 IN. x 16 IN. LOUVER
} = 6.07 SQ.FT.

EFFECTIVE LOUVER AREA = 4.58 SQ. FT.

ITEM NO.	COMPONENT NAME	COMPONENT DIMENSIONS (IN.) L	W	H	COMPONENT BASE AREA ($IN.^2$)	MAXIMUM UNIT STEADY STATE HEAT DISSIPATION (WATTS)	Q/A BASE $\left(\frac{WATTS}{IN.^2}\right)$	COMPONENT TEMPERATURE LIMIT MAX. (^oF)	MIN. (^oF)	LOUVER AREA REQUIRED ($IN.^2$)	CONTACT CONDITION REQUIRED $\left(\frac{BTU}{HR-FT^2}\right)$	RESULTANT LOUVER Q/A $\left(\frac{WATTS}{IN.^2}\right)$	LOUVER TEMPERATURE (^oF)	BASE PLATE TEMPERATURE (^oF)	COMPONENT TEMPERATURE (^oF)	BASE PLATE THICKNESS (IN. TOTAL)
13	PRIMARY COMPONENT AND SEQUENCER	8	8	7.5	64	20	0.312	110	30	92	20	0.22	89	100	108	0.032
14	BACK UP COMPONENT AND SEQUENCER	8	8	6.5	64	*	0.312	110	30	*	20	0.22	89	100	104	0.032
15	COMMAND UNIT	7	7	3.6	49	13	0.270	110	30	60	20	0.22	89	100	108	0.032
19	RELAY LINK RECEIVER	7	6	1	7	7.5	1.060	110	30	34	25	0.22	89	100	110	0.064
19	RELAY LINK RECEIVER	7	6	1	7	7.5	1.060	110	30	34	25	0.22	89	100	110	0.064
20	RELAY LINK DEMODULATOR	7	6	1	7	1.0	0.144	110	30	5	10	0.22	89	100	106	0.064
20	RELAY LINK DEMODULATOR	7	6	1	7	1.0	0.144	110	30	5	10	0.22	89	100	106	0.064
25	DC/DC CONVERTER COMMAND AND SEQUENCER	6	6	3.5	36	10	0.280	120	-20	46	10	0.22	89	100	114	0.032
25	DC/DC CONVERTER TEMPERATURE CONTROL	6	6	3.5	36	10	0.280	120	-20	46	10	0.22	89	100	114	0.032
25	DC/DC CONVERTER	6	6	3.5	36	10	0.280	120	-20	46	10	0.22	89	100	114	0.032
28	J-BOX	9	6	6	54			160	10		10		89	100	102	0.032
30	GUIDANCE AND CONTROL ELECTRONICS	11	7	6	77	25	0.323	130	-30	112	20	0.22	89	100	108	0.032
	TOTAL				444 (0.73 SQ. FT.)	105				480 (3.3 SQ.FT.)		0.22				

Figure 5-13

EQUIPMENT PANEL NO. 7, Command, Computing, Sequencing and Power subsystem.

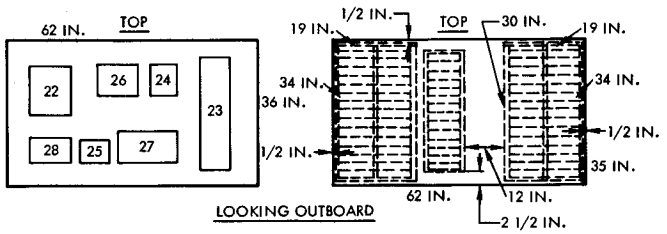

(2) DOUBLE 19 IN. x 30 IN. LOUVERS
(1) SINGLE 10 IN. x 30 IN. LOUVER
} = 11.09 SQ. FT.

EFFECTIVE LOUVER AREA = 8.66 SQ. FT.

ITEM NO.	COMPONENT NAME	COMPONENT DIMENSIONS (IN.) L	W	H	COMPONENT BASE AREA ($IN.^2$)	MAXIMUM UNIT STEADY STATE HEAT DISSIPATION (WATTS)	Q/A BASE $\left(\frac{WATTS}{IN.^2}\right)$	COMPONENT TEMPERATURE LIMIT MAX. (°F)	MIN. (°F)	LOUVER AREA REQUIRED ($IN.^2$)	CONTACT CONDITION REQUIRED $\left(\frac{BTU}{HR - FT^2}\right)$	RESULTANT LOUVER Q/A $\left(\frac{WATTS}{IN.^2}\right)$	LOUVER TEMPERATURE (°F)	BASE PLATE TEMPERATURE (°F)	COMPONENT TEMPERATURE (°F)	BASE PLATE THICKNESS (IN. TOTAL)
22	POWER CONTROL UNIT	10	10	5	100	100	1.00	120	-20	460	25	0.22	89	100	119	0.064
23	SHUNT ASSEMBLY	25	6	6	150	100	0.67	150	-20	450	20	0.22	89	100	112	0.064
24	400 Hz INVERTER	7	7	5	49	0.5	0.010	120	-20	2.5	10	0.22	89	100	102	0.032
25	DC/DC CONVERTER CAPSULE	6	6	3.5	36	30	0.84	120	-20	144	20	0.22	89	100	120	0.064
26	DISTRIBUTION CONTROL UNIT	10	7	7	70	5	0.072	150	10	23	10	0.22	89	100	104	0.032
27	PYROTECHNIC CONTROL UNIT	15	7	7	105	2	0.02	150	10	10	10	0.22	89	100	102	0.032
28	J-BOX	9	6	6	54	–	–	160	10	–	10	0.22	89	100	101	0.032
	TOTAL				564 (3.9 SQ. FT.)	237.5				1089.5 (7.6 SQ.FT.)		0.22				

Figure 5-14

EQUIPMENT PANEL NO. 8, Power Distribution subsystem.

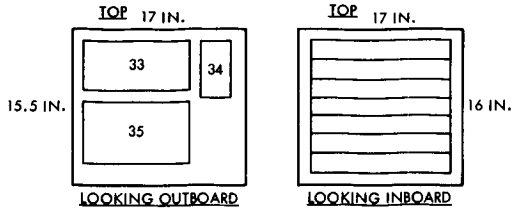

1 SINGLE 17 IN. x 16 IN. LOUVER 1.9 SQ. FT.
EFFECTIVE LOUVER AREA 1.46 SQ. FT.

ITEM NO.	COMPONENT NAME	COMPONENT DIMENSIONS (IN.) L	W	H	COMPONENT BASE AREA ($IN.^2$)	MAXIMUM UNIT STEADY STATE HEAT DISSIPATION (WATTS)	Q/A BASE $\left(\frac{WATTS}{IN.^2}\right)$	COMPONENT TEMPERATURE LIMIT MAX. (°F)	MIN. (°F)	LOUVER AREA REQUIRED ($IN.^2$)	CONTACT CONDITION REQUIRED $\left(\frac{BTU}{HR - FT^2}\right)$	RESULTANT LOUVER Q/A $\left(\frac{WATTS}{IN.^2}\right)$	LOUVER TEMPERATURE (°F)	BASE PLATE TEMPERATURE (°F)	COMPONENT TEMPERATURE (°F)	BASE PLATE THICKNESS (IN. TOTAL)
33	CANOPUS SENSOR	12	5	4	60	6	0.10	130	-30	28	10	0.22	89	90	94	0.032
34	J-BOX	6	4	6	24	–	–	160	10	–	10	–	89	90	92	0.032
35	INERTIAL REFERENCE ASSEMBLY	12	8	7	96	40	0.42	130	30	192	10	0.22	89	90	112	0.032
	TOTAL				180 (1.25 SQ. FT.)	46.0				220 (1.54 SQ.FT.)		0.22				

Figure 5-15
EQUIPMENT PANEL, Guidance and Control subsystem.

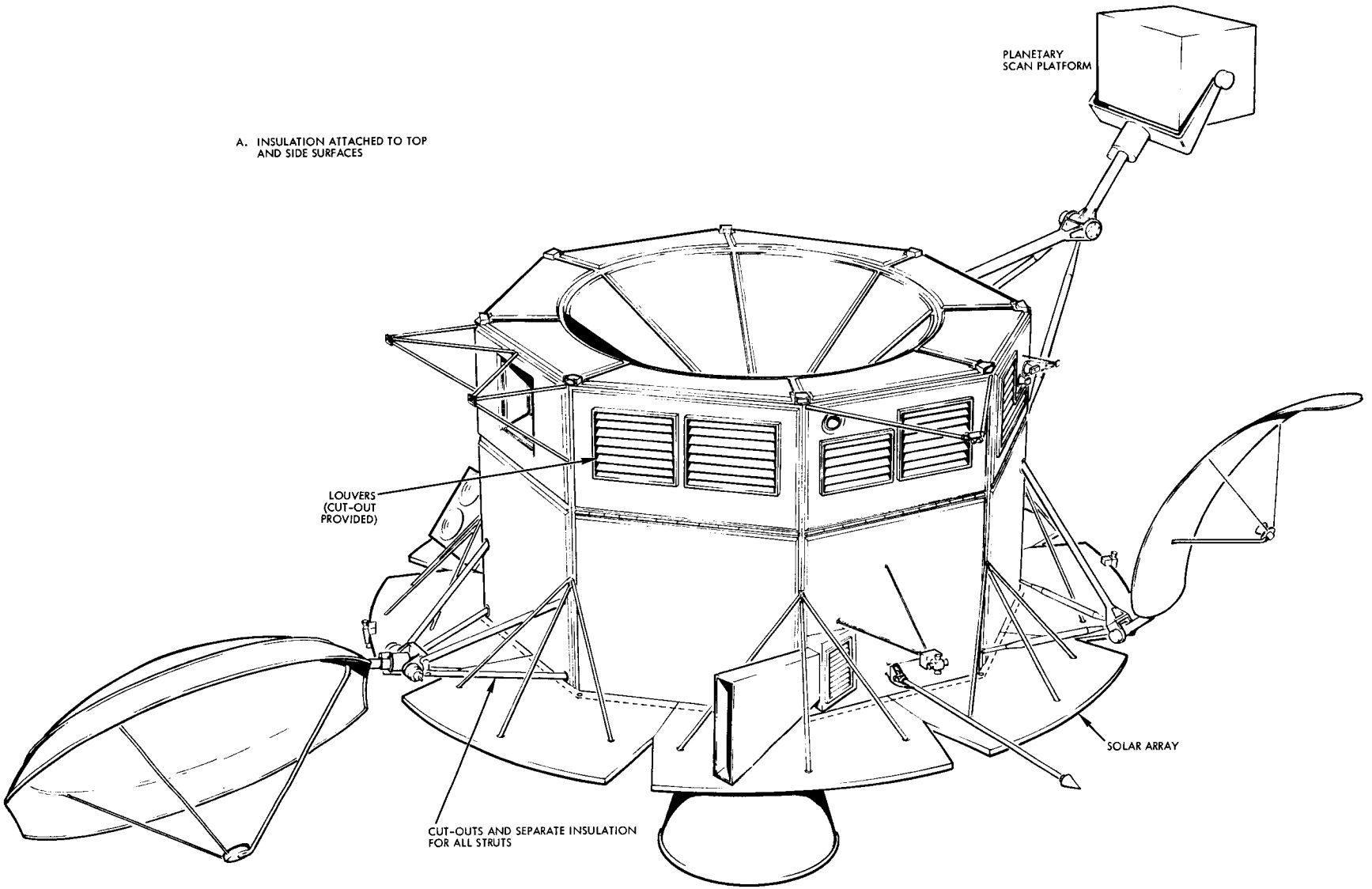

Figure 5-16
EXTERNAL COMPONENTS

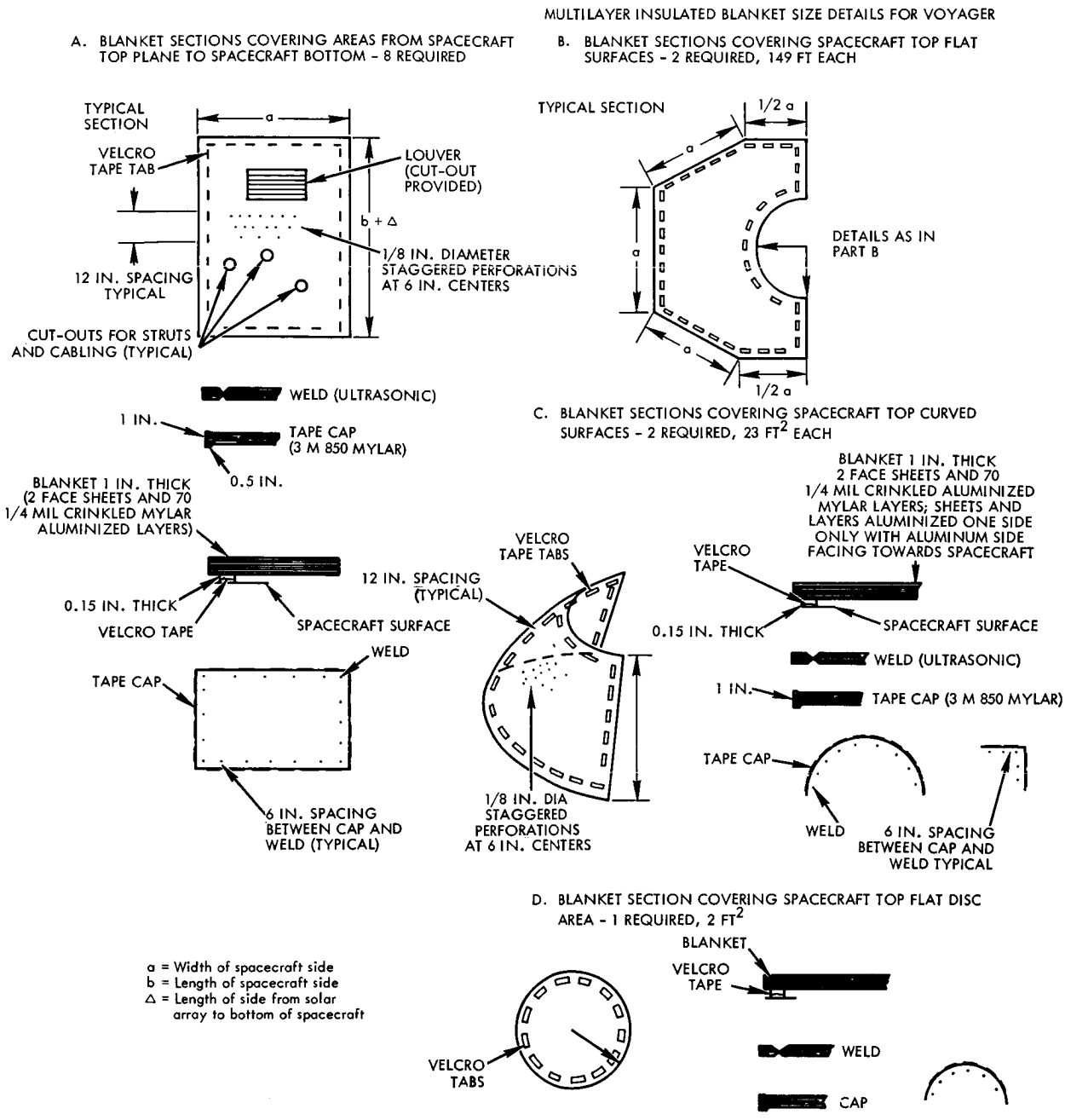

Figure 5-17

INSULATION DESIGN makes use of large, seamless blankets of multilayer, crinkled, aluminized Mylar. Blankets are attached to structure with Velcro tape.

Electrical components requiring temperature control are located on the equipment panels and are grouped by subsystems. The components are distributed on the panel so that the heat dissipation is distributed equally. In addition, all components on the equipment panels and within the equipment module will have a hemispherical infrared emissivity of 0.86 or greater to promote radiant interchange within the equipment module and the propulsion module. Conduction within the equipment panels and throughout the equipment module is promoted by good thermal conduction joints and materials. The equal distribution of heat-dissipation components, high-emissivity surfaces, and good thermal-conduction joints and structure reduces temperature gradients within the equipment module as much as possible.

5.4.2.4 Equipment Panel Temperature Control Details

Component design requirements, such as flatness (0.004 in/ft), component location (to equalize heat dissipation on panel and within equipment module), component orientation (maximum mounting area for heat description densities greater than 0.3 watt/in^2), baseplate area and baseplate thickness sufficient to reduce heat dissipation densities to acceptable levels, prevent electrical components from exceeding their temperature limits. Figures 5-9 through 5-15 show equipment panel component locations, required baseplate area, thickness, louver areas and locations, heat dissipation densities at component mounting area, and heat-dissipation densities. The baseplate and component temperatures are also given for contact conductances, baseplate areas, and thicknesses specified for each component.

The equipment panel transverse conductance was assumed to be 10 Btu/hr-ft^2 - ^oF (a minimum of 7 Btu/hr-ft^2 - ^oF is required). The one-inch thick aluminum honeycomb covered by 0.032-inch top and bottom face sheets supplies sufficient transfer of heat to the louvers. The lateral thermal conductance through the 0.032 aluminum cover sheets meets the general lateral thermal conductivity thickness product requirement of 6 Btu-in/hr-ft ^oF. Local increase in baseplate thickness enhances the lateral conduction, when required by high heat dissipation density units such as the TWT, shunts, and power control unit.

Equipment panel external surfaces, in the areas where louvers are to be mounted, are treated so that the hemispherical infrared emissivity is 0.85 or greater and the solar absorptivity is 0.25 or lower. The high emissivity allows maximum radiation of excessive heat through the louvers when they are open, while the low solar absorptivity limits heat absorbed should the louvers be facing the sun during non-sun-oriented periods.

5.4.2.5 External Equipment Temperature Control Details

External equipment is comprised of spacecraft components which are separately exposed to the spacecraft's induced and natural enviroments. The equipment shown in Figure 5-16 is usually located externally for a specific subsystem need, or, due to wide temperature limits, is not required to be located internal to the equipment module. The science equipment is grouped for ease of thermal control and orientation in the planetary scan platform package, which is covered in detail in Section 5.4.5.

An examination of the external equipment revealed that satisfactory temperature control could be achieved by appropriate use of surface finish control, insulation, and thermostatically-controlled heaters. Table 5-5 gives a list of external equipment requiring heaters and heat rating required.

The effect of plume heating on external equipment is small. The high-gain antenna experiences only a $50^{\circ}F$ rise during engine firing. There is no plume impengement on the spacecraft. A detailed description of plume effects is described in Volume 10, Section 4.

Table 5-5. External Mounted Equipment Requiring Heaters

Number Required Per Spacecraft	Component	Watts Required
1	High-gain antenna drive	1.0
2	Medium-gain antenna drive	1.0
4	Coarse sun	2.0 each (8.0)
1	Low-gain antenna deployment	
1	Planetary Scan Platform drive assembly	2.0
1	Planetary Scan Platform deployment mechanism	2.0
9		15

5.4.2.6 Solar Arrays

The solar arrays associated with the equipment module include the annular solar array, attached directly to the equipment module, and the solar panels suspended from the equipment module and attached to the propulsion module at assembly. Thermal control of the base-mounted solar arrays, which are insulated, is achieved by re-radiation from the sun side and conduction to other structures. Temperature control for the annular solar arrays is achieved by re-radiation from both the sun side and the back side. The minimum temperature experienced by the solar arrays occurs during Mars eclipse, at which time the temperature approaches the lower limit of -260°F. During engine firing, the solar array exceeds the upper steady-state limit of 250°F and briefly approaches 300°F. Tests on the VASP program have shown that the solar arrays can experience temperatures of this magnitude for a short period of time and maintain their integrity.

5.4.2.7 Louver Assemblies

The louver assemblies will be of the bimetallic actuator type used on Mariner, OGO, Pioneer and Pegasus. From these designs, those features which best suit the Voyager application will be selected. A preliminary specification for the louver assemblies is given in Figure 5-18.

PRELIMINARY SPECIFICATION

Louver Assembly

Purpose

To prevent excessive excursion of radiator temperature by varying its local effective emittance.

Performance Characteristics

1. The relationship between lower angle and actuator temperature shall be as shown in graph.
2. When mounted to an isothermal radiator (approximately 3 sq ft) whose emissivity is 0.85, the effective emissivity of the radiator shall be:
   - < 0.10 with louvers fully closed 0 deg
   - > 0.70 with louvers fully open 90 deg
3. The assembly shall tolerate temperatures resulting from exposure to solar radiation at 1 AU with a radiator solar absorpitivity of 0.20.
4. The performance shall not be compromised by exposure to the mission environment of 1.5 years.

Physical Characteristics

1. The assembly weight, for areas greater than 2 sq ft shall not be greater than 1.0 lb-sq ft.

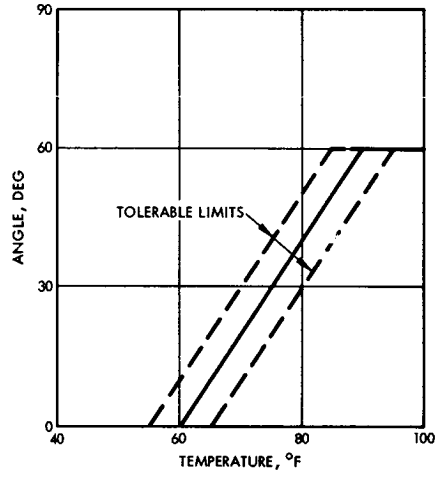

Figure 5-18

Generally the louver configuration shown in Figures 5-19 and 5-20, will be used. Each assembly will include a number of louver blades, each about 2 inches wide, made from two pieces of 0.005-inch aluminum suitably shaped to provide adequate strength. A bearing pin is attached on the central longitudinal axis through interposed insulation blocks at each end of the louver blade.

Continuous louver support brackets, formed from small gage aluminum, contain the louver bearings. Integral features serve to secure one end of each bimetallic actuator and to limit louver angle excursion (0 to 90 deg). Paired brackets, joined together at their ends, form frames for the louvers. The final louver assembly (less the actuator shields) thus becomes one part, for which handling and installation fixtures are built.

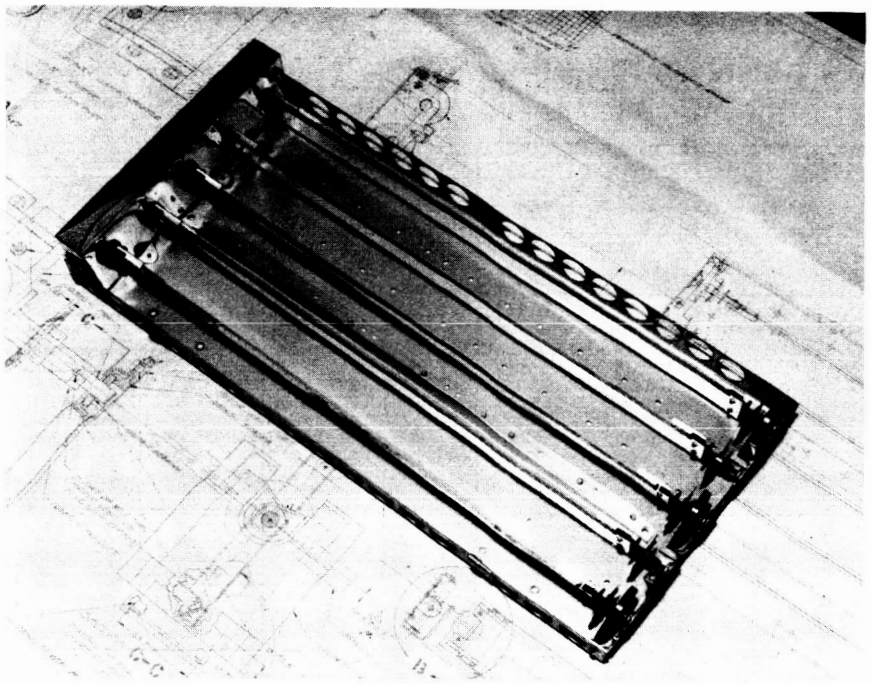

Figure 5-19

PREFERRED LOUVER ASSEMBLY has been space-qualified on the OGO series of scientific satellites and has been in trouble-free operation during more than two years in Earth orbit.

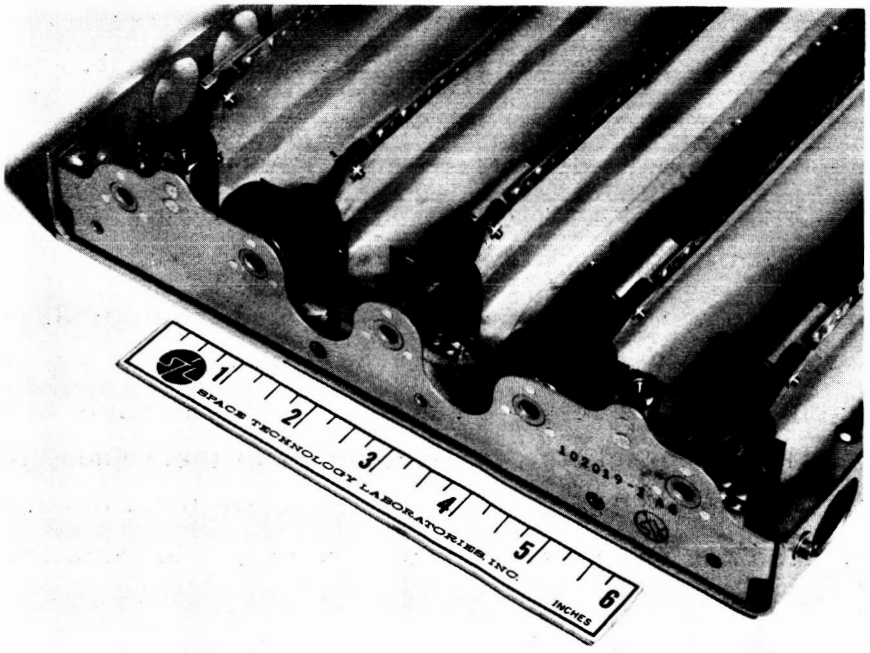

Figure 5-20

OGO BIMETALLIC ACTUATORS control blade settings automatically upper edges of blades open outward so that heat from solar arrays is reflected away from equipment.

Actuators for the louver blades will be of the type used on OGO spacecraft selected for their high output torque. Each actuator is a spiral coil, the inner end of which is secured to the louver axis by a device which also permits setting the louver angle. The other end is formed to extend down to the base of the support bracket, where it is held fixed. Actuators are placed at alternate ends of neighboring louvers.

To permit the actuators to be strongly responsive to the local temperature of the radiator surface, a radiation shield is provided. It is comprised of multi-layer aluminized mylar, formed to cover the actuators and the entire length of the support brackets. When installed, the only openings present are those required to permit free rotation of the louver blades and shaft.

The louver assemblies are located on each equipment panel and the two guidance and control panels. The locations of the louvers on the panels are given in Figures 5-9 through 5-15. Louver assemblies have been standardized as much as possible, consistent with component and equipment panel geometry. Generally, a single-row louver assembly 10 inches wide by 30 inches long, and a double row louver assembly 19 inches wide by 34 inches long, were selected. The louvers are 2 inches wide by 8 inches long. The relatively short louver length will ensures accurate louver angular actuation without excessive twist about the axis. In addition, the 8-inch length suited a standardized louver area for best equipment coverage. The louver assembly has a one-inch frame around the louver rows for actuators and attachments, and thus is not fully effective as a radiator surface. Figure 5-21 presents a description of the standardized louver assemblies, dimensions, total area, and effective radiation area. Table 5-6 summarizes the minimum effective radiating area required, total standardized louver area, and effective standardized louver radiating area.

5.4.2.8 Insulation

Insulation used on the equipment module will consist of blankets of multilayer aluminized Mylar. To facilitate handling, each blanket will have a 3-mil aluminized Mylar cover sheet on both sides. The outside layer has the aluminized surface facing toward the spacecraft. These blankets will consist of 70, 1/4-mil crinkled sheets aluminized on one side with aluminum side facing towards the spacecraft.

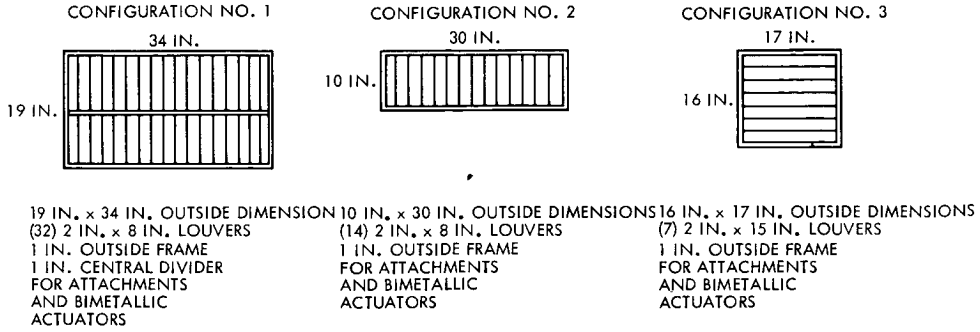

	CONFIGURATION NO. 1	CONFIGURATION NO. 2	CONFIGURATION NO. 3
OUTSIDE DIMENSIONS (IN.)	19 X 34	10 X 30	16 X 17
ATTACHMENT AREA (SQ FT)	4.50	2.09	1.89
EFFECTIVE RADIATING AREA (SQ FT)	3.55	1.56	1.46

Figure 5-21

STANDARDIZATION OF LOUVER ASSEMBLIES simplifies fabrication by requiring only three basic sizes.

Table 5-6. Summary Louver Area Required

Panel		Minimum Effective Radiating Area Required (ft^2)	Standardized Louver Mounting Area (ft^2)	Standardized Louver Effective Radiating Area (ft^2)
Power	I	12.00	13.50	10.70
Data Handling	III	4.15	6.07	4.58
S-Band	IV	5.25	9.00	7.10
Science	V	0.96	2.09	1.56
Command and Sequencing	VII	3.30	6.07	4.58
Power and Distribution	VIII	7.60	11.09	8.66
Guidance and Control		1.54	1.90	1.46
Guidance and Control		1.54	1.90	1.46
		36.34	51.62	40.10

The location of the insulation blankets on the equipment module, number of blankets, total square feet of insulation, and insulation thickness are given in Figure 5-17. In general, the insulation will be attached by means of Velcro tape to ease removal of blankets. The detailed design of the insulation is presented in Volume 10, Section 3.

5.4.2.9 Heaters and Thermostats

Electrical strip heaters and thermostats are utilized for temperature control of equipment external to the equipment module where power dissipation is inadequate or widely varying. The heaters are thin, flexible (e.g., silicone rubber) units of various sizes which can be adhesively-bonded to the surface. The resistive wire is bifilar-wound to reduce the magnetic field. With DC power applied, the magnetic field does not exceed 2 gamma at 2 inches. The units can be obtained from commercial sources per TRW Specification PT4-13004 in virtually any physical size and power rating required. Table 5-5 gives a list of external equipment requiring heaters, and the heater rating required. Four of these will be ground-command ON or OFF as required. Commercial thermostats are available in a broad spectrum of operating ranges. TRW Specification PT2-2004, for example, identifies ON-OFF differentials ranging from 9 to 20°F, setting accuracies of ±2 and ±5°F, and mean operation levels from 30 to 110°F.

5.4.2.10 Temperature Control Performance

A measure of temperature control subsystem performance can be achieved by comparing component and structure temperature limits for various "hot and cold" cases with the respective temperature limits. Tables 5-3 and 5-4 summarize information from the thermal model (Section 5.4.1) and individual component analyses for all the components and structure on the equipment list for the equipment module. All components are within the temperature limits.

5.4.3 Temperature Control Propulsion Module

Temperature control of the propulsion module is accomplished with multilayer insulation, high temperature insulation, surface finish, low thermal conductance structural attachments, and thermal interactions with the equipment module.

5.4.3.1 Insulation

Two types of insulation are to be used in the propulsion module, multilayer insulation and high-temperature insulation. One type of high temperature insulation is attached to the propulsion module structure around the engine opening (Figure 5-22). The insulation is attached so that, during engine gimbal operation, this blanket will slide over the adjacent insulation. The insulation to be used is 0.5-inch Refrasil batt, with a conductivity of 0.042 Btu/hr-ft-^{o}F, sandwiched between spun-metal enclosures of low emissivity. This insulation minimizes heat gain to the compartment during engine firing, minimizes heat loss to space during eht eclipse, and limits solar heat gains during the remainder of the remainder of the mission.

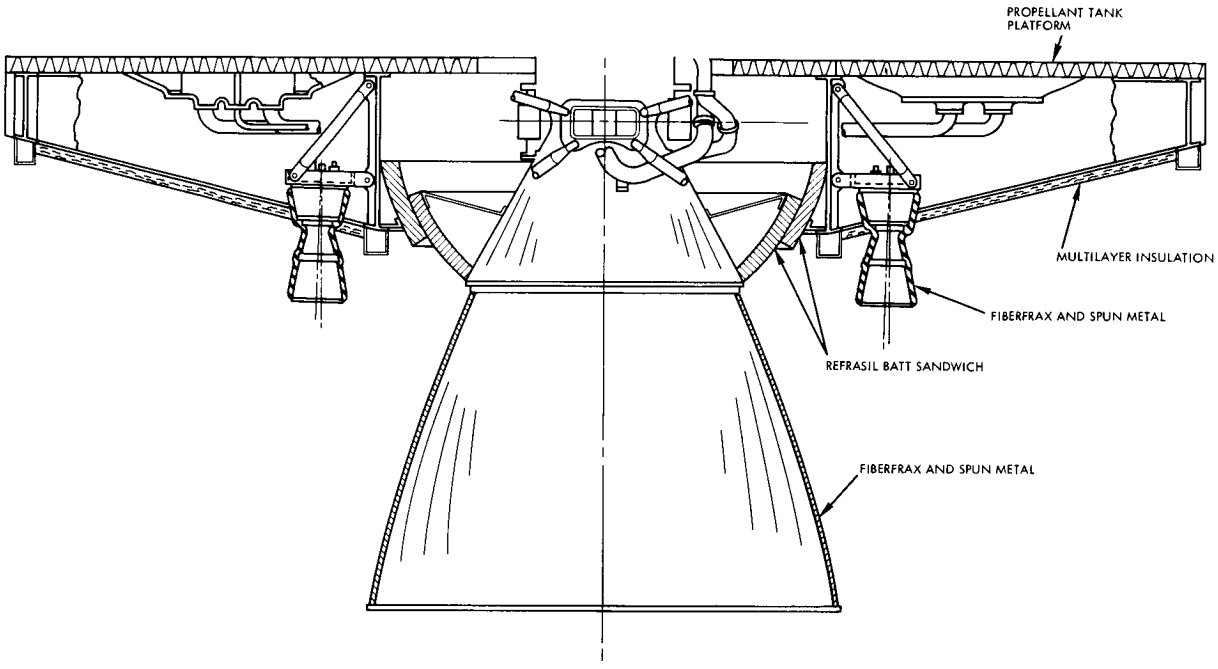

Figure 5-22
PROPULSION MODULE INSULATION consists of multilayer blankets on lower surfaces of module, high-temperature Refrasil around the base of the engine, and metal-coated Fiberfrax on the nozzle extension.

Other types of high temperature insulation will be used on the engine and nozzle extensions (Figure 5-22). The inside of engine will be covered with ablative material, from the combustion chamber to the location on the engine nozzle, where the area ratio is 16/1. The ablative material keeps the engine nozzle throat and nozzle section aft of the throat within operable temperatures.

The nozzle extension, from area ratio 16/1 to the exit plane, is covered by a blanket of Fiberfrax which in turn is covered with spun metal. The spun metal covering limits the hemispherical infrared emissivity to 0.2, thus providing radiative heating protection for the aft-mounted solar arrays during engine firing.

Multilayer insulation is attached to the base of the propulsion module to minimize heat loss to space and to minimize heat inputs from the sun (Figure 5-22). The multilayer insulation is one inch of aluminized Mylar, with 70 layers per inch. The conductance between the outer and inner layers, when attached, is 0.007 Btu/hr-ft^2-$^\circ$F for a hot side temperature of 246°F and a cold side temperature of 91°F. The multilayer blanket is layed so that the aluminized side faces the propellant tank platform. The hemispherical emissivity of the insulation with the aluminized side out is 0.04. This surface is to be coated for an emissivity of 0.24. The side of the insulation, radiating to space and the engine nozzle, has an emissivity of 0.78 (Mylar side out) and a solar absorptivity of 0.24. The multilayer insulation is vented to allow for changes in atmospheric pressure. It is layed in blankets and attached with Velcro tape. This method of attachment permits removal and replacement of the insulation blankets. Careful handling is required to minimize scratches on the insulation surfaces. A more comprehensive discussion of the insulation design development, and parameters affecting the design, is included in Section 3.5 of Volume 10.

5.4.3.2 Thermal Interaction, Equipment Module

The propulsion module, as discussed herein, is separate from the equipment module. Temperature control considerations, however, cannot separate the two modules because of thermal interaction. This iteraction is important because propellant tank temperatures depend on the amount of heat lost through the equipment module. Selection of insulation depends on tank temperature. Insulation blankets for the equipment module sections, based on propellant tank temperatures, will have a thermal conductance per unit area of no less than 0.007 Btu/hr-ft^2-$^\circ$F and no greater than 0.012 Btu/hr-ft^2-$^\circ$F. Table 5-7 presents computed propellant tank and line temperatures for extreme cases, using a unit area conductance of 0.007 Btu/hr-ft^2-$^\circ$F for the equipment module insulation blankets.

Table 5-7. Computed Tank and Line Temperatures*

Component	Temperatures from Steady-State Analyses, °F		Temperatures from Transient Analyses, °F		
	Near-Earth**	Near-Mars	Engine Firing Near-Earth, max	Engine Firing Near-Mars, max	Mars Eclipse at End of 2.6 hr
Fuel tanks	89	63	80	63	62
Oxidizer tanks	89	63	80	63	62
Fuel lines	90	62	86	63	62
Oxidizer lines	90	62	86	63	62
Helium tanks	90	71	82	71	70

*For extreme cases using an equipment module blanket insulation conductance per unit area of 0.007 Btu/hr-ft^2-°F.

**With capsule on, dissipating 7 kw.

5.4.3.3 Surface Finish and Coatings

The temperatures of most of the propulsion components must be maintained at 70 ± 20°F. All propulsion module components are connected within the feed lines, the pressurization system lines, or in the propellant tanks. The requirement then is to maintain all tanks and lines at 70 ± 20°F. This is accomplished by various surface coatings (Figure 5-23).

The propellant tanks and the helium pressurization tanks are coated with Cat-a-lac black paint (emissivity 0.86). The propellant tank platform has Cat-a-lac black paint on the forward side, and the aft side is coated with a silicone aluminum paint, which has a hemispherical emissivity of 0.24. The propellant lines are hung below the propellant tank platform. The lines are coated with a silicone aluminum paint having an emissivity of 0.24. The pressurization lines run between the pressurization tanks and the propellant tanks and are painted with Cat-a-lac black paint.

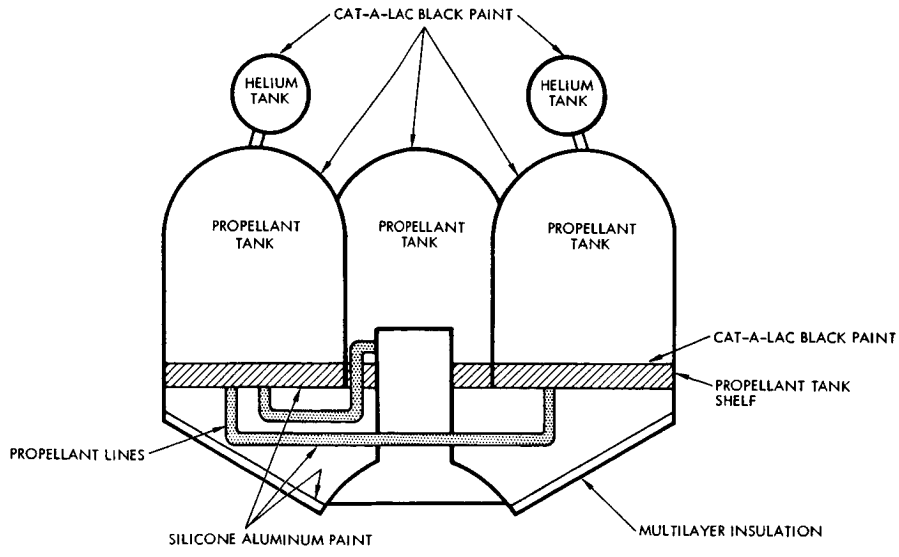

Figure 5-23

PROPULSION MODULE SURFACE COATINGS maintain internal temperature balance and radiatively couple propulsion components to the rest of the spacecraft.

5.4.3.4 Temperature Control Performance

All propulsion module components will be maintained within their temperature limits, as shown in Table 5-8, during all phases of testing, prelaunch activity, and launch, and throughout the Voyager mission.

5.4.4 Temperature Control Planetary Scan Platform

5.4.4.1 Description

The planetary scan platform houses the scientific instruments and related electronics. The instruments included are a photo-imaging system, high-resolution infrared spectrometer, broadband infrared spectrometer, infrared radiometer, ultraviolet spectrometer, and Mars sensors. The methods of temperature control include passive and active techniques: The passive techniques are insulation, radiators, and surface coatings which are state of the art; the active method is cryogenic refrigeration, which is under development.

Table 5-8. Temperature Limits (^{o}F)

Propellants	
Nominal bulk temperature	70 ± 20
T between unlike propellant tanks	5
T between like propellant tanks	2
Feed system component temperature	70 ± 20

5.4.4.2 Insulation

Multilayer insulation is attached to the planetary scan platform supports and within the planetary scan platform, the internal facing surfaces of the broadband infrared spectrometer, and the high resolution infrared spectrometer. This provides maximum insulation of the components of these two instruments from all other planetary-scan-platform-mounted equipment. The multilayer insulation is one inch (of 70 layers per inch) aluminized Mylar. The maximum conductance between the outer inner layers, when attached, is 0.001 Btu/hr-ft^{2}-^{o}F, based on a

hot side temperature of 85°F and a cold side temperature of -315°F. The insulation is attached with Velcro tape to satisfy remove-and-replace requirements. A more comprehensive discussion of the multilayer insulation design development and parameters affecting the design is included in Section 3.5 of Volume 10.

The planetary scan platform uses meteoroid shield in its construction. This shield is of foam sandwiched between aluminum face sheets, two inches thick, with a thermal conductivity of 0.02 Btu/hr-ft-°F. The meteoroid shield provides sufficient insulation to maintain the planetary scan platform environment within instrument temperature limits.

5.4.4.3 Heaters and Thermostats

Two-watt, thermostatically controlled heaters are attached to the planetary scan platform deployment and drive mechanisms to prevent freezing.

The heaters to be used are of the strip type. These are thin, variable-sized, flexible (e.g., silicone rubber) units which are adhesively-bonded to the surface. The resistive wire is bifilar-wound to reduce the magnetic field. The unit can be obtained from commercial sources in virtually any physical size and power rating required.

Associated with the heaters are thermostats having an Off-On range of 10°F. The heaters will be on when the temperature of the component to be heated is 10°F above its lower limit.

5.4.4.4 Radiators

The broadband infrared spectrometer and the high resolution infrared spectrometer contain components which must be radiatively cooled. Two 8-1/2 inch by 10 inch (0.59 square foot) radiators are used to control the temperatures of the broadband infrared spectrometer telescope, monochromator, choppers, and detectors. The high resolution infrared spectrometer detector is cooled by a 7 x 13 inch (0.63 square foot) radiator.

The radiators are 3/16 inch aluminum plates framed with fiberglass to prevent heat leaks (Figure 5-24). The aluminum plate also provides adequate micrometeoroid protection. The external surface of the radiator is coated with IITRI Z-93 white paint. The white paint has a hemispherical emittance of 0.9 and a solar absorptivity of 0.18. The paint was tested to determine the effect of solar exposure. After 1000 hours of exposure to solar radiation at a pressure less than 10^{-6} torr the solar absorptivity was 0.25. The surfaces of the planetary scan platform, where the radiators are located, are expected to be only briefly exposed to the sun.

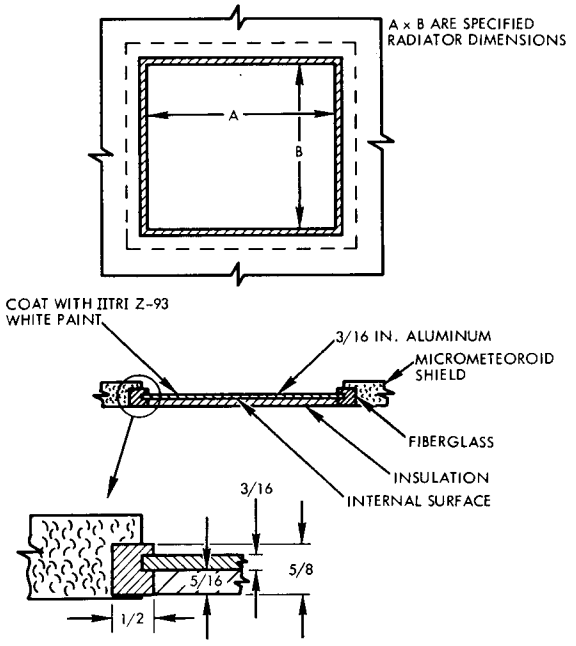

Figure 5-24

SPECTROMETER RADIATORS are fabricated from 3/16-inch aluminum sheets coated with white paint and insulated from the other science experiments within the planetary scan platform.

The components to be cooled are conductively tied to the radiators using high conductivity material. The inner surface of the radiator is insulated to provide isolation of those components which do not require cooling.

5.4.4.5 Cryogenic Refrigeration

The broadband infrared spectrometer contains an infrared detector which must be maintained at 45°K. A radiator operating at this temperature having an emissivity of 0.9 can remove 0.02 watts per square foot of radiating area. To radiatively cool the detector then would require the radiator and the detector to be perfectly isolated from any heat sources. Radiatively cooling the detector appears impractical. A radiator used with refrigeration can be effective.

There are four basic methods for spacecraft refrigeration: stored cryogenic fluids, thermoelectricity, sublimation and mechanical refrigeration. Storing cryogenic fluids for extensive periods is not practical since the weight of the initial fluid required, considering the loss due to boil-off would be prohibitive. Thermoelectric cooling in its present state of the art is only applicable to temperatures above 150°K, and thermomagnetic cooling is still under development. Present mechanical refrigeration techniques appear to be promising. Many developments have occurred in this field which should eventually lead to the development of several miniature cryogenic refrigerators appropriate for space applications. Even with refrigeration, careful design is required to limit heat leak into the detector.

The Voyager mission design life is 2 years, including 2 months in Mars orbit. This length of time, of course, rules out any type of open-cycle cooling. Closed-cycle refrigeration is, therefore, proposed to meet the 45°K requirement.

Research and development work on miniature cryogenic refrigerators is currently in progress. A miniature cryogenic refrigerator suitable for immediate spacecraft use has been developed by Norelco, called the "Cryogem". It operates on the Stirling cycle. A "Cryogem" unit has been developed to operate with 28 VDC instead of the more usual 3-phase 400-cycle and 60-cycle power. The current 28-volt model will pump 10 watts at 70°K with 300 watts input power and 1.5 watts at 20°K with 400 watts input. The system requires 400 watts input at turn-on and requires about 10 minutes to reach 70°K. For 45°K application, 350 watts of input will pump 5 watts. The "Cryogem" unit is suitable for use in the broadband spectrometer. It requires a large amount of power, however, and therefore places an additional burden on spacecraft power systems.

Table 5-9 lists additional cryogenic cooling devices which are under development and applicable for cooling the broadband infrared detector.

The efficiency of all these devices is quite low, requiring from 0.1 to 2 kilowatts of power for 0.1 to 5 watts of refrigeration. The external power requirement results in a system that is quite heavy when the power supply weight is included as part of the total cooling system weight.

At the present time, several approaches are being investigated for cryogenic refrigerators. These developments include both electrically powered refrigeration and gas-powered systems. Three different refrigeration cycles (Stirling, Joule-Thomson, and Claude cycles) and their variations are being considered as possible candidates for miniature cryogenic refrigeration and much research is being carried out in the development of high-speed miniature compressors.

As a result of this research and development activity, it is felt that several types of miniature cryogenic refrigerators could be available in the next few years, which will require no more than 50 watts of input power and meet the $45^{\circ}K$ cooling requirement.

Solid-cryogen refrigerators are currently under development. Such a refrigeration system consists of a container filled with a solid cryogen, which is thermally coupled to an infrared detector. The cryogen is thermally isolated from its surroundings. The size of this system is much less than the fluid cryogenic system since it takes advantage of two phase changes instead of one. The cryogen to be used is determined by the temperature at which the infrared detector is to operate. The desired detector temperature is maintained by controlling the vapor pressure over the solid. Development efforts have produced a solid-cryogen refrigerator, which will maintain an infrared detector at $52^{\circ}K$ and remove 17 milliwatts of heat from the detector. The cryogen used is Argon. The system weight is approximately 30 pounds and has a life of one year. The complete cycle of cooling and solidification of the Argon requires 24 hours.

Further development of solid cryogen refrigerators could result in a system suitable for use with the broadband infrared spectrometer. The solidification of the cryogen would occur prior to launch and would therefore require the solid cryogen to have a useful life in excess of 1 year.

Table 5-9. Cryogenic Refrigeration Systems Under Development

Type	T, ^{o}K	Cooling Capacity (watts)	Life (hr)	Power Required (watts)	Weight (pounds)
Joule-Thomson	80	0.25	500	50	9
Cryostat, closed cycle	88	2.5	500	200	9
Reverse Brayton	77	2	3 years	100	22
Nonreciprocating	77	2	1000	100	15
Closed cycle	77	4	500	1600	35
Closed cycle	22	0.2	500	500	32
Stirling cycle	25	0.5	500	450	35
Stirling cycle	77	1.5	500	45	8
Stirling cycle	77	0.5	500	25	5
Claude cycle	77	1.0	1 year	100	
Reverse Brayton	80	2	1000	400	
Reverse Brayton	15	1	1000	6600	
Stirling cycle	12	30	1000	650	
Solid cryogen	50	0.025	1 year	0	30

5.4.4.6 Science Equipment

The science equipment is arranged in the planetary scan platform to distribute the heat load. Exceptions to this are the broadband infrared spectrometer and the high-resolution infrared spectrometer. The broadband infrared spectrometer has two radiating surfaces and a viewing surface and, therefore, is placed in a corner. The high-resolution infrared spectrometer requires one radiating surface and one viewing surface. Figure 5-25 shows the relative location of these two units.

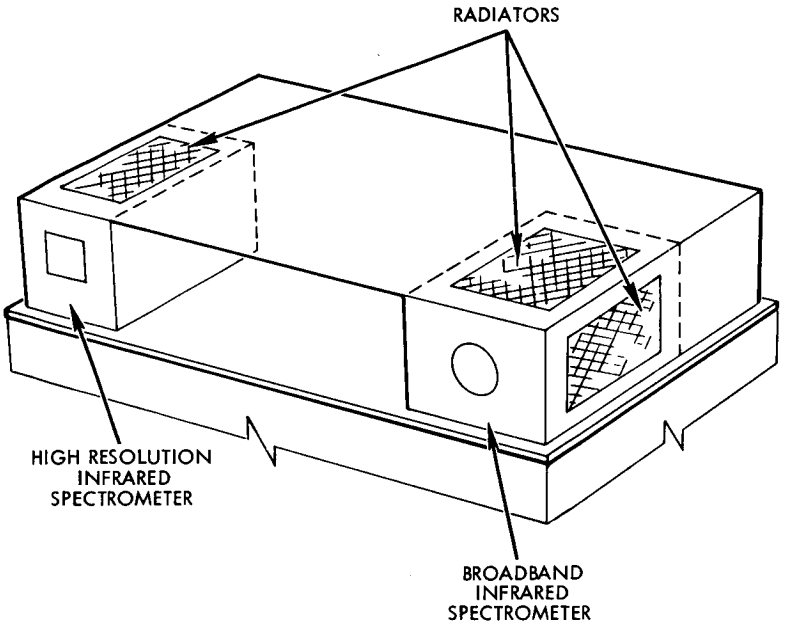

Figure 5-25

LOCATION OF SPECTROMETER RADIATORS, on portions of planetary scan platform normally facing away from sun, provides required performance with minimum area.

The broadband infrared spectrometer and the high-resolution infrared spectrometer are mounted on fiberglass standoffs and attached to the planetary scan platform structure. The Eastman Kodak film-type photo subsystem used in a candidate photo-imaging system is mounted on a 1/4-inch aluminum plate which is attached to the planetary scan platform structure. A more detailed discussion of the photo-imaging system is included in Section 4.4 of Volume 5.

The multilayer insulation on the broadband infrared spectrometer and the high resolution infrared spectrometer is attached with the Mylar side out, having an emissivity of 0.78. The remaining instruments and electronic units are to be coated with Cat-a-lac black paint, having an emissivity of 0.86.

5.4.4.7 Summary

Temperature control for the planetary scan platform and its science equipment is accomplished by the following state of the art, flight proven items: insulation, radiators, heaters and thermostats, thermal coatings, and thermal coupling. A broadband infrared spectrometer detector requires a cryogenic refrigeration system. This type of system is presently under development. The planetary scan platform and all its science payload will be maintained within their temperature limits, as presented in Table 5-10, during all phases of prelaunch activity, and launch, and throughout the Voyager mission by these temperature control techniques.

5.4.5 Reliability Estimate

The temperature control subsystem is a combination active-passive system. For this reliability estimate the following assumptions were made:

- The insulation is a passive, non-failing element
- Thermal finishes and thermal structural coupling are a passive, non-failing element
- Mission duration of the louvers is 2500 cycles
- Mission time of heaters/relays/thermostats is 6800 hours

Table 5-10. Planetary Scan Platform Equipment Temperature Limits

Equipment	Allowable Temperature, °F Minimum	Maximum
Baseline photo imaging system	35	85
High resolution infrared spectrometer		
Spectrometer	-76	50
Detector	-76	-76
Electronics	-22	122
Broadband infrared spectrometer		
Telescope	-44	-26
Monochromator	-44	-26
Channel 1 chopper	-235	-217
Channel 1 detector	-379	-379
Channel 2 chopper	-46	-28
Channel 2 detector	-226	-226
Electronics	-40	104
Infrared radiometer	4	58
Ultraviolet spectrometer	32	104
Mars sensor	0	113

Figure 5-26 presents a reliability block diagram for the temperature control subsystem. Type I louver assemblies cover radiating panels on the guidance and control equipment panels. For this reliability estimate it is assumed that no more than three blades can fail on a Type I louver assembly. Type II louver assemblies cover radiating panels on the equipment panels. For this reliability estimate it is assumed that no more than five blades can fail on a Type II louver.

Total mission success probability for the entire subsystem is 0.9943.

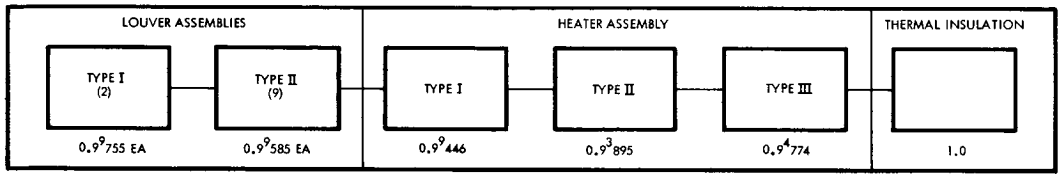

Figure 5-26
RELIABILITY BLOCK DIAGRAM-Temperature control subsystem.

The reliability expression for the subsystem is:

$$R_S = R_{louvers} \times R_{heaters} \times R_{insulation}$$

where

$$R_{louvers} = \left[R_{Type\ I}\right]^2 \times \left[R_{Type\ II}\right]^9$$

$$R_{heaters} = \left[R_{Type\ I}\right] \times \left[R_{Type\ II}\right] \times \left[R_{Type\ III}\right]$$

$$R_{insulation} = \left[R_{Type\ I}\right] \times \left[R_{Type\ II}\right] \times \left[R_{Type\ III}\right]$$

$$R_S = \left[0.9^{6}755\right]^2 \times \left[0.9^{9}585\right]^9 \times \left[0.9^{3}895\right] \times \left[0.9^{2}466\right]$$

$$\times \left[0.9^{4}774\right] \times \left[1.0\right]$$

$$R_S = 0.9943$$

Detailed calculations are presented in Volume 2, Section 3.8.10.

5.4.6 Weight Breakdown

Table 5-11 presents a summary of the weights for the various components of the temperature control subsystem. The weight for the temperature control subsystem components attributed to the equipment module is 177.3 pounds. This weight accounts for:

- Crinkled aluminized Mylar insulation (70 layers of 1/4 mil Mylar aluminized on one side with 3-mil Mylar aluminized on one side face sheets) covering on the outside and top of equipment module
- Attachments for insulation
- Louver assemblies which include blades, bimetallic actuators, enclosure, and attachment
- Heaters and thermostats

The weight for the temperature control subsystem attributed to the propulsion module is 61.2 pounds. This weight accounts for:

- Crinkled aluminized Mylar insulation (70 layers of aluminized on one side with 3-mil Mylar aluminized on one side face sheets) covering the base of the propulsion module
- Attachments for insulation
- High temperature Refrasil insulation

The total weight for the temperature control subsystem is 238.5 pounds. The weight associated with low-thermal-conductivity structural joints is attributed to the structure subsystem.

Table 5-11. Thermal Control System Weight Breakdown Recommended Configuration

Item	Weight (lb.)	
Equipment Module		177.3 lbs
Insulation	127.6	
Louvers	36.3	
Heaters and thermostats	4.0	
Attachments and miscellaneous	9.4	
Propulsion Module		61.2 lbs
Insulation, base panel	31.9	
Insulation, engine	29.3	
Total Thermal Control Subsystem		238.5 lbs

APPENDIX A

PROPELLANT SETTLING TIME AS A FUNCTION OF PROPELLANT TANK ACCELERATIONS

1. ANALYSIS

Consider the Voyager propellant tank in a zero-gravity environment with the propellant positioned initially at the opposite end of the tank from the propellant drain as shown in Figure A-1. If a constant thrust is applied, experimental results (Reference 2) indicate that for fluids having contact angles near 1 degree (as in the case for N_2H_4, Aerozine-50, and N_2O_4) the acceleration level required to destabilize the liquid-vapor interface and settle the propellant is obtained from the conditions that the Bond Number, B_o be greater than 0.83, i.e.,

$$B_o = \alpha g \, r^2 \, \frac{\rho}{\sigma} > 0.83$$

where α g is the applied acceleration, r the tank radius, ρ the density of the fluid, and σ the liquid surface tension.

In addition, the experiments of Reference 3 have established that the manner in which the liquid is settled (Figure A-2) is dependent upon the magnitude of the Weber number, W_e. W_e is defined as

$$W_e = V_L^2 \, r_o \, \frac{\rho}{\sigma}$$

where V_L is the velocity of the liquid sheet running down the tank wall at the tank drain as indicated in Figure A-2. More specifically, there are three distinct Weber number regions and associated settling mechanisms.

For a $W_e < 4.0$ there will be no geysering with the propellant sheets meeting at the tank bottom and the resulting ullage bubble

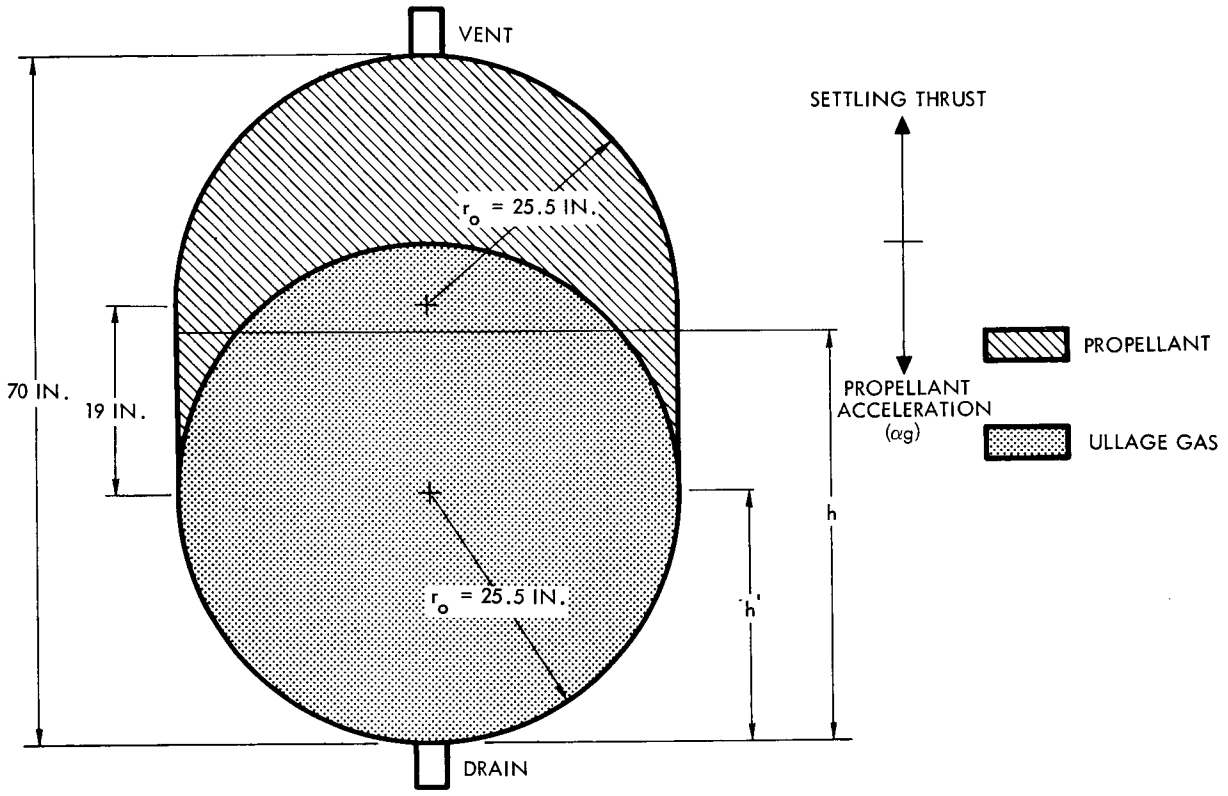

Figure A-1. Assumed Initial Tank Configuration

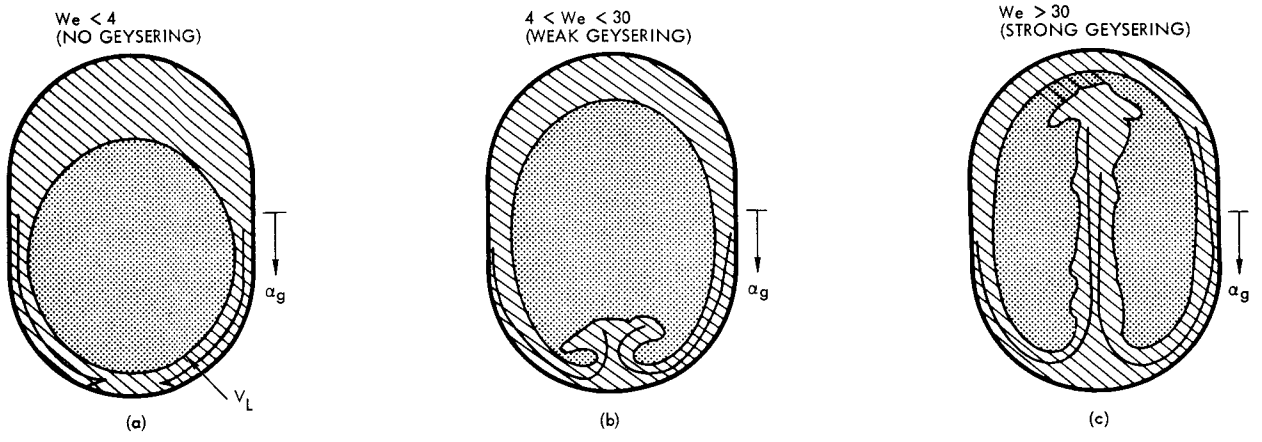

Figure A-2. Possible Flow Regimes

formed moving up the tank with a constant velocity given by

$$V_o = 0.48\ (\alpha g\ r_o)^{1/2}\ \left[1 - \left(\frac{.84}{B_o}\right)^{B_o/4.7}\right] \qquad (1)$$

This is illustrated in Figure A-2a.

In the region defined by $4 < W_e < 30$ there will be a very complicated mechanism of a weak geyser formation, growth and decay the exact nature of which is highly nonlinear and experimentally unobservable due to the long growth time of the geyser and the limited time available in drop tower tests (Reference 3, p. 15). This type of settling is shown in Figure A-2b.

For We > 30 there is strong geysering, the formation and growth of which, because of their short time scales, are observable in drop tower tests. The decay of such geysers was, however, not observable, again due to the short time available in drop tests. The observed geysers in this regime were found to proceed upward (Figure A-2c) against the impressed constant acceleration field with a velocity

$$V_g = K\ V_L \qquad (2)$$

where V_L is the velocity of the leading edge of the fluid as it reaches tank bottom, or

$$V_L = 2.76\ V_o \left(\frac{h'}{r_o}\right)^{1/2} \qquad (3)$$

with V_o defined in Equation (1) and h' equal to the height of the leading edge of the fluid above tank bottom when the acceleration field is initiated (see Figure A-1). The empirically determined constant K in Equation (2) varied from 1.9 to 2.9.

Based on the above experimental evidence it is possible to establish an approximate model for the settling problem in the Voyager spacecraft.

2. SETTLING MODEL

An acceleration level for each propellant volume to tank volume ratio and applied settling thrust was calculated using the relation

$$(\alpha g) = \frac{F}{W_T} = 386 \text{ in/sec}^2 \qquad (4)$$

where F is the applied settling thrust and W_T is the total weight of the accelerating vehicle. W_T as a function of the propellant to tank volume ratio (hereafter termed P_r) was obtained from Figure A-3.

The four levels of applied settling thrust used were 6, 12, 400, and 1050 pounds. Using the accelerations so obtained, lower bounds for the Bond and Weber numbers for each fluid were calculated in order that the flow regime could be determined. The accelerations used for this purpose were the lowest encountered, i.e., that determined by Equation (4) for a thrust level of 6 pounds and a $P_r = 0.9$. The results are:

$$B_o)_{N_2O_4} = 42.8 \qquad W_e)_{N_2O_4} = 37.4$$

$$B_o)_{N_2H_4} = 11.3 \qquad W_e)_{N_2H_4} = 9.7$$

$$B_o)_{A\text{-}50} = 23.3 \qquad W_e)_{A\text{-}50} = 20.8$$

The B_o is certainly greater than 0.83, as expected, and even the lowest thrust is more than enough to initiate settling.

In fact, the critical acceleration to cause $B_o > .83$ and initiate settling is, for the three fluids of concern

$$\alpha g)_{cr}]_{N_2O_4} = \frac{0.83}{(25.5)^2\ 0.866} = 1.47 \times 10^{-3} \text{ in/sec}^2 = 3.8 \times 10^{-6} g$$

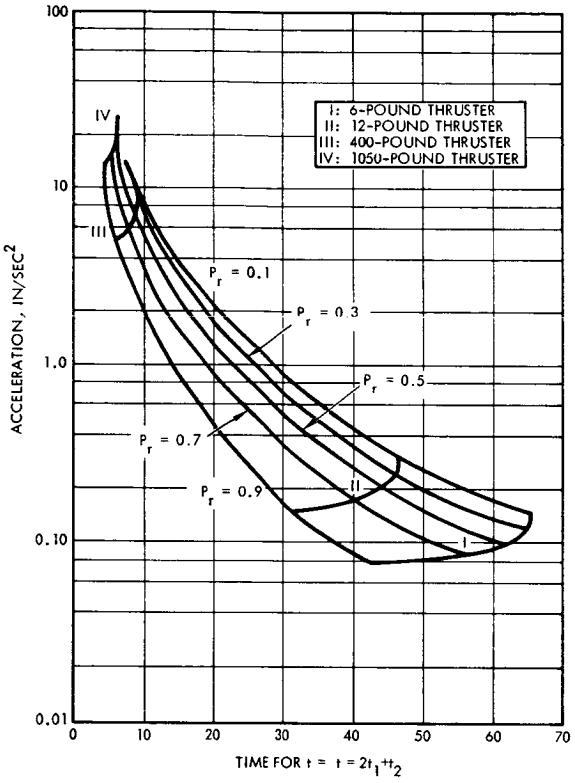

Figure A-3. Acceleration Versus Time for $t = 2t_1 + t_2$

$$\alpha g)_{cr}]_{N_2H_4} = \frac{0.83}{(25.5)^2\ 0.222} = 5.75 \times 10^{-3}\ \text{in/sec}^2 = 14.9 \times 10^{-6}\text{g}$$

$$\alpha g)_{cr}]_{A\text{-}50} = \frac{0.83}{(25.5)^2\ 0.48} = 2.66 \times 10^{-3}\ \text{in/sec}^2 = 6.9 \times 10^{-6}\text{g}$$

or two orders of magnitude less than the minimum acceleration of 2.02×10^{-4}g occurring here.

3. RESULTS

In the derivation of such a criterion some degree of approximation and engineering judgement is necessary, due to the lack of knowledge of the complicated process of geyser decay in the strong geysering regime

(We > 30). In view of this limitation, it is proposed that the processes a propellant undergoes before it may be considered fully settled for ullage-free starts are:

- A flow in the form of a cylindrical sheet down the tank walls
- A violent closing of this sheet on the bottom and the subsequent formation of a geyser traveling up to the height at which the fluid was initially
- A recirculating flow in a cylindrical sheet down the tank walls again
- A quiet closing of this sheet on the tank bottom with no geyser forming and the ullage bubble so formed moving up as the rest of the fluid drains down the walls to the bottom
- The rise of entrained ullage gas bubbles away from the tank drain.

Duration times required for each of these processes at each level of applied thrust (6, 12, 400 and 1050 pounds) and spacecraft weight (acceleration) will be calculated. Specifically, the times for each process are:

Process 1:

$$t_1 = \left[\frac{2h}{a_L}\right]^{1/2} \tag{5}$$

where:

$$a_L = 0.88(\alpha g)\left[1 - \left(\frac{.84}{B_o}\right)^{B_o/4.7}\right]^2$$

which, for $B_o < 12$ simplifies to

$$a_L = 0.88(\alpha g)$$

from Equation (1), for Bo > 12,

$$(\alpha g) = \frac{V_o^2}{r_o(0.48)^2}$$

so

$$t_1 = \frac{3.66\ h^{1/2}}{V_o} \tag{6}$$

where h is the height, the leading edge of the cylindrical wall sheet has to fall to the tank bottom and calculated as a function of P_r by (conservatively) assuming a flat fluid free surface (Figure A-1).

Process 2: Experiments of Reference 3 have shown that the geyser moves up with constant velocity [Equation (2)]

$$V_g = KV_L$$

with $V_L = 2.76\ V_o\ (\frac{h}{r_o})^{1/2}$ and an average value of $K = 2.4$ this becomes

$$V_g = 6.6\ V_o\ (\frac{h}{r_o})^{1/2}$$

$$\text{so} \qquad t_2 = \frac{h}{V_g} = 0.765\ \frac{h^{1/2}}{V_o} \tag{7}$$

Process 3: Same as Process 1:

$$t_3 = t_1 = 3.66 \cdot \frac{h^{1/2}}{V_o} \tag{8}$$

Process 4: The time used here is the time for the bottom surface of the bubble to rise to a height above the tank bottom corresponding to a volume of 25 percent of the propellant present in the tank or

$$t_4 = \frac{h''}{V_o} \tag{9}$$

where, for the purpose of determining h'' the free surface of the propellant is assumed flat as in Process 1.

The presentation of the acceleration - duration time results will be in two parts. The first graph, Figure A-3, defines the duration time as

$$t)_{\text{Figure A-3}} = t_1 + t_2 + t_3$$

This was done because it was felt that defining t_3 as the time to flow down the tank wall and not as the time for free fall was in itself conservative (as flow with drag down the tank walls will certainly take longer than a free fall). The photographs at the end of the drop tests in Reference 3 show the elongated geyser standing along the tank centerline. Since it is probable that without a side thrust the geyser will simply collapse against the tank bottom in free fall without touching the tank walls, using the time for process 3 instead of a free fall is definitely conservative.

In Figure A-4 the duration time is defined as

$$t)_{\text{Figure A-4}} = t_1 + t_2 + t_3 + t_4$$

and is probably overly conservative.

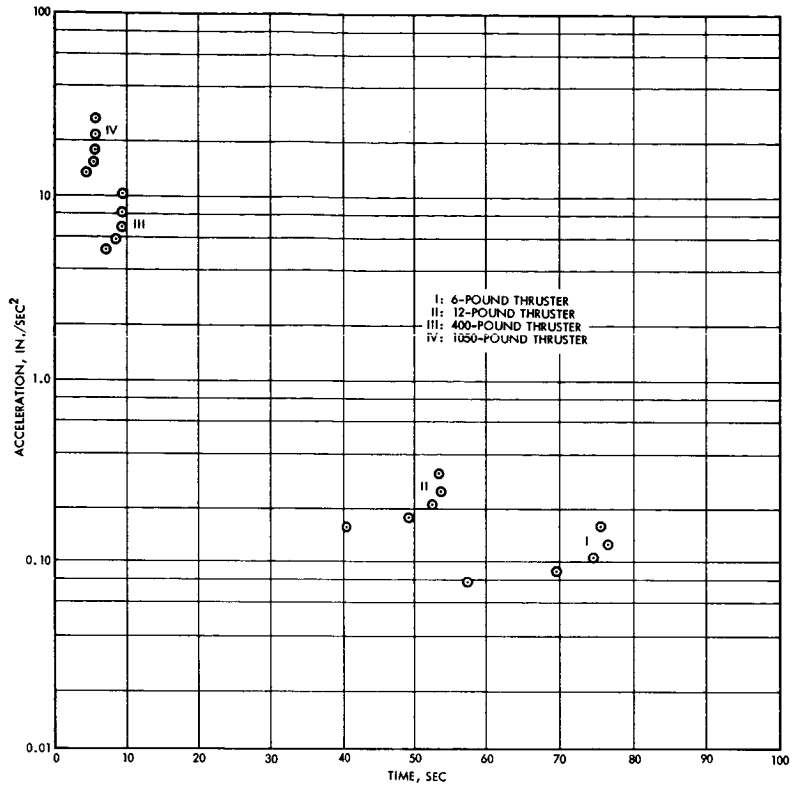

Figure A-4. Acceleration Versus Duration Time for $t = 2t_1 + t_2 + t_4$

4. REFERENCES

1) T. E. Bowman, "Liquid Settling in Large Tanks," Symposium on Fluid Mechanics and Heat Transfer Under Low Gravitational Conditions." Lockheed Research Laboratories, June 1965.

2) M. P. Hollister and H. M. Satterlee, "Low-Gravity Liquid Reorientation," Symposium on Fluid Mechanics and Heat Transfer Under Low Gravitational Conditions, Lockheed Research Laboratories, June 1965.

3) J. A. Salzman and W. J. Masica, "Experimental Investigation of Liquid-Propellant Reorientation." NASATN D-3780, Lewis Research Center, January 1967.

APPENDIX B

NET TRANSPORT OF PROPELLANT ACROSS A SCREEN DUE TO A TEMPERATURE GRADIENT

On the Voyager spacecraft it is likely that one end of the propellant tank will be at a different temperature than the other end. If the end opposite the propellant acquisition screen is the colder then it may be possible for propellant to migrate across the screen. Propellant vapor could evaporate off the wetted surface of the screen, migrate scross the tank by convection and condense on the colder end. After sufficient time all of the propellant trapped by the screen would be gone and starting the engine would be impossible. This is a serious question concerning the feasibility of using screens for propellant acquisition.

Figure B-1 shows an idealized sketch of a Voyager propellant tank. In the figure, T_1 is the temperature of the sun end, T_2 that at the liquid-vapor interface, T_3 at the cold end and $T_1 > T_2 > T_3$. It has been postulated that due to the temperature gradient existing in the tank, liquid might be transferred to the cold end by the following mechanism. The heat being conducted through the liquid from warm end to liquid-vapor interface evaporates liquid at the interface. The vapor formed as well as the pressurant gas there have a temperature equal to T_2 and the corresponding pressure. Since $T_2 > T_3$, this pressure will be higher than the pressure at the cold end causing the mass flow of vapor by convection to the cold end where the vapor will be condensed. Thus, after the passage of some time, depending upon the heat rate and the initial position of the ullage, the relative position of liquid and vapor within the tank will be as shown in Figure B-2. Obviously, if this process continued long enough it would result in all liquid on the cold end of the tank, the screen end containing only pressurant gas and vapor. This model is one concept of what might occur within the tank. It is based on the assumption that the presence of a temperature gradient within the tank implies the existence of a pressure gradient giving rise to convective flow of propellant from the hot to the cold end of the tank.

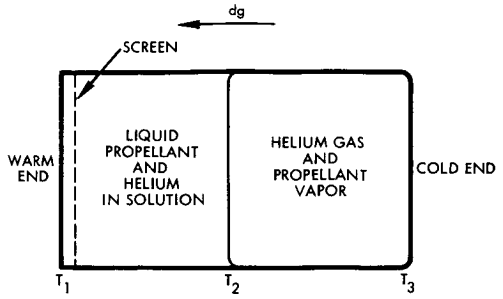

Figure B-1. Voyager Propellant Tank

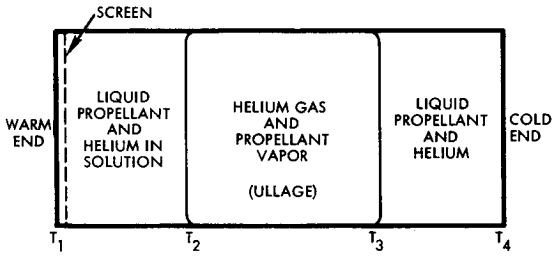

Figure B-2. Relative Positition of Liquid and Vapor Within Tank

A closed system is in thermodynamic equilibrium when both the pressure and the temperature are constant. However, as is well known, the existence of a temperature gradient does not necessarily imply the existence of a pressure gradient. There exists a certain threshold value of the temperature gradient which must be exceeded before the onset of convection. This threshold value of the temperature gradient depends on the physical parameters of the fluid and the gravity field present. In other words, states of partial thermodynamic equilibrium where a temperature gradient exists but the total system pressure is constant are possible.

The problem of the onset of convection in a fluid with a fixed temperature gradient in a gravity field has been extensively studied beginning with the work of Rayleigh in 1916. The results indicate that there will be no convection provided the product of the Grashof and Prandtl numbers are less than about 1100 for a fluid with a free surface, about 1710 for a fluid fixed between two parallel planes. That is, for thermal conduction without convection

$$GP = \frac{\beta \alpha g \ell^3 (T_1 - T_2)}{\nu x} < 1100 \qquad (1)$$

where G denotes the Grashof number, P the Prandtl number, and

β = coefficient of thermal expansion

αg = acceleration level

ℓ = length between two surfaces whose temperatures are T_2 and T_1

ν = kinematic viscosity = $\frac{\text{dynamic viscosity}}{\text{density}} = \frac{4}{\rho}$

x = thermal diffusivity = $\frac{\text{thermal conductivity}}{(\text{density})(\text{specific heat})} = \frac{k}{\rho c_p}$

and we have used the most conservative value of the product GP.

For liquid N_2O_4 the value of the product νx is 1.36×10^{-6} cm^4/sec^2 at 77^oF. The value of $\beta = 1/\rho \; \partial \rho / \partial T$, where ρ is the density and T is the temperature is not available in the literature, but for most liquids it is about $10^{-3}/^oK$. Thus, for liquid N_2O_4 there will be convection when

$$T_1 - T_2 > \frac{1.1 \times 10^3}{\beta \alpha g \ell^3} \nu x \qquad (2)$$

Using the value of the product νx given above, $g = 980$ cm/sec^2, $\beta = 10^{-3}/^oK$ gives, if $\alpha = 10^{-9}$

$$T_1 - T_2 > \frac{1.5 \times 10^6}{\ell^3} \; ^oK$$

Obviously, the temperature difference across the N_2O_4 to induce convection is a very sensitive function of ℓ the length through the liquid phase in the direction of the temperature gradient. If ℓ is as small as 10 cm, a rather large temperature difference is required to induce convection, whereas if the length ℓ is about a meter, convection will begin when $T_1 - T_2$ is of the order of $1^{o}K$.

ℓ	$T_1 - T_2$
10 cm	$1.5 \times 10^{3}\ ^{o}K$
100 cm	$1.5^{o}K$

For the ullage which is assumed to have the properties of Helium gas (it is a mixture of N_2O_4 vapor and Helium, but the concentration of N_2O_4 is small when the system temperature is not near the boiling point), the value of νx is $4.56 \times 10^{-2}\ cm^4/sec^2$. For an ideal gas the coefficient of thermal expansion is equal to $1/T$ where T is the temperature in ^{o}K. Thus, for Helium we find for the onset of convection for the same acceleration level (10^{-9} g)

$$T_2 - T_3 > \frac{1.1\,(4.56 \times 10^{-2})}{(3.33 \times 10^{-3})\ 0.98 \times 10^{-9}\ \ell^3} = 4.0 \times \frac{10^9}{\ell^3}$$

Clearly, in the gas phase convection is much more unlikely

ℓ	$T_2 - T_3$
10 cm	14.0×10^{6}
100 cm	14.0×10^{3}

From the above values of $T_2 - T_3$ required for the onset of convection we see that convection in the gas phase is extremely unlikely with the temperature gradients to be expected in the Voyager propellant tanks. On the other hand, convection within the liquid phase seems very probable.

It should be pointed out that the criteria being used for the onset of convection is based on a theoretical model which assumes one fluid with a free surface. The situation within the Voyager propellant tank only loosely agrees with the model since we have gas over liquid or possibly liquid over gas. It is likely that the presence of convection within the liquid would have the effect of inducing convection within the gas phase at least in the vicinity of the gas-liquid interface. However, the conditions in the gas are so far removed from the critical (unstable) condition that convection should not exist throughout the entire body of the gas. In other words, any small motion induced in the gas phase by the convection motion of the liquid could exist only near the liquid-gas boundary.

We conclude therefore that since convective motion of the pressurant gas is very unlikely, mass transfer of the vaporized propellant through the pressurant gas cannot occur by temperature gradient induced convection. In other words, a state of constant pressure in the pressurant gas is possible in the presence of quite large temperature gradients there. If there was a pressure gradient in the ullage, it would not persist since so long as the temperature difference $T_2 - T_3$ is less than the critical value the motion would die out in time.

With a constant pressure in the ullage space any N_2O_4 vapor transport from the hot to the cold end of the tank must be by molecular or diffusive transport at constant total pressure. By solving the one dimensional diffusion equation for the transport of N_2O_4 vapor through Helium gas we find that the rate of transport by diffusion is

$$\frac{\text{gms}}{\text{cm}^2\ \text{sec}} \quad \frac{D\mu}{RT} \frac{\Delta p}{\ell} = W$$

where D is the diffusion coefficient for the transport of N_2O_4 vapor through Helium gas, μ is the molecular weight, R the gas constant and T the absolute temperature. The quantity Δp is the difference between the vapor pressure of N_2O_4 at the temperature T_2 and that at T_3 and ℓ is the distance across the ullage. For a $\Delta T = T_2 - T_3$ of $10^{\circ}F$ around $40^{\circ}F$, Δp is about 0.204 atmospheres. The molecular weight of N_2O_4 is 92, the gas constant 82.05 $cm^3 atm/^{\circ}K$ gm-mole. The diffusion coefficients are not known, but for gaseous diffusion they are of the order of 1.0 cm^2/sec. Using a value of ℓ of about 10 inches we find for the order of magnitude of the mass transported in this manner a value of 4.00×10^{-5} $gms/cm^2 sec$. Using the maximum cross-sectional area which would be available for 59 inch diameter spherical tanks, this rate would be

$$4.0 \times 10^{-5} \frac{gms}{cm^2\ sec}\ 7.07 \times 10^4\ cm^2 = 2.8 \frac{gms}{sec}$$

or about 528 lb/day. Clearly, if this type of situation were to exist in the tank, large quantities of N_2O_4 could be transported from the warm to the cold end during the course of an 180-day mission. However, there must be heat available to evaporate and condense the propellant. For N_2O_4 the heat of vaporization is 178 Btu/lb. For the above numbers to hold a net heat flux through the tank of 22 lb/hr x 178 Btu/lb = 3,900 Btu/hr.

For the steady state, near-earth conditions the estimated heat loads on the tank are 6.4 Btu/hr-ft^2 on the top, 10 Btu/hr-ft^2 on the bottom, this total amount being gained by radiation and lost by conduction through supports and the tank ends. The maximum net heat flux going through the tank from bottom to top would be 3.6 Btu/hr-ft^2 or about 450 Btu/hr through the entire tank. The mass flow rate under these conditions would be no more than 2.53 lb/hr or 60 lb/day.

It should be pointed out that our calculations have considered an idealized tank model and worst conditions. In actual practice none of these circumstances is likely to apply.

We can summarize the results of the above order of magnitude calculations as follows. If a situation arises where the body of the ullage separates two bodies of propellant, a considerable transfer of mass from the warmer to the cooler body of liquid would take place by molecular diffusion of propellant vapor through pressurant gas. This rate is limited by the availability of heat to vaporize and condense the propellant. On the other hand, if there is a liquid path surrounding the ullage, free convection in the liquid is almost certain to occur. This would have the effect of reducing temperature and concentration gradients and thus eliminating mass transport of propellant due to diffusion through the pressurant.

The most critical period for this is of course the long coast phase following midcourse correction. During this period the tanks are nearly full of liquid and the heat flow is from bottom to top end of the tank. Initially, a spherical Voyager tank could have all the ullage in the cold end of the tank as shown in Figure B-3. A transfer of mass could occur by diffusion wetting the upper surface with condensate as shown in the figure. The fact that free convection will exist in the liquid now means that the great majority of the heat will be transferred from the warm end to the top end by free convection. This process will lead to a reduction in temperature gradients and concentration gradients throughout the entire tank. It therefore seems likely that the process of transporting liquid to the cold end will be definitely limited, the system approaching a final equilibrium configuration with the ullage removed from the tank cold wall.

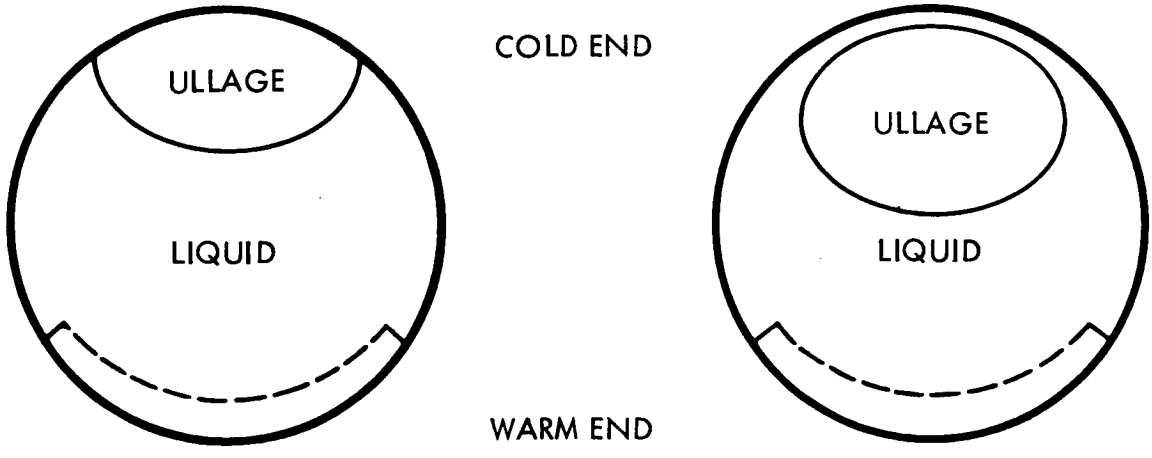

Figure B-3. Ullage in Voyager Tank

APPENDIX C

FRACTURE OF VOYAGER PROPELLANT TANKS BY METEOROID IMPACT

The mode of failure envisioned was catastrophic rupture caused by a crack that originated at the point of impact of a meteoroid and, driven by the pressure stress in the tank, propagated so extensively that it caused fragments of the tank or the adjoining spacecraft structure to fly off and possibly impact on Mars. The basic question was: what reduction in the probability of this event could be had by reducing the pressure in the tank when it wasn't needed?

The probability of suffering cracks several inches long if the tank is punctured by a meteoroid is reduced by a factor of 3 to 5 by lowering the stress. On the other hand, if the tank pressure is nearly zero, there is a possibility that crack arrest will occur when the overpressure caused by the impact is attenuated, and this possibility can be analyzed by the techniques of fracture mechanics.

The probability of rupture varies with meteoroid mass, and reaches a maximum at about 0.001 grams. Larger ones occur less frequently, and smaller ones have insufficient kinetic energy to create the impact overpressure after puncturing the tank wall. Assuming a mission time of 15 months and an exposed tank area of 10 square meters, the probability of encounter with a one milligram meteoroid is about 1 chance in 100

The accuracy of these estimates can best be judged by listing the four physical phenomena that must be analyzed in this problem. One is the frequency of occurrence of meteoroids and their mass, density, and velocity. Another is the severity of the fracture origin that they produce in the tank wall. Still another is the severity and duration of the shock pressure induced in the liquid by the penetration of the meteoroid. Finally, there is the fracture toughness of the material, its ability to resist crack initiation and propagation under these conditions.

The foregoing analysis applies to unshielded tanks. No analysis of the effects of shielding is given, except for the following cautionary note. Experiments have shown that a little shielding (or insulation) may be worse than none, for two reasons. Instead of a clean puncture, the tank wall may suffer cracking and extensive damage from impact by the fragments of the meteoroid and shield, i.e., a more severe fracture origin may be produced. Also, such fragmentation may cause the kinetic energy of the meteoroid to be converted to the pressure shock wave in a more efficient and devastating fashion. This phenomenon is probably the least understood of all.

1. EFFECT OF TANK PRESSURE

Puncture of a liquid-filled tank by a meteoroid has a two-fold influence on the tendency to rupture. The puncture and the damaged metal surrounding it constitute a fairly severe potential fracture origin. But also, the stress in the tank wall is raised, locally, by an expanding bulb of pressure in the liquid that results from conversion of the residual kinetic energy of the meteoroid (after puncturing the tank wall) into compression of the liquid. A hemispherical shock wave is formed, centered on the point of impact. Shock front pressures, measured in simulated meteoroid impacts, typically are of the order of 100,000 psi at a distance of 1 inch from the puncture. The shock front pressure diminishes rapidly as it expands, but it may exist long enough and be of such magnitude as to produce a local outward bulge of the tank wall and to initiate cracks radiating from the puncture.

Some test data by Ferguson (Reference 2) provide direct evidence of the influence of the pre-existing tank pressure on the tendency to rupture. He tested both 2219-T87 aluminum alloy and Ti-5Al-2.5Sn titanium alloy spherical test panels pressurized by liquid hydrogen and impacted by small aluminum spheres ranging in diameter from 0.063 to 0.250 inch. Only one projectile velocity was used, 21,600 ft/sec, which is about one-fifth the typical meteoroid velocity.

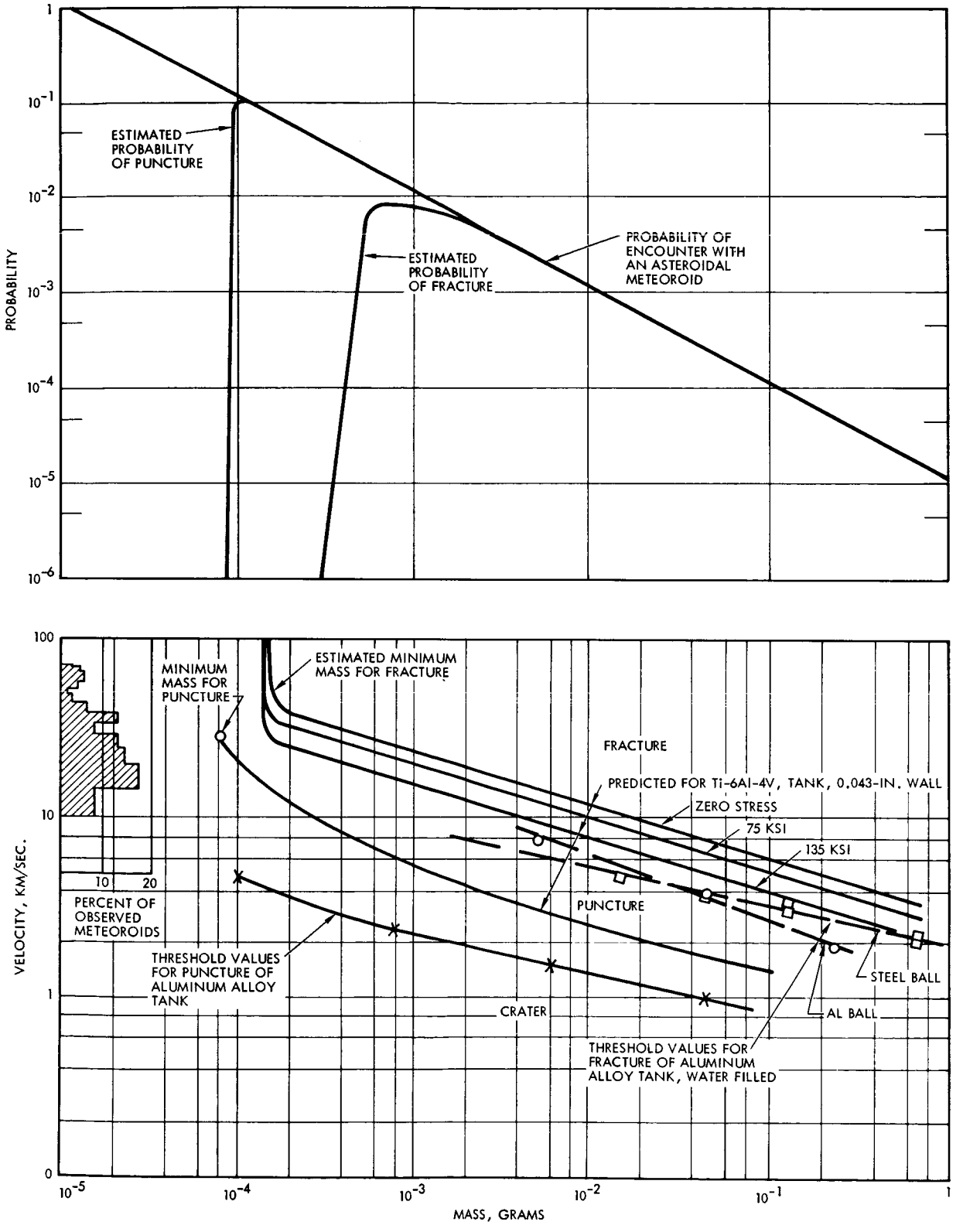

Figure C-1. Effect of Meteoroid Mass and Velocity on the Probability of Fracture of Liquid Filled Ti-6Al-4V Tanks

From Ferguson's correlation of his results, threshold values of projectile mass (those needed to barely cause fracture) corresponding to three stress levels in the tank wall were calculated. Also, from the NASA criteria document (Reference 3) the relative frequency of meteoroids of mass equal to or exceeding these threshold values were calculated. While Ferguson's test conditions do not simulate ours exactly, it is believed that the trends which he found will be true for our case also.

Pressure Stress, ksi	Relative Mass	Relative Frequency	
		Asteroidal	Cometary
135	1.00	1.00	1.00
75	2.30	0.44	0.32
40	3.00	0.33	0.18
0	3.78	0.26	0.16

Summarizing the evidence in the table, it shows that a reduction of the preexisting hoop stress from 135 to 40 ksi reduces the expected frequency of fracture-causing meteoroid impacts by a factor of three for asteroidal meteoroids and by a factor of about five for cometary meteoroids. Further reduction in stress would produce less benefit than the first two reduction steps. The reason for this is the very significant addition to the membrane stress, caused by the shock pressure itself.

2. EFFECTS OF METEOROID MASS AND VELOCITY

To consider this problem in terms of absolute values of meteoroid mass and velocity and of the projectile mass and velocity used in test, both kinds of data are plotted in Figure C-1. The data points which define the threshold values for fracture were taken from Reference 4. Both projectile mass and velocity were varied as shown. The tank wall was a 0.031 inch thick flat sheet of 7075-T6 aluminum, which contained water at atmospheric pressure. The data do not quite fit the inverse square root relationship that results from assuming that fracture is governed by the kinetic energy of the projectile. Small ones tend to cause fracture more readily than predicted, possibly because their energy is converted to shock pressure in the fluid more efficiently than for large projectiles.

To correct for differences in material, and wall thickness, and to apply the test results to our tank, reference is made to Ferguson's analysis of his data, which may be summarized in his Equation 6-17

$$\frac{\sigma_H}{\sigma_u} = 1 - 0.180\, R_1^{2.25}$$

$$R_1 = \frac{(K.E.)^{0.5}\, E_b\, (R_o)^{0.25}}{(K_C)^{1.5}\, t_s}$$

$\frac{\sigma_H}{\sigma_u}$ = the ratio of hoop stress caused by the pre-impact tank pressure to ultimate strength.

K.E. = kinetic energy, in-lb

E_b = bulk modulus of fluid, psi

R_o = characteristic length of projectile - taken as a constant, 0.110 inches

K_C = plane stress fracture toughness of the tank material, psi sq. in.

t_s = wall thickness of tank, in.

The expression does not correlate Morse's data with Ferguson's very well. The probable reason is the fact that "E_b" for liquid hydrogen is 20 times that for water, which requires more precision in the treatment of this term than Ferguson was able to achieve from comparison with results in liquid nitrogen, which is one-sixth as compressible as LH_2. Nevertheless, the formula contains terms that enable us to apply Morse's test results to our tank. Their validity needs checking, however. Fracture toughness, K_C, for 7075-T6 is about 40 ksi sq. in. (6), compared to an estimated minimum value of 70 ksi sq. in. for Ti-6Al-4V. Changing from 0.031 in. thick 7075-T6 aluminum to 0.043 inch thick

Ti-6Aℓ-4V increases the denominator of the expression for R_1 which means that an equivalent kinetic energy for fracture will be:

$$\frac{(K.E.)^{0.5}_{T_i}}{(K.E.)^{0.5}_{A_\ell}} = \left(\frac{70}{40}\right)^{1.5}\left(\frac{0.043}{0.031}\right) = 3.2$$

and

$$\frac{(mV^2)_{T_i}}{(mV^2)_{A_\ell}} = 10.2 \quad .$$

This result indicates that the threshold value of meteoroid mass for fracture is increased by a factor of 10 beyond that given by the data points.

The reductions in threshold mass when a pressure stress of 75 ksi or 135 ksi is present are also shown.

To complete the picture of the interaction of meteoroid mass and velocity, puncture data are also given in Figure C-1. The data points (from Reference 5) are for aluminum projectiles and 2024-T3 aluminum alloy targets. The data are given in terms of penetration relative to projectile diameter; but the latter is proportional to the cube root of mass and puncture was assumed to occur if penetration exceeded two-thirds of the thickness. The predicted curve for Ti-6Aℓ-4V was obtained by multiplying the meteoroid mass by the cube of the ratio of thicknesses and densities as follows

$$\frac{m_{(0.043\text{ in. Ti})}}{m_{(0.031\text{ in. A}\ell)}} = \left(\frac{0.043}{0.031}\right)^3 \times \left(\frac{0.16}{0.098}\right)^3 = 11.6$$

The end point of the puncture threshold curve at 30 km/sec. velocity was obtained from the NASA Criteria document (Reference 3), two paragraphs of which are reproduced for convenience:

"7. 1. 2. 3 Asteroidal Meteoroid Flux Model (Nominal Flux) [VII-3]

$$\log F_{>} = -13.54 - \log m$$

where $F_{>}$ is the number of impacts per unshielded square meter per second of particles with mass in grams exceeding m, the mass of an asteroidal particle.

$$\text{Meteoroid density} = 3.4 \text{ g/cm}^2 .$$

7. 1. 2. 3. 1 Asteroidal Meteoroid Puncture Flux Model [VII-3]

$$\log \phi = -12.95 - (54/19)(k_t + \log p)$$

where ϕ is the mean number of punctures per unshielded square meter per second, and the material parameter, k_t, is

$$k_t = -1.360 + \log \left(\epsilon_t^{1/18} \rho_t^{5/6} C_t^{2/3} \right)$$

with ϵ_t the ductility (relative elongation), ρ_t the specific gravity, C_t the sonic velocity (km/sec), and p the material thickness in cm."

By setting "F" equal to "ϕ", one finds the threshold mass to cause puncture at the average meteoroid velocity, 30 km/sec. Substituting $\epsilon_t = 0.08$, $\rho_t = 4.47$ and $C_t = 6.1$ km/sec. and p = 0.043 in. = 0.109 cm, the threshold value of m is found to be 8.2×10^{-5} grams. This mass corresponds to an aluminum sphere 0.013 inch diameter. Its kinetic energy is 27 ft-lb.

The lower limit of threshold mass to cause fracture can now be estimated -- at least, it must exceed 27 ft-lb. In Reference 3 the plot of threshold kinetic energy versus projectile diameter yields an extrapolated value of 50 foot lbs. for a sphere 0.013 inch in diameter. On these bases, the curve for threshold fracture in the presence of zero stress is given a vertical asymptote at a mass of twice the threshold mass for puncture.

Meteoroid frequency data are superimposed on the mode of failure data in Figure C-1. Only the asteroidal type are shown, for reason of simplicity and greater frequency. The expression from paragraph 7.1.2.3 of Reference 3 was used to compute the frequency of encounter, assuming an exposed area of 10 square meters and a time of 15 months (3.89×10^7 sec). Meteoroid velocity data were obtained from Reference 7.

Combining the fracture data with the probability of encounter data, it is possible to estimate the probability of fracture during the mission as a function of meteoroid mass, as shown at the top of Figure C-1. At mass levels near 1 gram, and at meteoroid velocities (30 km/sec, average) the fracture data show that the probability of fracture is very nearly one, if such a meteoroid impacts the tank. Because there is a threshold mass to cause fracture, however, the probability must decrease suddenly as the meteoroid mass drops to near the estimated threshold value of 1.6×10^{-4} grams.

The conclusion to be read from Figure C-1 is that the maximum probability of fracture is that for encounter with meteoroids of mass equal to 0.001 gram approximately, and that this probability is of the order of 1 chance in 100. This conclusion is for an unpressurized tank made of Ti-6Al-4V with 0.043 inch wall, filled with liquid of compressibility comparable to that of water. See the next section for the definition of fracture, in this case. The probability of puncture is about 1 in 10, based on a similar line of reasoning.

3. POSSIBILITY OF CRACK ARREST

There is one mitigating circumstance that may point to a means to avoid catastrophic rupture. The shock velocity diminishes, after a few inches travel, to sonic velocity, which means that the stress enhancement of the meteoroid impact phenomenon extends, according to several investigators, only 4 or 5 inches at most from the puncture. This being true, crack arrest should occur if the tank pressure is low enough and if the fracture toughness of the material is high enough. There is some experimental evidence (Reference 2 and others) that this is true.

Fracture mechanics provides a tool to treat this case. Picture maximum crack advance, "a", of 4 inches, radially, in opposite directions from the puncture before the shock pressure dies out. The nominal stress level, "σ", below which the crack should arrest is given by the expression:

$$1.77\,\sigma\,\sqrt{a} = K_C \quad .$$

The "plane stress fracture toughness", K_C is treated as a material constant, although it is dependent on wall thickness as well as temperature. For these propellant tanks, operating at 50-90°F, K_C for Ti-6Al-4V at a strength level of 165-180 ksi should be at least 70 ksi $in.^{1/2}$ Substituting these values, we find that the pressure stress must be less than 20 ksi to insure that a crack will arrest after it has propagated 4 inches under the influence of the shock pressure.

Note that the crack will propagate further if the pressure stress is subsequently raised; hence, some means to avoid subsequent pressurization must be provided, in case there is evidence that the tank has been punctured under conditions that caused some cracking.

4. REFERENCES

1) R. A. Benson, "Suitability of Using Low Pressure in the Propellant Tanks", I. O. C. VVV-465, August 3, 1967

2) C. W. Ferguson, "Hypervelocity Impact Effects on Liquid Filled Tanks", NASA CR-54852, March 31, 1966, Contract NAS 3-4193.

3) R. E. Smith and O. H. Vaughan, Jr.; George C. Marshall Space Flight Center, Huntsville, "Space Environment Criteria Guidelines for use in Space Vehicle Development 1967 Revision", NASA TM X-53521, February 1, 1967.

4) C. R. Morse and F. S. Stepka, "Effect of Projectile Size and Material on Impact Fracture of Walls of Liquid-Filled Tanks," NASA TN D-3627, September 1966.

5) C. J. Maiden and A. R. McMillan, "An Investigation of the Protection Afforded a Spacecraft by a Thin Shield", AIAA Journal, Vol. 2, No. 11, November 1964, pp. 1992-8.

6) J.C. Newman, Jr., "Fracture of Cracked Plates Under Plane Stress", Presented at the National Symposium on Fracture Mechanics, Lehigh University, June 1967.

7) A. A. Ezra, "The Meteoroid Hazard and Hypervelocity Impact", Martin, Denver, Research Report R-65-6, June 1965.

APPENDIX D

LOW-THRUST ORBIT INSERTION AS A BACKUP MODE

1. INTRODUCTION

The performance of low thrust propulsion as a backup to the LMDE high thrust mode normally employed for insertion of the Voyager planetary vehicle into orbit about Mars has been examined for suitability. This examination is performance oriented, and does not address in detail any questions relating to the implied requirements on various subsystems and on sequencing and control, to implement the low thrust mode.

The primary criteria which should be applied to establish the suitability of a backup propulsion system are:

- Ability to achieve an orbit about Mars
- Simplicity of the implementation and mechanization of the backup system and its programming
- Observance of the quarantine constraint. This requires that the periapsis altitude of the achieved orbit be not too low, and that the probability of secondary failures or glitches which would lead to impact of Mars by the spacecraft be low enough.
- Confirmation that the backup system does indeed improve overall system reliability
- Minimization of spacecraft resources (weight, space, power, etc.) required.

While candidate low thrust systems sustain substantial gravity losses when used for orbit insertion, resulting in highly eccentric, long-period orbits, it is felt that attaining even such a degraded orbit will permit a useful mission to be accomplished (Reference 1). However, what constitutes a "satisfactory degraded orbit" is a matter for consideration. Even though orbital decay due to atmospheric drag indicates greater orbit lifetimes for more eccentric orbits of the same periapsis altitude, it is prudent to require an increased minimum periapsis altitude

in these cases, because perturbations of the orbit (such as solar gravitational and high pressure forces, gas leaks) cause greater variations — both random and predictable — in periapsis altitude when the eccentricity is high (Reference 2). Therefore, we have raised the minimum periapsis altitude from 500 kilometers (nominal orbits) (Reference 3) to 700 to 1000 kilometers (highly eccentric orbits). Similarly, the maximum apoapsis altitude of the degraded orbit should be limited to:

- Avoid causing unduly large fluctuations in periapsis altitude
- Avoid extremely high orbital periods which would limit the usefulness of orbital science
- Facilitate the accurate estimation of orbital parameters
- Achieve the above objectives over the expected range of off-nominal approach trajectories and execution errors.

Maximum apoapsis altitudes (h_a) have been set at 100,000 kilometers, or possibly 200,000 kilometers, for the degraded orbit.

Simplicity of implementation and mechanization requires that the attitude control system and the command and sequencing functions of the spacecraft be applicable to the backup propulsion system without introducing special complexity. Compatibility with propulsion module design, of course, means the backup system must use the same propellants, tankage, and pressurization system as the primary propulsion.

2. BACKUP ENGINES

As noted in Table D-1, which presents a matrix of the combinations studied, the backup engines considered for use in the event of failure of the LMDE to fire at high thrust are:

- Four bipropellant engines, each of 100 pounds thrust. (The C-1 engine is one example.) This engine has a very long operating life, exceeding the 7100 seconds which will exhaust the propellant supply available at orbit insertion. I_{sp} is of the order of 295 to 300 seconds.

Table D-1. Suitability of Backup Orbit Insertion Methods

Backup Engines	Steering Law (attitude)	Failure Detection					
		In Advance		At Time of Attempted Ignition			
				Backup Automatically		Backup by Ground Command	
		Capture?	h_p Great Enough?	Capture?	h_p Great Enough?	Capture?	h_p Great Enough?
Four 100-pound Thrusters	Fixed	Yes		[Yes*]		?	
	Constant Pitch Rate	Yes		[Yes*]		?	
	Tangential	[Yes]	?	[Yes]	[No]	?	No
	Other						
LMDE Low Thrust (1050 lb for 600 sec)	Any	[No]	–	[No]	–	[No]	–
LMDE Low Thrust (1050 lb for 600 sec) + Four 100-pound Thrusters	Fixed	Yes		Yes		?	
	Constant Pitch Rate	Yes		Yes		?	
	Tangential	Yes	?	Yes	?	?	?
	Other						

[Yes] ... Answer determined by analysis

Yes ... Answer by inference

*Illustrated in Figure D-2.

- The LMDE in the low-thrust (1050 pounds) mode. Because of a limited life of 600 seconds in this mode, (Reference 4) it cannot achieve capture, and cannot by itself serve as backup for orbit insertion. Since a failure in the high-thrust mode is likely (but not certain) to prevent low thrust operation, it is not a realistic backup candidate. I_{sp} = 285 seconds.*

- The LMDE in the low-thrust mode (1050 pounds for 600 seconds) together with four 100-pound thrusters. Basically, the 400-pound thrust is depended on to effect capture and the LMDE low-thrust propulsion, if operative, would serve to reduce the orbit size considerably below that obtainable with the 400 pounds thrust alone.

3. STEERING LAW

The normal orbit insertion propulsion mode (LMDE high-thrust — 7750 pounds**) has a short enough burn time that "gravity losses" are held below a negligible 5 meters/sec, even with the simplest steering implementation — fixed inertial attitude for the vehicle while firing. However, with low-thrust propulsion, losses will arise from the extended burn arc, and it is appropriate to examine additional steering laws. The ones which have been studied are (Table D-1):

- Fixed. The planetary vehicle is maintained in a fixed inertial attitude while firing. (θ_o)

- Constant Pitch Rate. The vehicle assumes an initial attitude (pitch angle θ_o) at the onset of firing, and rotates at a constant pitch rate ($\dot{\theta}$) while firing. (Actually, to maintain the thrust vector in the plane of the approach orbit, this rotation probably involves both pitch and yaw proportionally, measured in spacecraft body axes.)

- Tangential. The thrust vector is rotated so as to remain tangent to the planetocentric trajectory at all times while firing. This required a programmed, non-constant rotation rate in the orbit plane, again probably involving body pitch and yaw motion.

---

*In the recent propulsion system design review, the LMDE low-thrust mode was proposed at 1700 pounds thrust, I_{sp} = 295 seconds. The above conclusions should be reanalyzed to see if they are valid, if such alteration is adopted.

**Recently proposed to be raised to 9800 pounds.

- Other. More sophisticated steering laws can be envisioned, which will improve or optimize performance of the low-thrust propulsion system. None of these has been studied here.

As shown in Figure D-1 pitch orientation (θ) in this memorandum is measured from the tangent to the approach hyperbola at its periapsis to the thrust axis, positive upward. With this definition, the fixed attitude of the normal, high-thrust, orbit insertion is $\theta = 0$.

4. FAILURE DETECTION AND BACKUP INSTITUTION

Three classes are identified (Table D-1):

1) The failure of the LMDE to operate in the high-thrust mode is detected well before arrival at Mars. The orbit insertion maneuver now can be timed to start earlier than the nominal firing to minimize gravity losses. Conceivably, the approach aim point can be retargeted at the last midcourse correction maneuver to cater to the backup mode also.

2) The failure of the high-thrust propulsion mode is detected only at the time of attempted ignition. Two possibilities exist for instituting the backup operation:

   a) The backup operation is instituted automatically by the sequencer, upon failure detection.

   b) The backup operation is instituted by ground command. Because of round-trip communication times of 19 to 27 minutes, depending on arrival date, the backup propulsion performance efficiency is penalized by the delay in firing.

For class 1, analyses of backup mode suitability can vary the time of initiation of firing to optimize performance. For class 2a, we have assumed no delay in instituting the backup mode; that thrust is initiated at the same point at which high thrust would have begun if no failure occurred (Figure D-1). No explicit analyses were made for class 2b.

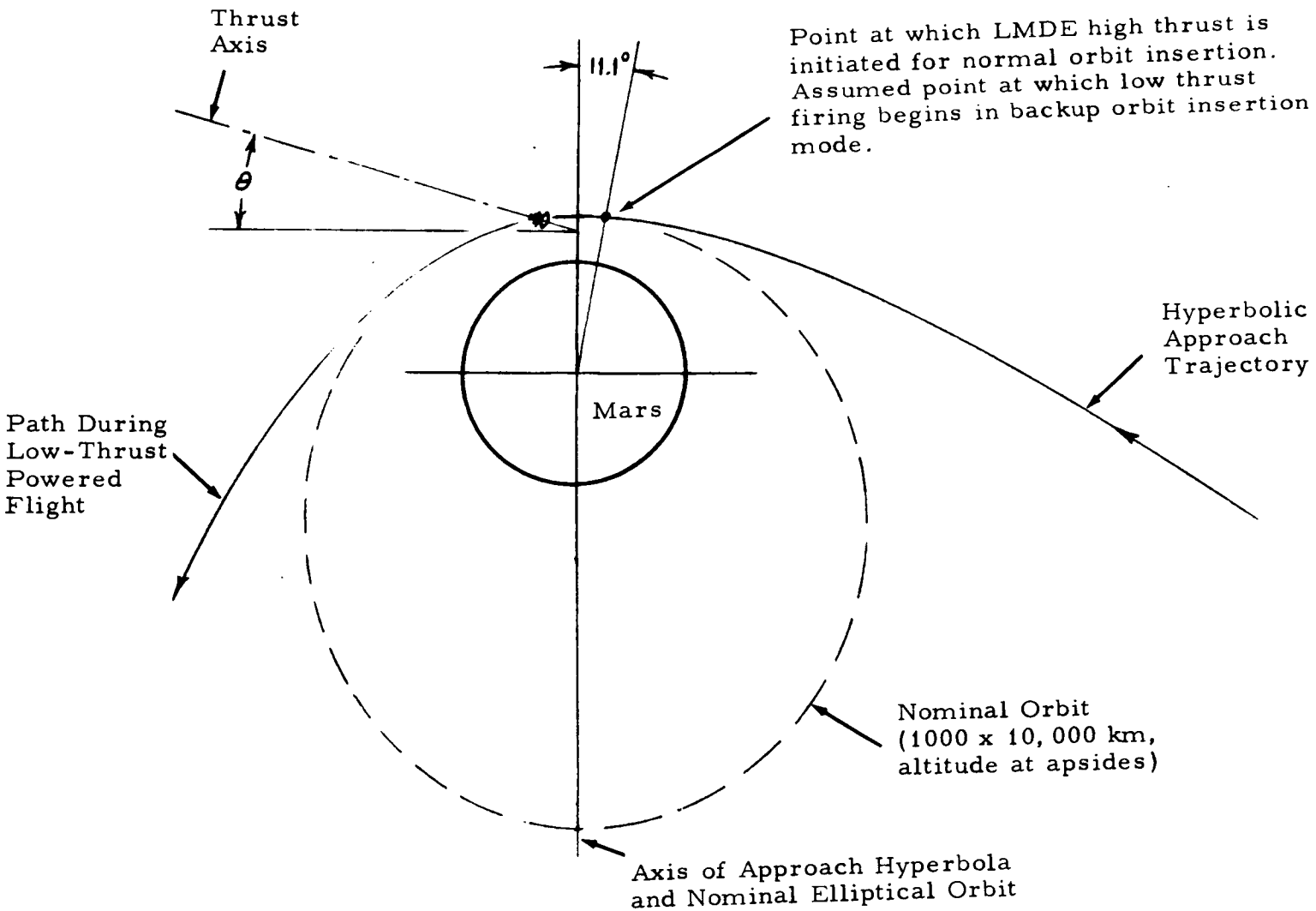

Figure D-1. Low-Thrust Insertion Into Orbit About Mars (Backup Mode)

5. CASES STUDIED AND RESULTS

Table D-1 presents a matrix of cases studied and qualitative results. All the performance analyses are based on the following mass allocations. The nominal mission allocates propellant for these velocity increments:

Maneuver	ΔV (meters/sec)	I_{sp} (sec)	Mass Ratio	Spacecraft Mass (lbs)
Interplanetary maneuvers	210	285	1.07825	21,500
Orbit insertion	1,760	305	1.80401	19,939.7
Orbit trim	150	285	1.05529	11,053.0
				10,473.9

For the backup mode it is assumed that the entire 1,560.3 pounds of propellant allocated to interplanetary maneuvers were expended for that purpose, so that at the time of initiation of the orbit insertion maneuver the planetary vehicle has a gross weight of 19,939.7 pounds, of which 9465.8 pounds is usable propellant. For the normal mode, 579.1 pounds of propellant is withheld from orbit insertion, and reserved for orbit trim maneuvers. However, for the backup mode, the entire 9465.8 pounds of propellant is considered available for use in the orbit insertion maneuver. Where the backup mode is at a 400-pound thrust level, I_{sp} was assumed to be 300 seconds.

It was also assumed that the asymptotic approach velocity of the planetary vehicle to Mars (a function of the launch and arrival dates) is 3.25 km/sec, the greatest permitted by the JPL Mission Specification, and that the approach trajectory (hyperbola) has a projected periapsis altitude of 1000 km.

Table D-1 indicates results according to two criteria: capture? (implying apoapsis altitude below 200,000 km); and h_p great enough? (implying periapsis altitude above 700 to 1000 km). For a tangential-thrust steering law, these questions are posed separately; both must be satisfied by a suitable backup system. For fixed-attitude and constant pitch rate steering laws, because one or two constants must be selected to specify the trajectory (θ_o, or θ_o and θ) a yes answer applies to both criteria, and implies that values of the constant(s) can be found so that both criteria are satisfied.

6. SOLUTIONS FOR 400-POUND THRUST (BACKUP INITIATED AUTOMATICALLY)

For a 400-pound thrust backup mode (instituted automatically, and a tangential steering law, the orbit resulting after depletion of propellant was found to have an apoapsis altitude of +57, 170 kilometer, and a periapsis altitude of -1583 km, leading to "yes" and "no" answers to the two criteria. (If thrust were terminated when capture was effected, these altitudes were found to be $+\infty$, +120 km, with periapsis radius still inadequate.) It can be shown that tangential retro-thrusting always reduces periapsis altitude, and, evidently, at the low, 400-pound thrust level, tangential thrusting reduces it too much for the resulting orbit to satisfy the planetary quarantine constraint.

Therefore investigation was directed to other steering laws which would approximate the efficiency of the tangential thrust in removing energy (i.e., reducing apoapsis altitude) but, by removing less angular momentum, would result in orbits with adequate periapsis altitude. The simplest family of these (from the standpoint of implementation requirements) is based on the constant-pitch-rate steering law, of which the fixed-attitude mode is a special case ($\dot{\theta} = 0$).

Figure D-2 displays the results of this investigation parametrically, showing both periapsis and apoapsis altitudes as functions of θ_o, the initial pitch angle, and $\dot{\theta}$, the pitch rate during firing. It is seen that it is possible to achieve the results

$$h_p \geq 1000 \text{ km}$$

$$h_a \leq 100{,}000 \text{ km}$$

over a broadband of choices of θ_o and $\dot{\theta}$. Notice that satisfactory (failure mode) orbits can be achieved with either

$$\begin{cases} \theta_o = 0 \\ \\ \dot{\theta} = -0.0034 \text{ deg/sec} \end{cases}$$

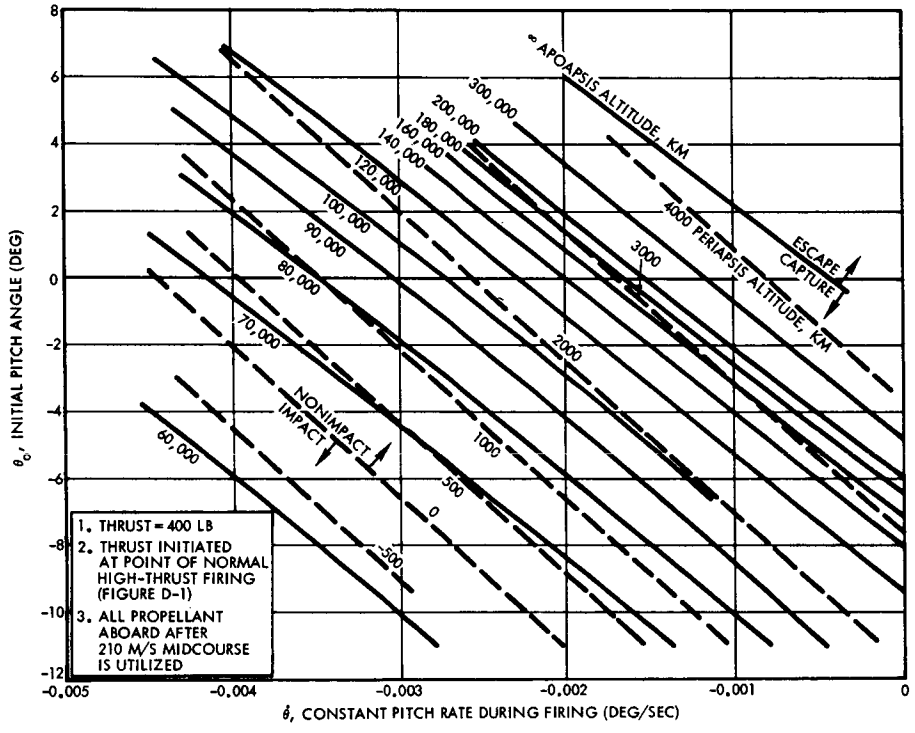
∞ APOAPSIS ALTITUDE, KM
300,000
200,000
180,000
160,000
140,000
120,000
100,000
90,000
80,000
70,000
60,000
4000 PERIAPSIS ALTITUDE, KM
3000
2000
1000
500
0
-500
ESCAPE
CAPTURE
NONIMPACT
IMPACT
1. THRUST = 400 LB
2. THRUST INITIATED AT POINT OF NORMAL HIGH-THRUST FIRING (FIGURE D-1)
3. ALL PROPELLANT ABOARD AFTER 210 M/S MIDCOURSE IS UTILIZED
θ_c, INITIAL PITCH ANGLE (DEG)
8
6
4
2
0
-2
-4
-6
-8
-10
-12
-0.005
-0.004
-0.003
-0.002
-0.001
0
$\dot{\theta}$, CONSTANT PITCH RATE DURING FIRING (DEG/SEC)

or

$$\begin{cases} \theta_o = -15 \text{ deg} \\ \dot{\theta} = 0. \end{cases}$$

The first of these corresponds to an initial attitude identical to that to which the planetary vehicle has been oriented for the intended high-thrust orbit insertion mode and therefore requires no immediate repositioning to initiate the backup. The second — deduced by extrapolating beyond the range of Figure D-2 — indicates that if the thrust axis is at once lowered 15 degrees, the backup firing could then be conducted in a fixed attitude until propellant depletion. (The 75 seconds required to achieve $\Delta\theta$ = -15 degrees, at the 0.2 deg/sec orientation rate, would not significantly affect this result.)

7. ORBIT PERIODS

The periods of the degraded orbits attained by the backup mode are very long compared with the desired 7- to 14-hour orbits. The period is given by

$$T = 0.5898(\alpha + \beta)^{3/2} \text{ hours,}$$

where

α = 1 + (apoapsis altitude)/3393 km

β = 1 + (periapsis altitude)/3393 km

For sample orbit sizes, periods are as follows

Periapsis Altitude (km)	Apoapsis Altitude (km)	Period (hr)
1,000	20,000	13.8
1,000	50,000	41.5
1,000	100,000	105.6
1,000	200,000	282.7

Thus, we are considering failure modes which will lead to orbital periods of 50 to 100 hours.

8. IMPLEMENTATION CONSIDERATIONS

Without attempting to be exhaustive, certain implementation requirements and considerations are reviewed which are pertinent to the backup orbit insertion mode. These are discussed in the context of the four 100-pound thrusters used in a constant-pitch-rate steering mode, and instituted automatically at the time of failure of the high-thrust mode to operate. However, other approaches would entail similar conclusions.

Of course, the propulsion system is affected. The low-thrust engines must be selected and incorporated into the design. Compatibility with the primary propulsion system must be assured, including ability to use the same propellants, the same propellant supply, the same feed system (where common to the primary system), and the same pressurization.

The stabilization and control system must encompass a provision for satisfactory thrust vector control during low-thrust engine firing. Depending on the number and type of engines employed, gimbaling or pulsing (off) of the engines and use of the cold gas attitude control system are candidate approaches. The implementation and institution of the pitch (actually pitch-yaw) program to mechanize the steering law is required, and a criterion for terminating the backup firing (timer, accelerometer, propellant depletion, ?) must be established.

The communication system operations will be affected in that no directive antenna will continue to be pointed toward the earth during backup firing, if either $\theta_o \neq 0$ or $\dot{\theta} \neq 0$, unless the backup implementation specifically programs corresponding changes in the antenna gimbal angle(s) to compensate for vehicle attitude changes during firing. An alternate communications mode would involve automatic switching of the spacecraft transmitter to a low-gain antenna, and appropriately reducing the down-link bit rate. Another communications effect is that the extended

burn arc of the backup mode might well extend into an earth-occultation zone, so that continuous monitoring of the propulsive maneuver is interrupted.

The sequencer must be programmed to initiate each of these events. Where the backup is initiated automatically upon detection of failure of the high-thrust mode to operate, the initiation of these events must proceed without interim verification (on the ground) of the readiness of the spacecraft to perform them.

There are also implications of the extended burn time on power and thermal control systems, but these effects are not expected to be serious.

Other factors, which should influence a decision on the incorporation of a backup mode for orbit insertion, and which have not been reviewed during this examination are noted below.

- Whether the capsule can be landed (with reasonably high probability of success) from the degraded orbit.
- Further implications of the planetary quarantine constraint. In addition to the achievement of an orbit with an adequately great periapsis altitude, we should examine whether the degraded control and verification during firing constitute a contamination risk and whether a failure or premature shutdown of the low-thrust mode could lead to an orbit which is too low.
- The relation of the improvement in reliability afforded by the backup mode to the weight and other resources of the spacecraft which must be devoted to it; and a comparison of this relation with alternate methods (in other subsystems, for example) of improving mission reliability.
- Whether the 400-pound thrust mode is satisfactory if it is decided that earth verification, diagnosis, and command must be employed before the backup mode is initiated.
- Whether other thrust levels are most appropriate.
- The orientation of the degraded orbit.

- The utility and exploitation of the degraded orbit.

- The examination of attainable orbits if the approach trajectory, rather than being the nominal, is within the limits of tolerable control, but is still higher or lower than the nominal approach.

- The effect on attainable orbits if the nominal orbit has its apsidal line (major axis) rotated appreciably from the "natural" orientation, i.e., that corresponding to minimum impulsive insertion ΔV requirement. In particular, if large retrograde rotations are scheduled, then the initiation of normal, high-thrust propulsion is logically delayed (relative to the periapsis of the hyperbolic approach). In such an instance, the backup propulsive capabilities are rendered less efficient if this mode is not instituted until the normal mode fails to operate, and the resulting failure mode orbit is correspondingly degraded.

- Whether it is appropriate to degrade the normal orbit-insertion maneuver — specifically, by programming it to occur somewhat earlier than the instant which is optimum for trajectory transfer efficiency alone — in order to improve the failure mode orbit. This would apply particularly to the rotated orbit discussed above, but is an appropriate consideration for any orbit.

9. CONCLUSIONS

It is determined that a backup propulsion system capable of using the primary system propellants and exerting 400 pounds of thrust can place the planetary vehicle into a tolerable orbit about Mars, if the backup mode is instituted automatically at the time the normal, high-thrust mode fails to ignite. Resulting orbit sizes are of the order of 1000 x 80, 000 km, and have periods about 80 to 100 hours. This orbit requires a different thrust pointing than the normal mode) attitude, or a constant-pitch-rate steering following the same initial attitude.

10. REFERENCES

1. For example, note that of the 11 competing characteristics of the JPL 1973 Voyager Mission Specification, none of the top five is achievable if the planetary vehicle fails to enter an orbit about Mars; however all five may be fulfilled, at least partially, if even a highly eccentric orbit is attained. section 3.1.3, 1 January 1967.

2. TRW Voyager Spacecraft Phase 1A Study Report (Task A), Volume 4, pp 230-232, 30 July 1965.

3. JPL 1973 Voyager Mission Specification, Section 3.1.4.4., 1 January 1967.

4. Communication from R.A. Benson, 7 July 1967.